



<https://theses.gla.ac.uk/>

Theses Digitisation:

<https://www.gla.ac.uk/myglasgow/research/enlighten/theses/digitisation/>

This is a digitised version of the original print thesis.

Copyright and moral rights for this work are retained by the author

A copy can be downloaded for personal non-commercial research or study,
without prior permission or charge

This work cannot be reproduced or quoted extensively from without first
obtaining permission in writing from the author

The content must not be changed in any way or sold commercially in any
format or medium without the formal permission of the author

When referring to this work, full bibliographic details including the author,
title, awarding institution and date of the thesis must be given

Enlighten: Theses

<https://theses.gla.ac.uk/>
research-enlighten@glasgow.ac.uk

Primary dysautonomias in domestic animals : A
study of neuronal protein metabolism

by

Marion Mathieson Pollin, B.V.M.S., M.V.M., M.R.C.V.S.

A thesis submitted for the degree of Doctor of Philosophy
in the Faculty of Veterinary Medicine
of the University of Glasgow

Department of Veterinary Surgery

February 1988

© M.M. Pollin

ProQuest Number: 10948190

All rights reserved

INFORMATION TO ALL USERS

The quality of this reproduction is dependent upon the quality of the copy submitted.

In the unlikely event that the author did not send a complete manuscript and there are missing pages, these will be noted. Also, if material had to be removed, a note will indicate the deletion.



ProQuest 10948190

Published by ProQuest LLC (2018). Copyright of the Dissertation is held by the Author.

All rights reserved.

This work is protected against unauthorized copying under Title 17, United States Code
Microform Edition © ProQuest LLC.

ProQuest LLC.
789 East Eisenhower Parkway
P.O. Box 1346
Ann Arbor, MI 48106 – 1346

TABLE OF CONTENTS

	Page no.
DECLARATION	i
ACKNOWLEDGEMENTS	ii
LIST OF TABLES	iii
LIST OF FIGURES	iv
LIST OF APPENDICES	x
SUMMARY	1
GENERAL INTRODUCTION	4
AIM OF THE THESIS	16
PROTEIN SYNTHESIS - A summary of structure and function, with particular reference to glycoproteins	17
The nucleus	17
Ribosomes and RER	19
The Golgi complex	22
GERL	26
Cytochemical demonstration of subcellular organelles	27
Summary of neuronal protein synthetic pathways	31
THE PATHOLOGY OF DYSAUTONOMIAS	33
BACKGROUND LITERATURE	
Gross pathology	33
Histology	33
Ultrastructure	35
Neuropeptides	35
AIM	37
MATERIALS AND METHODS : GANGLIA	37
(1) Paraffin wax section for light microscopy	38
(2) Plastic section for electron microscopy	39

TABLE OF CONTENTS (Cont'd)**Page no.**

RESULTS : GANGLIA	39
Light microscopy	39
Ultrastructure	
Normal peripheral autonomic neurones feline and equine	41
Affected peripheral autonomic neurones, feline	42
Affected peripheral autonomic neurones, equine	44
MATERIALS AND METHODS : XII NUCLEUS, FELINE	46
RESULTS : XII NUCLEUS, FELINE	47
Normal	47
Affected	48
MATERIALS AND METHODS : OTHER NEURONAL POPULATIONS	50
RESULTS : OTHER NEURONAL POPULATIONS	51
Dorsal root ganglia : normal	51
Affected	52
Ventral Horn Cells	53
Normal	54
Affected	54
Additional Finding	54
DISCUSSION	54
ENZYME CYTOCHEMISTRY	62
INTRODUCTION	62
BACKGROUND TO METHODS	62
General considerations	62
Preliminary work	64
Prolonged Osmification	65
MATERIALS AND METHODS	66
RESULTS	69
Normal	69
Affected	70

TABLE OF CONTENTS (Cont'd)	Page no.
DISCUSSION	71
Methodological Consideration	71
Results	75
Conclusion	78
ISOTOPE INCORPORATION <u>In vitro</u>	79
INTRODUCTION	79
BACKGROUND TO METHODS	79
MATERIALS AND METHODS	80
Protein estimation	83
Liquid scintillation counting	83
Data handling	84
Statistics	85
Validation of method	85
RESULTS	85
DISCUSSION	87
Method of killing	88
Time from death into label	89
Protein precipitation	90
Thickness of the slice	91
Interpretation of data	93
Choice of label	95
Conclusions	96
DISRUPTION OF GLYCOPROTEIN SYNTHESIS -	
The morphological consequences : A summary	104
The nucleus	104
The ribosomes and rough endoplasmic reticulum	105
The Golgi complex	108
The axon	110
ANTIMETABOLITES	114
INTRODUCTION	114
(1) Adriamycin	115
(2) Cycloheximide	115
(3) Tunicamycin	116
(4) Monensin	117

TABLE OF CONTENTS (Cont'd)

Page no.

MATERIALS AND METHODS

(a) <u>In vivo</u>	117
(b) Short term <u>in vitro</u>	118
(i) Cycloheximide	118
(ii) Tunicamycin	118
(iii) Monensin	119

RESULTS 120

(a) <u>In vivo</u> studies	121
Normal DRG	121
Adriamycin DRG	122
Normal autonomic neurones	123
Adriamycin - affected autonomic neurones	123
(b) Short term <u>in vitro</u> studies	124
(i) Cell survival	124
(ii) Cycloheximide	125
(iii) Tunicamycin	126
(iv) Monensin	126

DISCUSSION 127

Methodological considerations	127
Consideration of Results	130
(i) Adriamycin	130
(ii) Cycloheximide	132
(iii) Tunicamycin	133
(iv) Monensin	134

Tissue culture as an alternative in vitro model 135

(i) Methods	135
(ii) Results	136

GENERAL DISCUSSION 138

APPENDICES 147

REFERENCES 155

ACKNOWLEDGEMENTS

I would very much like to thank the following people for their help in the production of this thesis:-

- My supervisor Professor I.R. Griffiths for his friendly guidance and constant encouragement
- The Wellcome Trust for awarding me a Veterinary Research Training Scholarship
- Professor D.D. Lawson for allowing me to undertake these studies in his department
- The Surgery Department Laboratory staff for their technical assistance
- The Botany Department, University of Glasgow, for the use of their electron microscope
- Drs. D. Doxey, E. Milne and Mr. D. Pogson, Royal (Dick) Veterinary School, Edinburgh, for access to their clinical material
- Dr M. Ecob, Muscular Dystrophy Research Laboratories, Newcastle-upon-Tyne, for her help with the tissue culture methods
- Mrs. J. Nybo for typing the manuscript
- Mr. A. May for his help with the illustrations
- The owners of the animals, without whose cooperation this study would not have been possible

I could not have undertaken this study without the constant, much appreciated support of my parents, who have always given me every opportunity to further my education.

LIST OF TABLES

		Page no.
TABLE 1	Summary of distribution of neuronal damage in Dysautonomias	61
TABLE 2	Variations in method prior to labelling	98
TABLE 3	Rate of incorporation of labelled amino acid in the presence of cycloheximide	99
TABLE 4	Calculation of incorporation rates of tritiated glycoprotein precursors in normal and dysautonomic animals	100
TABLE 5	Summary of incorporation rates (absolute values) of tritiated glycoprotein precursors in normal and dysautonomic animals	101
TABLE 6	Correlation of rate of isotope incorporation in relation to the time taken between the death of the horse and the labelling of the tissue. (Shot control horses only)	102
TABLE 7	Effects of slice thickness and cutting damage on 103 the rate of incorporation of ³ H-leucine	103

LIST OF FIGURES

Following page 61:

- Figure 1 (a) Stellate ganglion, normal cat
(b) Stellate ganglion, affected cat (5 days duration)
- Figure 2 Affected neurones, coeliacomesenteric ganglion, dog (8 days duration)
- Figure 3 Stellate ganglion, affected horse (20 hours duration)
- Figure 4 Stellate ganglion, affected horse (20 hours duration)
- Figure 5 Normal autonomic neurone, stellate ganglion, cat
- Figure 6 Normal cytoplasm, autonomic neurone, stellate ganglion, cat
- Figure 7 Normal autonomic neurone, stellate ganglion, horse
- Figure 8 Normal autonomic neurone, stellate ganglion, horse
- Figure 9 Nuclear abnormalities, cranial cervical ganglion, cat (3 days duration)
- Figure 10 Affected neurone, coeliacomesenteric ganglion, cat (7 days duration)
- Figure 11 Affected neurone, cranial cervical ganglion, cat (3 days duration)
- Figure 12 Affected neurones, coeliacomesenteric ganglion, cat (7 days duration)
- Figure 13 Affected neurone, cranial cervical ganglion, cat (3 days duration)
- Figure 14 Affected neurones, stellate ganglion, cat (13 days duration)
- Figure 15 Affected neurone, stellate ganglion, cat (5 days duration)
- Figure 16 Affected neurone, stellate ganglion, cat (14 days duration)
- Figure 17 Neurones, stellate ganglion, chronically affected cat (6 weeks duration)

- Figure 18 Neurone, stellate ganglion, recovered cat
- Figure 19 Neurone, stellate ganglion, recovered cat
- Figure 20 Affected neurone, stellate ganglion, horse (20 hours duration)
- Figure 21 Affected neurones, stellate ganglia
- Figure 22 Affected neurone, stellate ganglion, horse (6 days duration)
- Figure 23 Affected neurone, stellate ganglion, horse (17 days duration)
- Figure 24 Affected neurones, stellate ganglia, horse
- Figure 25 Affected neurone, stellate ganglion, horse (17 days duration)
- Figure 26 Position of the XII nucleus in the brainstem
- Figure 27 Pre-processing trimming of blocks containing XII nucleus neurones
- Figure 28 Normal neurone, XII nucleus, cat
- Figure 29 Normal neurone, XII nucleus, cat
- Figure 30 Normal neurone, XII nucleus, cat
- Figure 31 Normal neurone and dendrite, XII nucleus, cat
- Figure 32 Abnormal nuclear structures, XII nucleus, cat (5 days duration)
- Figure 33 Affected neurone, XII nucleus, cat (3 days duration)
- Figure 34 Affected neurone, XII nucleus, cat (5 days duration)
- Figure 35 Affected neurone, XII nucleus, cat (13 days duration)
- Figure 36 Large light neurone, dorsal root ganglion, normal cat
- Figure 37 Large light neurone, lumbar dorsal root ganglion, cat (10 days duration)
- Figure 38 Large light neurone, lumbar dorsal root ganglion, cat (7 days duration)

- Figure 39 Large light neurone, lumbar dorsal root ganglion, cat (10 days duration)
- Figure 40 Normal ventral horn cell, cat
- Figure 41 Ventral horn cell, cat (3 days duration)
- Figure 42 Ventral horn cell, cat (3 days duration)
- Figure 43 Ventral horn cell, cat (3 days duration)
- Figure 44 Affected neurone, dorsal nucleus of the vagus, cat (13 days duration)

Following page 78:

- Figure 45 Mouse epididymis, TPPase, 17 hours incubation
- Figure 46 Mouse epididymis, TPPase, overnight incubation
- Figure 47 Dog ganglion, prolonged osmification
- Figure 48 (a) Normal horse, Stellate ganglion, TPPase lead capture
(b) Normal horse, Stellate ganglion, TPPase, cerium capture
- Figure 49 Normal horse, Stellate ganglion, TPPase, lead capture
- Figure 50 Normal cat, Stellate ganglion, TPPase, lead capture
- Figure 51 Normal horse, Stellate ganglion, AcPase
- Figure 52 Normal cat, Stellate ganglion, AcPase
- Figure 53 Normal horse, Stellate ganglion, AcPase
- Figure 54 Affected horse (20 hours duration) Stellate ganglion, TPPase lead capture
- Figure 55 Affected horse (30 hours duration) Stellate ganglion, TPPase lead capture
- Figure 56 Affected horse (7 days duration), Stellate ganglion, TPPase cerium capture
- Figure 57 Affected cat (7 days duration) cranial cervical ganglion, TPPase lead capture
- Figure 58 Affected cat (7 days duration) cranial cervical ganglion, TPPase lead capture

- Figure 59 Affected cat (6 weeks duration) Stellate ganglion, TPPase lead capture
- Figure 60 Affected horse (30 hours duration) Stellate ganglion, AcPase
- Figure 61 Affected cat (6 weeks duration) Stellate ganglion, AcPase

Following page 103:

- Figure 62 Summary of methods for the semi-quantitative assessment of protein synthetic function in vitro
- Figure 63 The effect on synthetic function in vitro of a delay between the death of the tissue donor and the onset of labelling
- Figure 64 Stellate ganglion, Normal horse, ^3H -leucine, 30 minutes labelling
- Figure 65 Stellate ganglion, affected horse (6 days duration), 30 minutes labelling
- (a) ^3H -leucine
(b) ^3H -mannose
- Figure 66 The calculated effects of cutting damage on the semi-quantitative assessment of ^3H -leucine incorporation in vitro.

Following page 137:

- Figure 67 Large light cell, non-incubated dorsal root ganglion, perfusion-fixation
- Figure 68 Dorsal root ganglion, Adriamycin (intravenous)
- Figure 69 Dorsal root ganglion, Adriamycin (intravenous) 3 days
- Figure 70 Dorsal root ganglion, Adriamycin (intraperitoneal) 5 days
- Figure 71 Dorsal root ganglion, Adriamycin, 7 days
- Figure 72 Normal autonomic neurone, rat, perfusion-fixation
- Figure 73 Autonomic ganglion, Adriamycin (intravenous) 6 hours
- Figure 74 Autonomic neurone, Adriamycin (intravenous) 7 days

- Figure 75 Dorsal root ganglion, control incubation, 3 hours
- Figure 76 Small dark neurone, dorsal root ganglion, control incubation, 3 hours
- Figure 77 Large light cell, dorsal root ganglion, control incubation, 6 hours
- Figure 78 Dorsal root ganglion, 3 hours incubation, Cycloheximide
(a) 80 ug/ml
(b) 20 ug/ml
- Figure 79 Dorsal root ganglion, 6 hours incubation, cycloheximide
(a) 20 ug/ml
(b) 80 ug/ml
- Figure 80 Dorsal root ganglion, tunicamycin 25 ug/ml, 6 hours incubation
- Figure 81 Dorsal root ganglion, 3 hours incubation, tunicamycin
(a) 10 ug/ml
(b) 25 ug/ml
(c) 50 ug/ml
- Figure 82 Dorsal root ganglion, 6 hours incubation, tunicamycin
(a) 10 ug/ml
(b) 25 ug/ml
(c) 50 ug/ml
- Figure 83 Dorsal root ganglion, monensin, 10 uM, 3 hour incubation
- Figure 84 Dorsal root ganglion, monensin 1 uM, 3 hours incubation
- Figure 85 Dorsal root ganglion, 3 hours incubation
(a) Monensin, 1 uM
(b) Monensin, 10 uM
- Figure 86 Dorsal root ganglion, monensin 1 uM, 6 hours incubation

Figure 87 Dorsal root ganglion, monensin 0.1 μ M

(a) 3 hours incubation

(b) 6 hours incubation

Figure 88 Embryonic mouse DRG after 12 days in vitro

Figure 89 Embryonic mouse DRG neurone, 14 days in vitro

Following page 153:

Figure 90 Perfusion apparatus for (i) cats (ii) rats

LIST OF APPENDICES

		Page no.
Appendix 1	Processing of samples for electron microscopy	147
Appendix 2	Staining of grids for electron microscopy	149
Appendix 3	Buffers	150
Appendix 4	Perfusion Fixation	152
Appendix 5	HEPES Buffered Salt Solution	154

SUMMARY

Primary dysautonomia has been recognised in horses for more than 70 years, a very similar condition was first observed in cats in 1981, and recently it has also been recorded in a small number of dogs. The occurrence of this condition appears to be confined almost exclusively to Britain and parts of Scandinavia, and young adult animals are the most susceptible in each population although younger and older animals are no less severely affected if they develop the disease.

In all species, cessation of gastrointestinal function is the predominant clinical finding, and the only consistent lesion demonstrable in each case is "chromatolytic" change in peripheral autonomic neurones, a finding now generally accepted as diagnostic of primary dysautonomia. The aetiology of these primary dysautonomias is unknown.

This thesis examines and compares the ultrastructural lesions of peripheral autonomic neurones in cats and horses, and describes the morphological damage sustained by feline XII nucleus, spinal ventral horn and dorsal root ganglion neurones.

In general, the changes in each population consist of a redistribution of rough endoplasmic reticulum, followed by loss of ribosomes from individual cisternae and distension of these cisternae by an electron-dense floccular material. This is closely related to a loss of the Golgi complex. Partial nucleolar segregation and crenation of the nuclear envelope are commonly found, and ring nucleoli are occasionally seen. Proliferated smooth endoplasmic reticulum is a frequent occurrence. Mitochondria appear relatively normal, although they

are frequently denser and more slender than normal, and occasionally increased in number. Neurofilaments, tubules and lysosomes all appear relatively normal.

The only major difference between the feline and equine lesions is the occurrence, in several feline peripheral autonomic neurones only, of complex smooth membranous stacks. Thiamine pyrophosphatase, an enzyme specific for 'trans' Golgi cisternae cannot be demonstrated in these stacks or any other abnormal structure in affected neurones, suggesting that if any unusual membranes are derived from the trans Golgi cisternae they do not retain their normal enzymic function. Similar results are obtained for acid phosphatase, an enzyme specific for GERL (Golgi-related Endoplasmic Reticulum producing Lysosomes) and lysosomes. Activity could only be demonstrated in lysosomes in the abnormal neurones.

An examination of the in vitro incorporation of tritiated glycoprotein precursors by a slice preparation of post-mortem autonomic tissue from normal and affected horses demonstrates a great decrease in the synthetic function of affected neurones.

The appearance of the dysautonomic neurones is compared to lesions resulting from specific disruption of protein synthesis at various levels in rodent dorsal root ganglia; mRNA synthesis (Adriamycin), polypeptide chain synthesis (cycloheximide), core glycosylation (tunicamycin) and terminal glycosylation and packaging within the Golgi (monensin). Based on these observed changes, together with those described in the literature of similar disruptions in various cell types, it is concluded that the primary lesion of dysautonomia occurs within the cytoplasmic

components of glycoprotein synthesis (rough endoplasmic reticulum and Golgi complexes), although the precise level of damage is not yet determined.

With the exception of the membranous stacks, the lesions in all the neuronal populations examined are very similar, and it is therefore extremely probable that the aetiological agent(s) in each case is also very similar, if not the same.

GENERAL INTRODUCTION

Primary dysautonomia has been recognised as a clinical entity in domestic animals in the United Kingdom for nearly 70 years. The first described, and probably best known, example of this is equine grass sickness.

Equine grass sickness (EGS), a disease of unknown aetiology, was first seen in Scotland in the early 1900's (Greig, 1928; Guthrie, 1940; Greig, 1942). Acute, subacute and chronic forms of EGS may occur, which were considered by Greig (1928) to be different degrees of "sympathicotonia", or perhaps related to a depression of the parasympathetic system as opposed purely to a primary stimulation of the sympathetic system.

In general, affected horses present with dullness and inappetence, difficulty in swallowing and inactive bowels which may at first suggest a subacute impaction of the colon. Fine muscle tremors are common over the shoulders and flanks, and there may be periodic patchy sweating (Mahaffey, 1959). Acute and subacute cases also have greatly elevated pulse rates.

Horses with the acute form of EGS show signs of abdominal uneasiness; rolling and tympany, sweating and attempted defaecation and urination. The animals salivate and there is a discharge of ingesta from the nose. Death is usually within four days (Edwards, 1987).

Subacute EGS has many features in common with the acute form although less marked, and the majority of horses die or are destroyed. A few become more chronic, and as the disease progresses there is a great loss of condition with the abdomen becoming markedly "tucked-up" (Guthrie, 1940; Mahaffey, 1959).

The muscles of the trunk and quarters are very hard to the touch.

Swallowing difficulties are common in acute and subacute EGS, and reverse peristalsis in the oesophagus is reported (Begg, 1936), with radiographic abnormalities also demonstrable (Greet and Whitwell, 1986; Greet and Whitwell, 1987). The most common finding of these authors was of delay and incoordination in the passage of barium in the oesophagus, with pooling at the thoracic inlet and oscillation of the accumulated barium between the thoracic inlet and the diaphragm. Dysphagia was present in less than half the cases where oesophageal abnormalities were demonstrated by this method.

Chronic cases demonstrate progressive emaciation, but do feed to some degree and may defaecate normally (Begg, 1936) although many animals have trouble with both defaecation and urination (Guthrie, 1940). Symptomatic treatment may prove helpful, but should only be attempted in cases which are feeding voluntarily. Horses may persist in this state for months before dying, or being destroyed.

Since it was first reported in Barry, Angus, EGS has been seen predominantly in Britain, although there have been reports of occasional cases elsewhere: a few subacute cases have been reported in Belgium (Brownlee, 1939); it has been recognised in Sweden for a number of years (Obel, 1955) and in one outbreak, 22% of a group of stabled trotters contracted the disease over a six-month period (Lannek, 1961). Only one of these was confirmed histologically. Reports have also been quoted of cases of this, or a similar condition in Brittany, West Flanders, Hungary,

Colorado, Denmark, Germany and Switzerland (Guthrie, 1940; Greig, 1942; Gilmour, 1987). A similar condition has been reported from Colombia (Ochoa et al., 1974), but this is now thought to be a distinct entity. Sporadic cases of suspected EGS have been seen in New South Wales during the early seventies, but were unconfirmed clinical diagnoses. In one instance, however (Stewart, 1977), the coeliaco-mesenteric ganglion was examined following death due to gastric rupture after 16 hours of illness and "typical" histological changes were found which were considered strongly suggestive of a positive diagnosis.

EGS is rare in animals of less than one year old and the clinical disease has never been seen in suckling animals, although one foal which survived only 24 hours after being born to an acutely affected mare was found to have some typical histological lesions (Gilmour, 1973).

In an attempt to find common epidemiological factors which might help in establishing an aetiology, numerous surveys have been undertaken (Begg, 1936; VCOU Report, 1970; Gilmour, 1973; Gilmour and Jolly, 1974). The following conclusions were reached by all the surveys:-

- the disease occurs most frequently in 2-8 year-old horses.
- animals kept solely outdoors are at greater risk than those stabled for even part of the day.
- those animals receiving no supplementary feeding, or a supplement of concentrate alone, are more likely to become ill than the others.

- horses resident on an affected premises for less than two months are at greater risk than the other animals.
- cases usually occur on premises with a history of previous EGS.

There was no significant difference, however, between those animals in previous contact with EGS and those which were not. There was no consistent history of concurrent disease in other horses on any farm, nor had the affected horses any significant history of previous disease. There was no sex predisposition. Never more than two horses were affected within 24 hours of one another, although a few "outbreaks" with several cases occurring over a 5-6 week period have been seen.

In Scotland during August to April cases tended to be near the coast, while in May to July the disease occurred inland and at higher altitude, but adjoining areas were not always affected sequentially. It tended to be associated with arable land, although any type of pasture could be affected (VCOU Report, 1970).

The geographical distribution of EGS being so precise, numerous workers have tried to establish a meteorological connection to account for this. The Scottish VCOU survey seemed to suggest that EGS is dependent on rain and increasing temperature. An early morning ground frost has been noticed to cause an apparent increase in the incidence of EGS, and there is a reduction with cold, wet conditions. Checking with meteorological records, however, has failed to establish any connection with a single climatic factor, although a combination of factors is still a possibility. Any apparent connection with

the weather could result from the effect of changing climatic conditions on the herbage; several people have reported that the disease is most prevalent in spring and early summer when the first "flush" of grass occurs and have proposed the possible involvement of a herbage factor (Guthrie, 1940; Greig, 1942; Gilmour and Jolly, 1974; Pickering, 1974). Horses with little or no supplementary feeding appear more at risk, and it has been suggested that a closer examination of the grazing behaviour of horses may help, since preliminary studies show that even on good pasture horses frequently select rough grazing (Fraser and Brownlee, 1974). Selenium deficiency has also been proposed, but not substantiated, as a possible aetiological factor (Anderson, 1978; Anderson et al., 1978; Macpherson, 1978).

Since EGS has been diagnosed in horses shortly after both turning out and being stabled (Greig, 1942; Ashton et al., 1977) some believe that it is a change of diet rather than the diet itself which could be implicated (Guthrie, 1940). In two instances, however, "outbreaks" occurred in stabled animals in which the only common factor appeared to be the food. Two groups of pit ponies in separate pits became ill simultaneously; the hay was the same since the pits had a common owner. This hay was traced as part of a consignment, the rest of which was returned by a large London stud following the occurrence of similar signs there (Forsyth, 1941).

In the "outbreak" in stabled trotters in Sweden (Lannek et al., 1961) the only difference found between affected and non-affected stable blocks was the linseed oil content of the food.

The HCN component of the linseed was suspected, but attempts to reproduce the disease by the feeding of the total volume of HCN to test horses were unsuccessful. These authors favoured a contagious aetiology, given the pattern of a sudden flare-up and the restriction of the disease to adjoining stables.

Infectious agents have been considered as a possible aetiology, but no evidence has been found to support this (Gordon, 1934; Begg, 1936; Guthrie, 1940; Greig, 1942; Chandler and Brownlee, 1967), with the exception of the cases of EGS in Colombia (Ochoa et al., 1974; Ochoa and de Velandia, 1978). An as yet unidentified neurotoxin of unknown origin has also been implicated in this disease (see page 59).

The domestic horse, and occasionally the donkey, is almost exclusively affected, but there is one report of two cases (Ashton et al., 1977), confirmed histologically in other equidae at Whipnade Park; one a ten year old Przewalski horse with acute EGS, the other a two year old zebra which showed the signs of chronic EGS, the onset of which coincided with a short period of being housed off grass for management purposes. These cases occurred within two months of each other.

In the last six years another clinical entity classifiable as a primary dysautonomia has become apparent, this time in cats. The syndrome, consisting most commonly of persistent pupillary dilation, protrusion of the membranae nictitans, dryness of the mucous membranes, constipation and regurgitation, was first described by Key and Gaskell (1982), and became recognised with increasing frequency over the following year (Nash et al., 1982; Janz, 1982; Koch, 1982; Power and Temple, 1982; Madeiros, 1982).

Feline dysautonomia occurs predominantly in young adult animals, six months to three years old, but is also seen in very young and much older animals in which, although less common, it is no less severe. Cats generally become noticeably ill over a period of 24-48 hours, but in a few extreme cases the onset is so rapid that a road traffic accident might be suspected initially (Nash, 1987).

In addition to the originally described signs, reduced tear production and megaesophagus are very common clinical findings in more than 90% of cases, while a bradycardia (<120 beats per minute), areflexic anus, and faecal and/or urinary incontinence are presenting signs in at least a quarter of the affected cats. Occasional cats also demonstrate mild proprioceptive deficits and episodes of collapse (Sharp et al., 1984; Rochlitz, 1984; Pollin, 1985; Nash, 1987). There is no consistent history of any previous significant illness in these cats.

One of the first problems noticed by the owners may be dysphagia, or the regurgitation associated with megaesophagus. The radiographic appearance of barium swallows in affected animals is very consistent. It may be slight, with only a distension of the thoracic inlet and pooling of barium, and sometimes some pooling in the caudal oesophagus too. More severe changes may also occur with dilation of the full length of the oesophagus, and retention of the barium, none of it reaching the stomach within at least the first five minutes (Pollin, 1985).

Affected cats rarely die, unless a secondary infection is contracted, but the majority (75-80%) are destroyed on humane

grounds within the first month of illness. Those which do recover do so slowly, and signs such as megaesophagus, while ceasing to be a clinical problem, are still demonstrable radiographically. Body condition is rarely regained, and recently the problem of occasional cats relapsing or re-succumbing sometimes more than two years after the initial illness has been noted (personal observation). The outcome in these cases so far has been the destruction of the animal.

In general only one cat in a household is affected, although there are a few reports of two cats becoming ill within a relatively short period of one another (Madeiros, 1982; Power and Temple, 1982; Macholc and Macholc, 1985; Pollin, 1985; Nash, 1987; Gaskell, 1987). An "outbreak" of suspected feline dysautonomia with a high morbidity but atypically low mortality has also been seen in a closed cat colony. No causal agent was identified in this instance.

Although initial reports indicated that the incidence of this feline dysautonomia (or Key-Gaskell syndrome) was apparently confined to Great Britain, there have been several confirmed cases elsewhere subsequently, notably Scandanavia (Flagstad et al., 1986; Edney et al., 1986) but also two in Dubai, one in the USA of a cat imported from the UK, and one unconfirmed report from Venezuela (Gaskell and Edney, 1985).

Despite a large number of cats being affected, no cause for this condition has become apparent, and several studies of epidemiological factors have been undertaken in an effort to elucidate the aetiology (Sharp et al., 1984; Rochlitz, 1984; Gaskell, 1987). Apart from the fact that the greatest incidence

involves young cats, no other single factor could be associated with the disease. Diet, toys, previous illnesses and treatment in the affected cat and any others in the household, access to domestic chemicals, how much time was spent outdoors, whether or not the cat hunted, the breed and sex of affected animals were all investigated. The conclusions reported from the most comprehensive of these (Gaskell, 1987) are preliminary, and since no single factor has been identified, further studies, with careful controls allowing detailed comparisons and cross-correlations to be made, may be of value if the problem is multifactorial.

Many similarities can be noted between the feline and equine dysautonomias; in general the onset is rapid, but may be more gradual, and the usual presenting signs include dullness, inappetence, dysphagia, gut stasis and radiographically demonstrable oesophageal dysfunction. A considerably greater proportion of acutely affected horses die rather than are destroyed, but this could possibly be accounted for by the differing alimentary tract physiology of the two species, ileus being more catastrophic in the horse than in the cat.

Numerous comparisons may also be drawn regarding the geographical distribution of primary dysautonomias, but by far the most striking similarity between the two is the appearance and distribution of the histological lesions within the nervous system. "Chromatolytic"-type neurones are found within sympathetic and parasympathetic ganglia in all affected animals, and some may, in addition, have specific lesions of the dorsal

root ganglia, the ventral horn cells and intermediolateral grey matter of the spinal cord and certain brainstem nuclei, not all of which are autonomic. Patterns of peripheral neuropeptide depletion are also closely comparable in these two conditions, and both this and the pathological changes are discussed in detail later (pages 32-61).

The only other species in which a primary dysautonomia has been recorded is the dog. Three cases have been reported, all from Britain (Rochlitz and Bennett, 1982; Pollin and Sullivan, 1986), presenting clinically with the same signs as the cat. They showed a generalised ileus, and radiographic abnormalities of the oesophagus. One case had a bradycardia which did not respond to stress or exercise, and a loss of anal tone; another showed impaired bladder function. They were all young adult dogs, and pathologically the lesions in the nervous system were indistinguishable from those in the cat and the horse.

The spectrum of human autonomic failure is much greater than that in other species. A wide range of autonomic signs is seen in conditions such as familial dysautonomia (Dancis, 1983) and pure pan-dysautonomia as described by Young *et al.* (1975); several cases of acute autonomic neuropathy have also been reported (McLeod, 1983). Acute primary pan-dysautonomia is rare however, the majority of patients presenting with a chronic secondary autonomic failure, most being middle-aged or elderly (Mathias, 1987).

The aetiology of pure autonomic failure in man is not known. The better documented and understood problems are those occurring as secondary complications in conditions such as amyloidosis,

diabetes, Parkinsons's disease, Multiple System Atrophy, syringomyelia, the Holmes-Adie syndrome, Chagas disease, traumatic cervical or thoracic cord transection and old age (Bannister, 1983; Mathias, 1987).

In most occurrences of autonomic failure in man there are marked vasomotor disturbances manifested by orthostatic hypotension and a lack of response of the heart to stress. General malaise, gastrointestinal disturbances and constipation, dry mucous membranes and fixed dilation of the pupils are present in many cases. In some patients urinary retention, loss of rectal tone and abnormal sweating may be seen. More localised syndromes are seen too, the eyes being the organ most frequently affected (Johnson, 1983).

Some syndromes also include non-autonomic components; the Holmes-Adie syndrome for instance, where there may be a disturbance of the deep tendon reflex in the knees in association with pupillotonia, a condition occurring rapidly, mainly in young people and appearing to persist for life.

One case has been described (Inamdar et al., 1982) where only the cholinergic components of the autonomic nervous system appeared to be involved. An alert young girl of eight presented with abdominal pain, absence of bowel sounds, dilated intestines, urinary retention, fixed dilated pupils, dry skin and mouth and decreased lacrimation. No orthostatic hypotension was seen, but there was no response of the heart rate to carotid sinus massage. Clinically this would appear to be the closest example of a comparable human condition, but the girl recovered, so the nature

of the underlying lesion remains unknown.

Autonomic failure in man has a varied pathology. Specific areas of the central and peripheral nervous systems are involved in each condition, and all the dysautonomic states have a distinctive distribution of lesions. In many cases the intermediolateral grey matter of the spinal cord is involved, and lesions are frequently seen in the dorsal nucleus of the vagus (DNV) of patients with progressive autonomic failure (Bannister, 1983; Mathias, 1987). However, abnormalities are generally seen in areas of the CNS not known to be involved in the dysautonomias of other species.

If the number of cases and the precise geographic location of primary dysautonomia in domestic animals is taken into consideration, together with the specificity of lesion distribution, it becomes apparent that there is no comparable human condition.

AIM OF THE THESIS

The primary dysautonomias of domestic animals appear to be very similar with regard to the geographical distribution of cases, the age of susceptible animals, the clinical signs and the nature and distribution of the associated neurological lesions. The aetiology and precise pathogenesis in each species is unknown.

The aim of this thesis is to investigate the ultrastructural lesion within the perikaryon, with particular reference to the structure and function of the organelles involved in glycoprotein biosynthesis, which are thought to be primarily involved in dysautonomias, and to establish a putative structure-function relationship in affected cells.

Comparisons will be made between the ultrastructure of neurones affected by the natural disease and those in which synthetic activity has been specifically disrupted by antimetabolites of known action.

It is hoped that this will provide evidence regarding the primary site of damage in dysautonomic neurones, and hence some indication of the possible nature of the causal agent(s).

PROTEIN SYNTHESIS

A summary of structure and function, with particular reference to glycoproteins

The nucleus

The genetic information required for the synthesis of protein is contained within the nucleus in the two helical polynucleotide chains of deoxyribonucleic acid (DNA). Synthesis of protein occurs within the cytosol, and therefore there must be a transfer of the genetic information from the nucleus to the cytoplasmic synthetic machinery. This is effected by ribonucleic acid (RNA), a single-standed polynucleotide chain complementary to a specific area of DNA. The specificity of DNA and the complementary RNA is determined by the sequence of the nucleotide bases, forming a very precise 'code'.

RNA synthesis from DNA is known as transcription, and comprises the four main stages of 'binding' to the DNA template, chain initiation, chain elongation and chain termination. Random, rapidly reversible binding of RNA polymerase with DNA occurs until a promoter region - a specific sequence of base-coding - is found. This leads to a local unwinding of the DNA. Elongation of the RNA in a 5' to 3' direction is by phosphodiester bonding of nucleoside triphosphates in a sequence complimentary to that of the base sequence in DNA. To form RNA, uracil corresponds to the adenine of DNA, adenine to thymine, guanine to cytosine and cytosine to guanine.

Those areas of DNA that have been transcribed regain their double-helical conformation as the next section unwinds.

There are specific signals on DNA which terminate

transcription, some of which can be recognised by RNA polymerase itself, others by a specific protein 'termination factor'.

These RNA molecules are then modified or split in highly selective ways - mechanisms known as maturation or processing. Some RNA molecules are the information-carrying intermediates of protein synthesis, others are a part of the synthetic machinery. There are three main types of RNA:-

mRNA (messenger) contains the information required for the correct sequencing of the amino acid chain of proteins groups of three bases coding for each amino acid.

tRNA (transfer) recognises the specific mRNA base sequences for individual amino acids, each tRNA molecule containing a specific 'anticodon' of three bases and the binding site for the amino acid specified by that codon;

rRNA (ribosomal) is one of the many components of ribosomes, the structures which actually synthesise the polypeptide chains.

The structural-functional correlation within the nucleus has not been fully elucidated.

The nucleolus comprises two main structural components; the fibrillar and granular elements which represent nucleolar chromatin and pre-ribosomal particles respectively (Daskal, 1979). It is thought that rRNA processing occurs initially in the fibrillar region of the nucleolus, transferring later to the granular components (Bouteille and Dupuy-Coin, 1979).

Chromatin may be present in both condensed and dispersed forms. The exact relationship between these is still to be described.

Perichromatinic granules are a universal component of the eukaryotic nucleus, but their precise structure, function, origin and composition are as yet unknown (Daskal, 1979) although it is thought that they may carry mRNA/protein complexes (Bouteille and Dupuy-Coin, 1979). The interchromatin granules also have no assigned function.

The nucleus is bounded by a double membrane - the nuclear envelope - which contains numerous 'pores'; structured holes through the double membrane containing transverse fibrils which pass through the pores and extend into both the karyoplasm and the cytoplasm.

These pores are closed by the two membranes of the nuclear envelope (Arechaga and Bahr, 1985) and act as a selective 'gate' for nucleocytoplasmic exchange (Feldherr, 1985; Maul and Schatten, 1985).

The pore complex appears to be a very dynamic structure, the numbers being doubled during cell division and halved subsequent to ischaemic damage (work carried out in kidney), the number at any given time being dependent on the balance between the numbers forming and disappearing (Maul and Schatten, 1985).

The nuclear envelope bears cytochemical similarities to the endoplasmic reticulum (Cataldo and Broadwell, 1984) and is continuous with it (Smuckler and Clawson, 1985).

Ribosomes and RER

Cytoplasmic protein synthesis involves the 'translation' of the coded nucleotide sequence of mRNA into the specific amino acid sequence of polypeptide indicated by each mRNA molecule. This entails the coordinated interplay of more than 100 different

macromolecules; mRNAs, tRNAs, activating enzymes and protein factors, and the ribosomes.

Ribosomes comprise large and small subunits, both of which consist of many proteins and various RNA components. These are apparently formed by 'self-assembly' when all the various component parts are present.

The activation of amino acids and their linkage to the relevant tRNAs is effected by specific synthetases and is energy dependent. Polypeptide chain synthesis occurs in three main stages - initiation, elongation and termination.

Initiation is by a complex comprising a ribosomal subunit, mRNA, Met-t-RNA and energy in the form of GTP. The Met-t-RNA binds to the 'P' site, one of two binding sites present on the ribosome.

Elongation consists of the binding of an aminoacyl-tRNA into the other empty site - the 'A' site - of the ribosome, a process which requires energy (GTP) and a protein 'elongation factor'.

A peptide bond is formed between the peptide in the P site and that in the A site, this reaction being catalysed by peptidyl-transferase.

Translocation then occurs, with the unchanged tRNA leaving the P site, the peptidyl tRNA moving from A to P, and the mRNA moving a distance of three nucleotides. This requires a translocase. The A site is then ready for the next aminoacyl-tRNA.

'Stop' codons are not recognised by tRNAs; instead they are recognised by proteinaceous release factors. This initiates

peptidyl transferase to hydrolyse the polypeptide-tRNA bond at the P site and the polypeptide chain leaves the ribosome.

Many polypeptides formed by the translation of mRNA are not the final products. Glycoproteins, for example, are formed by the attachment of sugars to the side-chains of specific amino acids.

Some ribosomes are free in the cytosol, others are membrane bound, forming the RER, the relative proportions of these depending on the individual cell type. Newly synthesised membrane and secretory proteins are transferred from the bound ribosomes into the cisternae of the RER, directed there by a short peptide "recognition sequence" which is later cleaved from the main polypeptide. Cytoskeletal and various other proteins are formed on free ribosomes.

RER is multi-functional, being concerned mostly with protein synthesis, but it is also involved in lipid synthesis and glycogenolysis in some cells (Broadwell and Cataldo, 1983).

In cell bodies and the proximal dendrites it consists of an anastomotic and fenestrated network of sacs and tubules with attached ribosomes, but the endoplasmic reticulum in the distal portion of the dendrites is aribosomal. Cisternae found close to the cell membrane appear similar to other areas of RER, but there are no ribosomes on the side adjacent to the plasmalemma (Broadwell and Cataldo, 1983).

The volume of endoplasmic reticulum is governed by the importance of protein synthesis to the cell. Neurones are dependent on well-developed RER and SER for their function. Its perikaryal distribution can vary from highly organised, discrete

stacks of parallel cisternae, to strands of varying length, distributed apparently at random, but predominantly along the long axis of the cell, depending on the neuronal type (Broadwell and Cataldo, 1983).

In the RER, mannose-rich oligosaccharides are added to nascent polypeptide chains soon after or even before completion of the polypeptide backbone (Leblond and Bennett, 1977), prior to their transportation to the Golgi (Torrise and da Silva, 1984). The enzymes involved in the translocation of polypeptides and this proximal glycosylation serve as RER markers (see later) (Farquhar and Palade, 1981). These glycoproteins appear to be membrane-bound in the RER (Tartakoff, 1980). Before this complex has left the RER, some trimming of the oligosaccharide by glucosidases occurs.

The boundary between RER and SER is poorly defined, some cisternae being smooth on one side, the other side carrying ribosomes. This is known as transitional ER, and is often found closely parallel to the 'cis'-most element of the Golgi complex.

The Golgi complex

There are no apparent connections between these two membranous organelles (RER and the Golgi complex), and since there is no soluble transport in the cytoplasm (Morre et al., 1971) numerous authors have suggested a vectorial form of transport (Morre et al., 1971; Novikoff et al., 1971; Tartakoff, 1980; Rothman, 1981; Cataldo and Broadwell, 1984; Yamamoto, 1985). They propose 'transfer vesicles' budding from the transitional ER and fusing with the forming face of the Golgi

complex, thus transferring not only their contents but also selected membranes (Tartakoff, 1980; Yamamoto et al., 1985). Novikoff et al. (1971) proposed an additional theory of membrane flow by means of larger 'transfer sheets', and presented evidence for both types of vector in DRG neurones.

Since intracellular transport has been demonstrated to proceed in the absence of protein synthesis, it has been proposed that the vesicles 'shuttle' back and forth (Tartakoff, 1980) and that membranes are at least partially conserved.

Although, as mentioned, occasional glucose and mannose residues are removed in the RER, the bulk of the modifications occur in the Golgi complex where mannose is trimmed and other oligosaccharide residues are added (Rothman, 1981; Dunphy and Rothman, 1985).

The Golgi complex plays an important role in a variety of cellular activities including the assembly of secretory proteins, the formation of lysosomes, the differentiation of membranous organelles, phospholipid synthesis, glycosylation and sulphation (Leblond and Bennett, 1977; Rothman, 1981; Lin et al., 1982), but the mechanisms by which it transports, modifies, concentrates and packages its contents are poorly understood (Doine et al., 1984).

Biochemical reactions accompanying the passage of proteins through the Golgi include proteolytic cleavage and modifications to bound oligosaccharides. The Golgi also concentrates its contents (Tartakoff, 1980). Materials leaving this organelle are packaged into vesicles which often contain more than one product (Novikoff and Holtzman, 1970).

Different types of glycoprotein can be synthesised

concurrently, and are classified by their exit from the Golgi as either membrane proteins, secretory proteins or lysosomal enzymes (Leblond and Bennett, 1977; Griffiths and Simons, 1986). They appear to be sorted in the 'trans' most element of the Golgi complex, or perhaps even after exit.

The Golgi complex consists of three distinct functional compartments which have a polarity (see below), and transport within these appears to be by means of 'transport vesicles', and occurs in a cis-trans direction (Dunphy and Rothman, 1983 and 1985; Dunphy, Brands and Rothman, 1985).

The functional reasons for this compartmentalisation of the Golgi complex are as yet unclear, but it is thought to prevent stereochemical blocking of one enzyme by the premature action of another (Dunphy and Rothman, 1985).

There has been no demonstration, however, that secretory products must pass through successive cisternae. The cisternae may be immobile (Tartakoff, 1980) although several workers support a theory of flow or progression of cisternae from cis to trans. Fucose is added in the Golgi complex (Hammerschlag and Lavoie, 1979), but experimental evidence shows no preferential localisation of fucose uptake in any one Golgi cisterna - it would appear to be random (Leblond and Bennett, 1977).

Studies have enabled the functional grouping of Golgi enzymes, but have not yet allowed systematic correlation between the morphological and enzymatic characteristics of all Golgi complex components (Tartakoff, 1980).

The Golgi complex shows a great diversity of size and shape

depending on the cell type studied. Examination by light microscopy of neurones and secretory cells reveals it to be a widespread, interconnecting network throughout the cytoplasm in a broad area roughly concentric with the nucleus (Novikoff et al., 1971). The volume of this network is reported as being directly proportional to the size of the cell (Shanthaveerappa and Bourne, 1965).

The Golgi complex consists of stacks of closely spaced, membrane delimited saccules (cisternae) of which three to seven is the normal number in neurones. These saccules are separated by a relatively constant distance, but the nature of the force holding them together is unknown (Novikoff and Holtzman, 1970).

The membranes of the cisternae are never associated with ribosomes, and the complex is frequently curved or "cup-like". The cisternae often appear quite flat, but may be dilated, especially at the periphery. These peripheral regions of the saccules may include tubules and fenestrations.

The Golgi complex often shows an obvious polarity, and various terms have been used to describe this; cis and trans, top and bottom, outer and inner, convex and concave, forming and mature. The cis saccules may differ from the trans in thickness, content and size and frequency of budding vesicles (Novikoff and Holtzman, 1970). Polarisation is not always clear in neurones, however, with vesicles not necessarily being found consistently on one side of the stack (Bloom, 1973).

Cytochemical variations may also be seen (see later) as may differing dimensions of delimiting membranes (Tartakoff, 1980). There is also a graded increase in the cholesterol content of the

Golgi membranes, increasing from the 'cis' face to the 'trans' face (Dunphy and Rothman, 1983).

The transmost layer of the stack is composed of tubules in a hexagonal array, enclosing areas known as polygonal compartments. In transverse section these tubules may appear to be a region of Golgi-associated vesicles. The conformation of the 'cis'-most element varies from one cell-type to another. In neurones it is an anastomosing system of highly irregular small tubules and saccules. The intermediate saccules appear to be fenestrated, but their precise structure is not yet clear.

The saccules also have a transverse heterogeneity (Tartakoff, 1980), a number of phosphatase reaction products are more abundant in the dilated rims than in the centres of the cisternae.

GERL

In close proximity to the 'trans' most Golgi elements there are areas of GERL, so called because it is a region of "Golgi-Associated Endoplasmic Reticulum which produces Lysosomes" (Novikoff et al., 1971; Novikoff, 1976). This GERL is not fenestrated; it is composed of cisternae and smooth-surfaced tubules which in certain cells (e.g. rodent ganglia) have been demonstrated to extend into the polygonal compartments of the trans element of the Golgi, forming an anastomosing network (Novikoff et al., 1971). The functional significance of the spatial relations of the GERL and the Golgi complex is not yet fully understood (Novikoff, 1976).

GERL is considered to be smooth ER since connections have

been demonstrated between it and distally disposed clumps of RER and there is no indication of direct continuity with the Golgi stack (Tartakoff, 1980).

There has been subsequent debate, however, as to whether this structure derives from the ER as suggested by its name, or from the 'trans' element of the Golgi complex (Broadwell and Cataldo, 1983; Cataldo and Broadwell, 1984; Doine et al., 1984; Griffiths and Simons, 1986). Neither hypothesis has been fully proved.

Although its origins may still be questioned, there is agreement about the function of this organelle. GERL is involved with the packaging of the cell's secretory products, and lysosomes are thought to originate from it (Holtzman et al., 1967; Novikoff, 1976; Bainton, 1981).

All lysosomal enzymes are glycoproteins, and sorting of these occurs by means of mannose-6-phosphate receptors derived from the cis Golgi cisterna, which recognise mannose-6-phosphate groups on the lysosomal enzyme (Pohlmann et al., 1982; Geuze et al., 1985)

Lysosomes, which vary in size and have heterogenous contents are the primary components of the intracellular digestive system.

Cytochemical demonstration of subcellular organelles

Cytochemical techniques have been used increasingly in recent years to establish functional-morphological correlations within the protein synthetic pathway.

However, several findings have led to differing theories on the origins and functions of certain areas in the pathway, notably the Golgi complex and GERL.

Acetylcholinesterase activity is consistently found in the nuclear envelope and RER (Holtzman et al., 1967; Flumerfelt and Lewis, 1975) and not in other regions of the perikaryon. Glucose-6-phosphatase can be demonstrated in these areas, but is also found in the 'cis' cisternae of the Golgi complex (Tartakoff, 1980; Farquhar and Palade, 1981; Broadwell and Cataldo, 1983; Cataldo and Broadwell, 1984). Prolonged osmification results in specific deposits in RER and the Golgi complex - again specifically the 'cis' region (Novikoff et al., 1971).

Thiamine pyrophosphatase is found only in 'trans' Golgi regions, never in RER or less "mature" areas of the Golgi complex, although it is very occasionally found in GERL under specific circumstances (see below) (Novikoff et al., 1971; Cataldo and Broadwell, 1984; Doine et al., 1984).

Immunocytochemical techniques using antibodies raised against sub-cellular fractions (Louvard et al., 1982) or specific enzymes and proteins have also been frequently used to identify organelles, or to localise Golgi-associated enzymes to particular areas; for example, galactosyl transferase has been co-localised with TPPase in the trans Golgi cisternae (Roth and Berger, 1982).

Wheat germ agglutinin, an indicator of AcNGlc terminal glycoconjugates, strongly stains lysosomes, vacuoles, secretory granules and the plasma membrane, but Golgi complexes are poorly stained, with 'trans' cisternae being more strongly positive than the 'cis' region. No staining is seen in the nuclear envelope, RER or mitochondria (Torrison and da Silva, 1984).

The Golgi complex is also rich in binding sites for Concanavalin A, an indication of terminal mannose groups in glycoprotein assembly (Wood et al., 1974).

GERL and lysosomes have a common cytochemical marker in AcPase, the first lysosomal enzyme to be identified (Novikoff et al., 1971; Bainton, 1981; Doine et al., 1984; Griffiths and Simons, 1986).

These markers therefore outline three main functional divisions, with the nuclear envelope and RER strongly associated, the GERL and lysosomes closely related and the Golgi complex associated with, but distinct from both these populations of organelles.

A major controversy arises with regard to the formation of Golgi membranes and the transport of newly synthesised peptides through this region. Two separate theories exist.

There is no dispute over the fact that material is most probably transported from the RER to the Golgi complex by means of vesicles.

Studies by Yamamoto et al. (1985) of specific membrane proteins have demonstrated that RER proteins appear to be efficiently "sorted out" from the areas of transitional ER giving rise to the transport vesicles, with only the proteins destined for Golgi, plasma membranes or lysosomes being transferred to the Golgi complex.

Conversely, the presence of glucose-6-phosphatase in the 'cis' Golgi cisterna, and the affinity of this region for osmium, have been interpreted as an indication that this "sorting out" either does not occur, or is inefficient (Novikoff et al., 1971;

Rothman, 1981). This has led to the concept of vesicles returning from cis Golgi cisternae to RER with 'unwanted' protein, the "sorting out" having occurred in the Golgi complex.

There are also two schools of thought regarding movement within the Golgi complex. There is intercisternal vesicular transport, experimental evidence for which is still elusive (Griffiths and Simons, 1986) and additionally, some workers favour a theory of membrane "flow", with cis cisternae being constantly formed, and a cisternal progression through the stack leading to the ultimate conversion of the trans cisterna to GERL (Broadwell and Cataldo, 1983; Doine et al., 1984).

Many find it hard to reconcile this theory with the functional heterogeneity of the Golgi complex and the abrupt cytochemical delineation between the trans Golgi region and GERL however, and favour more static, distinct sub-sections (Novikoff and Yam, 1978; Tartakoff, 1980; Rothman, 1981).

Recent experimental evidence has been reported which would seem to favour a close functional correlation between the trans Golgi cisternae and GERL. Working with immature secretory cells, Doine et al. (1984) demonstrated that TPPase was present in GERL in addition to the expected AcPase. This was most pronounced when the rats were 20 days old. By 40 days old, TPPase was confined to the Golgi complex, but a similar redistribution of TPPase to include GERL was found when the secretory granule production was accelerated.

This has been used to substantiate the argument that GERL is initially Golgi-derived. It does not necessarily mean, however,

that there is a constant membrane flow between these structures.

An additional problem in the interpretation of these data is that the relative development and cytochemical properties of the various compartments varies between cell-types (Malchiodi et al., 1986).

There is still no conclusive experimental evidence which will allow a confident statement of precise functional mechanisms within this complex, vital organelle.

Summary of neuronal protein synthetic pathways

All proteins synthesised by the neurone have a common pathway initially, with genetic material in the nucleus being transcribed by mRNA which passes to the cytoplasm for translation by ribosomes. After this stage however, the route taken through the cytoplasm depends on the ultimate nature and destination of the protein.

This chapter has concentrated on the pathway for secretory and membrane proteins, where polyribosomes become associated with RER. Secretory proteins transfer to the lumen of RER where they undergo modification by proteolytic cleavage and the addition and subsequent partial removal of sugar residues. They then transfer to the Golgi complex where further glycosylation of the protein moieties occurs, with the addition of terminal oligosaccharides such as N-acetylglucosamine, galactose, sialic acid and fucose, and the phosphorylation of lysosomal enzymes (Siesjo, 1978; Bainton, 1981; Schwartz, 1985; Malchiodi et al., 1986).

These mature glycoproteins are then concentrated and packaged in the Golgi/GERL complex, and distributed to their 'target' organelles e.g. secretory granules, lysosomes and the

plasma membrane by mechanisms which have not yet been fully elucidated. Some final modifications are thought to occur within these organelles (Schwartz, 1985).

Membrane polypeptides are never fully released into the lumen of RER; instead they are "threaded" through the lipid bilayer during synthesis (Schwartz, 1985).

Some ribosomes do not attach to RER, and polypeptide is formed in the cytoplasm on free polyribosomes. These cytosolic proteins comprise the cytoskeletal proteins and numerous biosynthetic and degradative enzymes. Very little modification of these polypeptides occurs subsequent to translation (Schwartz, 1985).

Mitochondria are also endowed with the capacity to synthesise some protein. These proteins appear to be structural, mitochondrial enzymes being cytosolic in origin and transported to the mitochondria after synthesis (Siesjo, 1978; McIlwain and Bachelard, 1985; Schwartz, 1985).

Most neuronal protein is perikaryal in origin, but it has been demonstrated that some independent axonal synthesis occurs. Experimental evidence suggests that this is ribosomal rather than mitochondrial, but the precise mechanisms are as yet unknown (McIlwain and Bachelard, 1985).

Protein synthesis is therefore a very complex, diverse, variable cellular mechanism relying on the close interdependent relationships of its many structural and functional components.

THE PATHOLOGY OF DYSAUTONOMIAS

BACKGROUND LITERATURE

Gross pathology

The gross pathological findings in dysautonomias tend to be non-specific, other than evidence of severe gastrointestinal disturbance, and in general the animals are emaciated and dehydrated. Hard faeces are common in the colon of cats (Sharp et al., 1984; Pollin, 1985), and evidence of inhalation pneumonia may be found. Megaoesophagus is a frequent finding in cats, and in horses longitudinal oesophageal erosions have also been reported (Obel, 1955; Gilmour, 1987).

In acute EGS the stomach is greatly distended by gas and fluid, which has occasionally resulted in gastric rupture (Obel, 1955; Stewart, 1977), and food may be present in the nasal cavity. Sub-acute and chronic cases may have little evidence of disease with the exception that the gastrointestinal tract is depleted of its contents, and chronically affected animals are generally emaciated, with a tacky discharge from the bowel mucosa (Begg, 1936; Mahaffey, 1959; Gilmour, 1987).

Fatty degeneration of the liver has been noted (Holman et al., 1944; Obel, 1955) and the spleen is often much enlarged (Mahaffey, 1959; Gilmour, 1987), but in none of the species is there consistent gross pathological changes which could be considered to be of a primary nature.

Histology

The clinical appearance of dysautonomia suggests a predominantly autonomic involvement, and this is confirmed by the strikingly similar lesions found in the autonomic nervous system

(ANS) in horses, cats and dogs. Typical, specific changes are also found outwith the ANS (see below) for which there are few, if any, associated clinical signs.

Original examinations of material from cases of EGS failed to demonstrate any consistent changes (Greig, 1942; Holman et al., 1944). In 1955 however, Obel described lesions in the autonomic ganglia which have since been confirmed and elaborated upon by numerous authors (Brownlee, 1959; Mahaffey, 1959; Chandler and Brownlee, 1967; Barlow, 1969; Gilmour, 1973; Howell et al., 1974; Gilmour, 1975; Gilmour, 1976; Hodson et al., 1984; Brownlee, 1985; Gilmour, 1987).

"Chromatolytic" changes in autonomic neurones with little increase in the non-neuronal cell population were found by Obel (1955) in all autonomic ganglia examined, but in only one case was there evidence of a lesion in the CNS. These ganglionic findings were substantiated by all later reports but unlike Obel, Barlow (1969) found marked CNS lesions in more than 50% of his cases. He reported no lesions in the dorsal root ganglia (DRG) but Gilmour (1973b) in addition to finding similar CNS changes, described affected DRG in all but two of the horses he examined.

The histological lesions of feline dysautonomia were first described by Griffiths et al. (1982) and confirmed and discussed in some detail by Sharp et al. (1984). Very similar lesions have been seen in three dogs (Rochlitz and Bennett, 1982; Pollin and Sullivan, 1986). As in EGS, consistent "chromatolytic" changes are seen, principally in the peripheral ANS, frequently progressing to a marked depletion of neuronal numbers with a

corresponding increase of the non-neuronal cell population.

Neurones in all autonomic ganglia are generally involved to approximately the same degree within any given cat (Pollin, 1985), a finding considered confirmatory of the clinical diagnosis. In more severe cases, damaged neurones may also be seen at a lower frequency in certain other areas. This distribution of lesions closely relates to those in both horses and dogs (see Results).

Ultrastructure

The ultrastructure of peripheral autonomic lesions has been reported in both the horse (Gilmour, 1975; Hodson and Wright, 1987) and the cat (Griffiths and Sharp, 1983; Sharp *et al.*, 1984; Griffiths *et al.*, 1985). Even at this level changes are very similar, with the Nissl substance of dysautonomic neurones showing a great variety of changes, and Golgi complexes not being identifiable in any form in affected cells. These and other changes are discussed in detail later in this chapter.

Dysautonomic horses and cats also exhibit axonal abnormalities involving both myelinated and unmyelinated fibres (Gilmour, 1975; Griffiths *et al.*, 1985; Hodson and Wright, 1987). Commonly, neurotubules are increased and mal-aligned in a non-longitudinal manner, and vesicles and branched vesiculo-tubular arrays of smooth endoplasmic reticulum (SER) are frequently observed. Mitochondria and various membrane-bound vacuoles and dense-cored vesicles may also be present.

Neuropeptides

In addition to the "routine" histological and ultrastructural findings, major corresponding abnormalities in

gut peptidergic innervation have been demonstrated in both EGS and feline dysautonomia.

The neuropeptides vasoactive intestinal polypeptide (VIP) and Substance P affect the secretion, blood flow and motility of the normal gut; VIP increases water and electrolyte secretion and Substance P is a vasodilator. They are both found in neurones concerned with peristalsis.

Hodson et al. (1982) found marked changes in the regulatory peptide profile of each of the EGS horses. The number of fibres immunostained for VIP and Substance P was reduced in each layer of the gut wall. In certain areas no immunoreactive fibres could be found (Hodson et al., 1982; Sabate et al., 1983).

Ultrastructurally there was extensive degeneration of fibres in the gut of affected horses (Hodson et al., 1982). In the ileum there was an almost total reduction of neuronal vesicles, especially VIP and Substance P, and in the proximal ileum a loss of vesicles with no other degenerative changes suggesting that this is one of the earliest morphologically identifiable events in EGS (Bishop et al., 1984).

In cats too, there is a great loss of VIP immunoreactivity with only a few cell bodies and fibres in the myenteric plexus, and a scarcity of VIP immunoreactive fibres in the circular muscle layer (Vaillant and Sharp, 1984). Only a small number of Substance P-containing fibres could be demonstrated, mainly in the myenteric plexus, and no immunoreactive cell bodies were

found in four of the six cats studied (Vaillant, 1987). In routinely stained sections however, there was little evidence of neuronal loss, only a small number of abnormal, apparently degenerating perikarya in the enteric plexuses. Thus it is possible that levels of immunoreactive materials are reduced within peptidergic nerves.

AIM

The aim of this section is to review and confirm the findings of previous authors regarding the light microscopy and ultrastructural appearance of the peripheral autonomic lesion in cats and horses, and to directly compare these.

A comparison will also be made between the changes in autonomic and non-autonomic neurones, using the feline XII nucleus, ventral horn cells and DRG as the non-autonomic populations.

MATERIALS AND METHODS : GANGLIA

Twenty dysautonomic cats which presented at Glasgow University Veterinary Hospital (duration 3 days - 7 weeks) and four non-affected cats were available for post-mortem examination. One recovered case was also studied.

Five affected cats and three control animals were killed by perfusion-fixation with buffered aldehydes, this method being fully described in Appendix 4. A further five affected cats were killed by intravenous overdose of barbiturate and perfusion-fixed post-mortem within 40 minutes of death.

The remaining twelve cats were killed by barbiturate overdose and the tissue fixed by immersion in the appropriate fixative (see below).

Ten dysautonomic horses presented either at Glasgow or Edinburgh Veterinary Hospital (duration 20 hours - 10 days) were also examined. One horse was shot, the remaining nine being killed by barbiturate overdose, either at the request of the owner or on the operating table following elimination of the possible diagnoses of other causes of 'colic' by exploratory laparotomy. Normal equine tissue was kindly supplied from an experimental pony being shot by Mr. S. Love, Department of Veterinary Medicine, Glasgow University. All equine tissue was immersion-fixed (see below).

Tissue from two dogs with dysautonomia (duration eight days and four months) was available following the natural deaths of both animals. Several hours delay occurred between death and immersion-fixation of the tissue in these cases.

The stellate ganglion was removed entire from every animal, and in the cats and dogs the coeliacomesenteric, cranial cervical, jugular and dorsal root ganglia were also removed. Following removal, tissue from all animals regardless of species or means of death, was handled in one of two ways:-

(1) Paraffin wax section for light microscopy

Feline and canine ganglia were halved, and samples not exceeding 3 mm cubed were cut from the centre of equine ganglia. These blocks were immersion-fixed in 4% buffered neutral formalin (BNF) for a minimum of 48 hours. Tissue perfusion-fixed with buffered aldehydes was rinsed in 0.85% saline for 24 hours prior to the introduction of 4% BNF.

All samples were processed on a 24 hour cycle in a Shandon-

Elliott automatic tissue processor; they were dehydrated through ascending concentrations of alcohol, 'double' embedded in 1% celloidin in methyl benzoate, cleared with histoclear then embedded in paraffin wax.

Sections were cut at 8 um and stained with either haematoxylin eosin or cresyl violet.

(2) Plastic section for electron microscopy

Blocks not exceeding 1.5 mm cubed were cut from the ganglia of each animal, either fresh or following perfusion-fixation, and immersed in 2.5% gluteraldehyde in 0.025% sodium cacodylate buffer for a minimum of 48 hours.

Samples were post-fixed in 1% osmium tetroxide, dehydrated through alcohols and embedded in Araldite resin as described fully in Appendix 1.

One micrometre sections, stained with methylene blue, were used to select the best areas for ultrastructural examination. Thin sections were then cut using a Reichert OmU3 ultratome, supported on 200 mesh copper grids, stained with Reynolds lead citrate and uranyl acetate (Appendix 2) and examined in a Phillips 301 electron microscope.

RESULTS : GANGLIA

Light microscopy

The light microscopic appearance of the neuronal lesion in feline dysautonomia has been fully described and discussed elsewhere (Pollin, 1985). It is summarised here to enable direct comparison both with the lesions in other species, and the associated ultrastructural morphology.

The only consistent histopathological finding in

dysautonomias was chromatolytic change in peripheral autonomic neurones. This is considered confirmatory of the clinical diagnosis.

The appearance of damaged neurones was strikingly similar in all three species when examined in paraffin sections, and easily distinguishable from normal tissue (Figs. 1, 2 and 3). The cytoplasm loses the basophilic granular appearance of the Nissl substance, becoming homogenously pale-staining in both haematoxylin eosin and cresyl violet-stained sections. Some neurones also demonstrated vacuolation of the cytoplasm. Affected perikarya were rounded and moderately swollen in the early stages, but later became shrunken and irregular, while the nuclei were commonly pyknotic.

As the disease progressed, the autonomic ganglia showed a reduction in the number of neurones, with an increase in the non-neuronal cell population. This was most marked in the cat, and in extreme examples neurones were difficult to find. In cases where clinical disease had been present for more than two weeks, few chromatolytic neurones could be demonstrated, remaining neurones mostly appearing normal.

The proportion of autonomic neurones affected in any animal varied (Table 1) and the pattern of involvement within a ganglion appeared to be random (Fig. 3). In the acute lesions it was usual to find more morphologically normal neurones in equine ganglia than in the feline disease.

Any differences between affected neurones were not readily distinguishable in paraffin sections, but examination of 1 um

plastic sections revealed a wide spectrum of lesions, varying from slight dispersion of the Nissl substance to extensive cytoplasmic vacuolation (Fig. 4). These lesions could be clearly defined at ultrastructural level.

Ultrastructure

Normal peripheral autonomic neurones, feline and equine (Figs. 5-8)

The perikaryon was rounded or oval with a large, circular, centrally-placed nucleus containing a prominent nucleolus with a 'honeycomb' appearance. The remainder of the karyoplasm contained randomly distributed heterochromatin granules.

Golgi complexes were numerous, and found concentric to the nucleus in an area not closely associated with either the nuclear envelope or the cell membrane. They consisted of 3-7 parallel cisternae, frequently in a curved configuration. Numerous small coated and non-coated vesicles were associated with the Golgi complex, particularly the 'trans' (concave) side.

RER was generally found throughout most of the cytoplasm except in those areas directly related to the nuclear envelope and cell membrane. It occurred as groups of cisternae, or branching vesiculo-tubular arrays, and was also seen as smaller configurations or individual cisternae. SER occurred as small single cisternae frequently related to the RER or Golgi complexes.

Mitochondria and lysosomes were numerous, and distributed evenly in those areas not occupied by the other large organelles.

The remaining cytoplasm was occupied by neurotubules and filaments. These became increasingly oriented around the long

axis of the cell as they approached the cell process, and the density of the other organelles decreased, with only occasional mitochondria, lysosomes and RER fragments being found more distally.

Affected peripheral autonomic neurones, feline

Nuclei were frequently eccentric, with crenation of the nuclear envelope. Abnormal nuclear structures such as ring nucleoli were seen, although not in every affected cell. The distinctive 'honeycomb' appearance of the normal nucleolus was not always clearly defined (Fig. 9). In no instance was the perinuclear cistern distended.

In the earliest case examined (3 days duration) cytoplasmic changes were already pronounced. No Golgi complexes, either normal or abnormal, could be identified.

No normal RER remained in these cells, and the cytoplasm frequently contained many distended cisternae filled with electron-dense floccular material. Occasional ribosomes adherent to the limiting membranes of these cisternae indicated their probable origins in RER (Fig. 10).

Mitochondria were normal or, in some cases, slightly denser and more slender than usual. Lysosomes appeared normal, many showing signs of secondary activity.

The remainder of the cytoplasm was packed with proliferated SER in short vesiculo-tubular arrays (Fig. 11).

In addition to these changes, some neurones contained abnormal accumulations of approximately parallel smooth membranes. These varied greatly in size and complexity from

almost linear arrangements containing only a few membranes (Fig. 11), to complex stacks and whorls containing many (Fig. 12). The membranes in these stacks appeared to be doubled, in the form of flattened cisternae. They occurred most commonly at the periphery of the cell, although not closely related to the cell membrane. In one cell from a case of three days duration they were found distributed in the cytoplasm in the area, concentric with the nucleus, in which Golgi complexes are normally found (Fig. 13). No Golgi complexes were visible in this cell. These stacks were not found in every cell which showed the other cytoplasmic changes, and their origin is unknown.

Membrane-bound accumulations of glycogen granules are observed in some cells (Fig. 14); some were single membrane structures, probably autophagic vacuoles, others have a double membrane and may represent degenerating mitochondria. They were occasionally associated with membranous stacks. These were an infrequent occurrence, the significance of which is unknown.

In cases of longer duration, the cytoplasm contained a greatly increased number of relatively normal mitochondria (Fig. 15). Lysosomes and a variety of vacuoles were also numerous and the remaining cytoplasm was filled with SER, neurotubules and filaments.

Very large membrane bound accumulations of floccular material were seen round the periphery of a few cells in cases of more than a week's duration. No normal cellular features could be identified in these degenerating neurones (Fig. 16).

The neurones of the chronic case were less rounded and

regular than normal, the nuclei were frequently eccentric and the nuclear envelope slightly crenated (Fig. 17). In the recovered cat, the nuclei and the perikarya tended to be a more normal rounded shape (Fig. 18). The nucleoli in both cases appeared normal, and the cytoplasmic findings in these two cats were very similar (Figs. 17-19).

Normal cisternae of RER with their associated ribosomes were present, well-distributed throughout the cytoplasm, predominantly in discrete Nissl granules. Golgi complexes, although present, were much less prominent than normal, and greatly diminished in number. Those that were present, however, appeared relatively normal although some cisternae appeared dilated in places. Mitochondria, lysosomes, neurotubules and filaments appeared normal.

The cytoplasm also contained numerous small 'cleared' areas which consisted only of a sparse, fine reticular structure, where any was visible. These areas were not obviously bound, and occurred most frequently, but not exclusively, in association with areas of RER (Fig. 19). The possibility that these are artefactual cannot be discounted, but both long-standing cases demonstrated these changes, which were not seen in any of the other routinely-handled cases.

Affected peripheral autonomic neurones, equine

A wide range of ultrastructural changes was seen in affected equine autonomic ganglia, the greatest variation of lesion being seen in a horse that was shot 20 hours after the appearance of clinical signs.

A few neurones appeared normal. Crenation of the nuclear envelope was the only consistent nuclear abnormality, and in severely affected cells the nucleus was eccentric and pyknotic.

The first cytoplasmic change to occur appeared to be a dispersion of the Nissl substance throughout the cytoplasm (Fig. 20), which was followed by a loss of volume of this dispersed RER, accompanied by disappearance of the Golgi complex and an increase in the numbers of mitochondria (Fig. 21). Occasional small, smooth, membrane-bound vacuoles were also seen in these cells.

An increase in the number of mitochondria was also suspected on visual inspection of some neurones with Golgi complexes and relatively normal RER, but this was not quantified. Increased numbers of mitochondria were not a ubiquitous feature of abnormal neurones.

More severely affected cells had accumulations of distended cisternae, filled with electron-dense floccular material, the great majority of which were found in an area of cytoplasm at the periphery of the cell (Fig. 22), which was often sharply demarcated from the central portions (Fig. 23). This area contained, and the rest of the cytoplasm consisted of, numerous vesiculo-tubular profiles of SER, neurotubules and filaments. Mitochondria and lysosomes were also present in variable numbers. No Golgi complexes were present, and no normal RER remained.

In very severely affected cells, numerous vacuoles were found in the peripheral region together with the cisternae described above. Vacuoles also occurred in more central areas of the cytoplasm, but they tended to be fewer in number and smaller

than those in the periphery (Fig. 24).

The central areas also contained mitochondria and numerous smooth membranous profiles, but cytoplasmic detail was indistinct in these neurones.

The membranous stacks found in feline autonomic neurones were not seen in horses, but one small structure of apparently similar morphology was found in a neurone which had relatively normal-looking cytoplasm (Fig. 25).

MATERIALS AND METHODS : XII NUCLEUS, FELINE

Five dysautonomic cats which had been ill for less than 14 days, and three non-dysautonomic cats were studied.

Each cat received 1500 units of intravenous heparin sodium (Evans) prior to induction of anaesthesia by intravenous thiopentone. Anaesthesia was maintained by O₂, N₂O and halothane administered by a respiratory pump via an endotracheal tube.

The aorta was cannulated and the cats killed by perfusion with mixed aldehydes in 0.08M sodium cacodylate buffer as described in detail in Appendix 4.

The brain was removed entire, and further fixed by immersion in 2.5% glutaraldehyde in 0.025M sodium cacodylate buffer for a variable period of not less than 48 hours. It was then halved along its midline, and selected areas from one side processed for ultrastructure examination.

Using a razor blade, 8-10 transverse sections approximately 1mm thick were cut through the brainstem by hand, working rostrally from an initial cut approximately at the caudal border of the cerebellum (Fig. 26). These sections were then trimmed

(Fig. 27) to leave only the dorsomedial region of the brainstem which contained the neurones of the XII nucleus.

The resulting blocks were post-fixed for 1-2 hours in 1% osmium tetroxide and processed through graded alcohols and propylene oxide as described in Appendix 1 prior to embedding in an Araldite-based resin.

One micrometre sections, stained with methylene blue, were used to select the best areas for ultrastructural examination. Thin sections of 60-80nm were cut on a Reichert OmU3 ultratome, supported on copper grids, stained with Reynolds lead citrate and uranyl acetate (Appendix 2) and examined in a Philips 301 electron microscope.

RESULTS : XII NUCLEUS, FELINE

Normal

The perikarya of neurones within the normal XII nucleus were large and multipolar, with organelles well-dispersed throughout the cytoplasm. They had a prominent round or oval nucleus, with pale-staining karyoplasm containing a variety of randomly distributed granules. The nucleolus was usually round and had a typical "honeycomb" appearance (Fig. 28).

The Nissl granules - discrete stacks of 3-12 flattened, approximately parallel cisternae of rough endoplasmic reticulum (RER) - were distributed throughout the cytoplasm occurring more frequently close to the nucleus, and rarely associated with the cell membrane (Fig. 29). SER tended to occur as isolated single cisternae not always associated with the RER.

The prominent Golgi complexes were concentric with the nucleus, though not closely related to it or the cell membrane,

and were associated with many coated and non-coated vesicles, particularly on the "trans" side.

Numerous mitochondria of a fairly uniform appearance were evenly distributed throughout the cytoplasm, being found most frequently in those areas not occupied by the other large organelles. They were, however, occasionally seen within an area of RER (Fig. 30).

Several "dense bodies" and occasional multivesicular bodies were found, and the cytoplasm also contained numerous neurotubules and filaments which were orientated approximately along the long axes of the cells' dendrites.

In the dendrites, neurotubules and neurofilaments were the most prominent organelles, although all other organelles could be found proximally, mitochondria occurring with the greatest frequency (Fig. 31).

Affected

A proportion of the neurones in the XII nucleus remained ultrastructurally normal in all affected cats. Abnormal neurones also had large multipolar perikarya with prominent nuclei, most of which appeared normal, although some showed slight crenations of the nuclear envelope, and ring nucleoli were occasionally seen (Fig. 32).

The Nissl substance showed a great variety of changes. In the earliest case examined (three days after onset) the only abnormality seen in some neurones was an unusual distribution of the RER. Individual cisternae with ribosomes attached were no longer arranged into discrete "granules", but were more dispersed

throughout the cytoplasm, surrounding other organelles, and not distinct at low magnifications (Fig. 33).

In slightly later cases, (i.e. 3-6 days duration) the changes in the RER became much more pronounced, with no normal cisternae visible. Instead the cytoplasm was filled with numerous distended cisternae containing an electron-dense floccular material. The presence of occasional ribosomes adherent to the membranes of these cisternae indicated their origins in the RER (Fig. 34).

Other neurones in these cases showed no evidence of any RER, but had a great increase in the number of SER profiles. This was very pronounced in a case of two weeks clinical duration, where some neurones and dendrites were packed with proliferated SER, slender mitochondria, multivesicular bodies and lysosomes being the only other recognisable organelles (Fig. 35). Degenerating "ghost" cells contained only smooth membranous profiles, and vacuoles, with occasional lysosomes and mitochondria.

The Golgi complex was also very severely affected. It appeared normal in some cells in which the only abnormality was a dispersion of otherwise unchanged RER, but in all other affected cells no Golgi complexes, either normal or abnormal, could be recognised.

Mitochondrial numbers were perhaps increased in early cases and definitely increased in lesions of longer duration, where individual mitochondria appeared to be more slender than those in normal neurones.

With the exception of the earliest case, there was an increased number of lysosomes (many of which showed secondary

activity) in most affected neurones. Multivesicular bodies and autophagic vacuoles were also seen. Neurofilaments and neurotubules appeared normal in all the cases examined.

MATERIALS AND METHODS : OTHER NEURONAL POPULATIONS

In addition to the areas of the nervous system already described in this chapter, paraffin sections were examined from the brainstem, spinal cord and dorsal root ganglia of the cats (details previously given, page 37) and the dog which had been ill for eight days. The spinal cord and dorsal root ganglia of the chronically affected dog were also available.

The distribution of neuronal damage found in the cats was subsequently combined with data from a previous study (Pollin, 1985). The results from these cats and dogs were then tabulated, together with data from the literature on the lesion distributions in EGS, to enable a direct comparison in the three species.

Dorsal root ganglia and spinal cord samples from those cats which were perfusion-fixed were also taken for ultrastructural examination.

Blocks not exceeding 2mm^3 were cut from the DRG and further fixed by immersion in 2.5% glutaraldehyde in 0.08M sodium cacodylate buffer for not less than 48 hours.

The spinal cord was removed entire from each animal and further fixed under slight longitudinal tension by suspension in a measuring cylinder of fixative (as above) with a small weight attached to the dependent end.

Using a razor blade, 3-4 transverse sections approximately

1mm thick were cut by hand from the mid-cervical and mid-lumbar regions of the spinal cord. Under a dissection microscope these slices were then trimmed to leave only the ventral horn on either side of the cord. The resulting 6-8 blocks were processed collectively as 'cervical ventral horn' or 'lumbar ventral horn'.

All samples for electron-microscopic examination were post-fixed in 1% osmium tetroxide, dehydrated, embedded in Araldite, sectioned, stained and examined in a Philips 301 electron microscope (Appendices 1 and 2).

RESULTS : OTHER NEURONAL POPULATIONS

The peripheral autonomic region of the nervous system is the only area to be consistently involved in dysautonomia. Non-autonomic ganglion and ventral horn neurones were involved in some cases and specific brainstem nuclei, not all of which are autonomic, may also contain neurones demonstrating the typical 'chromatolytic' appearance described earlier (Table 1). Not all of these regions were necessarily affected in each animal.

Dorsal root ganglia and ventral horn cells were examined ultrastructurally.

Dorsal root ganglia : normal

At light microscopic level, two main neuronal populations can be seen, the large light neurones and the small dark ones. The main difference between these populations is their nuclear to cytoplasmic volume ratio.

Workers investigating rodent DRG have subdivided these categories into six or seven distinct populations using ultrastructural and histochemical methods, and these are discussed in more detail elsewhere in this thesis.

For the purpose of this study, only the two major categories were considered.

The general ultrastructural appearance of the DRG neurone was very similar to that of the other neuronal perikarya described in this chapter.

The nucleus was large, round and prominent with a typical 'honeycomb' nucleolus. The cytoplasm contained much RER, arranged into discrete Nissl granules of varying size. Small single profiles of SER were occasionally found, usually, but not always, associated with the RER. The Golgi complexes were numerous and had the usual configuration of approximately 4-5 curved, parallel cisternae with numerous vesicles, associated particularly with the 'trans' side. Mitochondria had a well-defined internal cristal pattern, and the lysosomes were very dense.

In some large light DRG neurones these organelles were separated by very prominent bands of neurofilaments and tubules (mostly filaments) (Fig. 36).

Affected

As can be seen from Table 1, DRG were not affected in every animal, and where chromatolytic neurones were visible they formed only a small percentage of the total neuronal population. Small dark neurones appeared predominantly affected in paraffin sections.

At ultrastructural level however, slight changes were found in a much greater number of neurones than anticipated (approximately 50%), which were unlikely to be detectable at

light microscopic level in either paraffin or plastic sections. Both neuronal populations were equally involved.

No consistent nuclear abnormalities occurred, although a small ring nucleolus was seen (Fig. 37). In occasional cells, Golgi complexes were difficult to find and were possibly reduced in number. Mitochondria and lysosomes were normal.

The one specific abnormality identifiable in these cells was the occurrence of long, fairly straight smooth membranes which on close inspection appeared to be very flattened cisternae. In some cases, one of the membranes was thicker and more dense than the other (Figs. 37 and 38). They were associated with the RER, most of which looked normal and was still arranged into discrete Nissl granules. In a few cells however, these Nissl granules appeared less dense than usual and no normal rough cisternae were seen; instead numerous clumps of ribosomes were associated with many small, smooth membranous 'vesicles' (Fig. 38).

Occasional neurones showed a much more marked disruption of the normal cellular architecture. RER was dispersed throughout the cytoplasm, and numerous small vesicles were associated with the remaining ribosomes. Normal mitochondria were greatly increased in number and Golgi complexes could not be seen (Fig. 39).

Ventral Horn Cells

Like DRG, very few of these neurones appeared to be affected when assessed at light microscopic level. Unlike DRG, this low incidence of abnormality was also found ultrastructurally.

Normal

The normal structure of the ventral horn cell was essentially similar to the other neuronal types described earlier with a large, prominent nucleus, abundant Nissl granules, frequent Golgi complexes and numerous mitochondria and dense lysosomes distributed throughout the cytoplasm in their usual relationships to one another (Fig. 40).

Affected

In affected cells, normal RER and Golgi complexes could not be found. Mitochondria were greatly increased in number in some neurones, and SER profiles were common (Fig. 41).

Distension of the RER by electron-dense floccular material, very similar to that seen in autonomic and XII nucleus neurones, was also seen in the ventral horn cells, ribosomes adherent to these cisternae confirming their origins (Figs. 42 and 43).

Additional Finding

A grid prepared for examination of the XII nucleus from a cat of 13 days duration included some neurones from the region of the dorsal nucleus of the vagus. One of these neurones had markedly disrupted cytoplasm. That part of the cell which was visible contained numerous vesicles, vacuoles and distended cisternae, in addition to which there was a large stack of parallel smooth membranes apparently identical to those seen in some affected autonomic neurones (Fig. 44).

DISCUSSION

The earliest lesion examined in feline autonomic neurones (3 days) already involves pronounced cytoplasmic change, and is of little value in elucidating the evolution of degeneration within

the cell. The early changes in feline XII nucleus and equine autonomic ganglia are much more informative, there being a greater spectrum of damage within these neuronal populations.

Golgi complexes are rarely present in any cell showing signs of a disturbance in the normal pattern of RER, and slight alterations in RER density and distribution are the only abnormalities present in cells where the Golgi complexes are still visible. The distension of RER cisternae or marked disruption of this organelle, typical of the more advanced lesion, is never seen in neurones with normal Golgi complexes.

In those few neurones with no Golgi complexes and little other cytoplasmic change, no structures can be found which might be abnormal Golgi complexes, or derived from them. This would suggest that the earliest morphological change involves the distribution of RER, but is rapidly followed by loss of the Golgi complex.

Although RER, or structures derived from it, are severely affected in some cases, it can still be identified. This is not the case with the Golgi complex. The membranous stacks found in some peripheral autonomic neurones in diseased cats bear several similarities to the Golgi complex, consisting of smooth, flattened cisternae with slightly dilated ends which may, very occasionally, be in a similar cytoplasmic orientation to the absent Golgi complexes. They occur, however, only in a single neuronal population in one species and, even then, not in every affected cell. Their appearance is certainly not a consistent sequel to Golgi loss.

In many cells, however, the typical Golgi loss is not accompanied by the consistent appearance of any identifiable structure. The possible origins of the membranous stacks and the fate of the Golgi complex are further investigated and discussed later.

Despite this apparent anomaly between the lesion in feline peripheral autonomic neurones and other neuronal populations, all the other changes of RER disruption, generalised proliferation of SER, nuclear and nucleolar changes and the relative normality of lysosomes and mitochondria suggest that dysautonomia in the horse and the cat is very similar.

A major drawback in the investigation of conditions such as dysautonomia is the inability to reproduce the disease experimentally and therefore examine the pathogenesis more completely. Reliance on clinical material has a tendency to confine available material to two main categories - the acute early cases and the chronically ill - with little access to the intermediate stages of disease, or recovered cases. Material was available from one chronically ill and one recovered cat in this study, and the findings in these cases were interestingly similar, with relatively normal RER, small Golgi complexes greatly diminished in number but generally looking normal, and no abnormalities apparent in the other organelles. Without examining further cases after a shorter illness, it cannot be stated whether these neurones were ever markedly disrupted and have 'recovered', or whether they were only mildly, or not, affected and 'survived' in that condition throughout the course of the disease. The presence of the small "cleared" areas is not

readily explained, however. The similar changes in the neighbouring satellite cell in Fig. 19 would suggest that this is most likely artefactual change, but the mitochondria, usually very sensitive to fixation artefact, are only slightly "blown", and similar changes have not been observed in more acute cases.

Conclusions cannot be drawn until either more cases have been reported with similar changes, or an experimental model enables the serial monitoring of changes from the acute stages, through to 'recovery', enabling the origin of these 'patches' to be defined, if indeed they are a genuine change.

The appearance of the cytoplasm in the chronically-ill and "recovered" cats is closely comparable, suggesting that the function of these neurones will also be similar. The very marked differences in the clinical appearance of the two animals can only be accounted for, therefore, by the fact that the 'recovered' cat had considerably more neurones remaining than the chronically ill animal.

The strong similarities between dysautonomias in the various species extends beyond the morphological changes themselves to the distribution of these changes within the nervous system. Damage within the nervous system is very specific, unique to this disease, and its distribution has not yet been fully explained. While the autonomic and brainstem neurones all have connections with the alimentary tract, this is very tenuous in the case of the ciliary ganglion (Gilmour, 1973b; Pollin, 1985) and does not include the neurones of the ventral horn, for example. In addition, while autonomic neurones are the only ones consistently

affected not all autonomic regions are involved, nor are all affected areas autonomic.

It has still not been shown whether all the clinical signs arise as a result of this neuronal damage, or whether gut stasis occurs primarily, and allows retrograde transportation of the causal agent(s) from the gut. This latter theory would only explain damage in those areas with direct connections to the alimentary tract.

There is some reported evidence which suggests that the perikaryal damage might be secondary to an axonal lesion. Formaldehyde-induced fluorescence (identified as noradrenaline (NA)) was absent from ganglion cells of both normal and affected horses, but present in the nerve-fibre tracts of the ganglia in 75% of EGS cases (Gilmour, 1976). Decreasing fluorescence with extended clinical duration was suspected but not quantified. By comparison with experimental axonal ligation in cats and rats, this author proposed that NA accumulation in EGS demonstrated by this fluorescence represents primary morphological damage to the axons as opposed to the perikarya.

The loss of vesicles from enteric nerves and subsequent reduction of immunofluorescent staining for neuropeptides (as described earlier) could be accounted for either by this accumulation of transmitter within the axon, or a cessation of production at perikaryal level. However, while peptide losses were similar in cats and horses, degeneration of enteric neurones is reported to be marked in horses (Hodson *et al.*, 1982) but only a few abnormal neurones could be found in cats (Vaillant, 1987).

Obel (1955) who first described the ganglionic lesions was

satisfied that they explain the clinical course, and the diagnostic significance of myenteric plexus degeneration has been questioned by Gilmour (1973b) who maintains that these changes are not uncommonly a feature of equine intestinal disorders. He also suggests that neuronal degeneration occurs coincidentally with or preceding the alimentary signs of EGS, but points out that to establish this as fact, much further work needs to be done.

The great majority of authors are therefore in agreement that the perikaryal changes are of primary significance in the pathogenesis of dysautonomias and this will be discussed more fully in the General Discussion.

An apparent anomaly arises however, when the work by Gilmour (1973a) regarding the transmission of EGS is considered. By intraperitoneal injection of "acute phase serum" from clinical cases of EGS into experimental ponies, he produced apparently "classic" chromatolytic neurones in the autonomic ganglia. The ponies however, remained clinically normal throughout. It has been clearly shown that ultrastructural examination of tissue reveals differences not visible by light microscopy, and it is unfortunate that this was not carried out on these ganglia. It might be the case that the neuronal damage produced by this method is not, in fact, the result of transmission of a specific disease process but instead non-specific neuronal damage as a result of some abnormal component of affected serum, for example a non-specific anti-autonomic-neurone-antibody arising from the damaged neurones in the diseased horses.

Regardless of the cause of this damage, however, it is still difficult to reconcile the fact that these apparently severely damaged autonomic neurones failed to result in any clinical problems in these ponies.

The clinical signs in dysautonomia can be interpreted in terms of the lesions described in this study. Autonomic neurones are the most consistently and severely affected neurones, and autonomic signs predominate clinically. While lesions frequently occur in areas such as the XII nucleus and ventral horn cells with no apparently referable clinical signs, it must be taken into consideration that the proportion of cells affected is fewer, and the apparent spectrum of lesions greater in these regions, thus reducing further the total number of severely disrupted neurones. The activity of the less affected neurones may be sufficient to maintain the overall functioning of the system despite individual neuronal deficits. In the small number of cats which show dysphagia or mild proprioceptive deficits this could be attributable to the damage in these areas being more severe than average.

The perikaryal changes reported in this chapter are therefore considered to be the primary lesion in dysautonomia, and the possible precise location of the damage within the glycoprotein synthetic pathway is fully discussed in the General Discussion.

TABLE 1

SUMMARY OF DISTRIBUTION OF NEURONAL DAMAGE IN DYSAUTONOMIAS

AREA	Neuronal Lesions Present (% Cases)			Proportion of Cells Involved (d)		
	Cat (a)	Horse (b)	Dog (c)	Cat	Horse	Dog
Autonomic Ganglia	100	100	100	+++	+++	+++
Non-Autonomic Ganglia	50	83	50	+	+	+
Spinal Cord	62	91	50	+	++	+
Brainstem Nuclei						
XII	66	40*	100	+++	++	+++
X (DNV)	69	20*	100	+++	++	+++
VII	51	78	100	++	++	++
VI	-	NA	100	-	NA	++
V	47	NA	100	++	NA	+
III	25	97	100	++	++	+
Nucleus Ambiguus	40	NA	100	++	NA	++
Lateral Vestibular Nucleus	-	60*	-	-	+	-

NA - information regarding these areas was not available.

* - see (b)

(a) - Data from present study, Sharp et al (1984) and Pollin (1985)

(b) - Data from Barlow (1969) and Gilmore (1973b) combined (40 horses) except figures marked* - these from Barlow (1969) only (5 horses)

(c) - Data for autonomic ganglia and spinal cord - 2 cases; brainstem, 1 case.

(d) - Some variation occurred between individual cases; these cases are average semi-quantitative assessments:-

+++ - many affected cells

++ - several affected cells

+ - occasional affected cells

Figures I - 44

Figure 1

(a) Stellate ganglion, normal cat

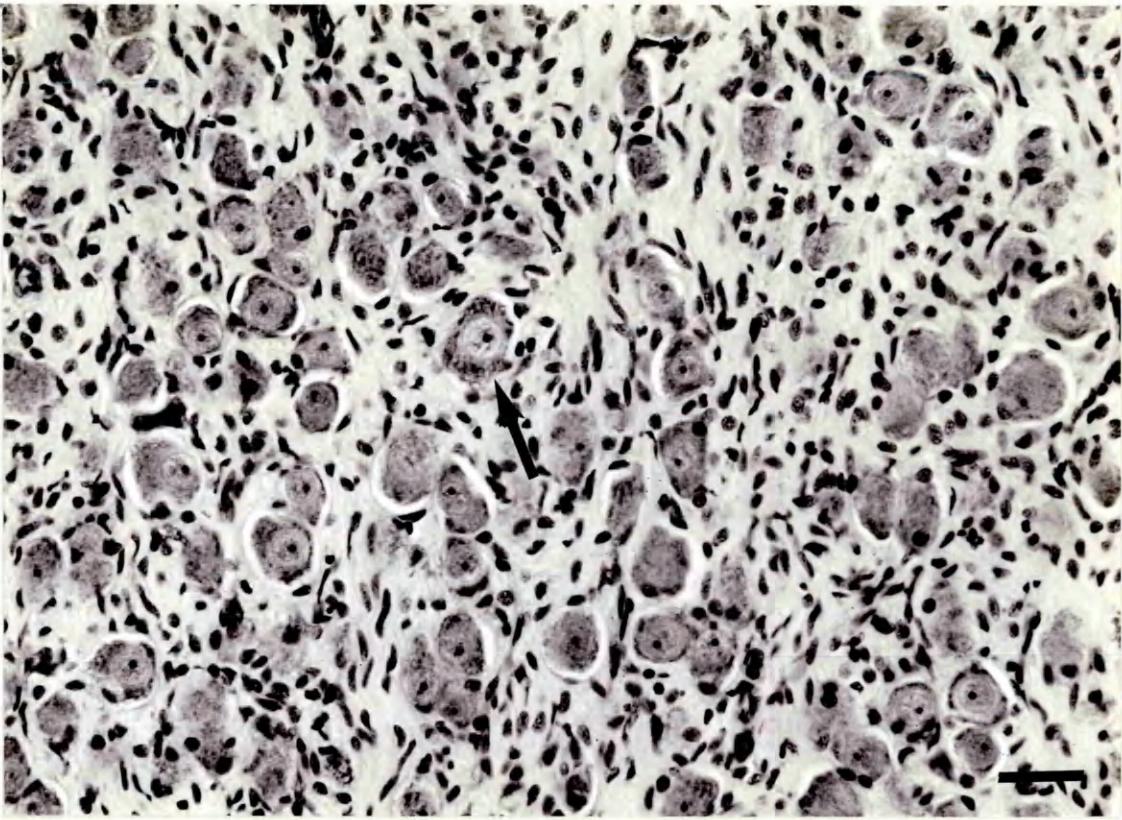
Normal autonomic neurones (arrow) are rounded with large, centrally placed, prominent nuclei and basophilic granular cytoplasm. The numerous smaller dark nuclei of the non-neuronal cell population can also be seen. H & E.

(b) Stellate ganglion, affected cat (5 days duration)

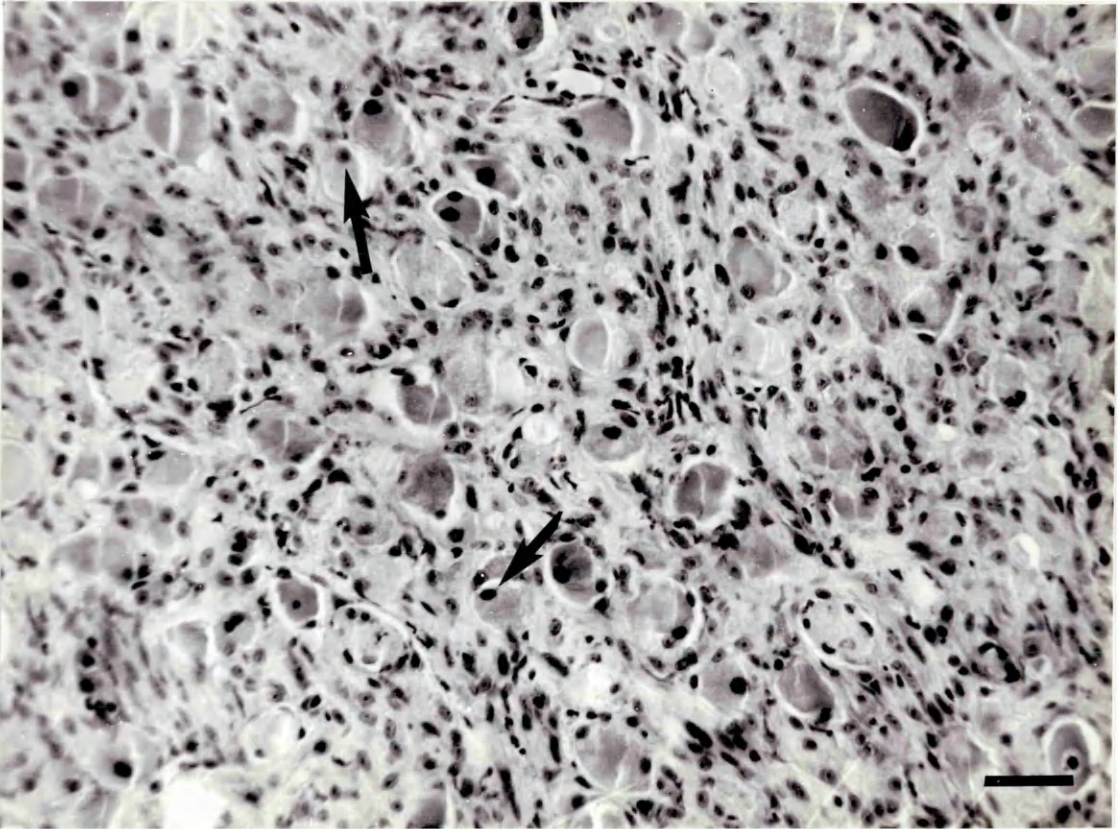
The non-neuronal nuclei are unchanged, but the neuronal perikarya have lost their granular appearance and are homogenously pale-staining. The neuronal nuclei are pyknotic and eccentric (arrows). H & E.

(a) Bar = 20 μ m.

(b) Bar = 20 μ m.



a



b

Figure 2

Affected neurones, coeliacomesenteric ganglion, dog

(8 days duration)

Note the rounded, swollen appearance of the abnormal pale-staining perikarya (*) and the eccentric, pyknotic nucleus (arrow) as compared to the rough, basophilic cytoplasm and prominent nucleus of the adjacent normal neurone (arrowhead).

H & E.

Bar = 20 μ m.

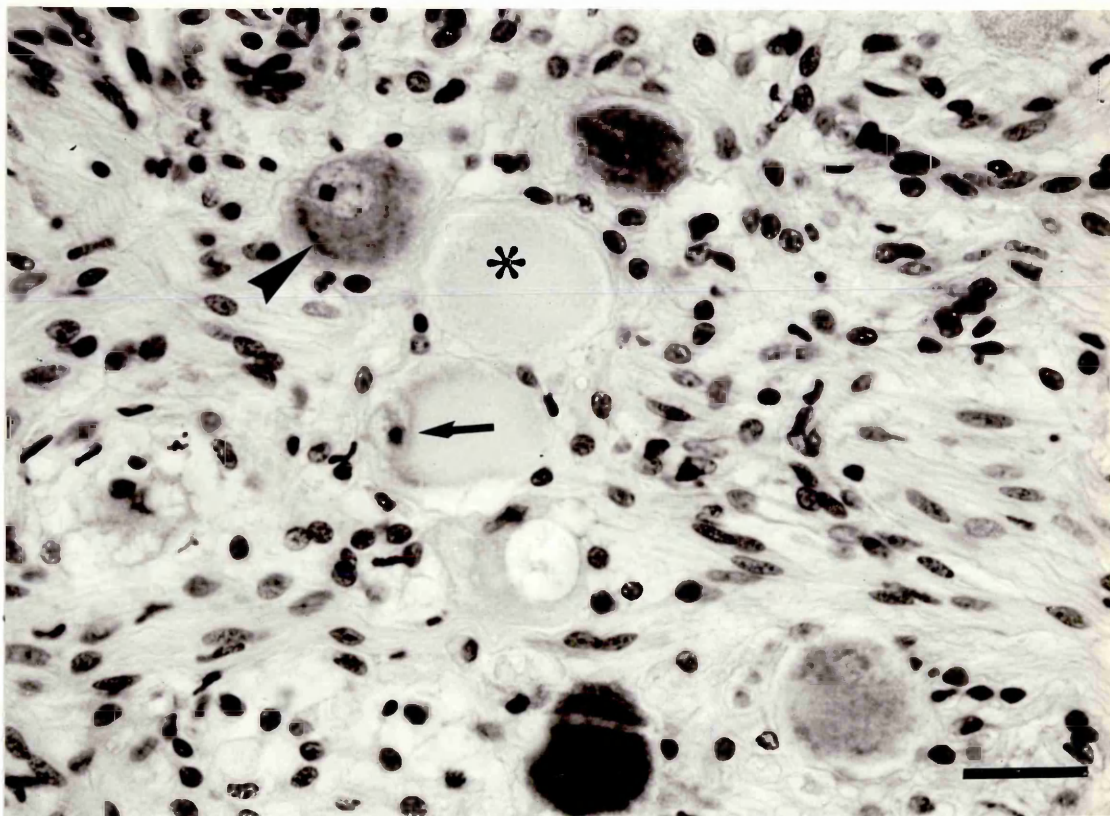


Figure 3

Stellate ganglion, affected horse (20 hours duration)

The pale-staining "chromatolytic" neurones occur apparently at random amongst the granular, basophilic normal neurones. Note also the prominent, pale nuclei of the normal neurones as compared with the shrunken, more darkly staining nuclei of the affected cells. Cresyl Violet.

Bar = 20 um.

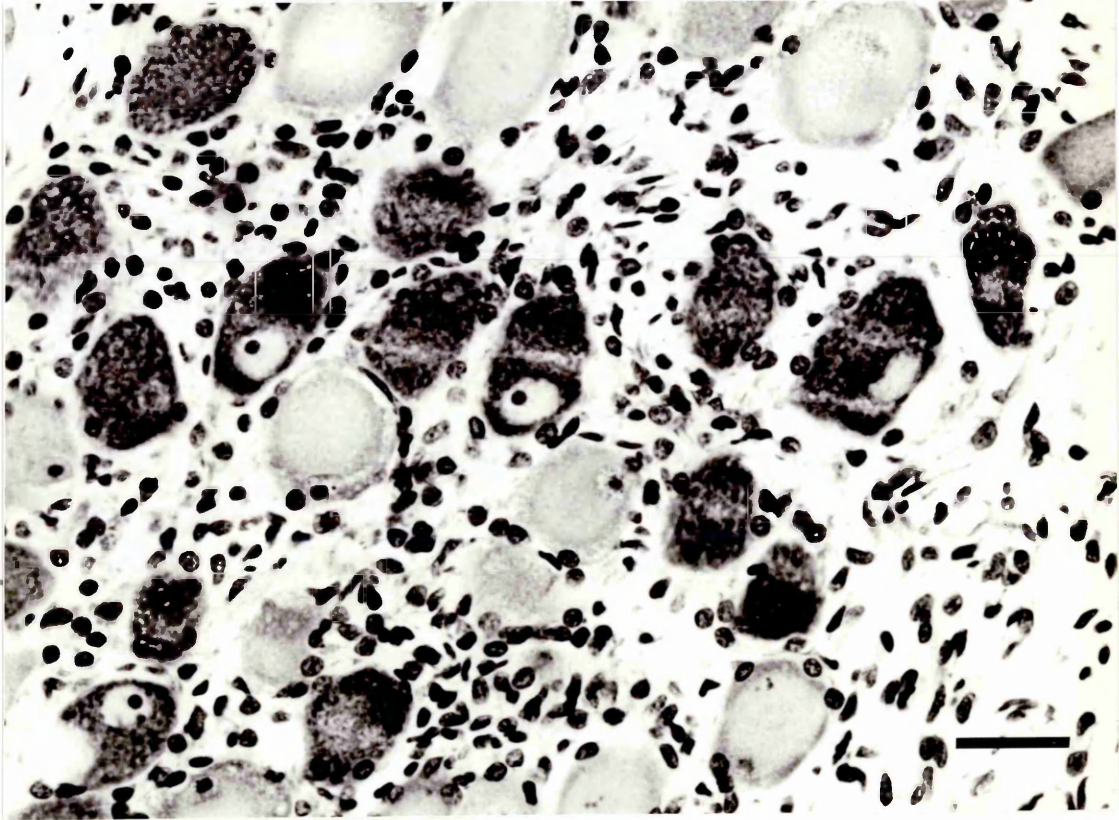


Figure 4

Stellate ganglion, affected horse (20 hours duration)

The spectrum of lesions within a ganglion can be appreciated in 1 μ m plastic sections.

Occasional neurones appear normal (arrow) with a prominent light nucleus and cytoplasmic Nissl granules. Others show loss of Nissl substance and in some perikarya there is extensive cytoplasmic vacuolation (arrowhead).

Bar = 10 μ m.

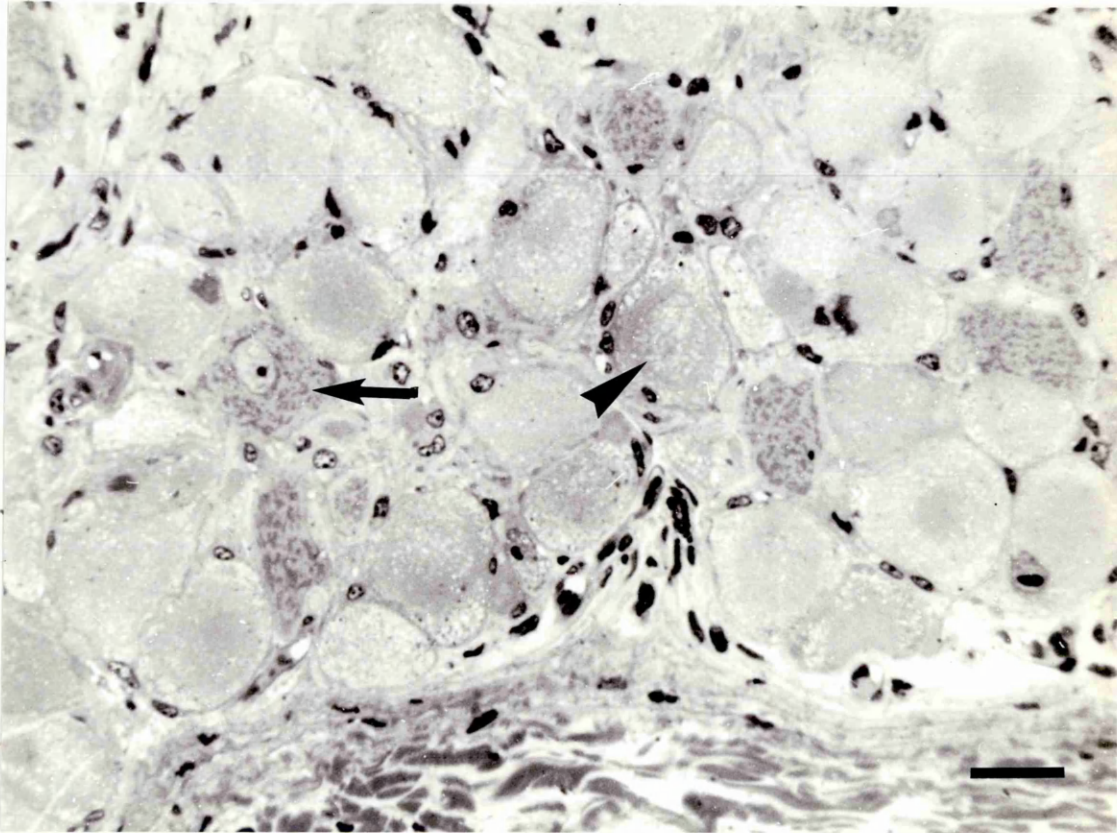


Figure 5

Normal autonomic neurone, stellate ganglion, cat

The nucleus (N) is large and circular with a prominent nucleolus. Golgi complexes (*) are frequent and found in an area of cytoplasm approximately concentric with the nucleus. The granular appearance of the cytoplasm is attributable to RER (RER), some areas of which are prominent. Numerous dense lysosomes are present, and mitochondria can be seen throughout the cytoplasm.

Bar = 2 μ m.



Figure 6

Normal cytoplasm, autonomic neurone, stellate ganglion, cat

The Golgi complex (G) consists of several approximately parallel smooth membranous cisternae in a curved configuration. Numerous coated and non-coated vesicles of various size are associated with this complex, the majority being on the 'trans' (T) rather than the 'cis' (C) side. The Golgi cisternae are closely connected with the RER (RER).

The RER forms an array of branched vesiculotubular cisternae, with ribosomes adherent to their outer surface. Areas of RER tend to be exclusive of other large organelles. Mitochondria (M) and dense-staining lysosomes (L) can be seen.

Bar = 1 μ m.

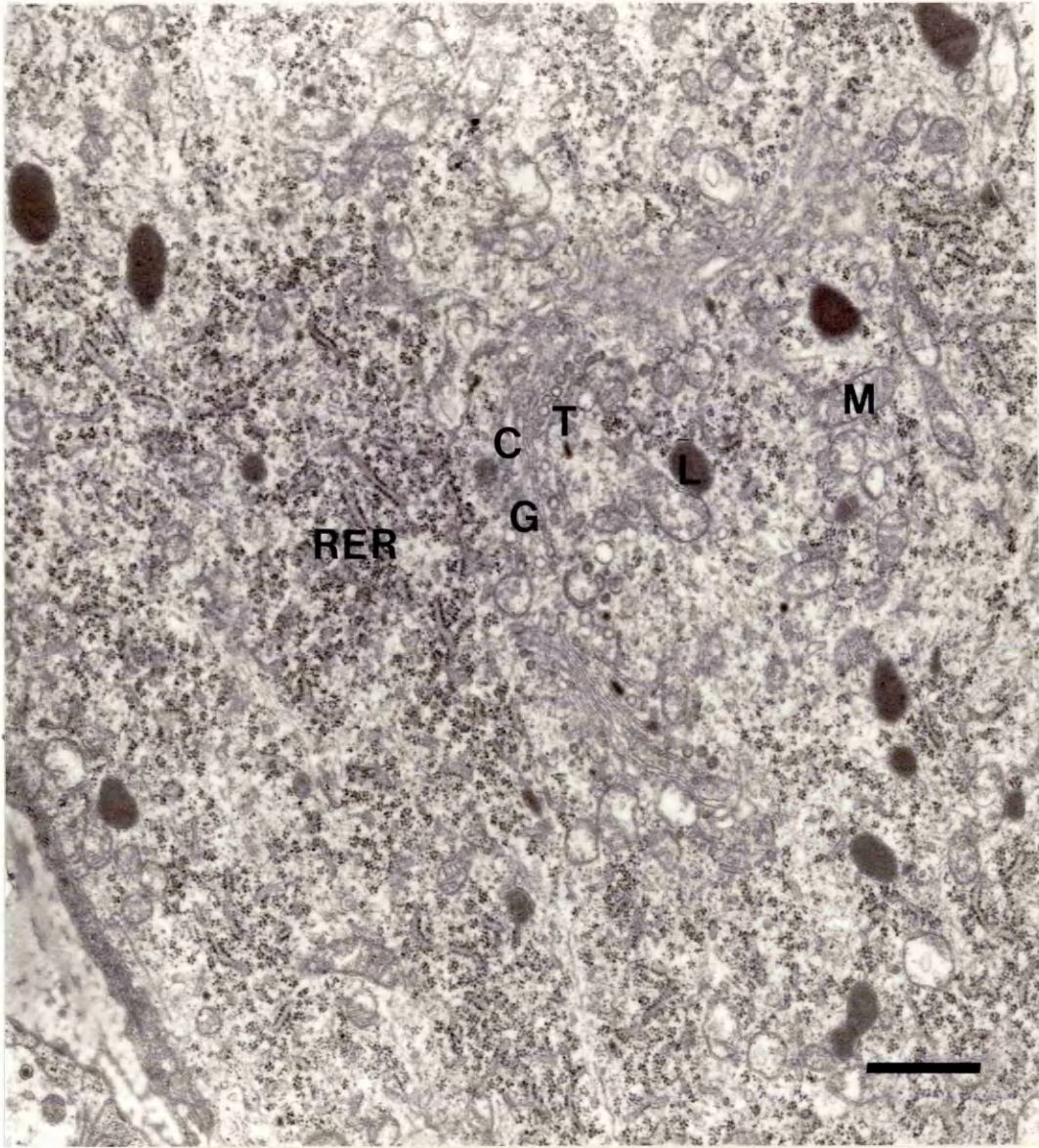


Figure 7

Normal autonomic neurone, stellate ganglion, horse

Normal neuronal features are very similar in the cat and the horse (see previous figures).

The curved stacks of Golgi cisternae (G) are prominent, and discrete areas of RER (RER), varying in size, can be found throughout the cytoplasm. Lysosomes and mitochondria are distributed at random in the perikaryon, but the occurrence of all these large organelles decreases proximal to the cell process (arrowheads).

Apart from the longitudinally oriented neurotubules and filaments, mitochondria are the only organelles occurring with any frequency in the cell process.

Bar = 2 μ m.



Figure 8

Normal autonomic neurone, stellate ganglion, horse

Golgi complexes (G) and Nissl granules (RER) are both prominent, and not closely associated with the nuclear envelope (N). Mitochondria and lysosomes are distributed throughout the cytoplasm, the remainder of which is filled with neurofilaments and tubules.

Bar = 1 μ m.

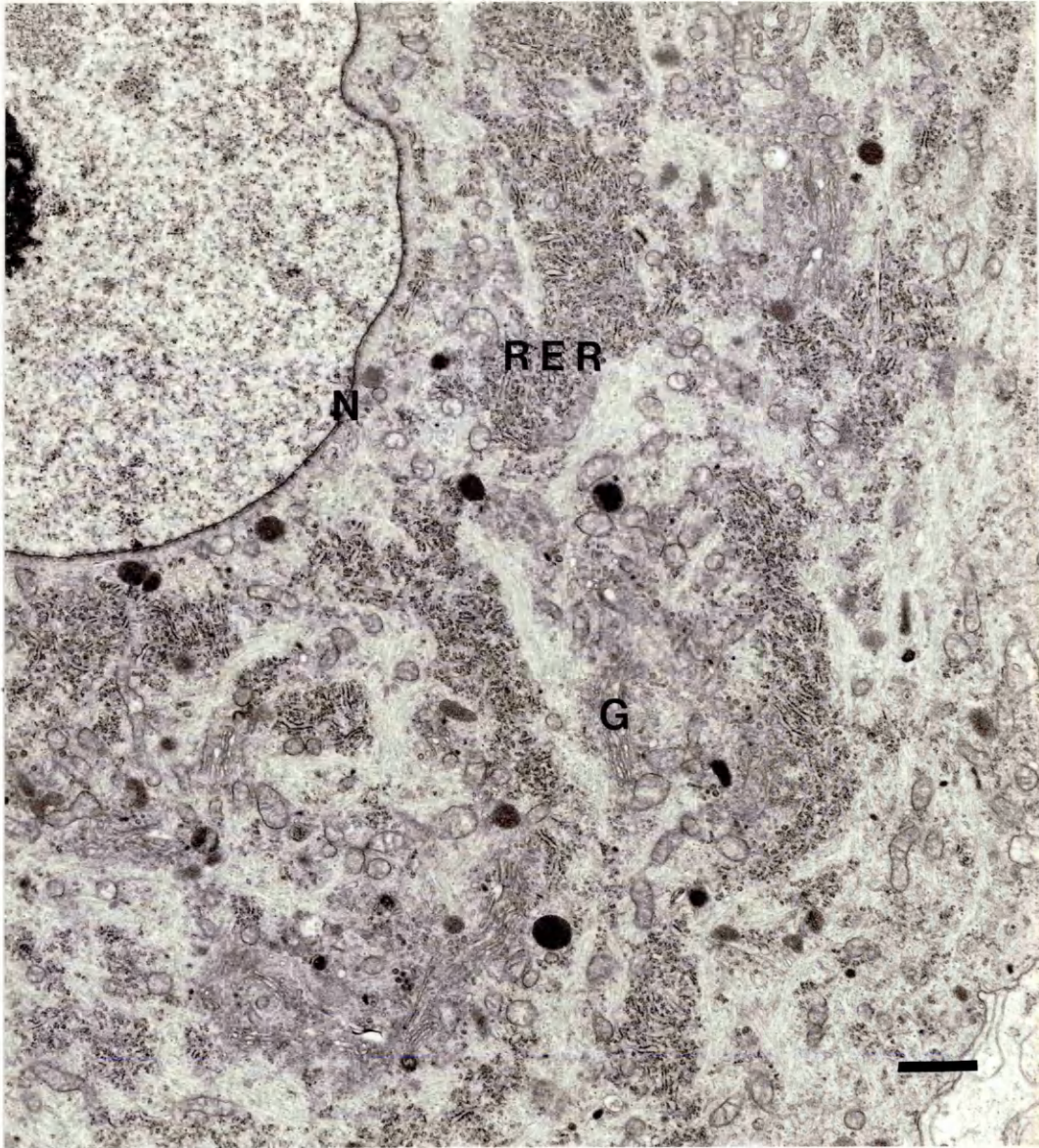


Figure 9

Nuclear abnormalities, cranial cervical ganglion, cat

(3 days duration)

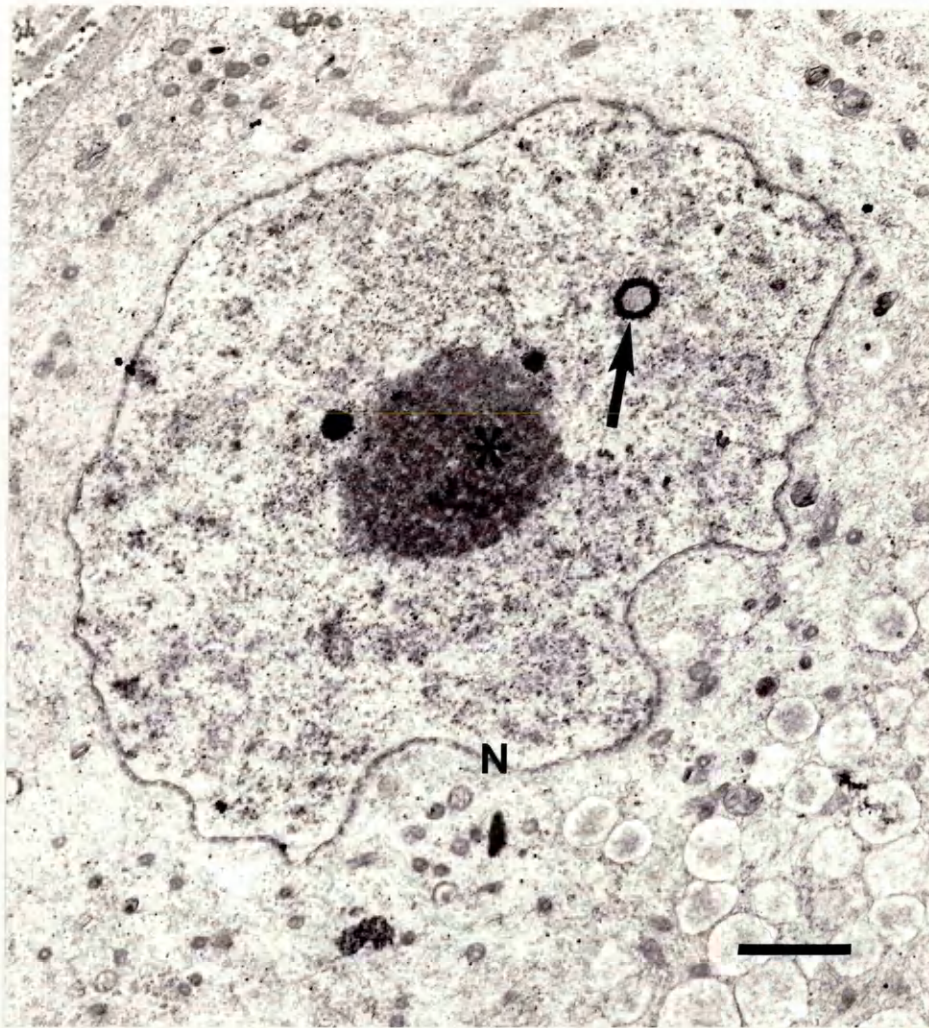
(a) The nuclear envelope (N) is crenated, and the nucleolus (*) has lost its normal well-defined "honeycomb" appearance. There is a ring nucleolus (arrow).

(b) Nucleolar morphology is indistinct (*) and an abnormal membranous structure (M) is present in the karyoplasm.

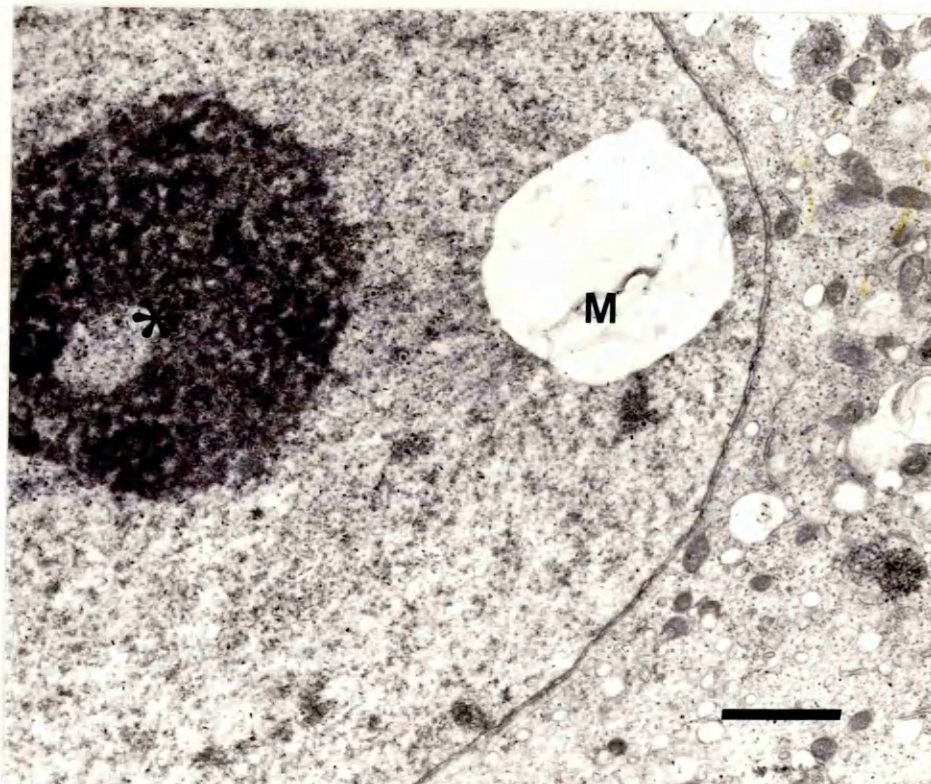
The perinuclear cisterns are not distended in either figure. None of these abnormalities occurred consistently in cells showing cytoplasmic changes.

(a) Bar = 1 μ m.

(b) Bar = 1 μ m.



a



b

Figure 10

Affected neurone, coeliacomesenteric ganglion, cat

(7 days duration)

The cytoplasm contains numerous distended cisternae (C) filled with condensed, electron-dense floccular material. Occasional ribosomes (arrows) associated with their limiting membranes indicate their origin in RER.

Smooth parallel membranes are seen accumulated into stacks (S) at the periphery of the cell, and also as single, flattened cisternae deeper in the cytoplasm (arrowhead).

Bar = 1 μ m.

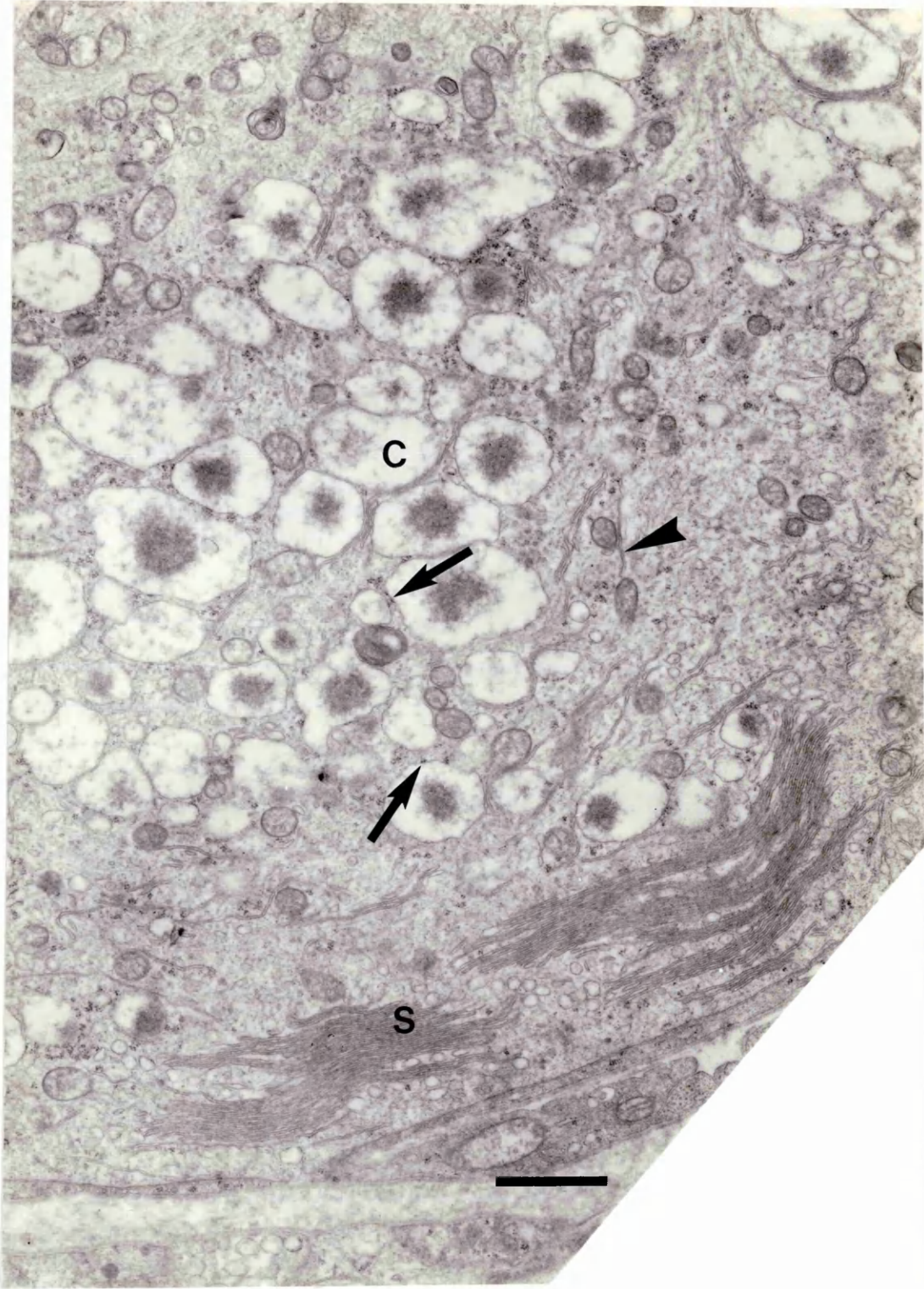


Figure 11

Affected neurone, cranial cervical ganglion, cat

(3 days duration)

The nuclear envelope (N) is crenated, and ring nucleoli (arrows) are present. The cytoplasm contains numerous SER profiles, and distended cisternae (C) containing electron-dense floccular material are seen. Occasional ribosomes are adherent to some of these cisternae (*). A few long smooth membranous profiles (arrowhead) can also be seen, oriented approximately parallel to one another. The few mitochondria present (M) appear normal.

Bar = 1 μ m.

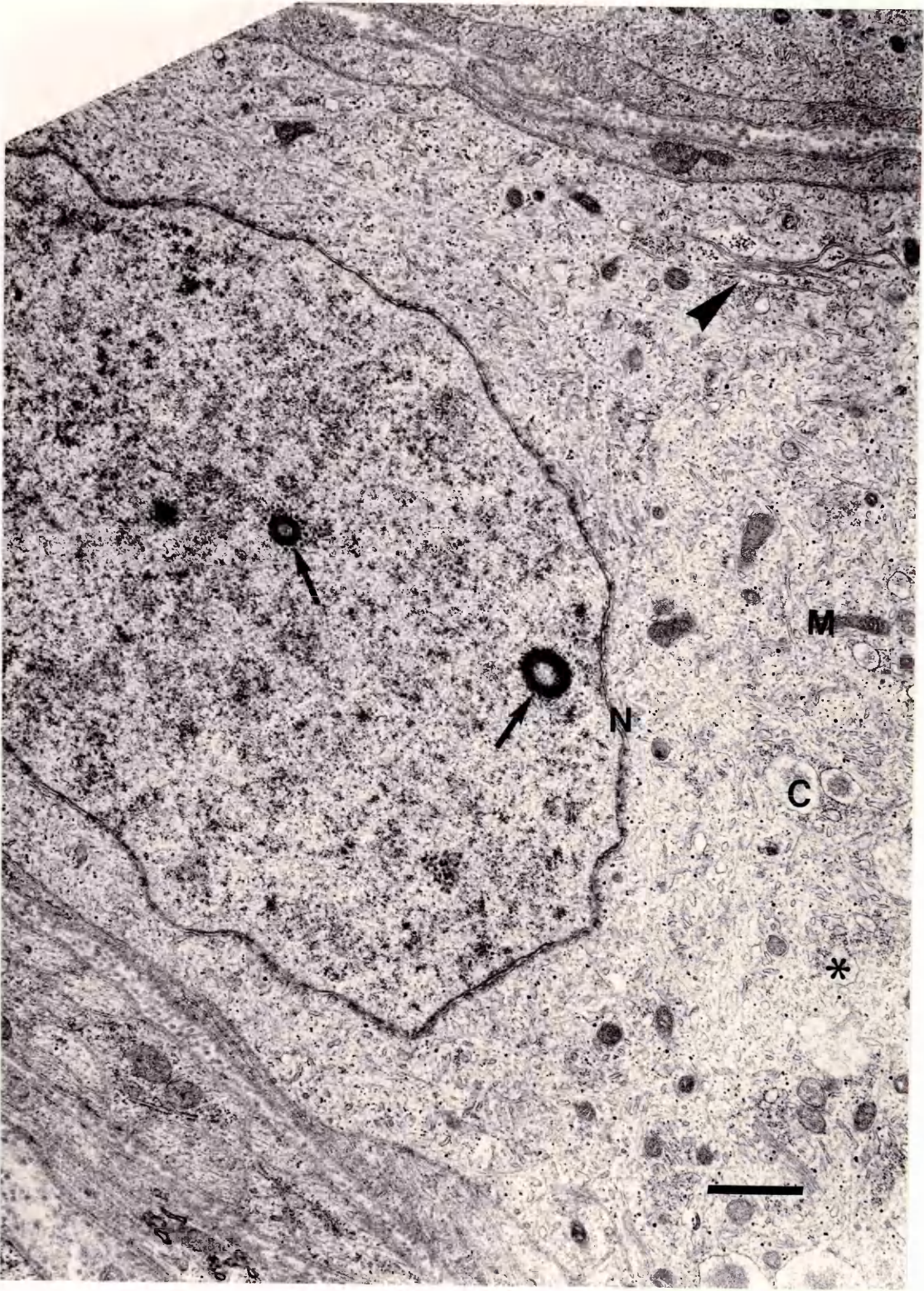


Figure 12

Affected neurones, coeliacomesenteric ganglion, cat

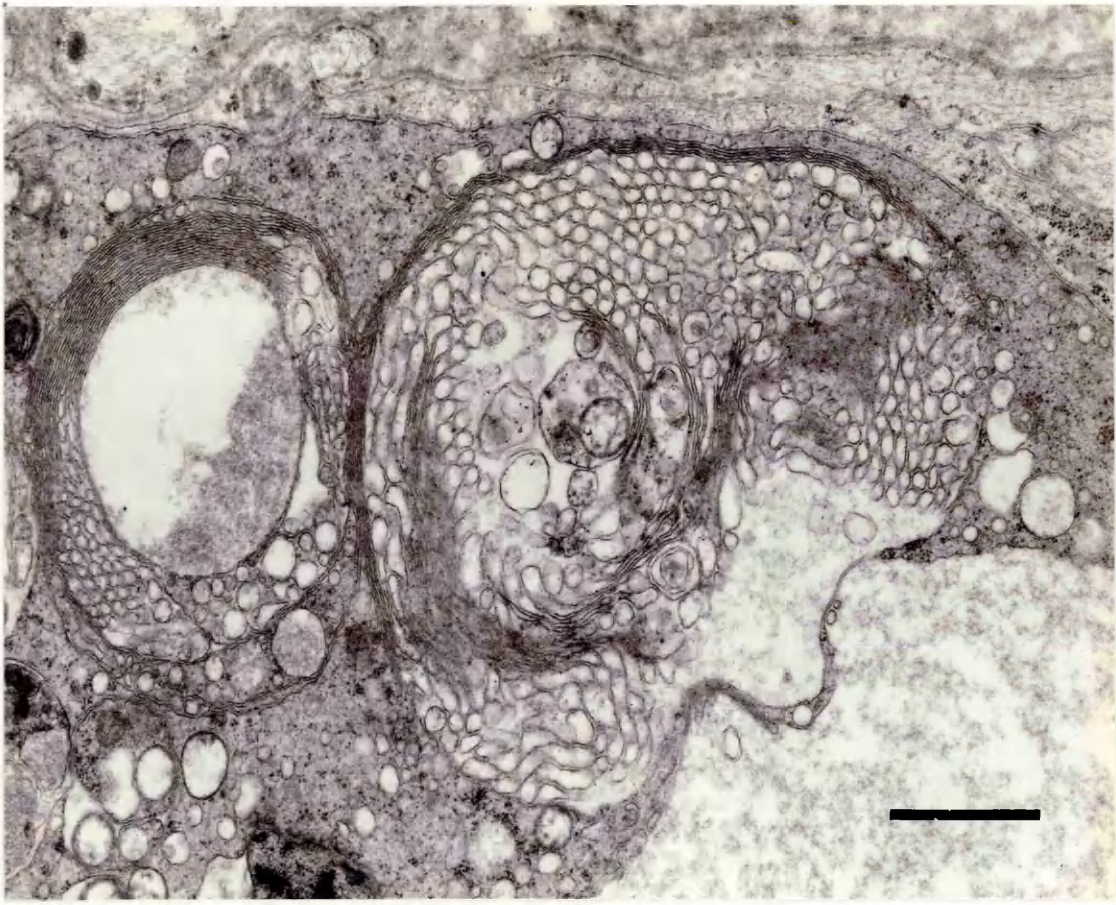
(7 days duration)

(a) The membranous 'stacks' described elsewhere may also be found as very complex "whorls", which appear in different planes of section. These vary in size and may be associated with vacuoles and distended cisternae.

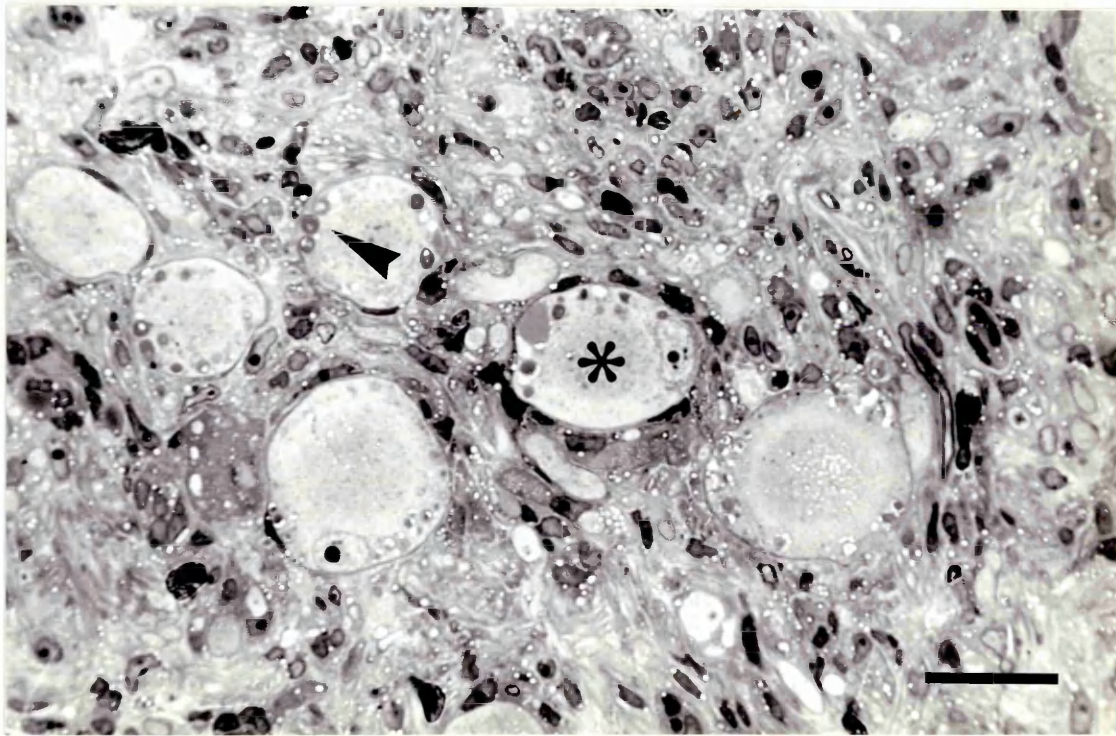
(b) Stacks and whorls may be identified in 1 μm sections - several may be present in a single neurone (*). They tend to be found at the periphery of the cell (arrowhead). They are not found in every neurone.

(a) Bar = 1 μm .

(b) Bar = 10 μm .



a



b

Figure 13

Affected neurone, cranial cervical ganglion, cat

(3 days duration)

The nucleus contains ring nucleoli, and the morphology of the nucleolus is indistinct. No RER is present. Mitochondria (M) appear dense and slender.

The cytoplasm contains several prominent stacks of parallel smooth membranes (*). These are present in the central region of the cytoplasm concentric with the nucleus, and not closely associated with either the nuclear envelope or the cell membrane (i.e. that area of cytoplasm normally occupied by the Golgi complexes). No Golgi complexes can be seen. The remainder of the cytoplasm is filled with short, disorganised profiles of SER.

Bar = 2 μ m.

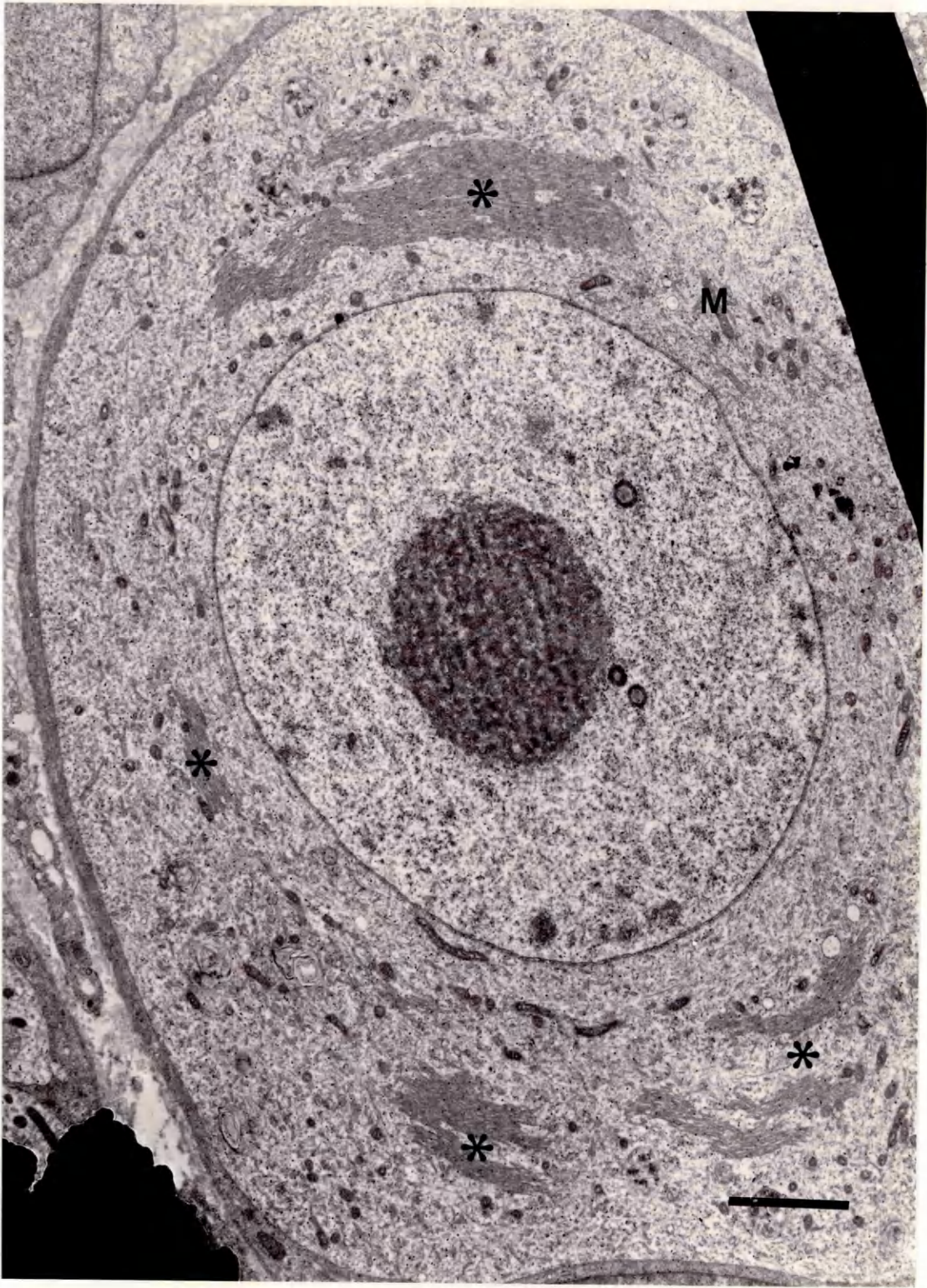


Figure 14

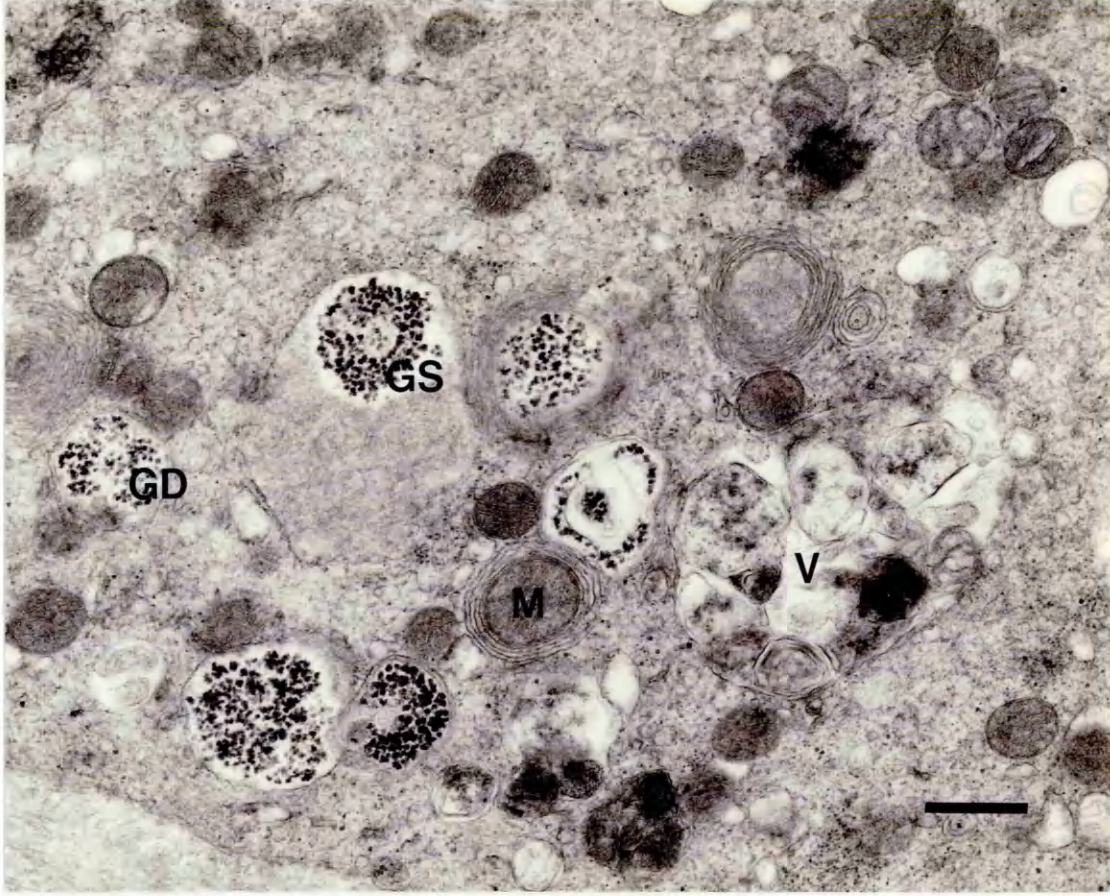
Affected neurones, stellate ganglion, cat (13 days duration)

(a) In this case, numerous accumulations of glycogen granules either bound by double (GD) or single (GS) membranes can be seen. Small configurations of smooth membranes, one of which is associated with a mitochondrion (M), a prominent autophagic vacuole (V) and other small vesicles are also present.

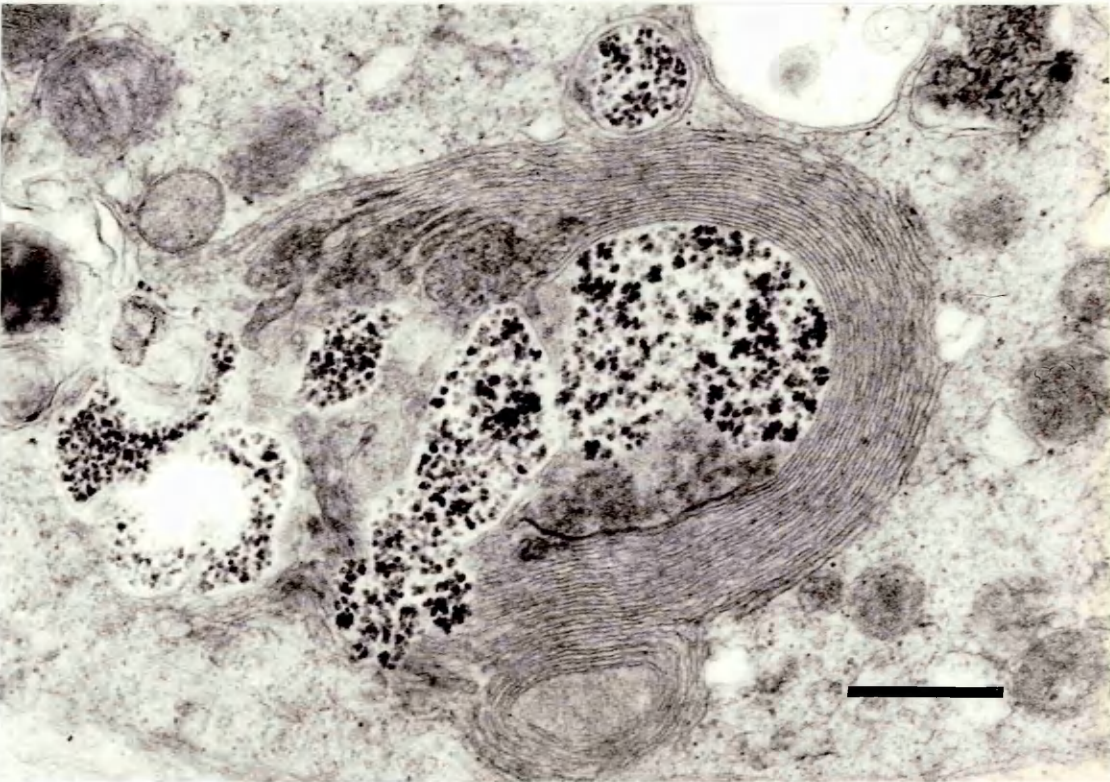
(b) The glycogen granules are occasionally closely associated with a membranous stack.

(a) Bar = 0.5 μ m.

(b) Bar = 0.5 μ m.



a



b

Figure 15

Affected neurone, stellate ganglion, cat (5 days duration)

A severely affected neurone. No RER or Golgi complexes can be seen. The cytoplasm contains greatly increased numbers of mitochondria (M) particularly in the more central areas, and there are also several accumulations of glycogen granules (G). Numerous small vesicles and vacuoles are found throughout the cytoplasm; these appear to be more frequent towards the periphery of the cell.

Bar = 3 μ m.

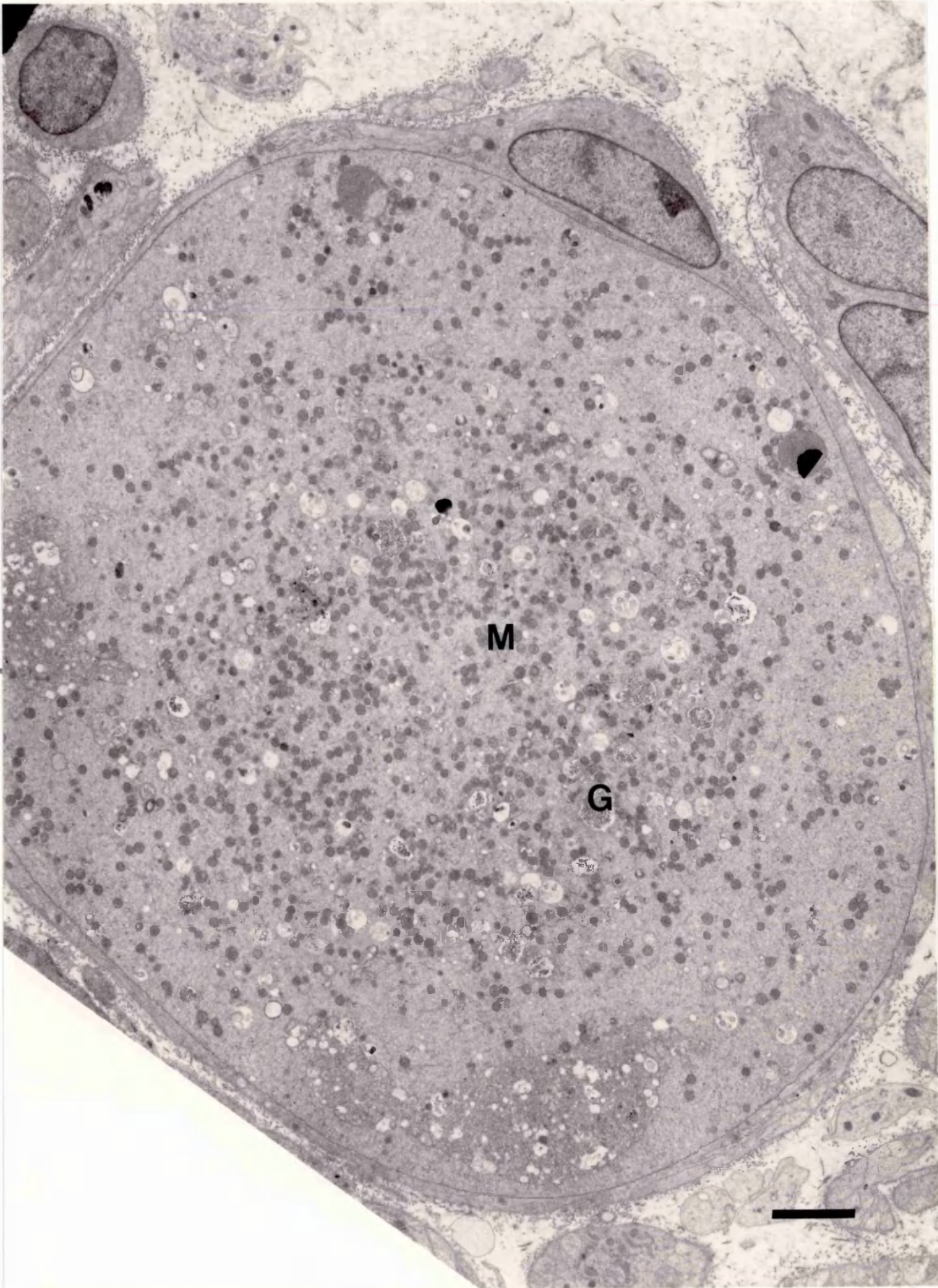


Figure 16

Affected neurone, stellate ganglion, cat (14 days duration)

A degenerating neurone. The nucleus (N) is pyknotic and eccentric. The peripheral areas of the cell are filled with extensive vacuoles (V) containing electron-dense floccular material, and the remaining cytoplasm consists mainly of lysosomes and small vacuoles.

Bar = 2 μ m.

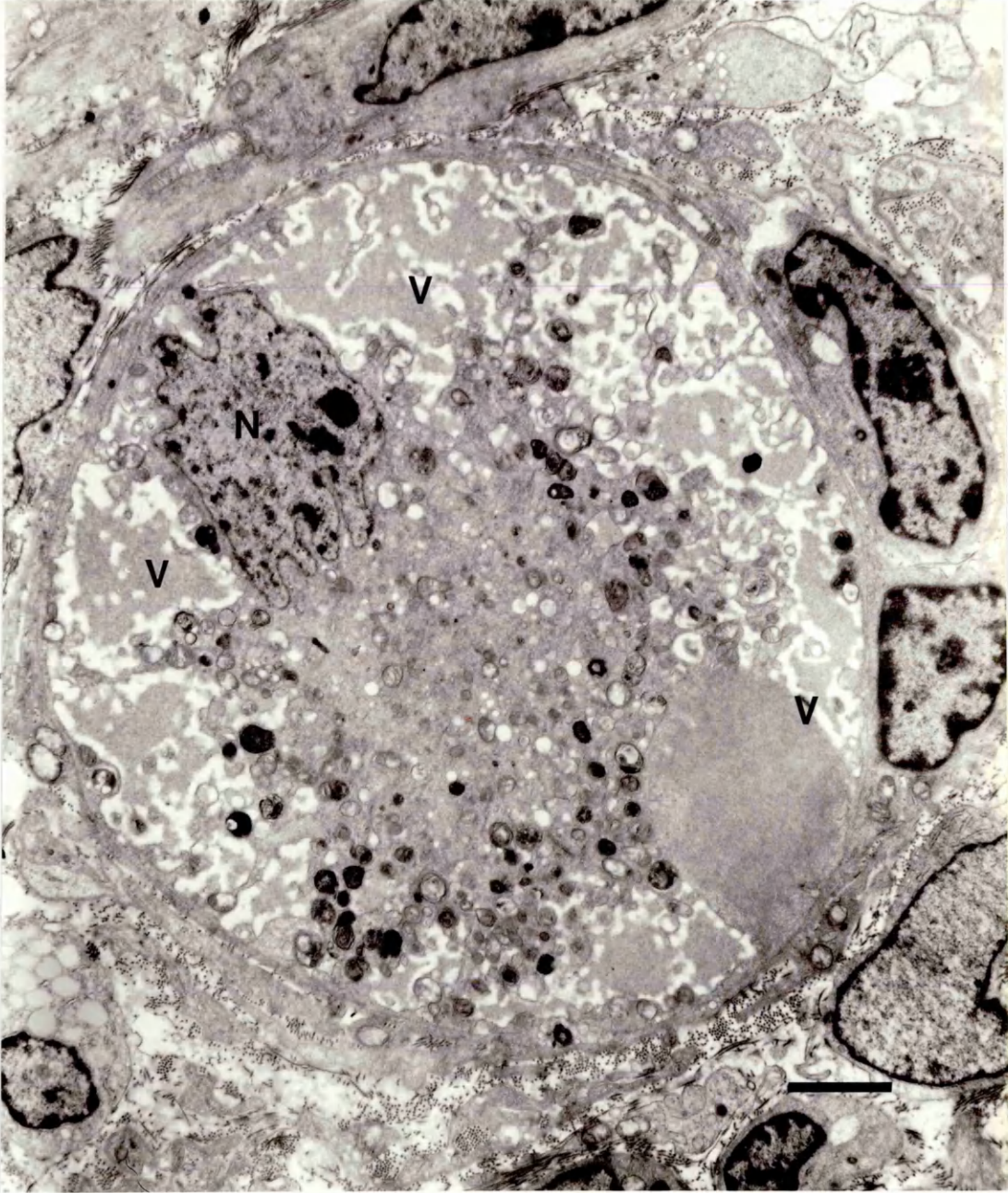


Figure 17

Neurones, stellate ganglion, chronically affected cat

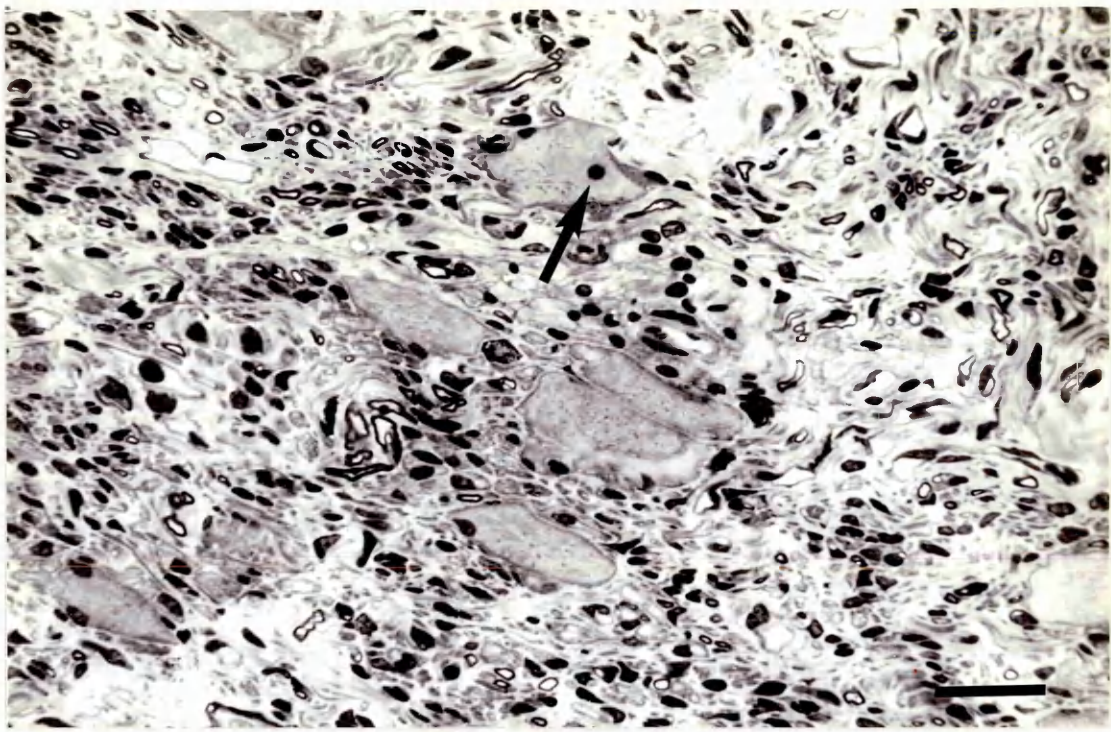
(6 weeks duration)

(a) 1 μ m section. The irregular elongated shapes of the neuronal perikarya can be seen. The nucleus (arrow) is large, with a prominent nucleolus, but it is eccentric. Darker areas in the cytoplasm, indicative of Nissl granules, can be seen in the cytoplasm of these neurones.

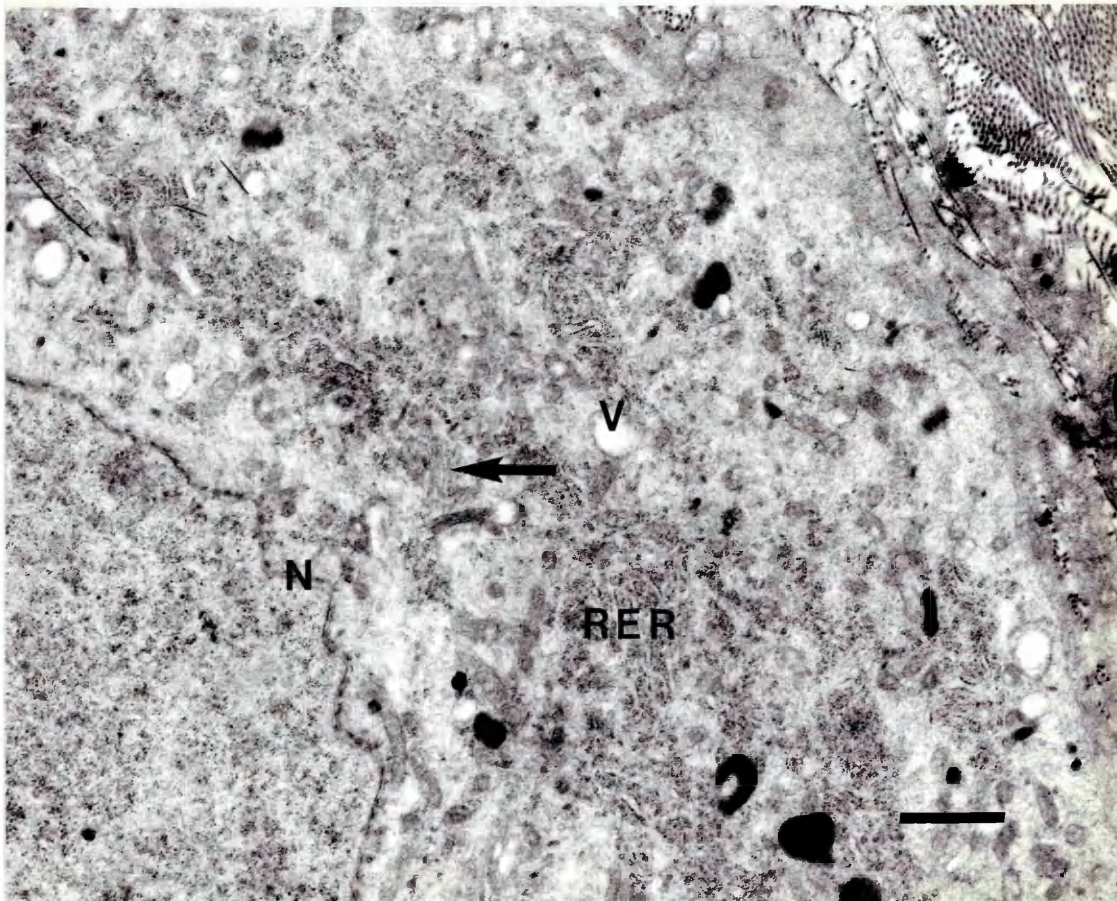
(b) The nuclear envelope (N) is slightly crenated. Areas of normal RER are prominent, although reduced in amount. A Golgi complex can be seen (arrow), but it is not as distinct or sizeable as normal. Occasional vacuoles (V) are present. Mitochondria and lysosomes appear normal.

(a) Bar = 10 μ m.

(b) Bar = 1 μ m.



a



b

Figure 18

Neurone, stellate ganglion, recovered cat

The perikaryon is rounded, and the nucleus (N) appears normal. RER (RER) is present but Golgi complexes cannot be readily identified as in normal tissue (see Figure 5, for comparison). Lysosomes and mitochondria are evenly distributed throughout the cytoplasm.

There are several small 'clear' areas, particularly round the periphery of the cell (*), the significance of which is unclear.

Bar = 2 μ m.

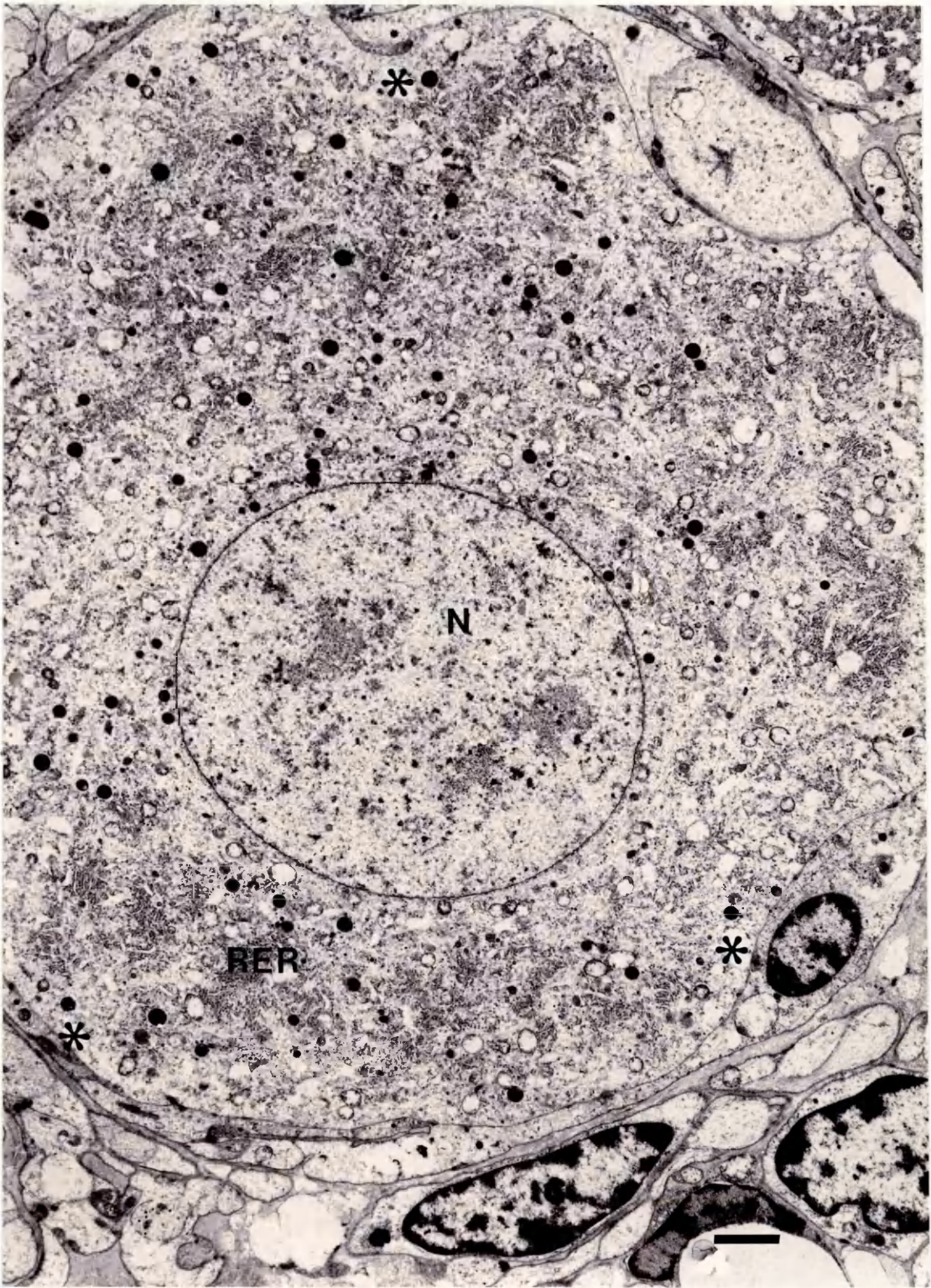


Figure 19

Neurone, stellate ganglion, recovered cat

The cisternae of RER (RER) appear normal, and are arranged into discrete areas. The Golgi complexes (G) are small, and appear to be partly vacuolated. There are several coated vesicles associated with them.

Numerous 'cleared' areas of cytoplasm can be seen with little, if any, definable structure (*). They have no well defined boundary, and occur most frequently in association with the Nissl substance. (These could probably be artefactual, since the satellite cell also contains cleared areas).

Mitochondria (M) appear slightly 'blown' (fixation artefact) but otherwise normal, and lysosomes, neurotubules and filaments also look normal.

Bar = 1 μ m.

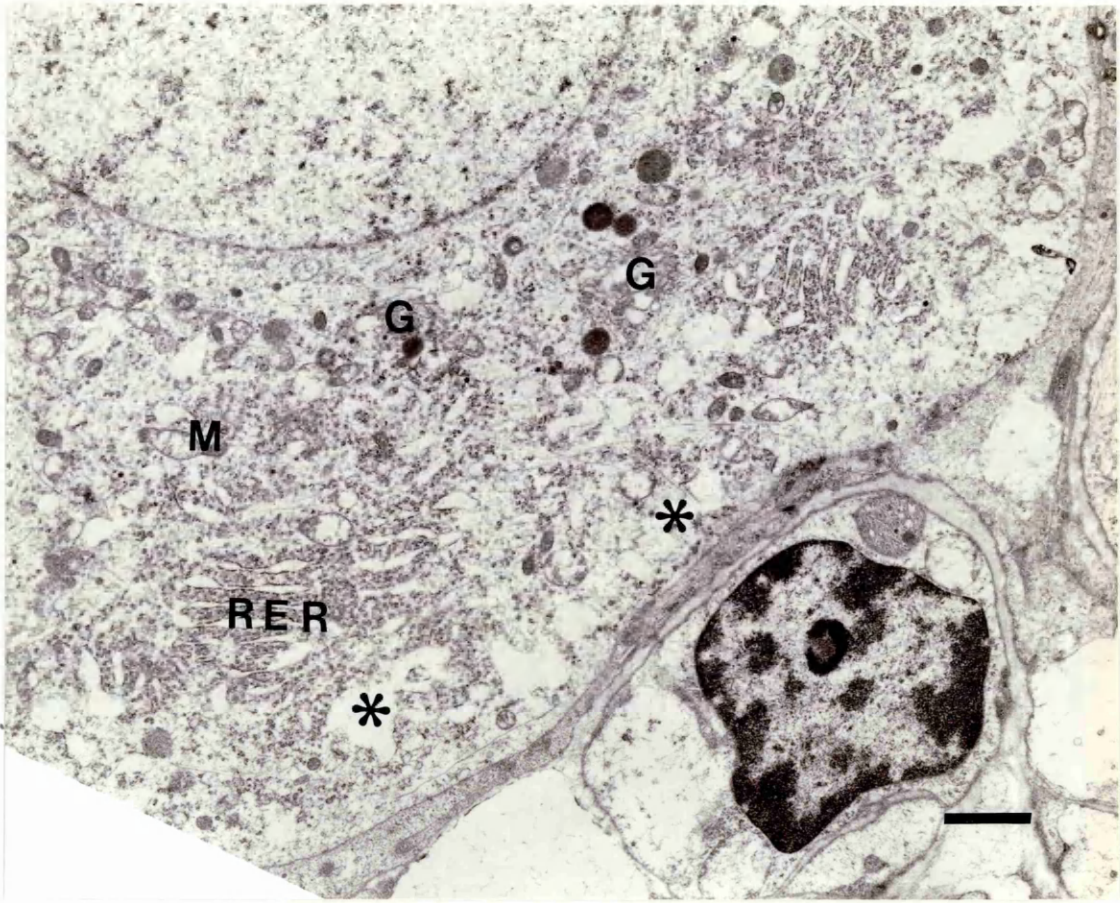


Figure 20

Affected neurone, stellate ganglion, horse (20 hours duration)

A mildly affected cell. The nuclear envelope (N) is slightly crenated. The RER (RER) looks normal, but its division into distinct Nissl granules is not as pronounced as usual, and there is very little in the area on the right of this figure (arrowheads). Only one Golgi complex (G) can be seen, and with the exception of a smooth membranous figure (arrow) which could be a small complex cut in an unusual plane of section, there are no abnormal structures to indicate where other Golgi complexes might have been. The mitochondria (M) are 'blown' (fixation artefact) but otherwise the remaining cytoplasmic structures appear normal.

Bar = 2 μ m.

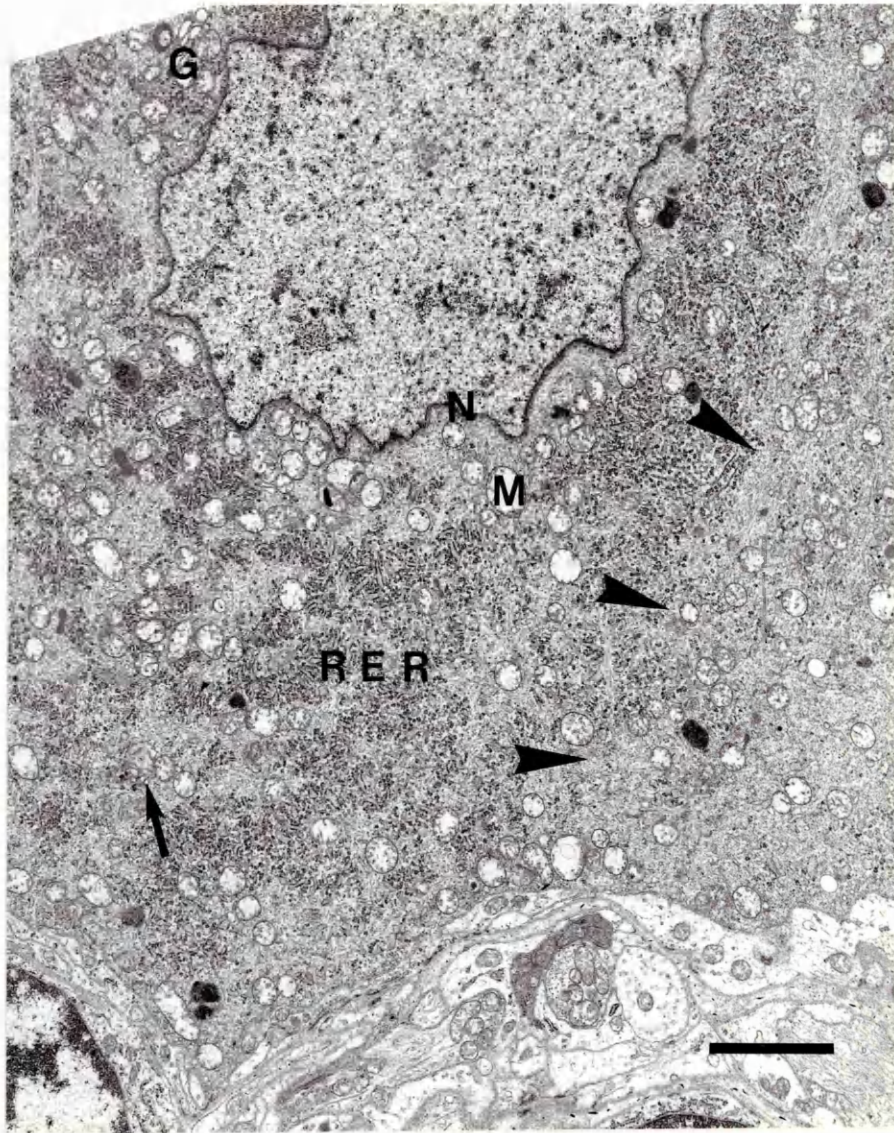


Figure 21

Affected neurones, stellate ganglia

(a) Horse, 20 hours duration

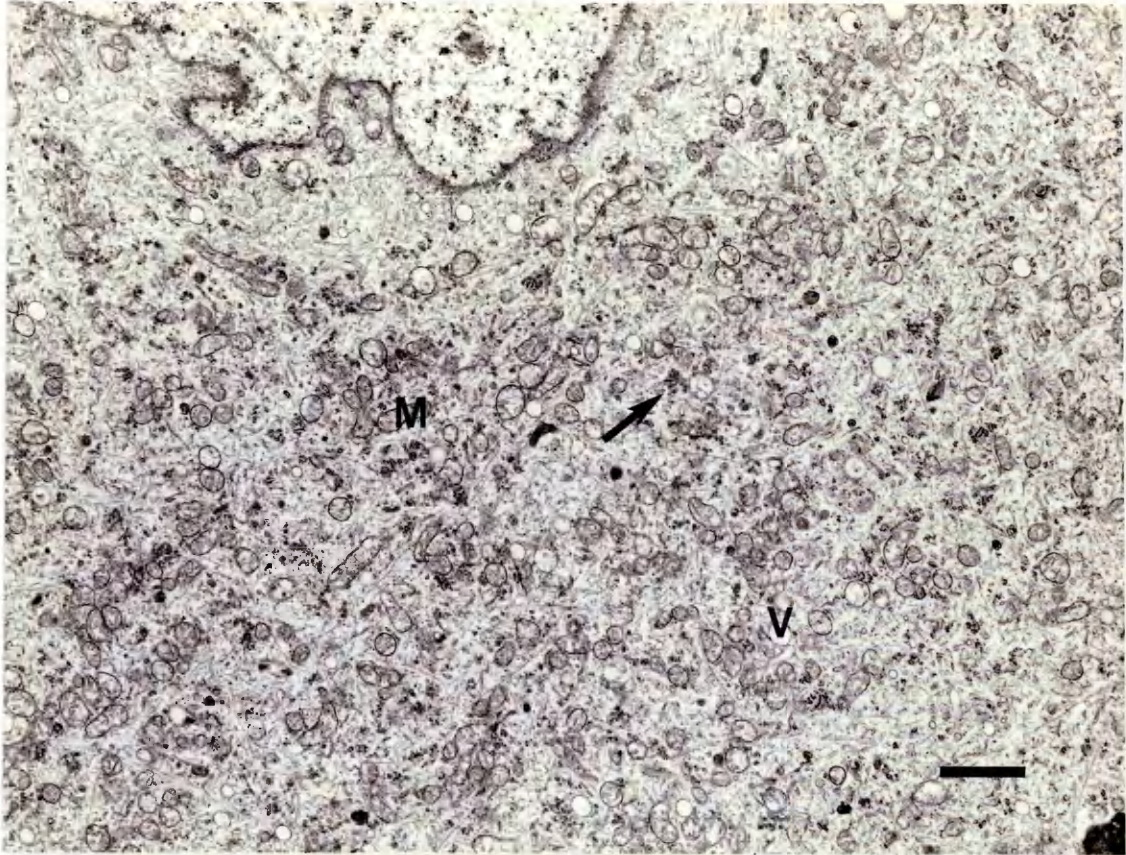
There is very little RER, occasional isolated single cisternae being distributed throughout the cytoplasm (arrow). No Golgi complexes can be seen. Occasional small vacuoles (V) are present, and mitochondria (M) appear increased in number.

(b) Horse, 30 hours duration

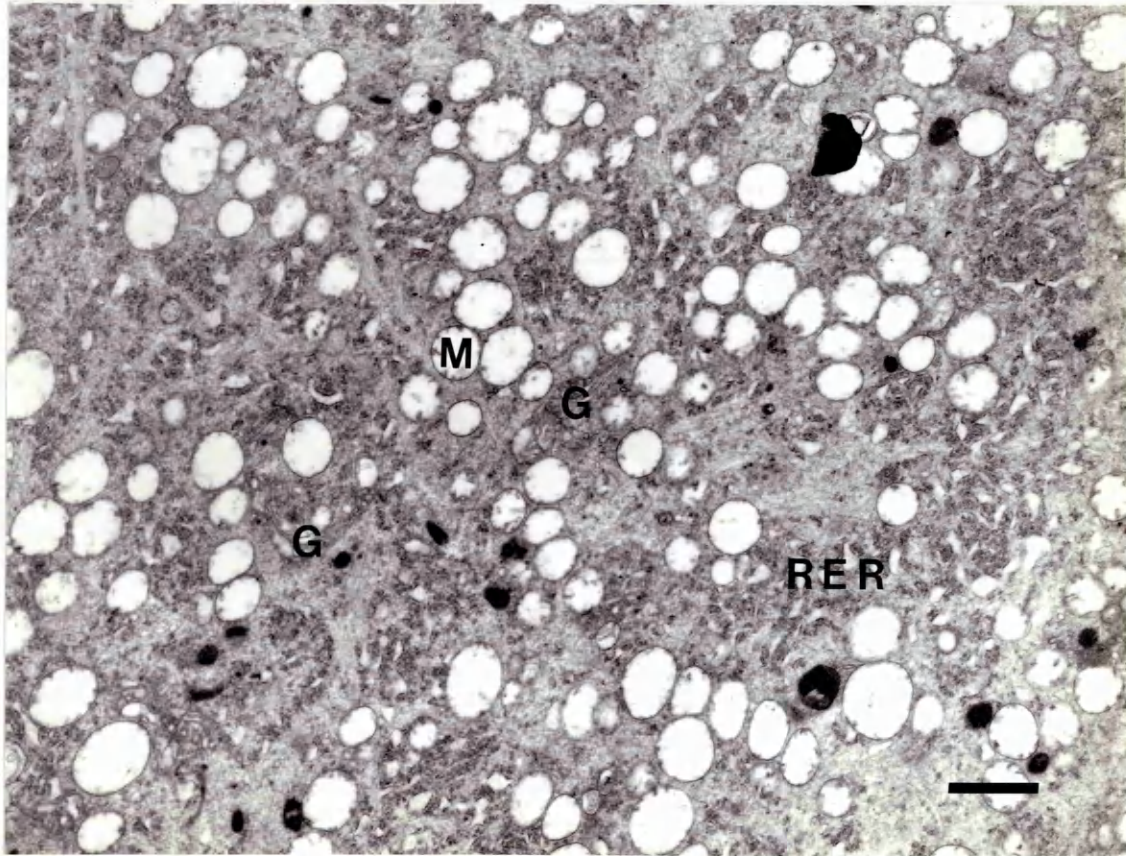
Mitochondria which are 'blown' (fixation artefact) (M) seem to be present in greater numbers than usual in a cell which has relatively normal Golgi complexes (G) and RER (RER).

(a) Bar = 1 μ m.

(b) Bar = 1 μ m.



a



b

Figure 22

Affected neurone, stellate ganglion, horse (6 days duration)

The periphery of this neurone contains numerous small cisternae (C) filled with electron-dense material amongst which small accumulations of ribosomes can be seen (arrow). Occasional vacuoles are also present.

Smooth membranous profiles (arrowheads), neurofilaments and tubules are numerous and present throughout the neurone, accounting for most of the cytoplasm outwith the peripheral area. A few small cisternae and vacuoles are also seen more centrally, together with occasional mitochondria (M) and lysosomes (L).

Bar = 1 μ m.

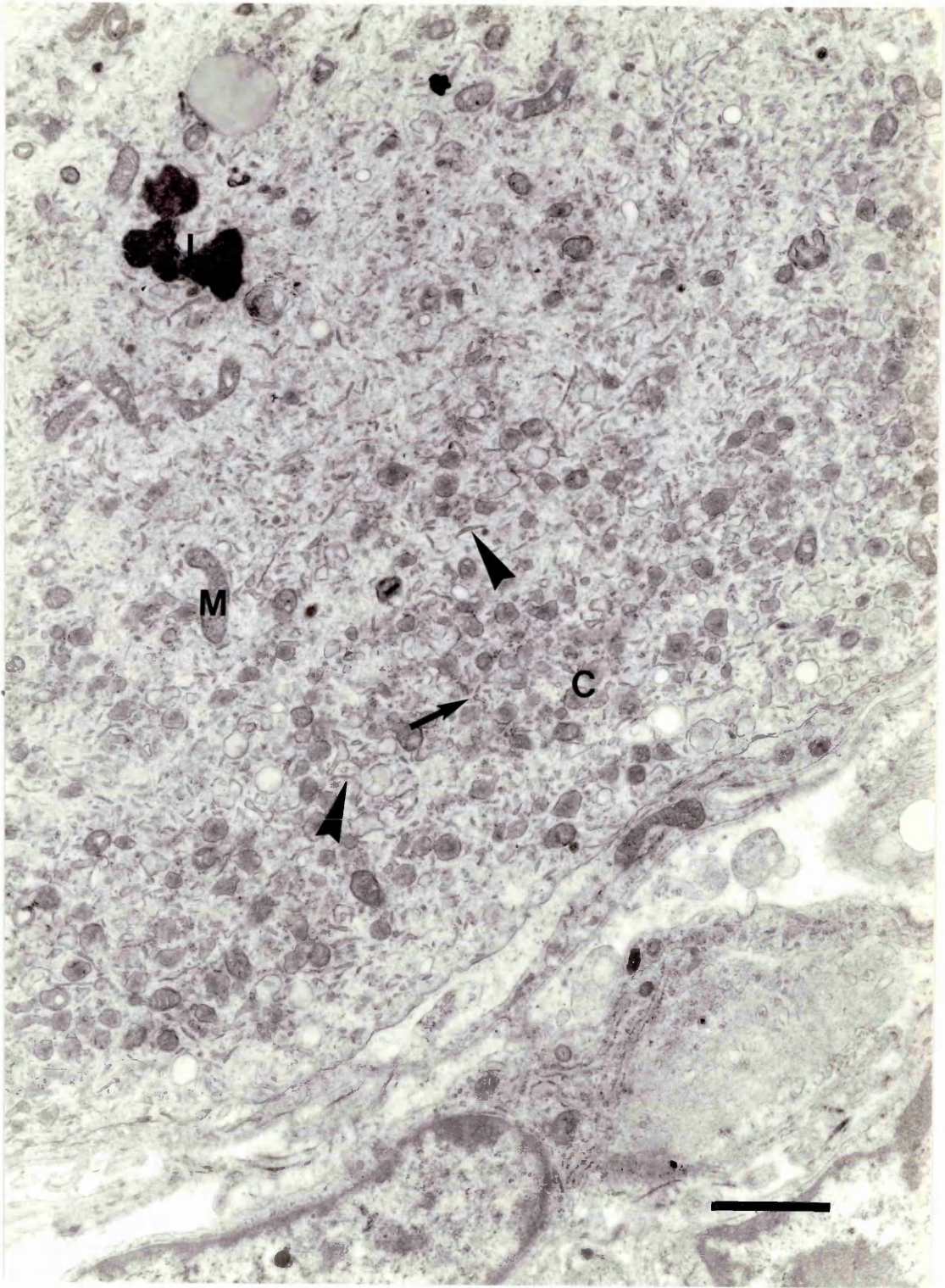


Figure 23

Affected neurone, stellate ganglion, horse (17 days duration)

The demarcation of the peripheral area containing distended cisternae (C) from the remaining cytoplasm can be very pronounced. Some small accumulations of RER and ribosomes (arrows) are found within the cisternal area or adjacent to it, becoming less frequent centrally. No Golgi complexes can be seen. The more central areas consist of occasional small vacuoles, large lysosomes (L) and mitochondria (M), with numerous neurofilaments and tubules.

Bar = 1 μ m.

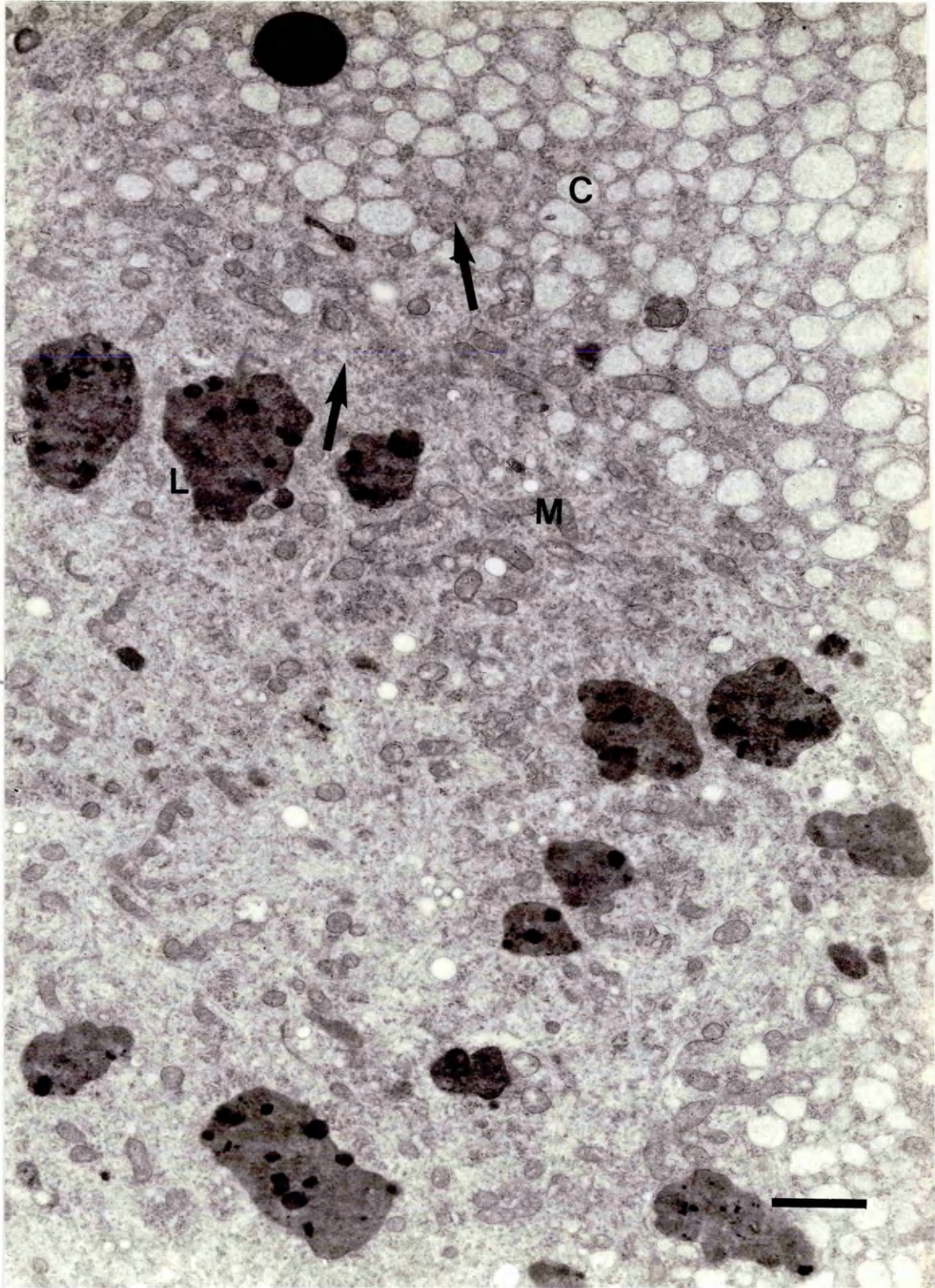


Figure 24

Affected neurones, stellate ganglia, horse

(a) 20 hours duration

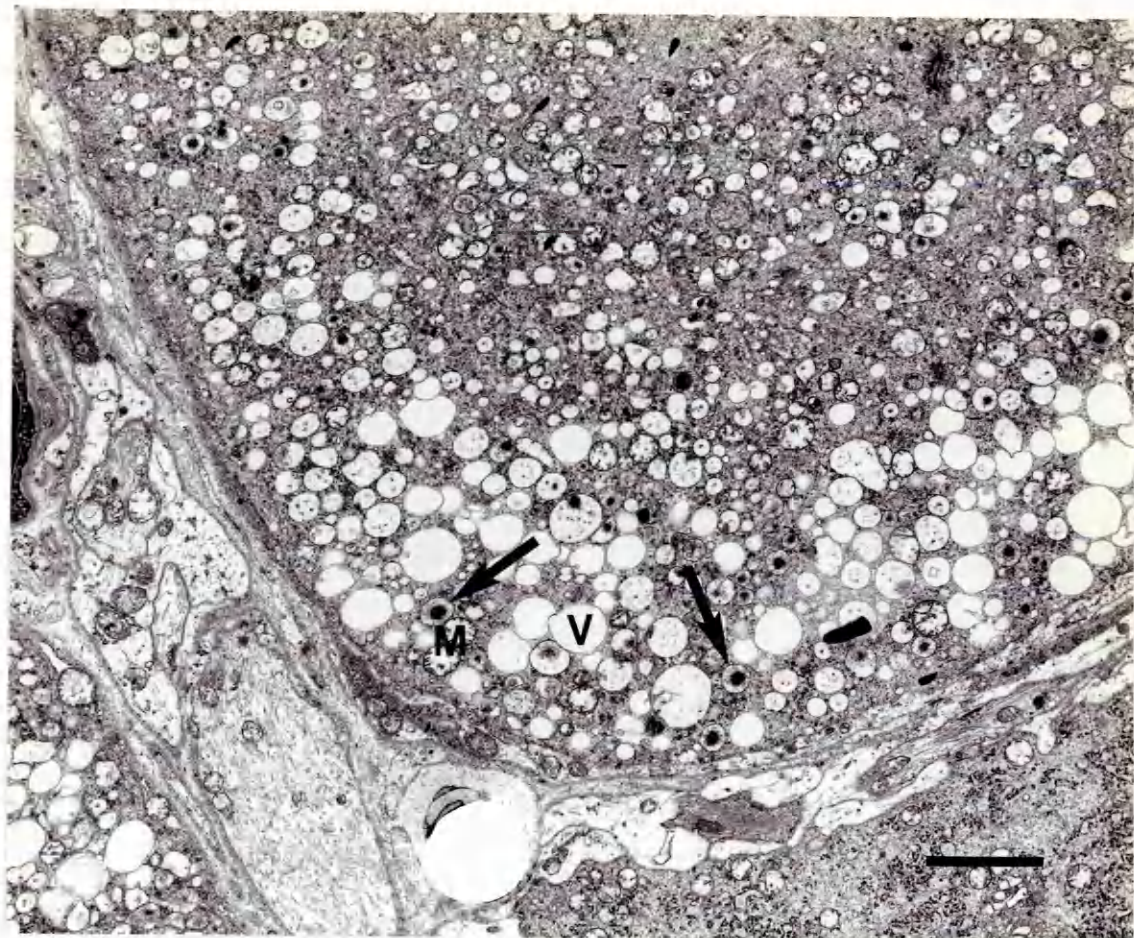
Cisternae containing condensed electron-dense material can be seen peripherally (arrows), and large vacuoles (V) are also prominent in this area. Smaller vacuoles, together with occasional cisternae and 'blown' mitochondria (M), SER, neurofilaments and tubules constitute the rest of the neurone. No RER or Golgi complexes are present.

(b) 17 days duration

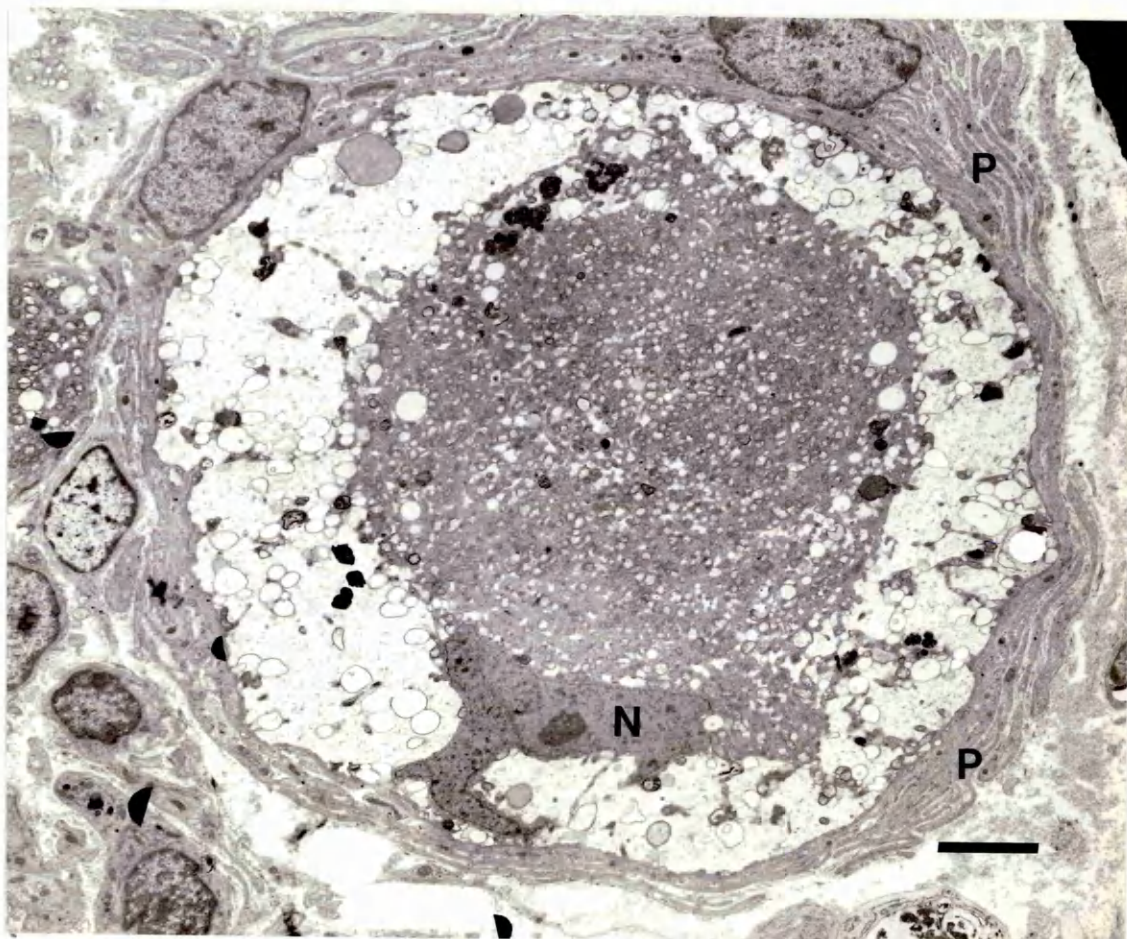
The nucleus (N) is shrunken and eccentric, and peripheral vacuolation is extensive. The central area contains vacuoles and mitochondria. There is also an increase in the number of satellite cell processes (P) surrounding the neurone.

(a) Bar = 2 μ m.

(b) Bar = 3 μ m.



a



b

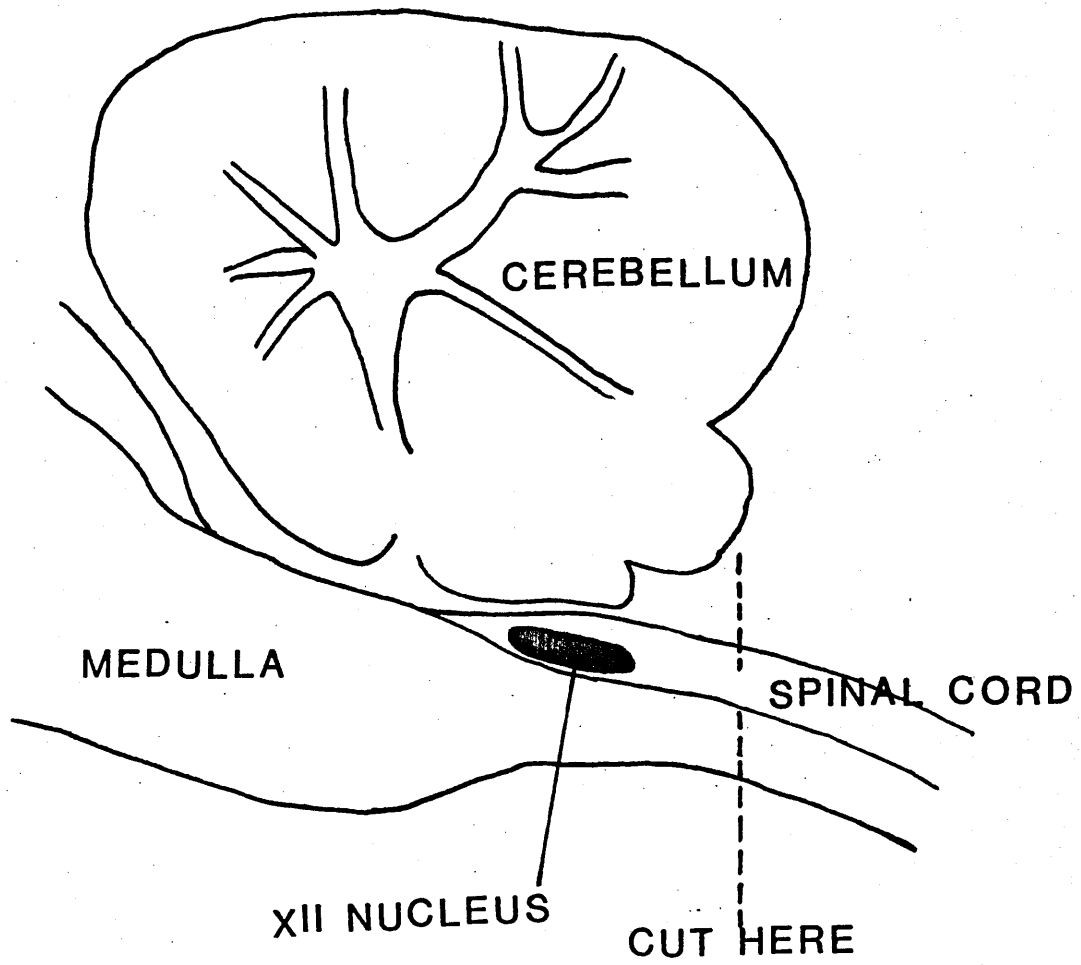


Figure 26. Position of the XII nucleus in the brainstem

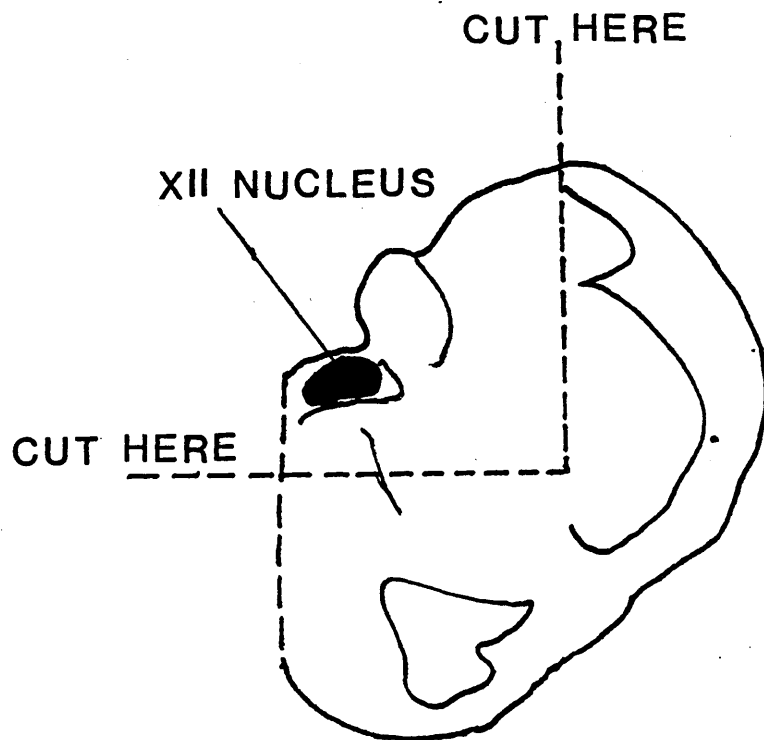


Figure 27. Pre-processing trimming of blocks containing XII nucleus neurones

Figure 28

Normal neurone, XII nucleus, cat

The nucleus is centrally placed, round and prominent, the karyoplasm (K) containing randomly distributed heterochromatin granules varying in shape and size. The circular nucleolus (N) has a typical 'honeycomb' appearance, the dense areas (nucleolonema) consisting of both granular and fibrillar components, not always readily distinguishable in routine sections. The pale areas within the nucleolus are the pars amorpha.

RER (RER) is seen as discrete areas occurring more frequently close to the nucleus and rarely associated with the cell membrane. These 'Nissl granules' are generally well distributed throughout the cytoplasm. Like Nissl granules the Golgi complexes (*) also occur centrally in the cytoplasm, roughly concentric with the nucleus.

Bar = 2 μ m.



Figure 29

Normal neurone, XII nucleus, cat

Nissl granules (RER) are a prominent feature. The typical appearance is of stacks of parallel flattened cisternae with ribosomes attached. Depending on the plane of section, tubular or vesicular configurations may be seen. Golgi complexes (G) are generally found close to the RER, but no other organelles occupy the same space as the Nissl granules except very occasional mitochondria.

The numerous mitochondria (M) are evenly distributed throughout the cytoplasm, appearing circular or oval depending on the plane of section, with a clearly defined cristal pattern internally.

The remaining membrane-bound organelles are predominantly dense-bodies (various lysosomes at different stages of development). While specific staining methods are required to accurately identify these, one type - lipofucsin granules (L) - are quite distinct. They are dense, irregularly shaped and may have associated pale areas.

Bar = 1 μ m.

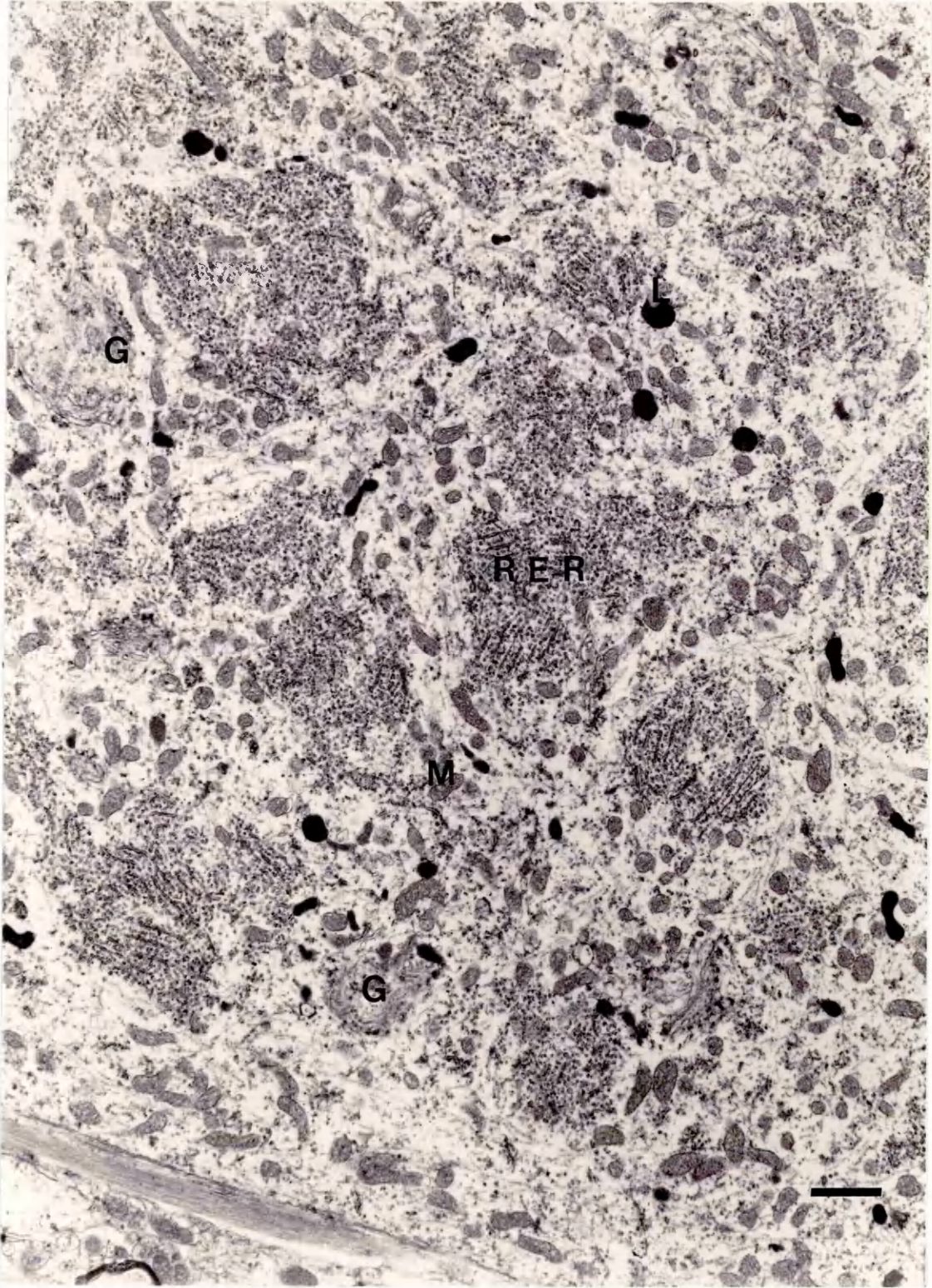


Figure 30

Normal neurone, XII nucleus, cat

Ribosomes can be seen attached in groups, at regular intervals, to the cytoplasmic surfaces of the cisternae of RER (RER). They also occur free in the cytoplasm either singly or in groups (polysomes). Small areas of SER may be seen close to, and associated with, RER (arrow).

The Golgi complex (G) comprises a curved stack of 3-7 flattened cisternae which may appear dilated at the rims. Numerous coated and uncoated vesicles are associated with the stack, particularly the "trans" (or concave) side.

Neurotubules and neurofilaments are seen in those areas of cytoplasm not occupied by the other organelles. Their direction through the perikaryon appears variable.

Bar = 1 μ m.

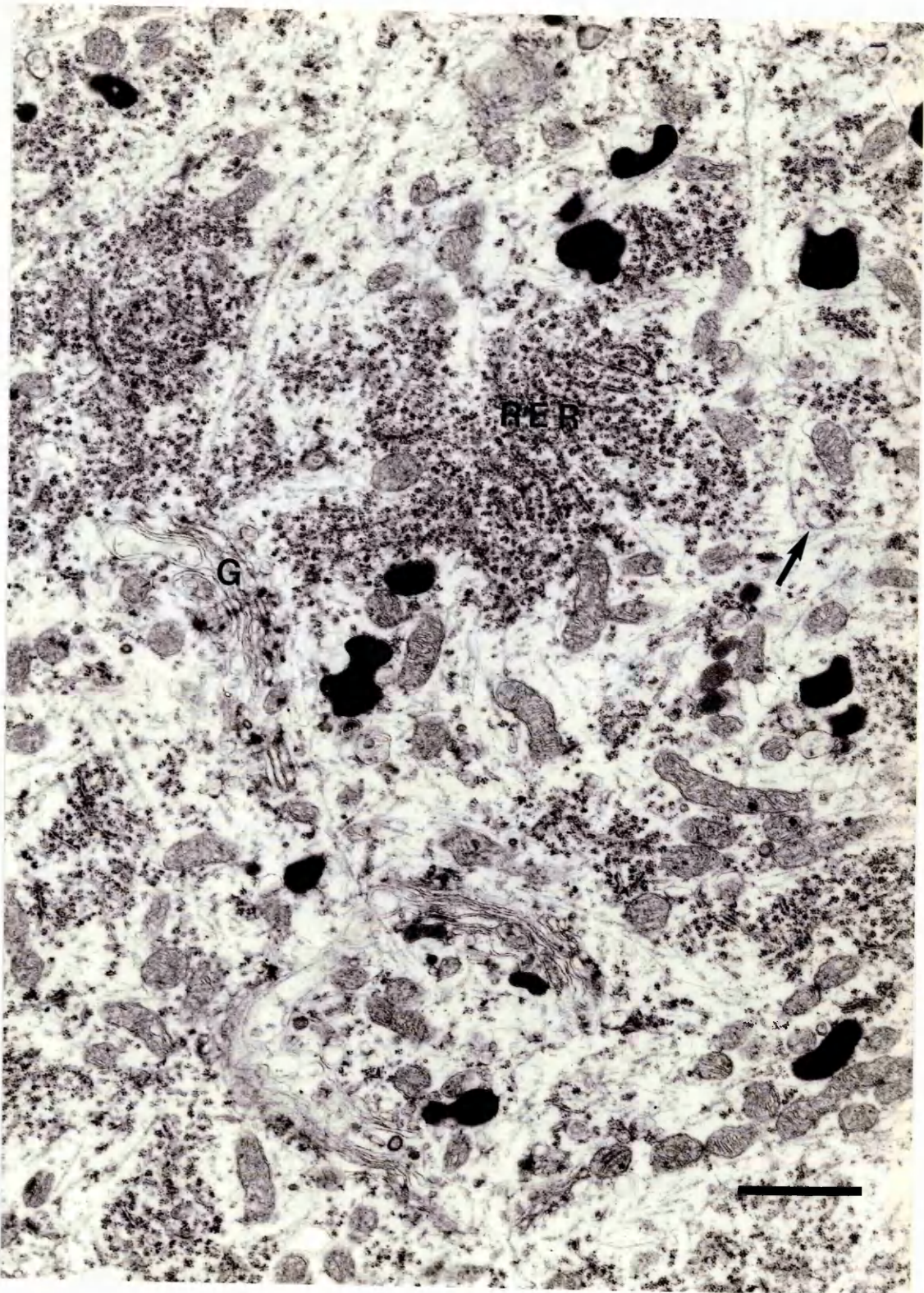


Figure 31

Normal neurone and dendrite, XII nucleus, cat

Small Nissl granules (RER) are found proximal to the cell body, although they may also occur more distally. Occasional Golgi complexes (G) are found.

Mitochondria are the most common membrane-bound organelles in this area. They are similar in size and shape to perikaryal mitochondria and occur in similar numbers proximally, becoming less frequent distally. There are occasional dense bodies.

The most prominent organelles are the neurotubules and neurofilaments which run past the other organelles and parallel to the long axis of the dendrites.

Bar = 2 μ m.

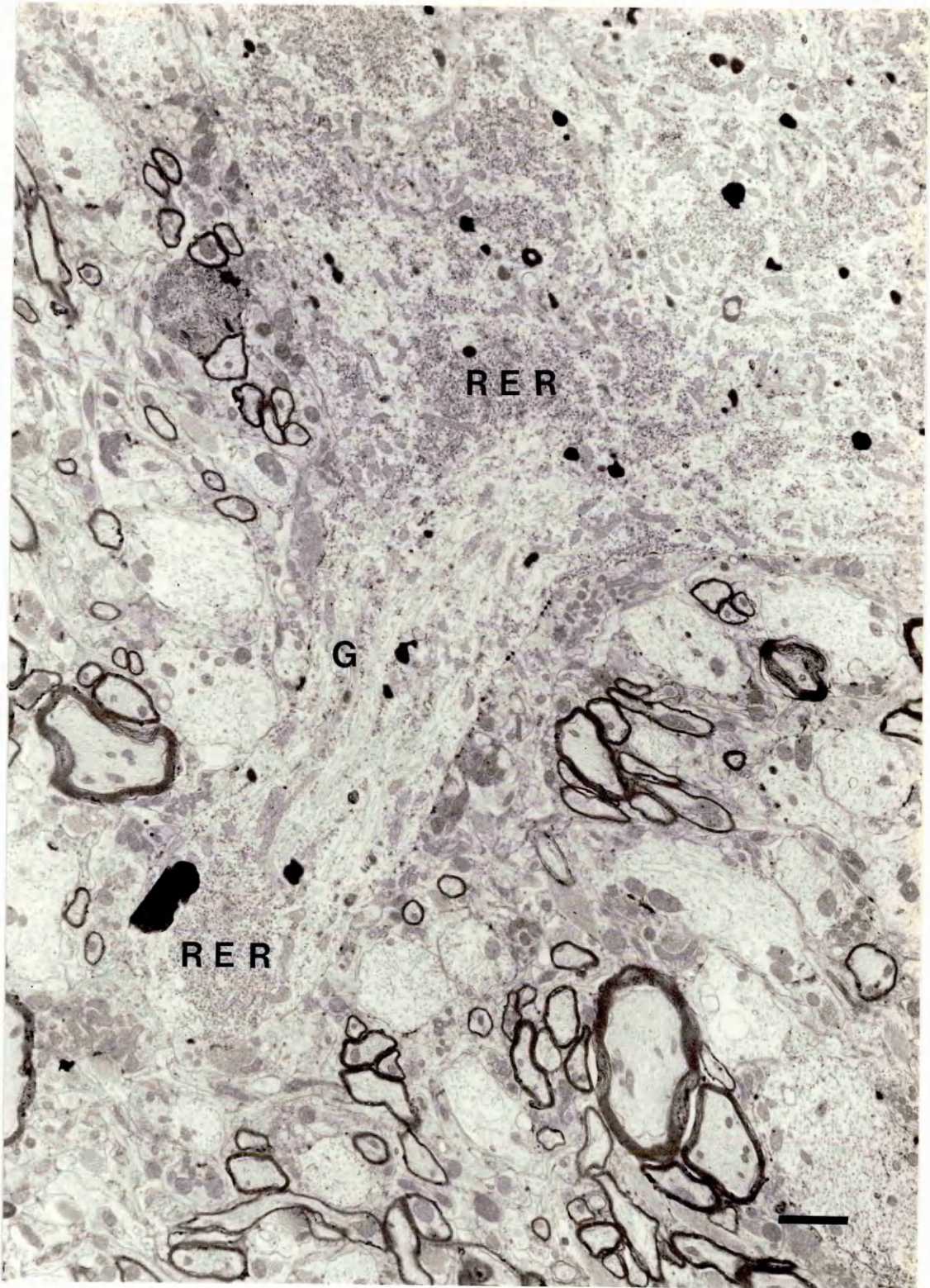


Figure 32

Abnormal nuclear structures, XII nucleus, cat (5 days duration)

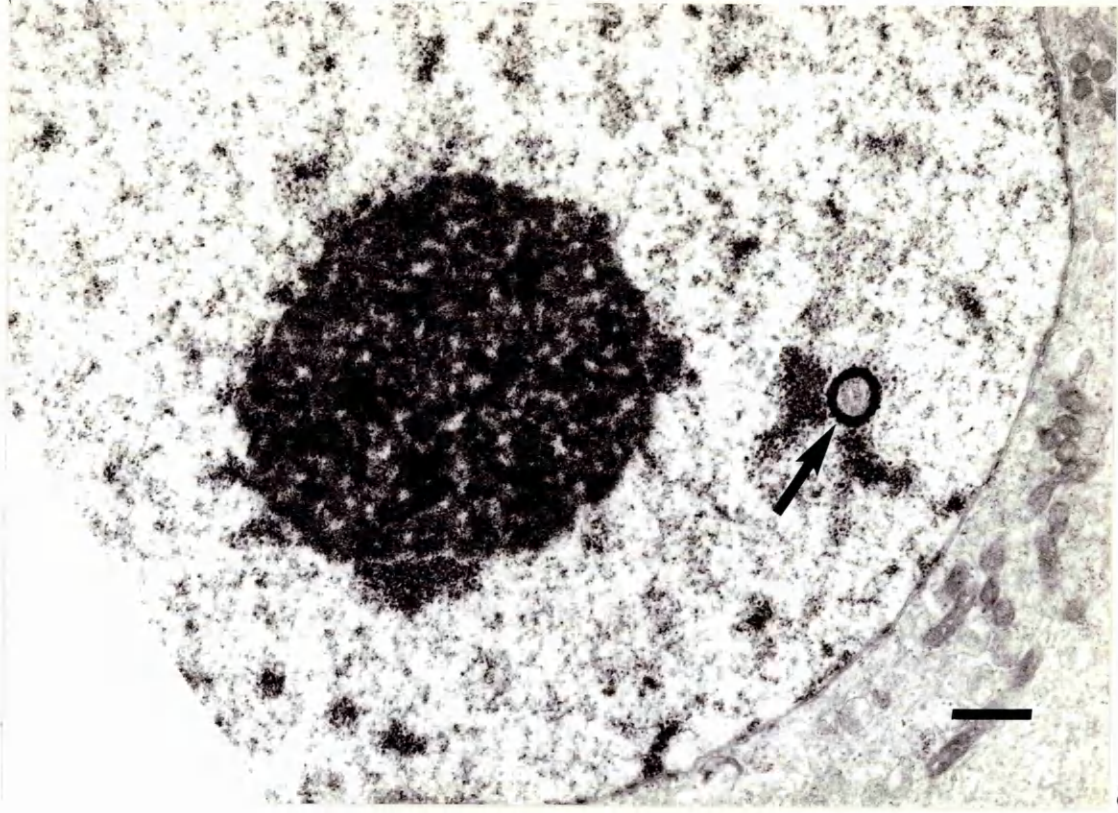
Occasional nuclear abnormalities were observed.

- (a) Ring nucleolus (arrow).
- (b) Membranous structure (arrows).

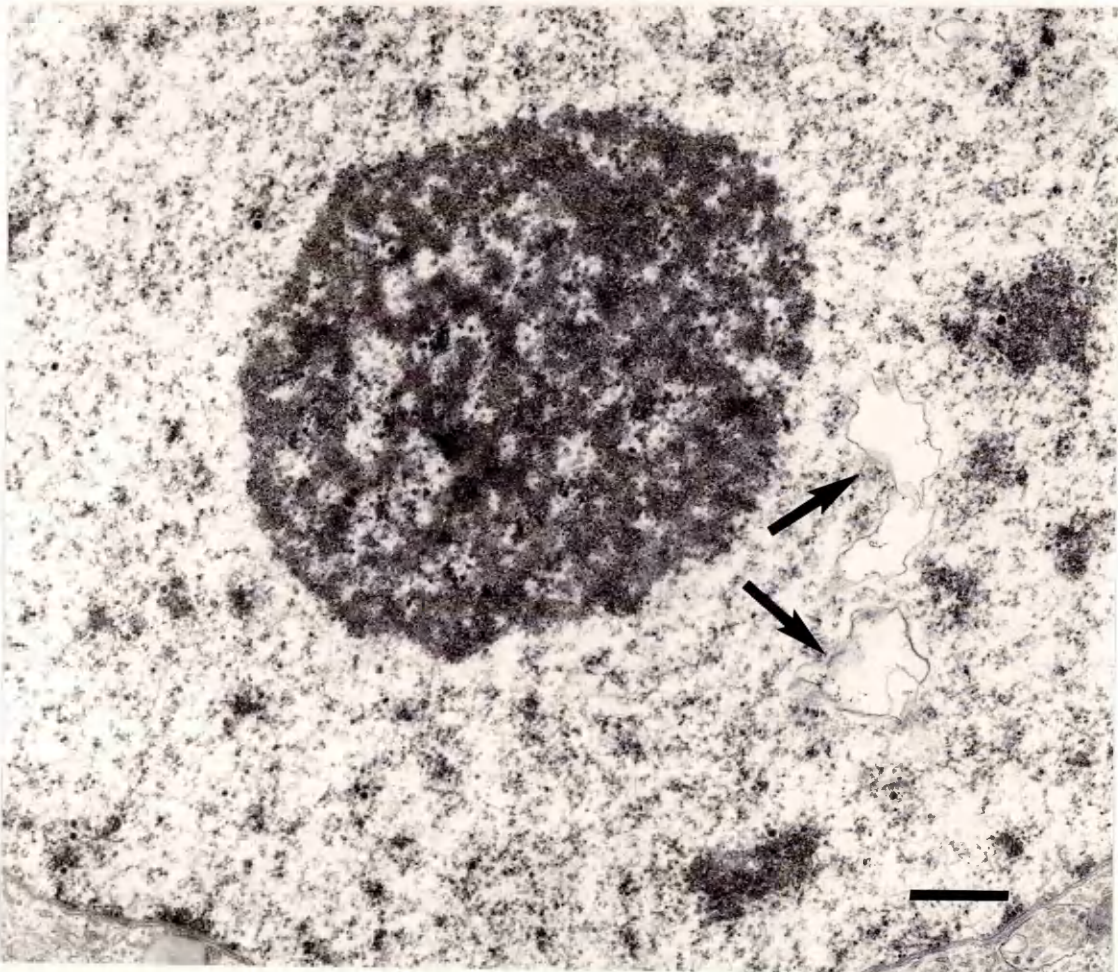
The significance of these structures is unclear, and they are only seen in a very small percentage of the neurones which show cytoplasmic changes.

(a) Bar = 0.5 μ m.

(b) Bar = 0.5 μ m.



a



b

Figure 33

Affected neurone, XII nucleus, cat (3 days duration)

There is a dispersal of the RER, with loss of distinctive Nissl granules. Small clumps and lengths of otherwise normal-looking RER are seen throughout the cytoplasm (arrow). The Golgi complexes (G) are prominent and relatively normal, although some cisternae appear slightly distended. The other organelles appear normal.

Bar = 2 μ m.

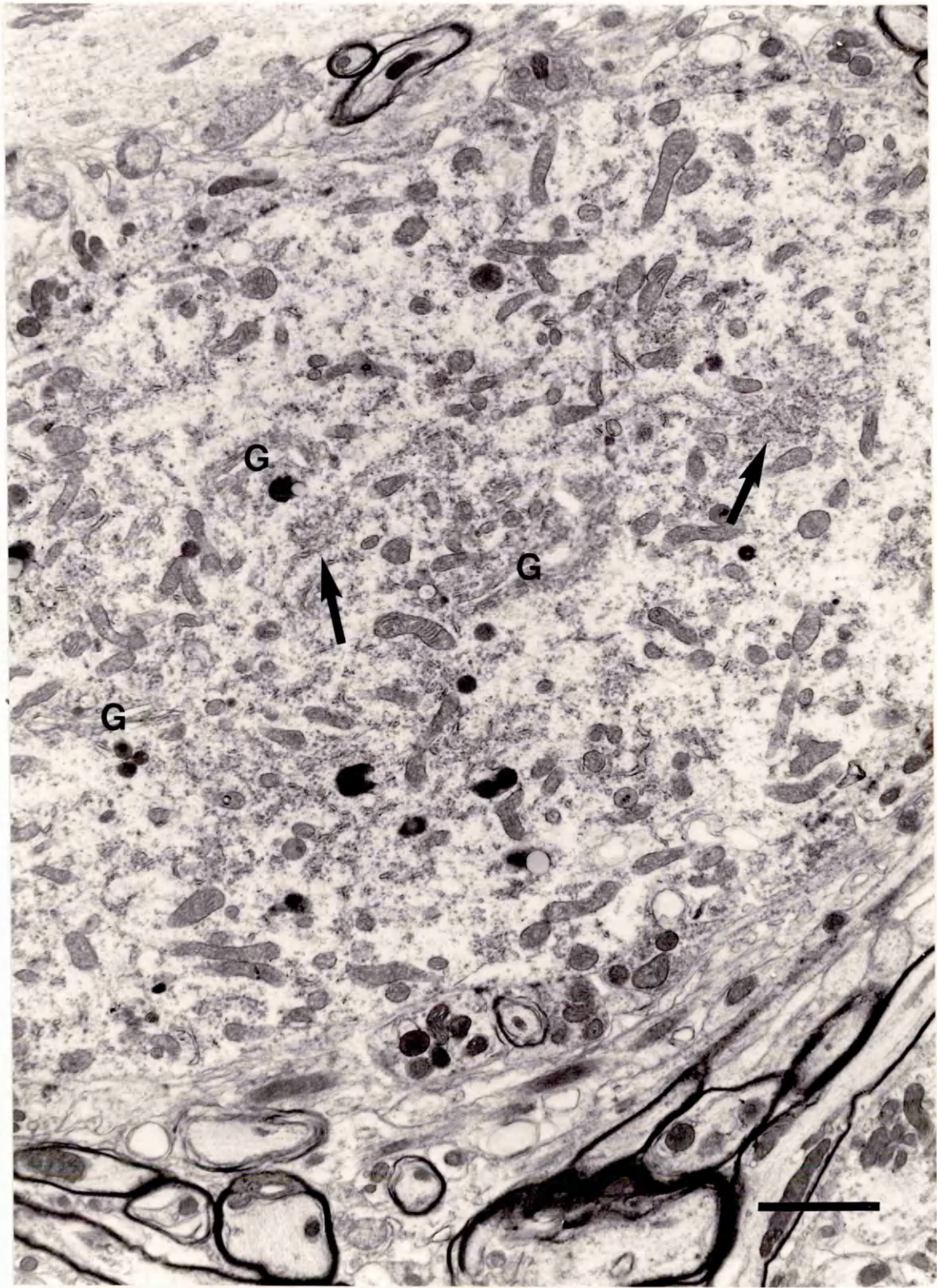


Figure 34

Affected neurone, XII nucleus, cat (5 days duration)

The cytoplasm is filled with proliferated SER profiles (SER) and numerous membrane-bound accumulations of electron-dense floccular material (C). A few ribosomes adherent to these structures (arrows) suggest that they are distended cisternae of RER.

Occasional normal-looking mitochondria (M) and lysosomes are present, but no Golgi complexes, either normal or abnormal, can be recognised.

The nucleus and nuclear envelope (N) appear normal.

Bar = 0.5 μ m.

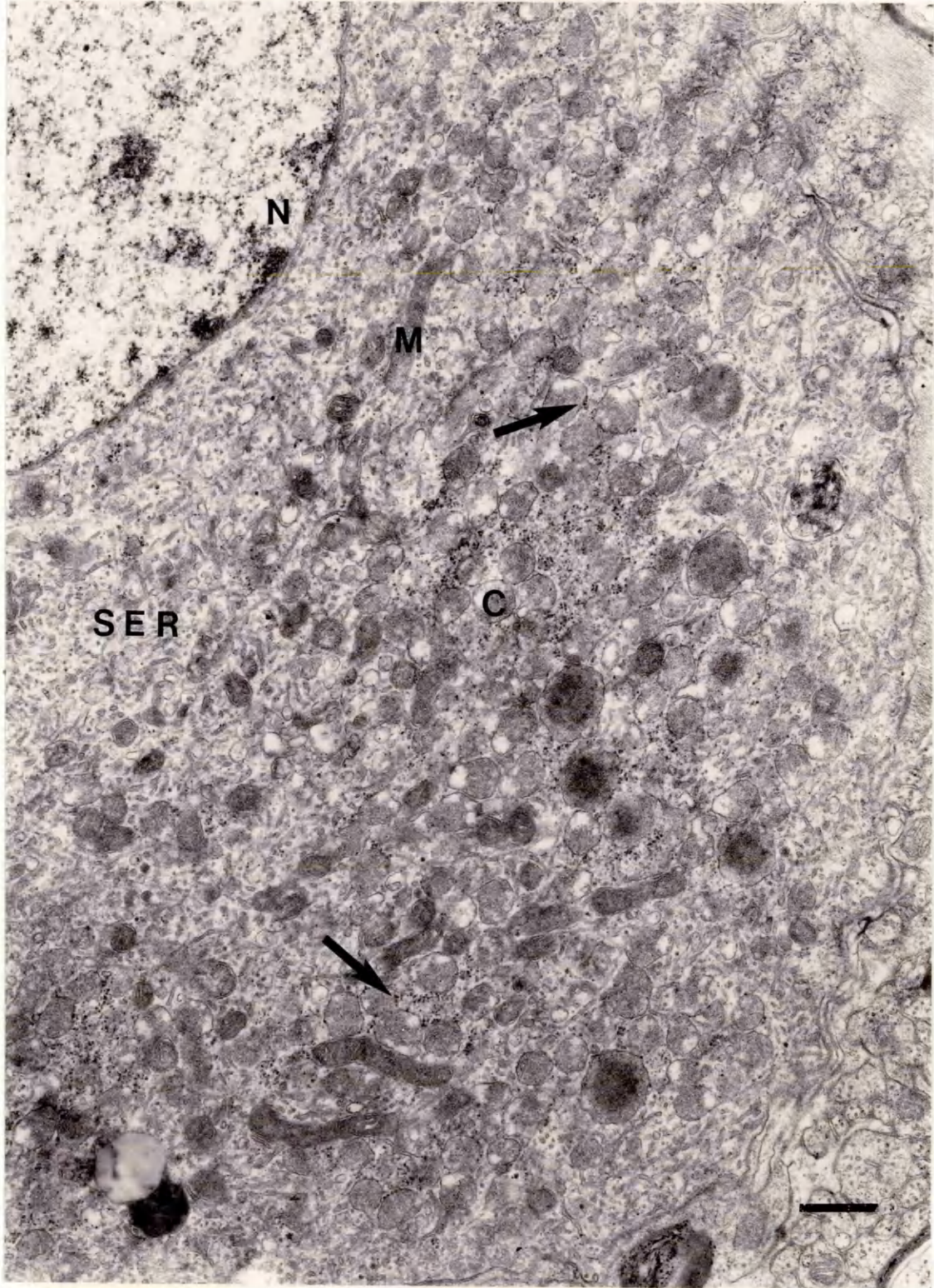


Figure 35

Affected neurone, XII nucleus, cat (13 days duration)

The cytoplasm contains proliferated SER profiles and numerous distended cisternae (as described in Figure 34), a much greater proportion of which have a very dense centre (C). The most prominent feature of this cell is the greatly increased number of mitochondria (M) occurring in clumps. These are more dense and slender than usual, but otherwise appear normal.

Numerous active lysosomes (L) are also present.

Bar = 1 μ m.

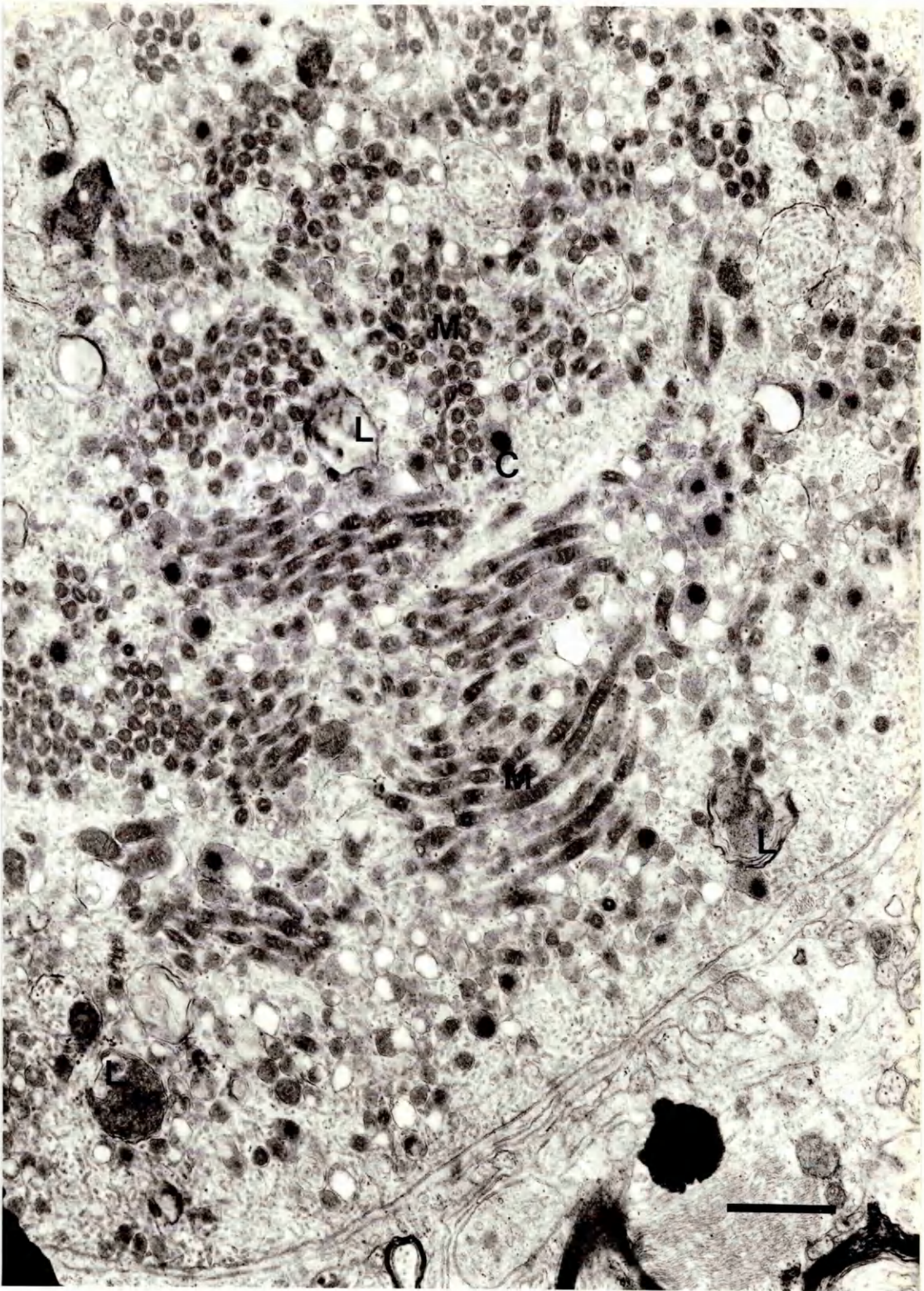


Figure 36

Large light neurone, dorsal root ganglion, normal cat

The curved smooth cisternae of the Golgi complexes (G) with their associated vesicles, the branched arrays of the RER (RER), the mitochondria (M) and lysosomes (L) appear the same as their equivalents in the cell types illustrated previously. They are separated from one another by prominent bands of neurofilaments (NF).

Bar = 0.5 μ m.

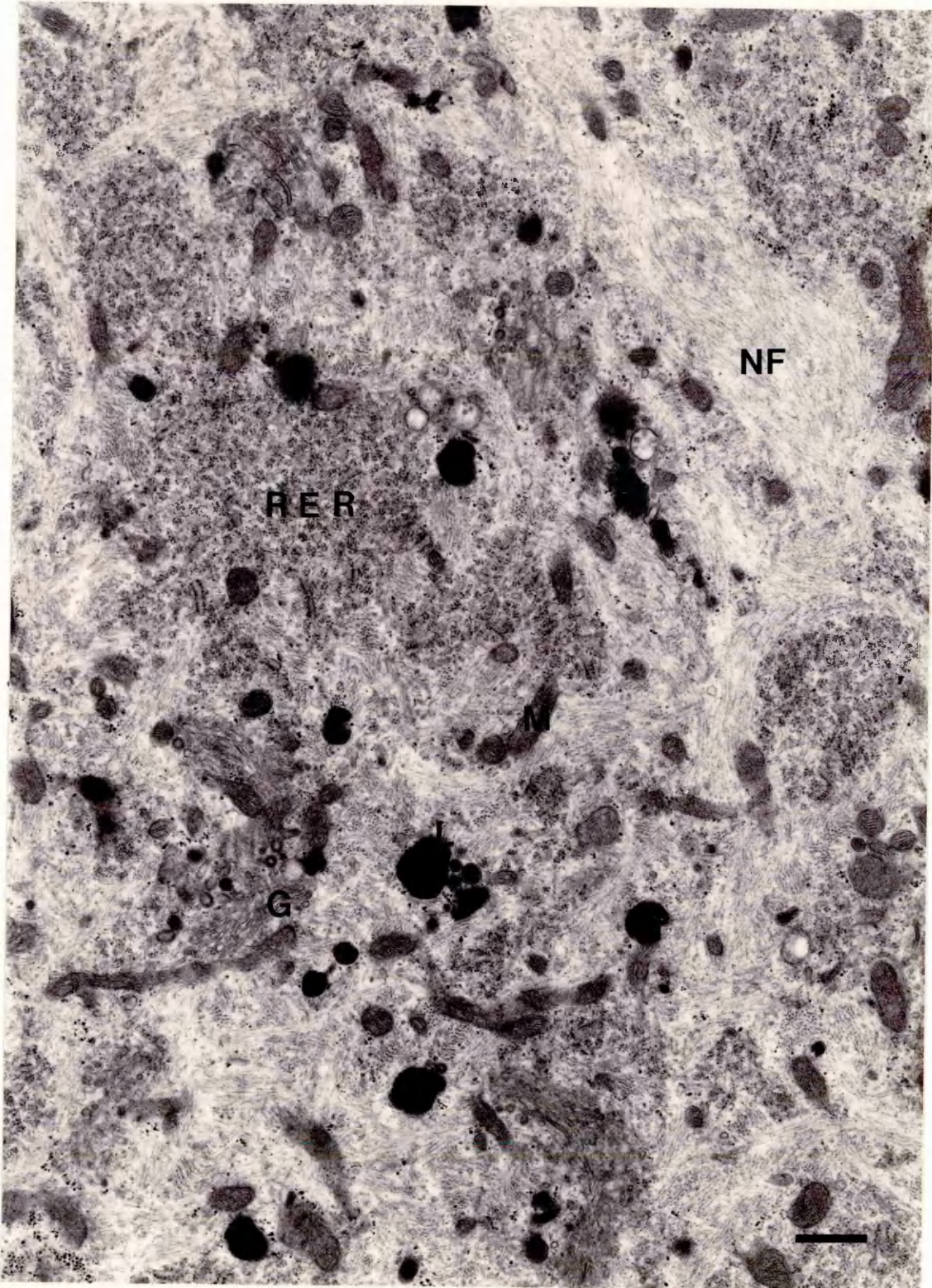


Figure 37

Large light neurone, lumbar dorsal root ganglion, cat

(10 days duration)

The nucleus and nucleolus appear normal, apart from the presence of a small ring nucleolus (arrow).

Golgi complexes (G) are hard to identify, and would appear to be greatly reduced in number. There are large quantities of normal-looking RER, but in one area (* and inset) the RER is disrupted by long, fairly straight smooth membranes. One of these appears to extend beyond the RER and passes through a structure which may be a Golgi complex (inset, arrowhead).

Bar = 2 μ m.

(Inset bar = 1 μ m).

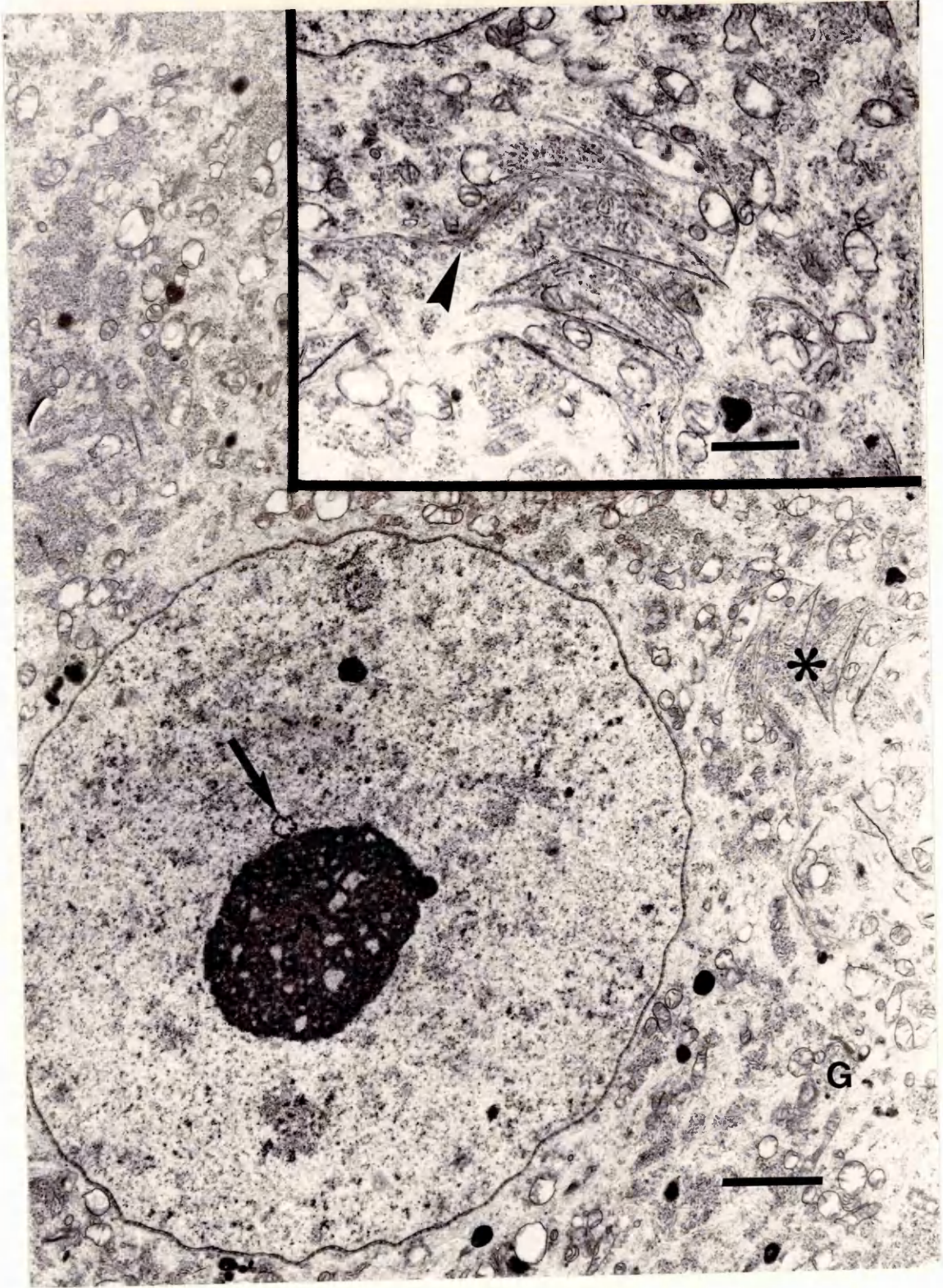


Figure 38

Large light neurone, lumbar dorsal root ganglion, cat

(7 days duration)

RER is present, but not in the usual cisternal pattern (RER). Ribosomes are clumped as polysomes and the membranous component formed into numerous small smooth-walled vesicles. This abnormal RER still tends to remain in discrete areas of the cytoplasm. One region of RER contains long, fairly straight, paired smooth membranes (arrows).

The Golgi complexes (G) are prominent and relatively normal, although their 'trans' most cisternae appear slightly more distended than normal.

Mitochondria, lysosomes, neurotubules and neurofilaments (where visible) all appear normal.

A small collection of smooth-walled vesicles, possibly denuded RER, can be seen at the periphery of this cell (arrowhead).

Bar = 2 μ m.

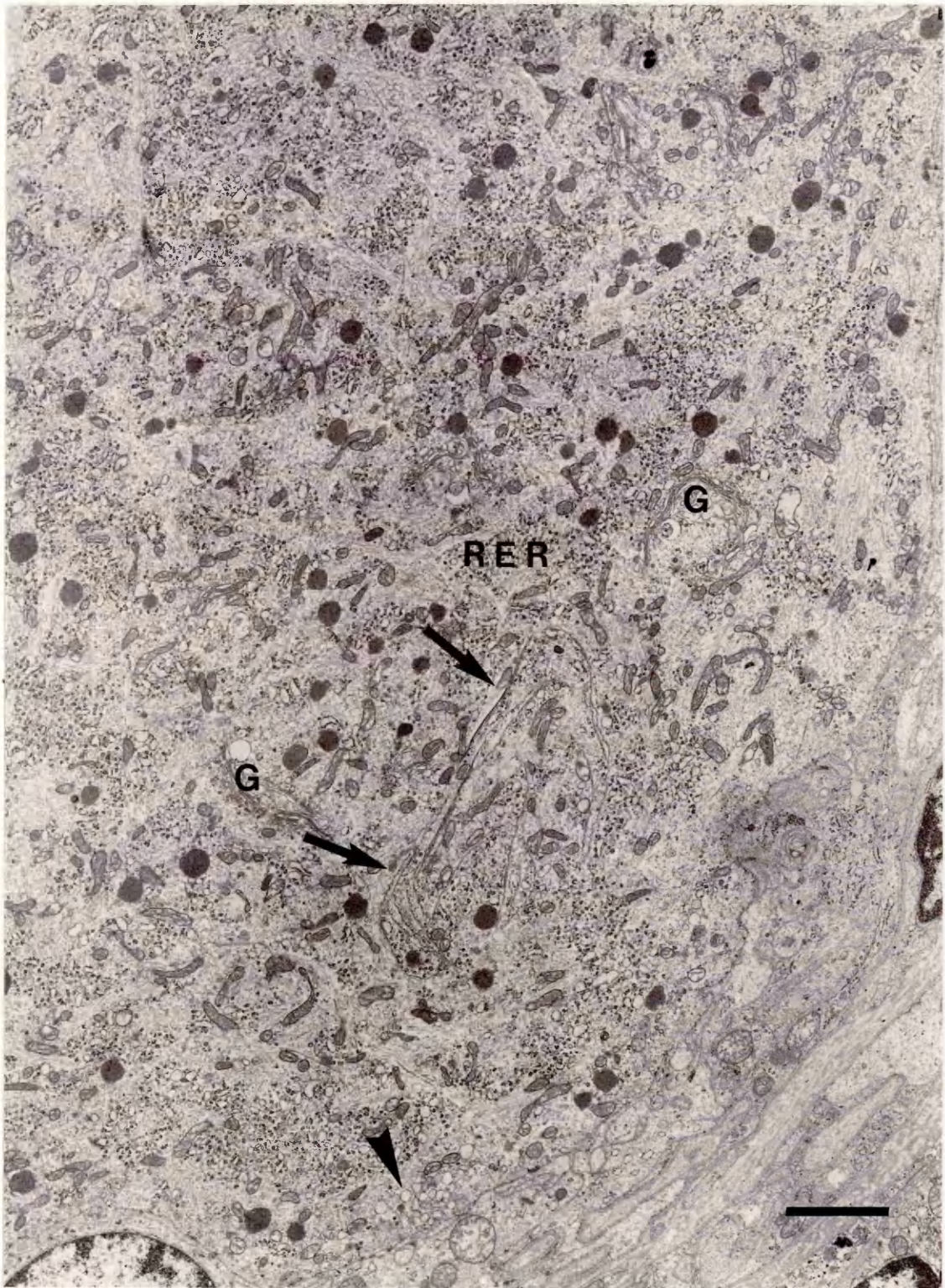


Figure 39

Large light neurone, lumbar dorsal root ganglion, cat

(10 days duration)

Normal RER and Golgi complexes cannot be identified. Mitochondria appear normal, but greatly increased in number. The cytoplasm is filled with numerous small vacuoles which on close inspection appear to be mostly related to areas of disrupted RER (arrow). Lysosomes appear normal.

Bar = 3 μ m.



Figure 40

Normal ventral horn cell, cat

These cells have a very similar appearance to normal neurones described earlier. The cytoplasm contains much RER, which occurs as discrete Nissl granules (RER). Golgi complexes (G) are prominent. Mitochondria are numerous. Lysosomes, neurofilaments and neurotubules are also visible.

Bar = 2 μ m.

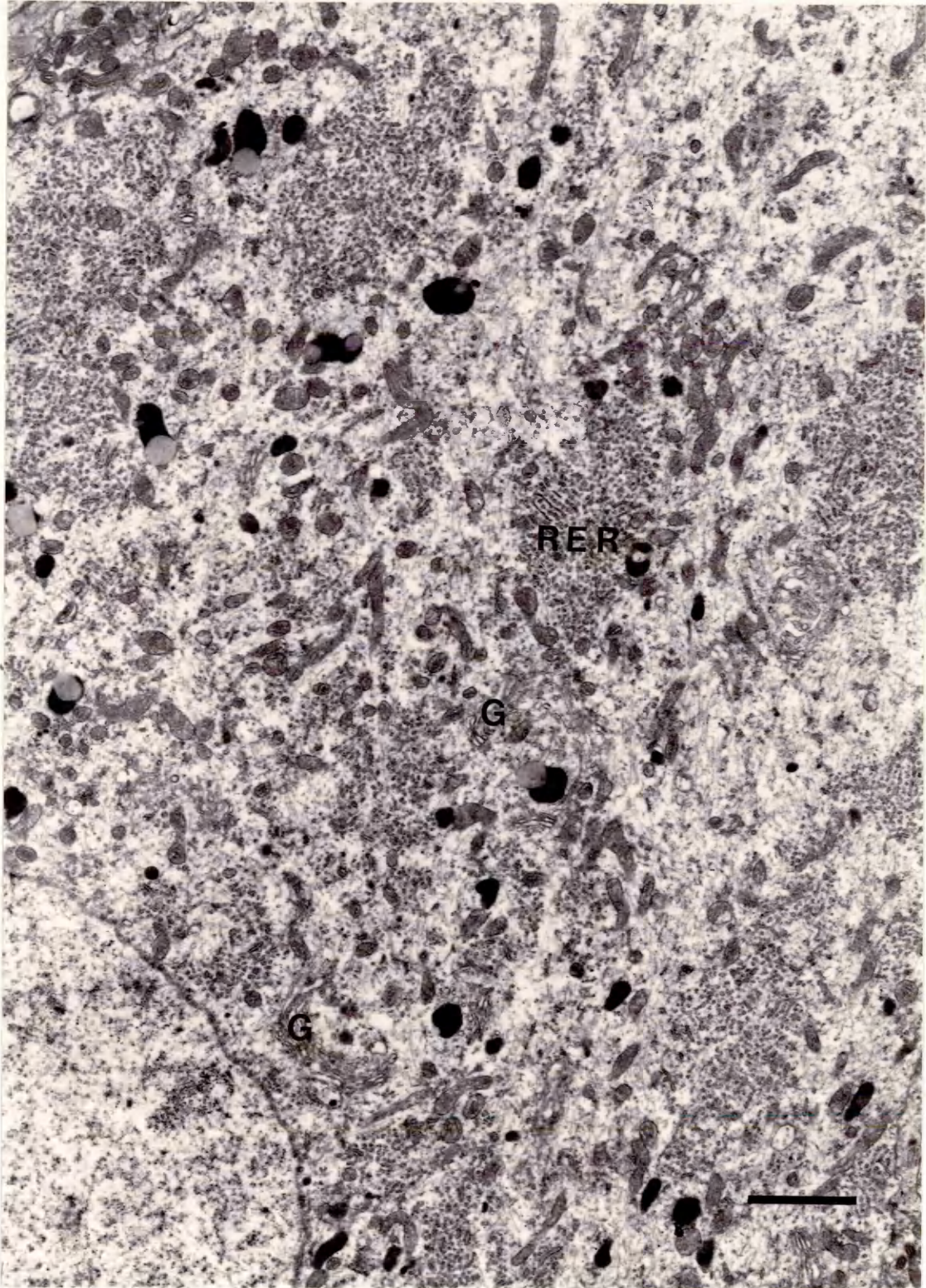


Figure 41

Ventral horn cell, cat (3 days duration)

No RER or Golgi complexes can be seen. The cytoplasm is filled with a variety of smooth membranous profiles and greatly increased numbers of apparently normal mitochondria (M).

There is an area of cytoplasm at the periphery of the cell (arrows) which contains very few of the mitochondria which fill the remainder of the perikaryon.

Bar = 1 μ m.

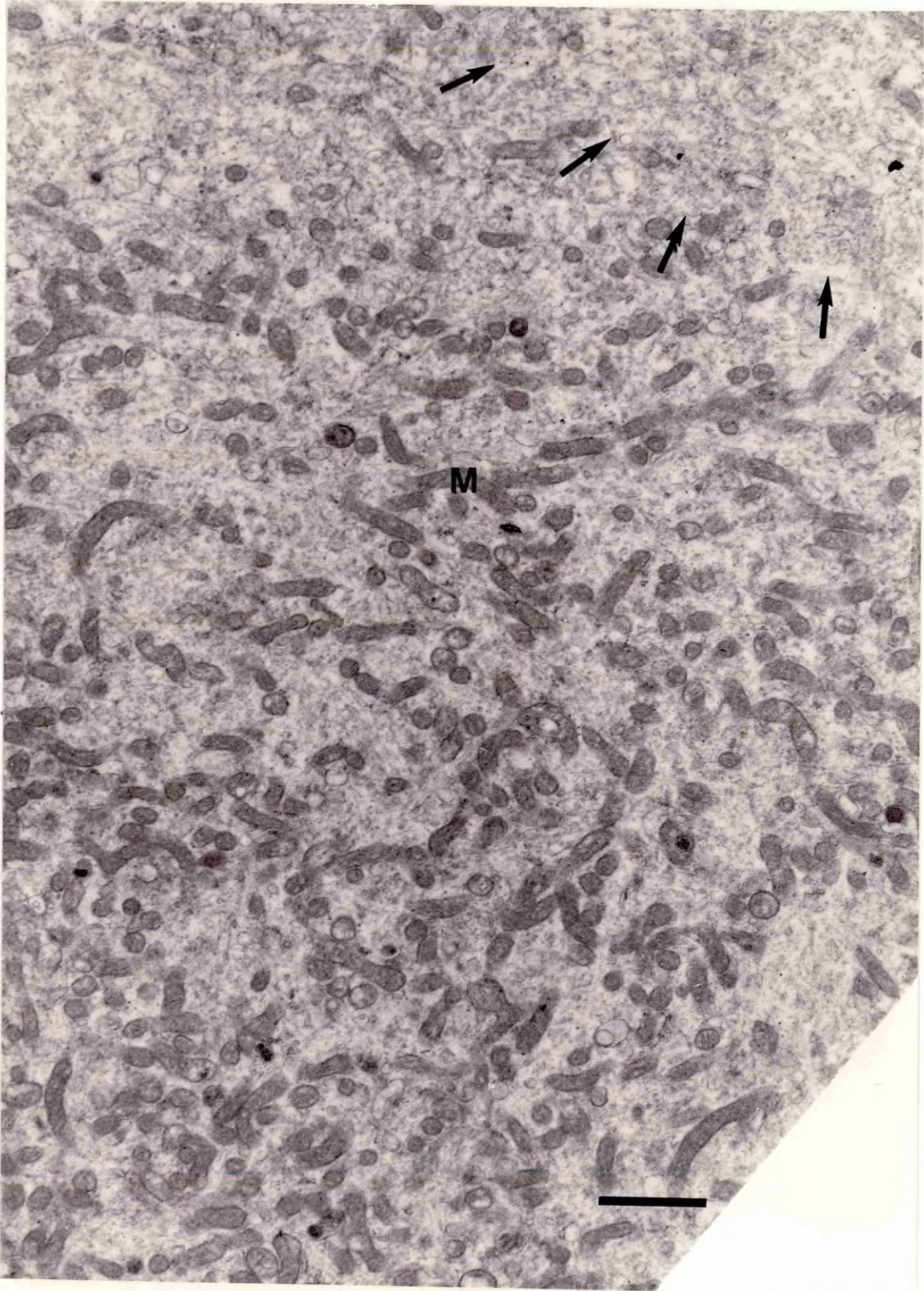


Figure 42

Ventral horn cell, cat (3 days duration)

Numerous distended cisternae of RER (arrows) at the periphery of a ventral horn cell, associated with small clumps of ribosomes (R). The cytoplasm also contains several arrays of SER (arrowheads).

Bar = 0.5 μ m.

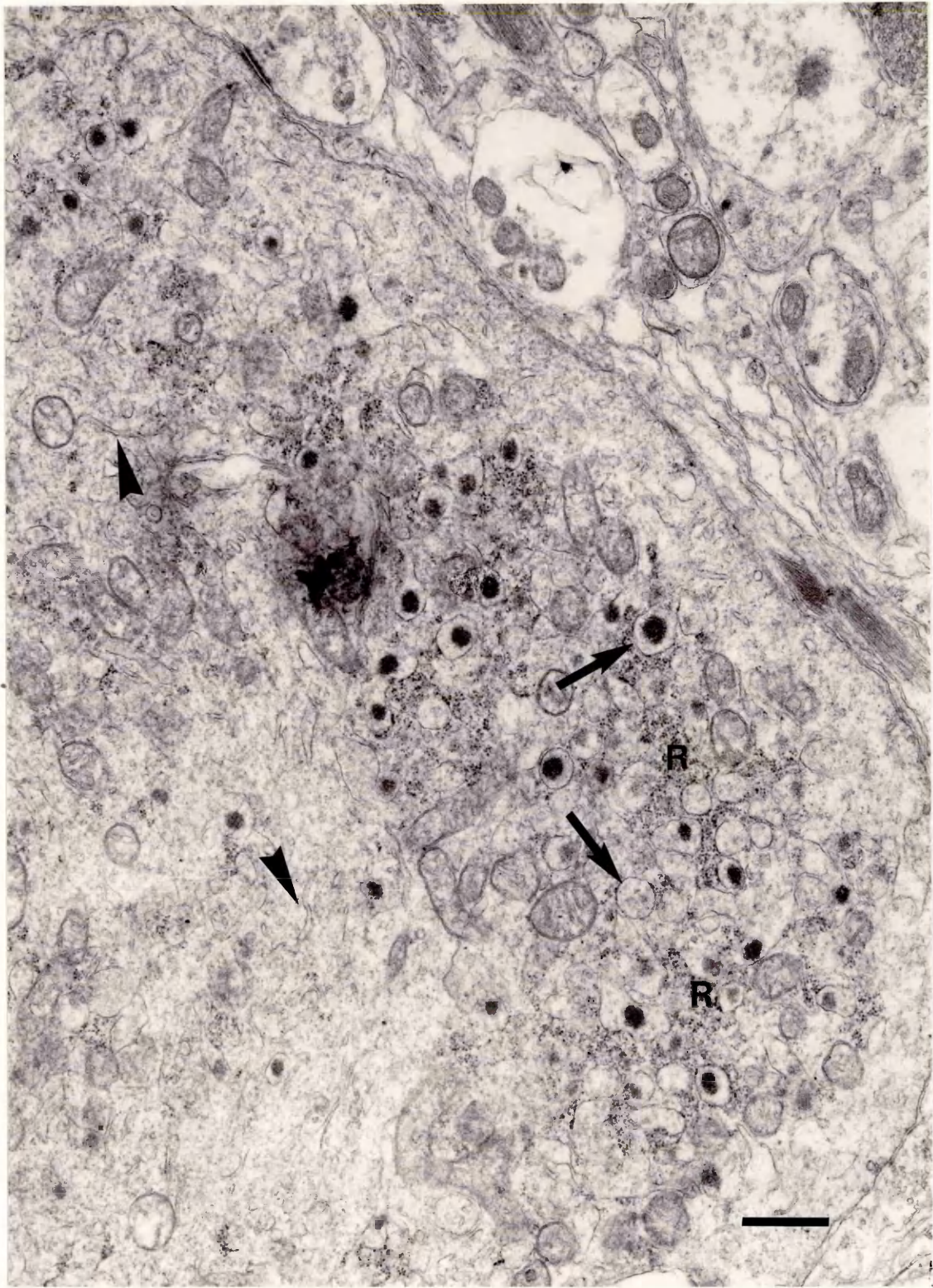


Figure 43

Ventral horn cell, cat (3 days duration)

The cytoplasm contains mostly small vesicular profiles of SER (SER). No normal RER can be seen, but there are occasional distended cisternae, filled with electron-dense floccular material, with ribosomes attached (arrows). Mitochondria (M) appear normal. The lysosomes (L) show secondary activity.

Bar = 0.5 μ m.

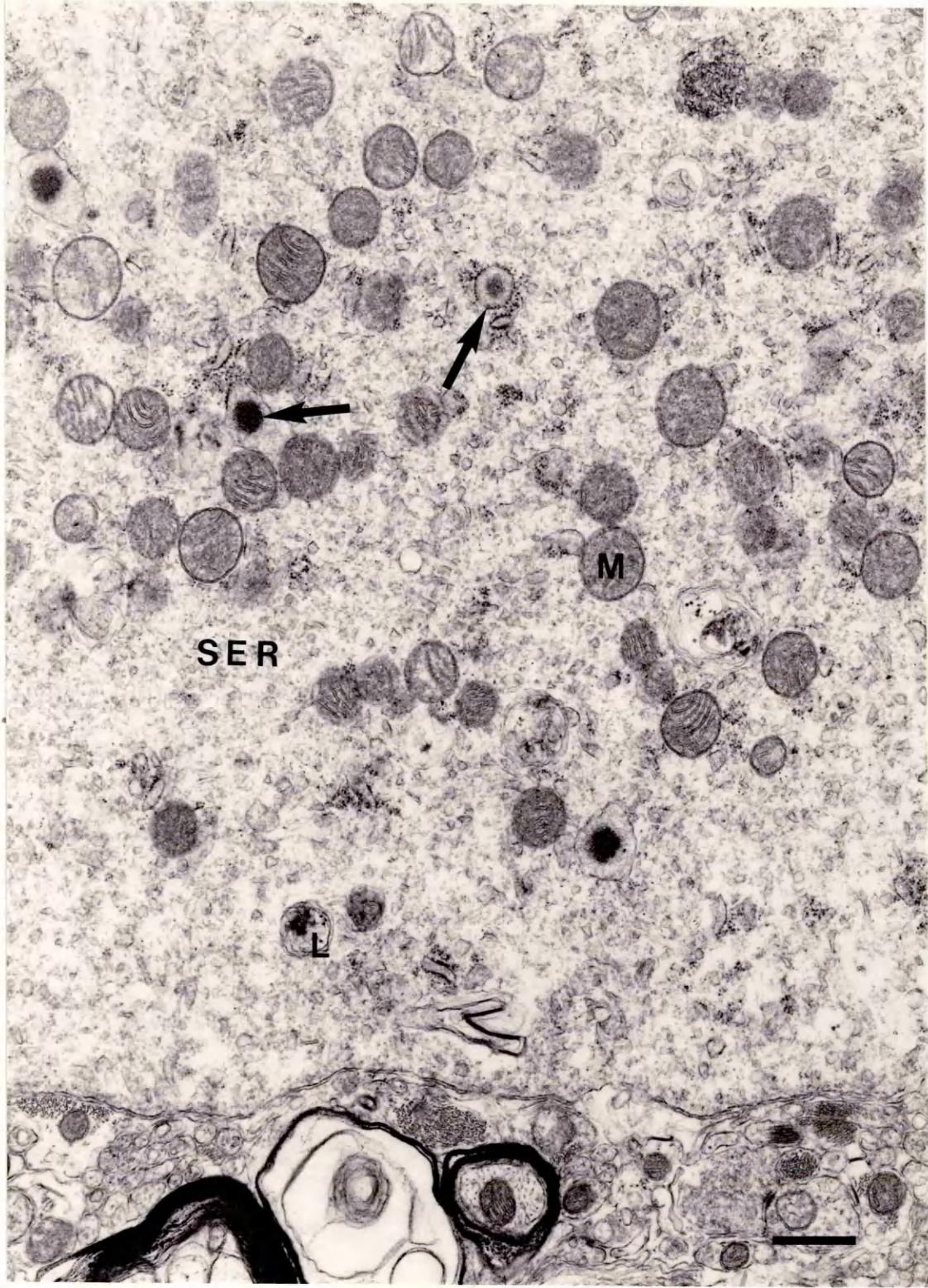


Figure 44

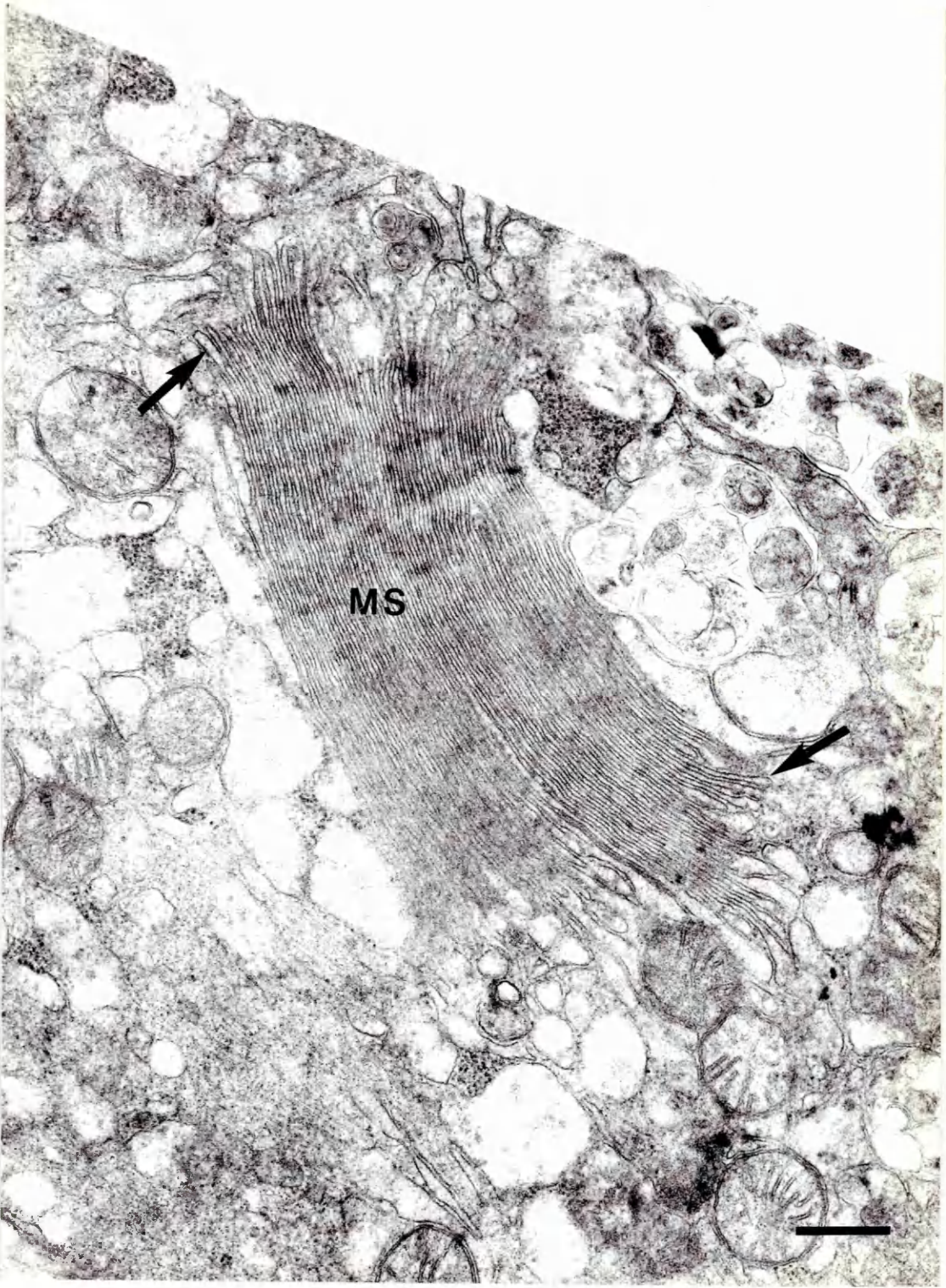
Affected neurone, dorsal nucleus of the vagus, cat

(13 days duration)

A membranous stack (MS) in a central autonomic neurone. Like those in peripheral autonomic neurones it consists of flattened, smooth membranous cisternae in a compact parallel array.

The 'cisternal' arrangement of these membranes can be clearly seen, where they are slightly distended at the edges of the stack (arrows).

Bar = 0.5 μ m.



ENZYME CYTOCHEMISTRY

INTRODUCTION

The ultrastructural morphology of the neuronal perikaryon in cases of dysautonomia has been well documented (Gilmour, 1975; Sharp *et al.*, 1984; Griffiths *et al.*, 1985; Pollin and Griffiths, 1987) and is discussed in detail in the previous chapter.

One of the earliest and most consistent changes in affected neurones is the absence of a recognisable Golgi complex and, in peripheral feline autonomic neurones, the frequent finding of stacks of parallel smooth membranes which have been postulated to arise from the Golgi apparatus (Sharp *et al.*, 1984).

Different areas of the Golgi complex have specific, discrete membrane components which can be demonstrated cytochemically, and numerous methods have been described for the specific staining of Golgi complexes at an ultrastructural level (see review, pages 27 and 28).

The aim of this study was to investigate whether any of the membranous profiles or cisternae in dysautonomic neurones could be shown to have originated from the Golgi complex by using specific ultrastructural cytochemical methods.

BACKGROUND TO METHODS

General considerations

Enzyme cytochemical methods are a well-documented means of localising enzyme activity ultrastructurally. They are based on the principle that a substrate is broken down by enzyme actions, and the product from this reaction then reacts with a 'capturing agent' which forms with it an insoluble compound known as the final reaction product. In the case of both enzymes studied in

this section, a free phosphate ion is split from the relevant substrate, and reacts with lead ions to form insoluble lead phosphate.

Although certain components of the incubation medium are specific for the enzyme being demonstrated, the following basic principles are observed in each case.

Fixation is required to preserve cellular structure and in general, substrate and capturing agent will diffuse much more rapidly if the semipermeable properties of the cell membranes have largely been destroyed.

Enzyme activity must also be preserved, and susceptibility varies greatly, not only between enzymes. The same enzyme may show differing susceptibilities to fixatives in various species, or even different tissues from the same species (Lewis, 1977). No generalisations can therefore be made regarding fixation procedures.

This sensitivity to fixation was also described by Novikoff et al. (1971) who demonstrated a decreasing stain intensity with increasing fixation time. Ogawa and Sakai (1982) also demonstrated that the activity of TPPase in fixed tissue was only 20-25% of that in fresh tissue.

Good penetration of reagents during incubation only occurs if the tissue block is thin enough, 50 - 100 μm in at least one dimension being the general rule for most enzyme cytochemical methods. Requirements for post-fixation of tissue depend on the stability of the final reaction product. Lead phosphate is considered relatively stable (Lewis, 1977), so post-fixation is

optional, unless primary fixation is minimal (e.g. if enzyme very susceptible to fixative, which was not the case in this study).

It was decided to examine two enzymes - thiamine pyrophosphatase, which is localised in 'trans' Golgi membranes, and acid phosphatase which occurs in lysosomes. Although the techniques for these are both well established, no references to their use in the autonomic nervous system could be found, and several problems were encountered in the introduction of these methods to this laboratory, which had no previous ultrastructural enzyme cytochemical experience.

Preliminary Work

This was carried out for TPPase, using epididymis from various species, chosen because of the presence of well-developed Golgi complexes in these cells, and the fact that the tissue could be obtained without killing the donor. Autonomic tissue from dogs being killed for other clinical reasons was also used, when available.

Several fixatives were tried, with varying concentrations of aldehydes:- 1% glutaraldehyde, 0.25% paraformaldehyde; 4% paraformaldehyde, 0.25% glutaraldehyde; 2.5% glutaraldehyde, 1% paraformaldehyde containing sucrose (I. Montgomery, personal communication) and 1.5% glutaraldehyde with 4% polyvinylpyrrolidone (PVP) (Angermuller and Fahimi, 1984), the sucrose and PVP being added to maintain the osmolality of the solution. Fixation time varied from 1 - 3 hours, and the fixation to incubation time was 16 - 48 hours.

The original TPPase incubation media were based on the lead capture methods of Novikoff and Goldfischer as cited by

Angermuller and Fahimi (1984) and those authors' own cerium capture method.

These methods led to varying success, with incubation times considerably longer than the more usual 90 minutes being required initially to achieve results (i.e. several hours, and in some cases overnight). The confining of lead phosphate deposits to the 'trans' cisternae of the complex did not obviously occur in these early examples although deposit was specific for Golgi membranes (Figures 45 and 46). Cerium capture appeared to have greater specificity, and the final reaction product was evenly dispersed along the cisternae, compared to the more irregular "blotchy" effects of lead capture.

Following personal communication with Dr. P.M. Novikoff, the methods described in detail below were adopted for TPPase. No problems were encountered in transferring this technique from epididymis to neuronal tissue.

For AcPase demonstration, the fixation protocol of Novikoff (personal communication) was followed, and the incubation medium was that of Novikoff and Yam (1978). This was not introduced until the TPPase methods were established.

In some cases the incubation media contained the permeabilising agent Triton-X (0.0001%) (Robinson, 1985). This had no appreciable effect on the outcome compared to control incubations containing no Triton-X.

Prolonged Osmification

Prolonged osmification (Lewis and Knight, 1977) was also attempted as a means of demonstrating the 'cis' membranes of the

Golgi complex. Tissue blocks were fixed in 1% osmium tetroxide in isotonic cacodylate buffer for one hour, then incubated in 1% aqueous osmium tetroxide at 37°C for 48 hours, this aqueous osmium being changed once after approximately 24 hours incubation.

The tissue was then washed several times in isotonic cacodylate buffer and dehydrated and embedded in the routine manner (Appendix 1). Despite apparently consistent technique, the success of this method was highly variable so, when demand on the tissue for other investigations was high, prolonged osmification was not used.

In those cases where it worked, however, it proved a very specific marker of Golgi membranes (Figure 47). This method was not used for any affected tissue, and is therefore not discussed elsewhere.

MATERIALS AND METHODS

Autonomic tissue (stellate, coeliacomesenteric or cranial cervical ganglion) was obtained from both normal (i.e. non-dysautonomic) and affected cats and horses post-mortem, as described on page 37. Tissue from three normal cats and 11 normal horses was available, and two affected cats (duration seven days, and six weeks) and nine affected horses (range of duration 20 hours to 17 days) were also examined.

Small blocks, approximately 1 - 2 mm³ were cut by hand within one hour of death, and immersion-fixed for three hours at 4°C in a fixative containing:-

2% paraformaldehyde and 2.5% glutaraldehyde (final concentrations) in 0.1 M sodium cacodylate buffer (pH 7.4)

(Appendix 3) with 7.5% sucrose (P.M. Novikoff, personal communication).

The tissue was then rinsed in buffer (0.1 M sodium cacodylate [pH 7.4] with 7.5% sucrose) at 4°C overnight.

The surface of the blocks was blotted dry, and the tissue mounted in a drop of cyanoacrylate adhesive on the specimen tray of a Polaron DSK Microslicer. When the glue had set (60 - 120 seconds) buffer (as above) was added, and 50 um sections of the tissue cut and collected into fresh buffer.

The slices were then divided into six groups and incubated for 90 minutes in one of the following media. All the components of these media were made within seven days of use (usually within 48 hours) and were mixed immediately prior to use.

(a) TPPase (lead capture) (P.M. Novikoff, personal communication).

Thiamine pyrophosphate chloride (Sigma)	25 mg
Distilled water	7 ml
0.2 M TRIS-maleate buffer (pH 7.2) (Appendix 3)	10 ml
0.025 M manganese chloride	5 ml
1% lead nitrate	1.25 g

The medium was filtered before use, and changed every 30 minutes.

(b) TPPase (lead capture). Control.

As (a) but with no thiamine pyrophosphate chloride.

(c) TPPase (cerium capture) (Angermuller and Fahimi, 1984).

Thiamine pyrophosphate chloride	25 mg
Distilled water	7 ml
0.2 M TRIS-maleate buffer (pH 7.2) (as above)	10 ml
0.025 M manganese chloride	5 ml
30 mM cerous chloride	3 ml
Sucrose	1.25 g

The medium was filtered before use, and changed every 30 minutes.

(d) TPPase (cerium capture). Control.

As (c) but with no thiamine pyrophosphate chloride.

(e) ACPase (lead capture) (Novikoff and Yam, 1978).

Sodium- β -glycerophosphate	25 mg
Distilled water	12 ml
0.05 M acetate buffer (pH 5) (Appendix 3)	10 ml
1% lead nitrate	3 ml
Sucrose	1.25 g

A precipitate was allowed to form, and the medium was then filtered before use.

(f) AcPase (lead capture). Control.

As (e) but with no sodium- β -glycerophosphate.

The slices were incubated in 5 - 10 ml of these media in 25 ml conical flasks in a Grant shaking waterbath.

Following incubation, all samples were rinsed in isotonic sodium cacodylate buffer (see Appendix 3) for 15 minutes, then transferred to fresh buffer and stored at 4°C until processed for electron microscopy by either the routine or 'short' schedule

(see Appendix 1), within three days.

The sections from each of the six groups were embedded as six blocks, rather than individually, and then 60 - 80 nm sections for electron-microscopy were cut with no prior reference to 1 μ m sections. The resulting examinable tissue tended to be long, but only 50 μ m wide.

These thin sections were collected onto copper grids, stained as follows:-

- (i) uranyl acetate only, or
- (ii) uranyl acetate and Reynolds lead citrate (Appendix 2) and examined under a Phillips 301 electron microscope.

RESULTS

Normal

Structural preservation was good in the normal animals, and final reaction product was deposited specifically in the 'trans' Golgi saccules with both the lead and cerium capture methods for TPPase. In a few instances, most of the Golgi cisternae appeared to be involved (Fig. 49), but more commonly only one or two of the cisternae were stained (Figs. 48 and 50).

Non-specific deposits were uncommon, and where present (Fig. 49) their fine nature did not interfere with interpretation of the result.

Reaction product for AcPase was not so readily visible, being superimposed on the most dense organelle in the cytoplasm, the lysosome.

However, close examination of the numerous dense bodies revealed collections of small lead phosphate deposits associated

with the great majority of these (Figs. 51 and 52) and in occasional neurones the vesicles associated with the 'trans' Golgi cisternae contained AcPase activity (Fig. 53).

The appearance of the results of these cytochemical techniques was essentially similar in the cat and the horse, and hence the above comments are applicable to both species.

Affected

Any attempt to demonstrate TPPase activity in affected equine neurones was unsuccessful (Figs. 54 - 56). The fixation was adequate for the identification of the abnormal structures and none of these was stained by this method. Some non-specific deposit was seen in most cases.

Only two affected cats, one of seven days' duration, the other of six weeks' duration, were available for enzyme cytochemistry. Non-specific staining was present in the sections from the more acute case, but there were no concentrated areas of deposit which would suggest specific TPPase activity (Figs. 57 and 58). Small abnormal smooth membranous configurations were present in this case. In the chronic case, section thickness was variable (see Discussion) and structural definition poor, but dense deposits of reaction product in discrete areas of cytoplasm in approximately single, curved configurations would be strongly suggestive of TPPase activity specific to Golgi complexes (Fig. 59).

In contrast, AcPase activity was present in all affected animals, both feline and equine. Lysosomal structures were densely stained, but no abnormal cytoplasmic structures showed reaction product for AcPase (Figs. 60 and 61).

DISCUSSION

The problems associated with establishing the technique have been described at an earlier stage. This discussion is confined to the method ultimately chosen, and the consequent results.

Methodological Considerations

The major difficulty was the small number of neurones which could be examined from each animal; there were a number of contributory factors.

Due to the small number of affected animals available, abnormal autonomic tissue was limited.

Incubated tissue slices were only 50 μm thick; this was necessary to ensure good penetration of the reagents, but very thin samples proved difficult to embed. Initial attempts to embed these for cutting parallel to their greater surface area were unsuccessful, since the slices tended to move about in the Araldite as it warmed before polymerising. It was then decided to cut perpendicular to this surface, which resulted in very long, thin "cross-sections". Several slices were embedded together so that 3-4 different tissue slices could be included on one grid.

These sections were therefore, at most, two neurones wide, and the number of neurones present along the length of the section varied depending on the density of neurones in the original tissue block. Blocks from nearer the edge or ends of the ganglion tended to have a greater proportion of non-neuronal tissue than the central areas, and in animals where tissue was being taken for in vitro protein synthesis studies (see later) the blocks for cytochemistry were mostly obtained from

these peripheral regions.

In affected cats this number was further reduced as overall numbers of neurones in the ganglia can become greatly diminished as the disease progresses.

The cutting of these blocks frequently resulted in fragile sections which were inclined to tear or curl under the electron beam, or contained Araldite with holes where the tissue had been completely torn out during cutting.

The processing schedule had been shortened (Appendix 1) on the basis that slices were so thin that penetration of Araldite would be complete in a shorter time, and the cutting difficulties were initially attributed to the possibility that, in fact, penetration of the Araldite was inadequate with this schedule. However, these difficulties persisted when the normal 3-day schedule was reintroduced.

It was then decided that this tearing could be caused by the differing physical properties of the reaction product and the tissue. The metallic reaction product is much harder than the surrounding tissue and therefore more difficult to cut, especially if the knife was not new. It could also cause uneven wear of the cutting edge resulting in possible poor quality of other parts of the section. Any non-specific deposits on the surface of the slice might similarly interfere with cutting, weakening the surrounding section and resulting in holes and a tendency for tearing to occur in the microscope beam. This was confirmed by Lewis (1977) who states that, with regard to enzyme cytochemistry methods, "the cutting of ultrathin sections may

pose many problems even to workers with plenty of experience of routine EM material".

The sections tended to be no more than one 'grid square' wide, therefore the tearing of one square resulted in the loss of the section at that level. Also, if positioning of the section on the grid was unfortunate, almost the entire section could be occluded by a single grid-bar.

In good sections there were rarely more than 10-12 neurones, several of which might have sustained some form of cutting artefact, but more usually only 3-4 neurones were examinable. While being sufficient for defining 'normality', this greatly restricted the observations possible in affected neurones, particularly in the cat, where there were fewer neurones to start with.

The membrane stacks found in some affected peripheral neurones in the cat were of particular interest in this study. It was extremely disappointing that only one cat in the acute stages of the disease was available for examination. From this case it would appear that there is no specific staining of these membranes. There was, however, more non-specific staining than in the normal animals.

An undoubted criticism of this experimental protocol is that while negative controls were provided by omission of the substrate, there was no positive control to ensure that the method was working.

Several options were considered for the provision of a normal control. As the technique had been established in epididymis, it was decided to use that tissue from affected

animals (where possible) as a control. Unfortunately all the animals available were either females or castrated males so this was not possible. Liver samples were taken from two cases, but only non-specific deposit was seen. Given the sensitivity and tissue variability of the enzymes to fixation (as discussed in the introductory section of this chapter) these results were not interpretable. A similar argument applies to the introduction of species' variables by using rodent tissue as a control. A further factor in the case of samples obtained from equine cases in Edinburgh was the transport back to Glasgow during fixation in a potentially variable environment.

It was therefore decided to rely on the unpredictable occurrence of normal neurones in the equine tissue, and to use the non-autonomic jugular ganglion from cats, since only a very small percentage of neurones in this ganglion are affected in dysautonomia. Unfortunately the one neurone on the jugular ganglion section from the dysautonomic cat was affected and contained no Golgi complexes.

As an additional safeguard, the method was routinely 'tested' on normal tissue, when available, as a form of "spot-check" on laboratory and operator techniques, and at no time during the period when the affected tissue was being handled did these methods fail to work on normal tissue. As a consequence of this, it can reasonably be assumed that the results obtained were genuine.

Results

There was no TPPase activity in any abnormal structure in affected neurones, and AcPase activity could still be demonstrated in morphologically normal lysosomes, even amid marked cytoplasmic disruptions.

This negative result for TPPase activity does not, however, mean that none of these structures could originally have derived from Golgi membranes.

The enzyme would only be present in membranes derived from the 'trans' side of the Golgi (see page 27). Another possibility is that membranes in abnormal configurations may themselves be abnormal, and that the enzyme is either absent, or present in a non-functioning state, i.e. the only conclusive proof that these membranous stacks, or any other abnormal structure were derived from Golgi complexes would have been the demonstration of TPPase activity. A negative result does not prove this, but nor can it disprove it.

The AcPase results are also difficult to interpret. No neurones were found on grids from cases of medium duration; the animals examined had been ill for either a short period i.e. less than 4-5 days, or much longer, i.e. the chronically ill cat, in which Golgi function was demonstrated by the TPPase method.

AcPase is a glycoprotein, and must therefore undergo modification and packaging in the Golgi prior to its transportation to lysosomes (Bainton, 1981). No reference could be found regarding its half-life, however, so no conclusions can be drawn regarding whether or not glycoprotein is still being produced on the basis of the presence or absence of AcPase. An

assessment of this would require examination of a wide range of disease durations, and information on the half-life of AcPase.

The fact that AcPase activity was demonstrable in abnormal tissue would, however, suggest that the cytochemical methods were indeed working normally on the occasions that affected animals were examined, and that the negative result for TPPase was genuine.

There has been very little work published regarding the use of ultrastructural enzyme cytochemistry as an investigative tool in pathological states. Novikoff and Essner (1962) working in liver, showed that the normally poor-staining, very thin TPPase activity in Golgi membranes seen only in a few cells, became stout, deeply stained threads easily visible in all hepatocytes following bile duct ligation.

Conversely, a failure to demonstrate TPPase activity does not necessarily indicate an absence of the enzyme. Martinez-Rodriguez et al. (1980) suggested that TPPase is synthesised in the ER, but that this area does not stain either because the enzyme is present in insufficient concentration, or that it is in an inactive state.

Laszlo and Knyihar (1975) have studied TPPase activity in axotomised motor neurones. In addition to chromatolytic change and increased numbers of neurofilaments, they demonstrated an increase in the length and number of Golgi cisternae. These cisternae, however, had considerably decreased demonstrable TPPase activity.

It would appear, therefore, that neither the relative proportions of membranes and their associated enzymes, nor the specific activity of these enzymes need necessarily remain the same in cells in which metabolic disturbances have occurred.

Increased acid phosphatase activity, localised to lysosomes has been observed within perikarya following axotomy in both sensory and motor neurones by light microscopic techniques. Chronologically, neurones revealed an increased activity by 24 hours post-operatively, with a peak activity occurring between 15 and 20 days. This is thought to indicate an increase in cellular metabolism in response to regenerative requirements. A return to control levels, reflecting a return to normal morphology, was seen between 30 and 60 days (Glover, 1982).

For regeneration to occur successfully however, a functioning protein synthetic pathway is required. These examples are concerned with altered metabolism of the whole cell in response to general cellular damage and cannot therefore be directly compared with the findings in dysautonomic tissue in which specific disruption of the protein synthetic pathway is postulated.

As mentioned in the summary of protein synthesis, immunocytochemical techniques can be used to demonstrate many specific Golgi membranes and enzymes.

We obtained antibody against bovine galactosyl transferase, kindly donated by Dr. Neil Watt, Department of Veterinary Pathology, Edinburgh University. While this worked well on bovine tissue it was, as is often the case with immunocytochemical methods, species specific, and could not

therefore be used to demonstrate this enzyme, or lack of it, in feline and equine tissue.

Conclusion

While the study cannot confirm or refute the Golgi apparatus as the origin of the membranous stacks it can be stated with reasonable certainty that the majority of affected neurones do not contain Golgi-associated or derived membranes with functionally active TPPase.

Figures 45 - 6I

Figure 45

Mouse epididymis, TPPase, 17 hours incubation

This tissue was fixed for 90 minutes in 2.5% glutaraldehyde, 1% paraformaldehyde (containing sucrose) and incubated for 17 hours in the medium for lead capture after Novikoff and Goldfischer (1961).

The section is stained with uranyl acetate only, and the very dense, profuse lead phosphate deposits present in the Golgi complexes can be easily seen (e.g. arrowhead). Each cell contains one large complex. Some non-specific staining occurs (arrows) but most of the deposit is confined to the Golgi complexes.

Little cytoplasmic detail is distinguishable in this section, Golgi complexes being identified by their characteristic conformation of curved cisternae.

Bar = 2 μ m.

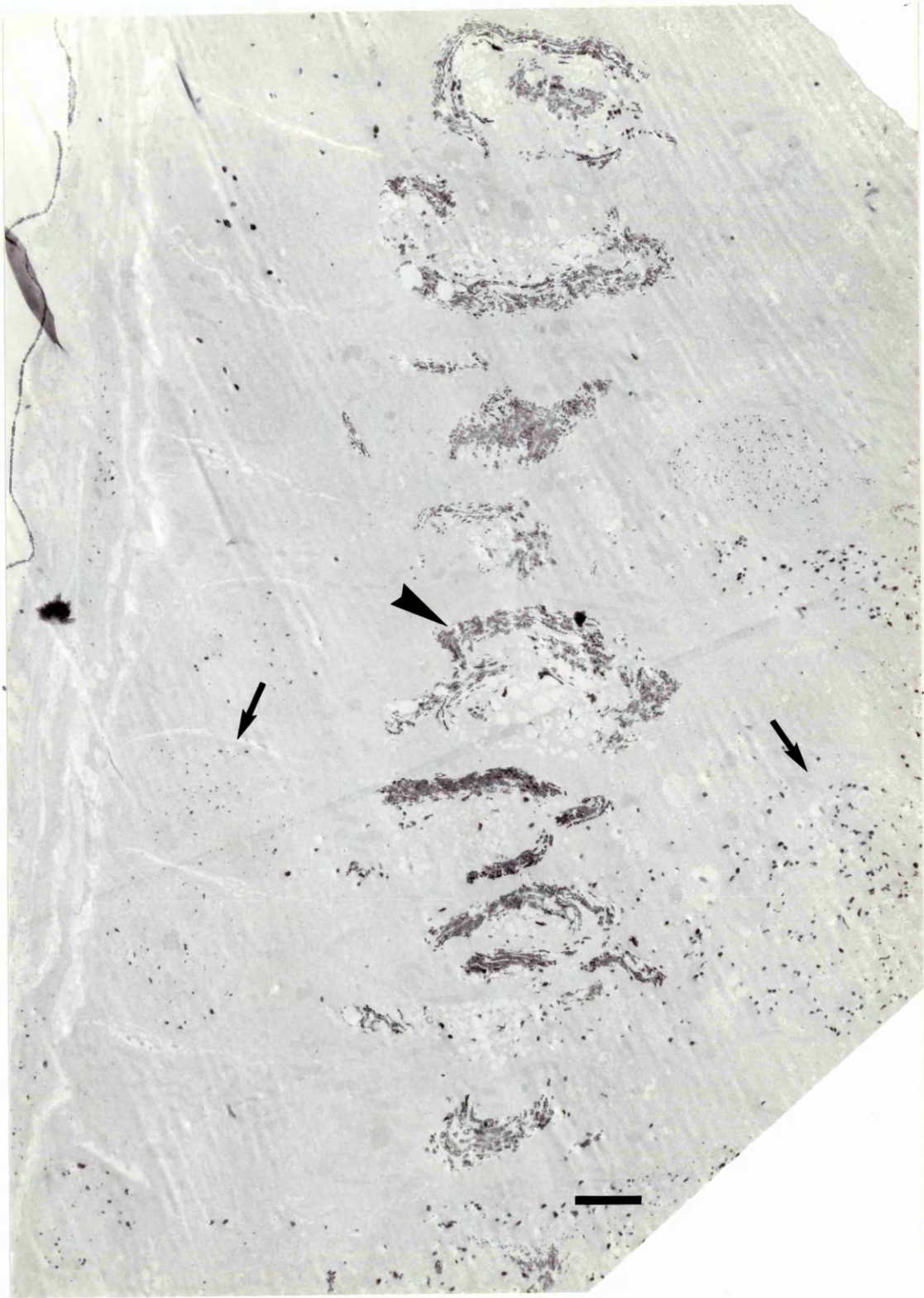


Figure 46

Mouse epididymis, TPPase, overnight incubation

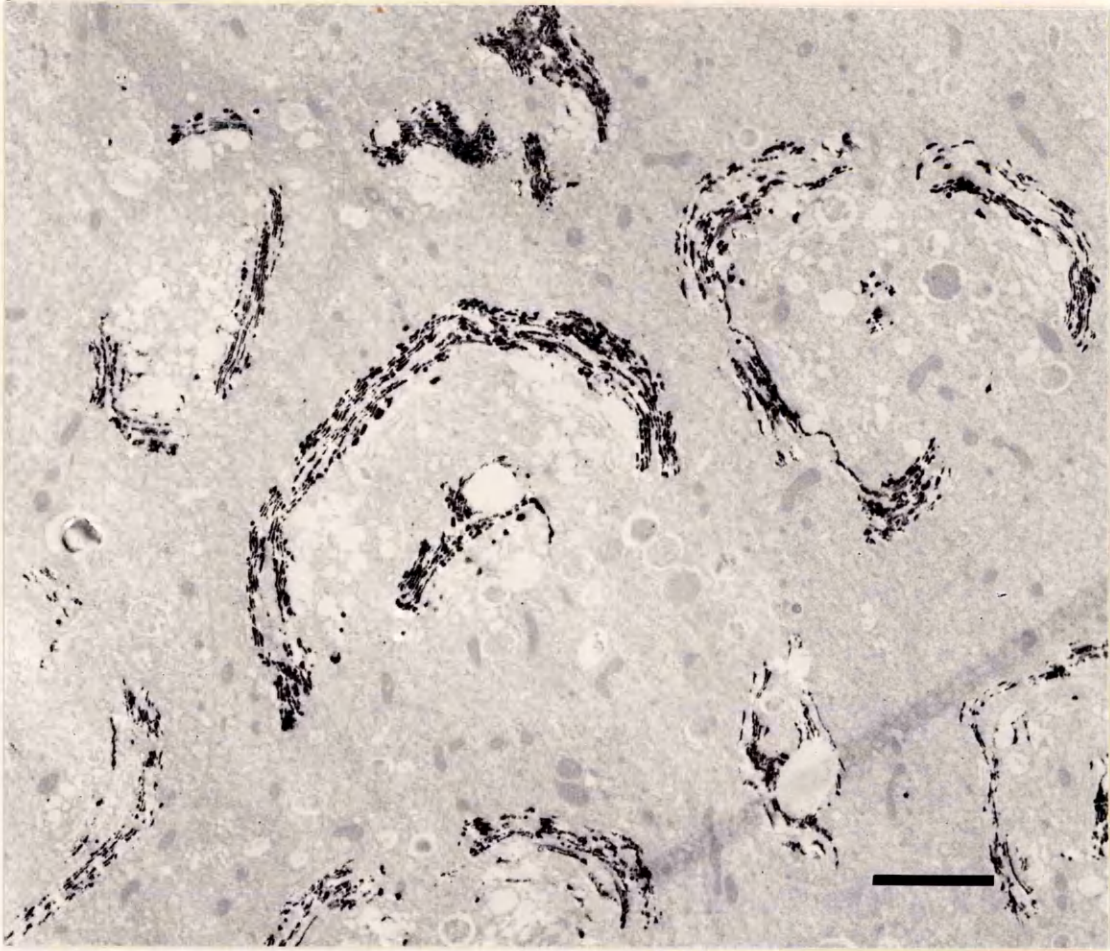
This tissue was fixed for 90 minutes in 2.5% glutaraldehyde, 1% paraformaldehyde (containing sucrose) and incubated overnight for TPPase in either the lead capture medium (Novikoff and Goldfischer, 1961) or cerium capture medium, both presented by Angermuller and Fahimi (1984). In neither section is structural preservation good, with marked distension of some Golgi cisternae.

(a) Lead capture. Stained only with uranyl acetate. Irregular heavy deposits of lead phosphate can be seen throughout the Golgi complexes.

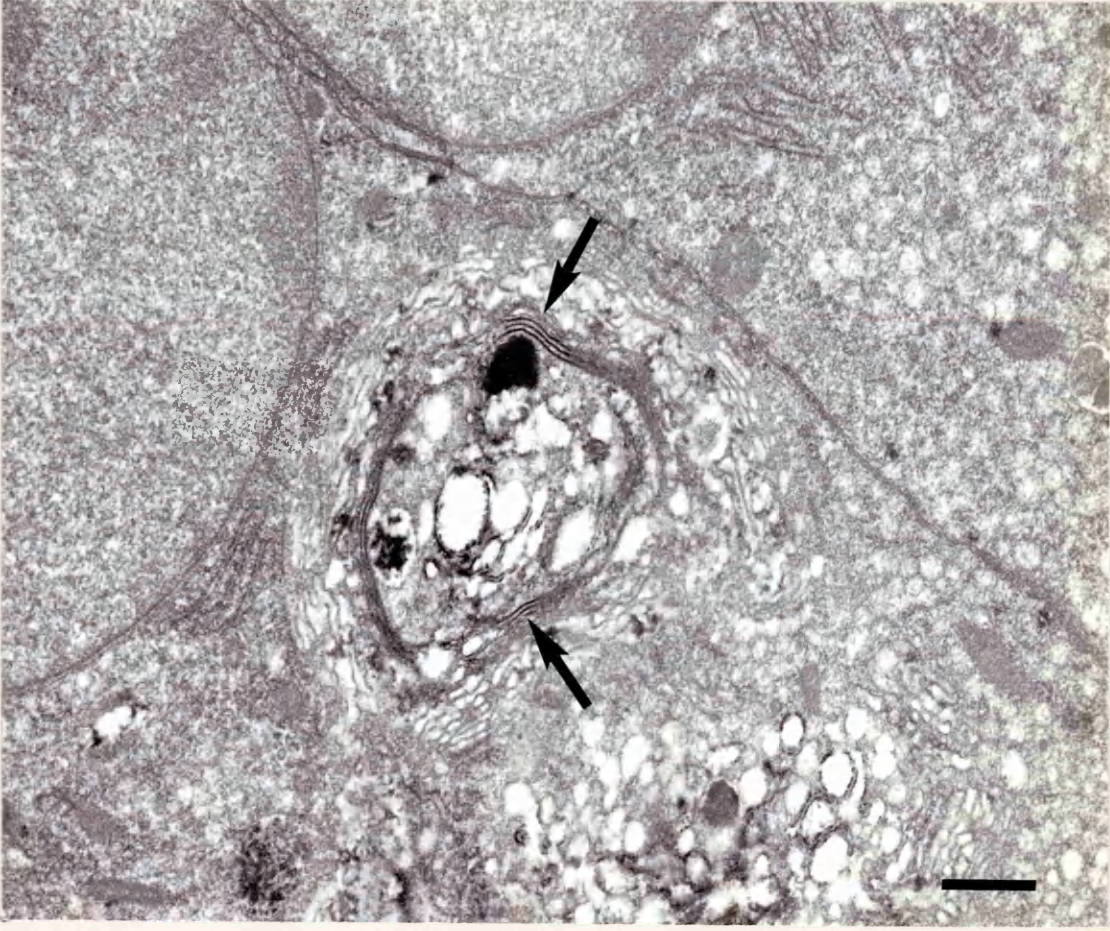
(b) Cerium capture. Stained with lead citrate and uranyl acetate. The much finer, more even deposit appears to be confined to the 2 or 3 trans-most cisternae of the complex (arrows).

(a) Bar = 2 μ m.

(b) Bar = 0.5 μ m.



a



b

Figure 47

Dog ganglion, prolonged osmification

It can be seen that the dark staining is specific for the 'cis'-most cisternae of the Golgi complexes (G).

Bar = 0.5 μ m.

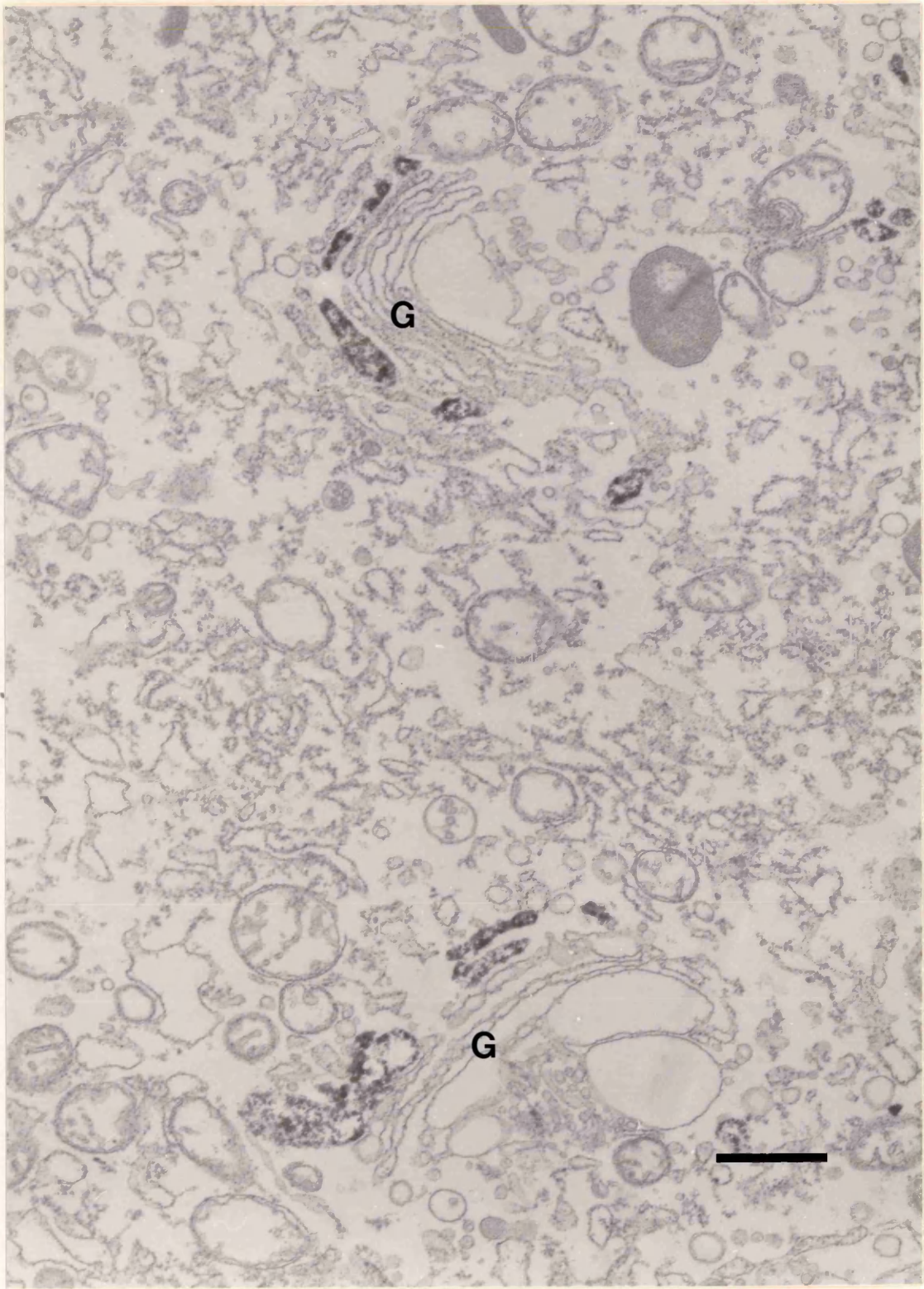


Figure 48

(a) Normal horse, Stellate ganglion, TPPase lead capture

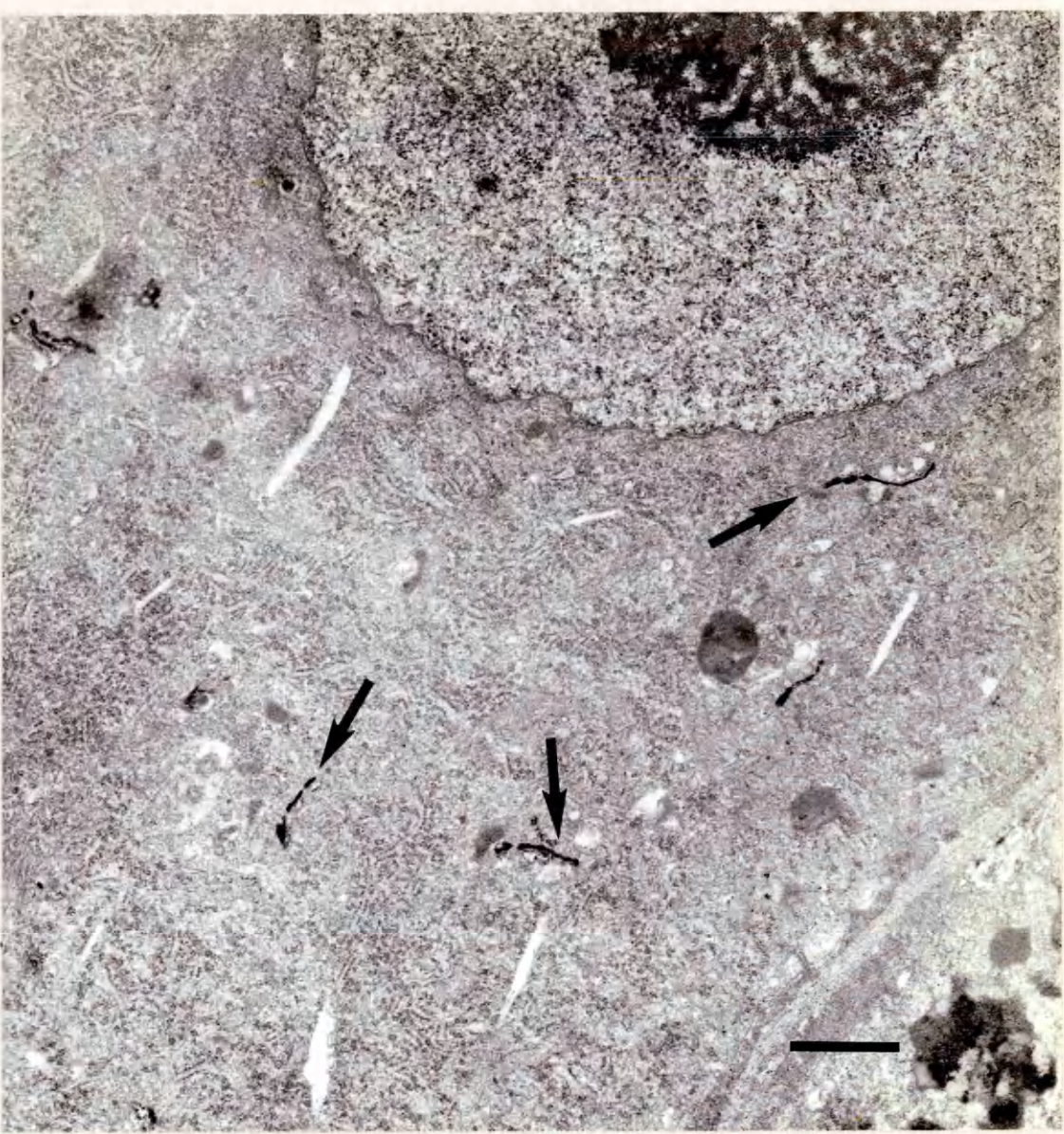
Structural preservation is good, and the perinuclear positioning of the Golgi complexes can be readily identified by the dense reaction product in their 'trans' cisternae (arrows). In general, only single cisternae contain deposit. Stained with uranyl acetate and lead citrate.

(b) Normal horse, Stellate ganglion, TPPase, cerium capture

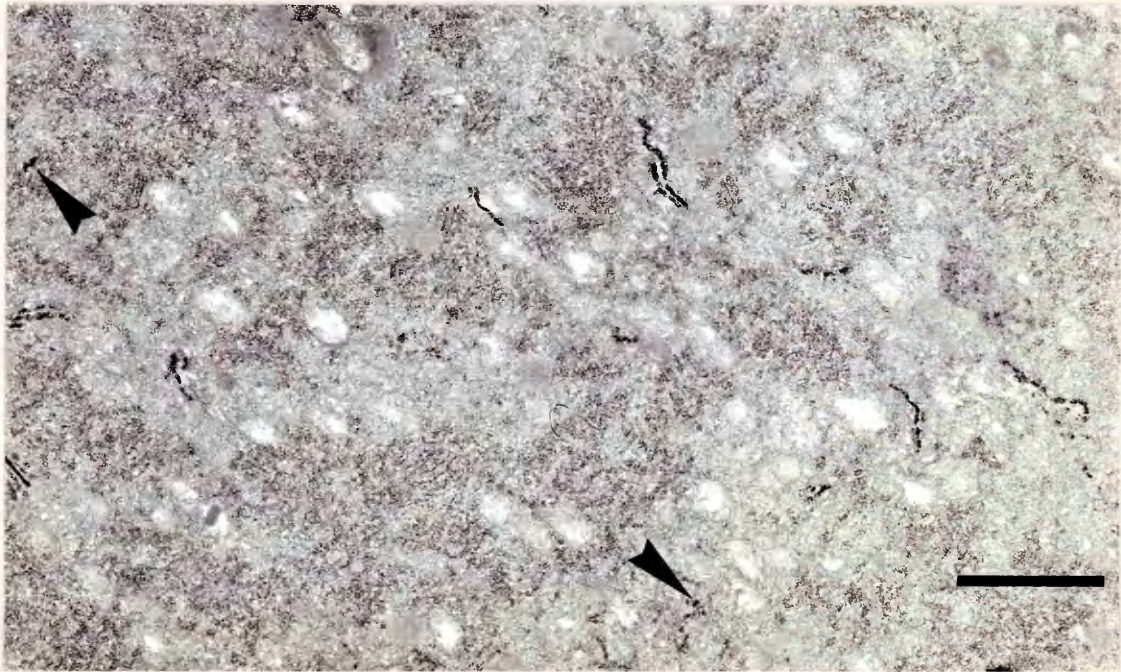
As in (a), Golgi complexes are readily identifiable by the presence of reaction product in their cisternae. Structural preservation is not as good as in (a) and there are occasional areas of deposit (arrowheads) which may be non-specific. Stained with uranyl acetate only.

(a) Bar = 1 μ m.

(b) Bar = 1 μ m.



a



b

Figure 49

Normal horse, Stellate ganglion, TPPase, lead capture

Dense reaction product is present in most of the readily identifiable Golgi cisternae. Occasional associated vesicles also apparently contain reaction product (arrows) but this may be a combination of patchy staining and the plane of section through the 'trans' most cisterna. The rest of the section is covered by a fine, non-specific deposit. Stained with uranyl acetate only.

Bar = 0.5 μ m.



Figure 50

Normal cat, Stellate ganglion, TPPase, lead capture

Reaction product is mostly confined to the 'trans' cisternae of the Golgi complexes and associated vesicles (arrowheads). Several small, apparently non-specific deposits are also present (arrows), but these are not generalised, as in Figure 5.

Structural preservation is very good. Stained with uranyl acetate and lead citrate.

Bar = 0.5 μ m.

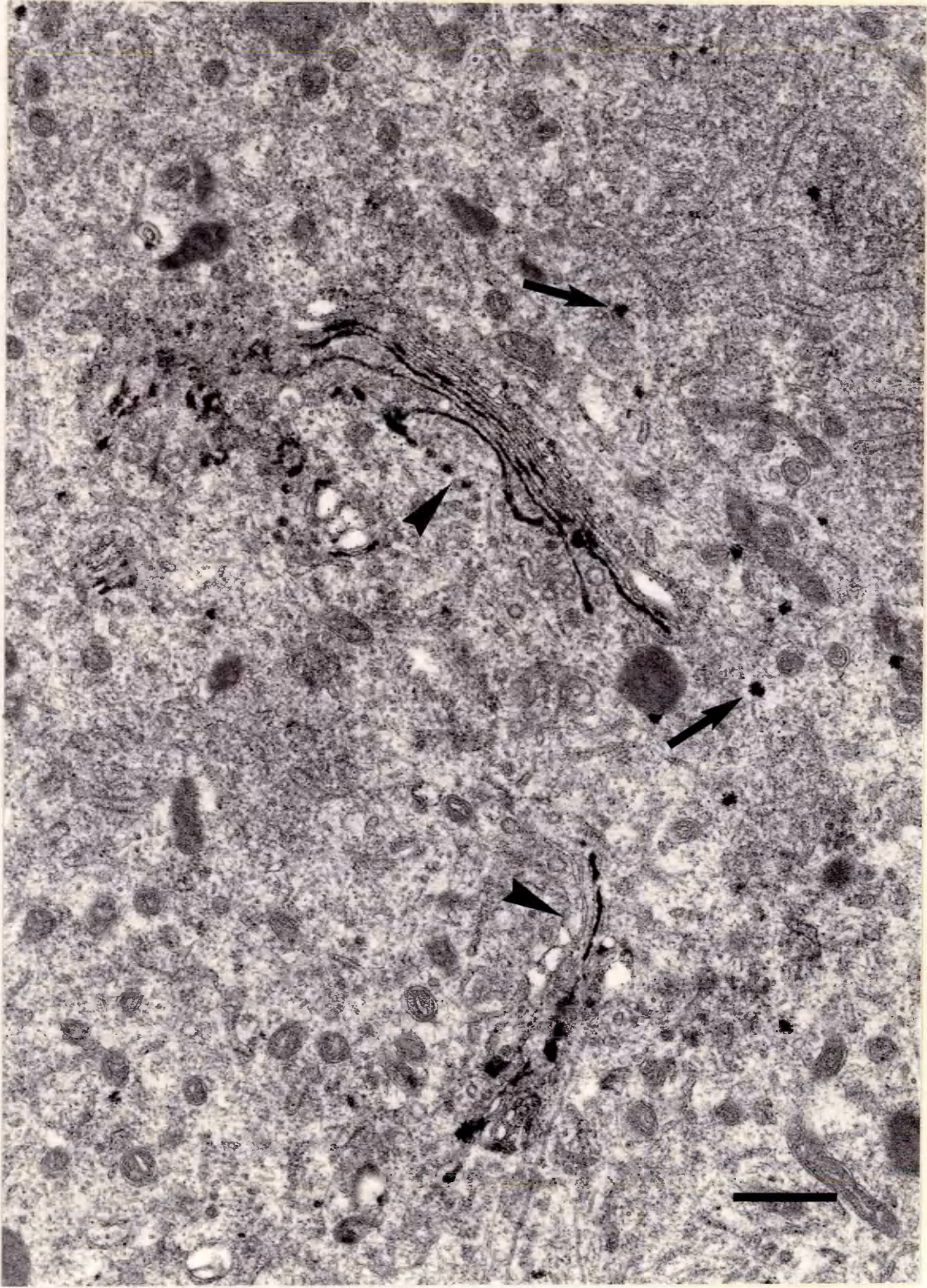


Figure 51

Normal horse, Stellate ganglion, AcPase

Small, dense, irregular deposits of reaction product can be seen in most of the dense bodies (arrowhead), although a few smaller lysosomes appear unstained (arrow). This can be more clearly seen at a higher magnification (inset, arrowhead). There is no non-specific deposit.

Stained with uranyl acetate and lead citrate.

Bar = 1 μ m.

(Inset bar = 0.5 μ m).

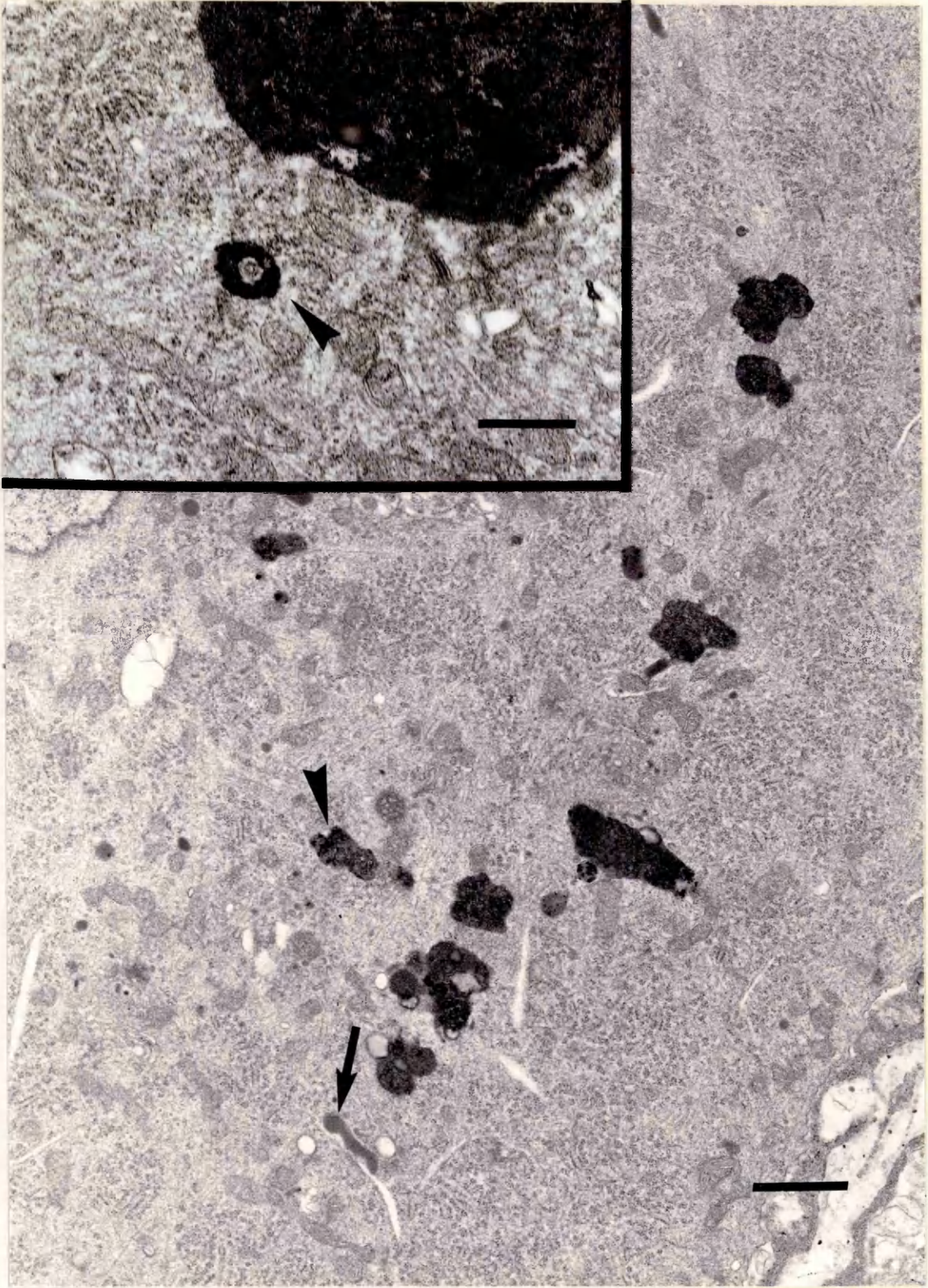


Figure 52

Normal cat, Stellate ganglion, AcPase

Reaction product is superimposed on the lysosomes. Some appear more densely stained than others, and occasional dense bodies do not demonstrate any AcPase activity in this section (arrow). Some non-specific deposits are present (arrowheads). Stained with uranyl acetate and lead citrate.

Bar = 0.5 μ m.

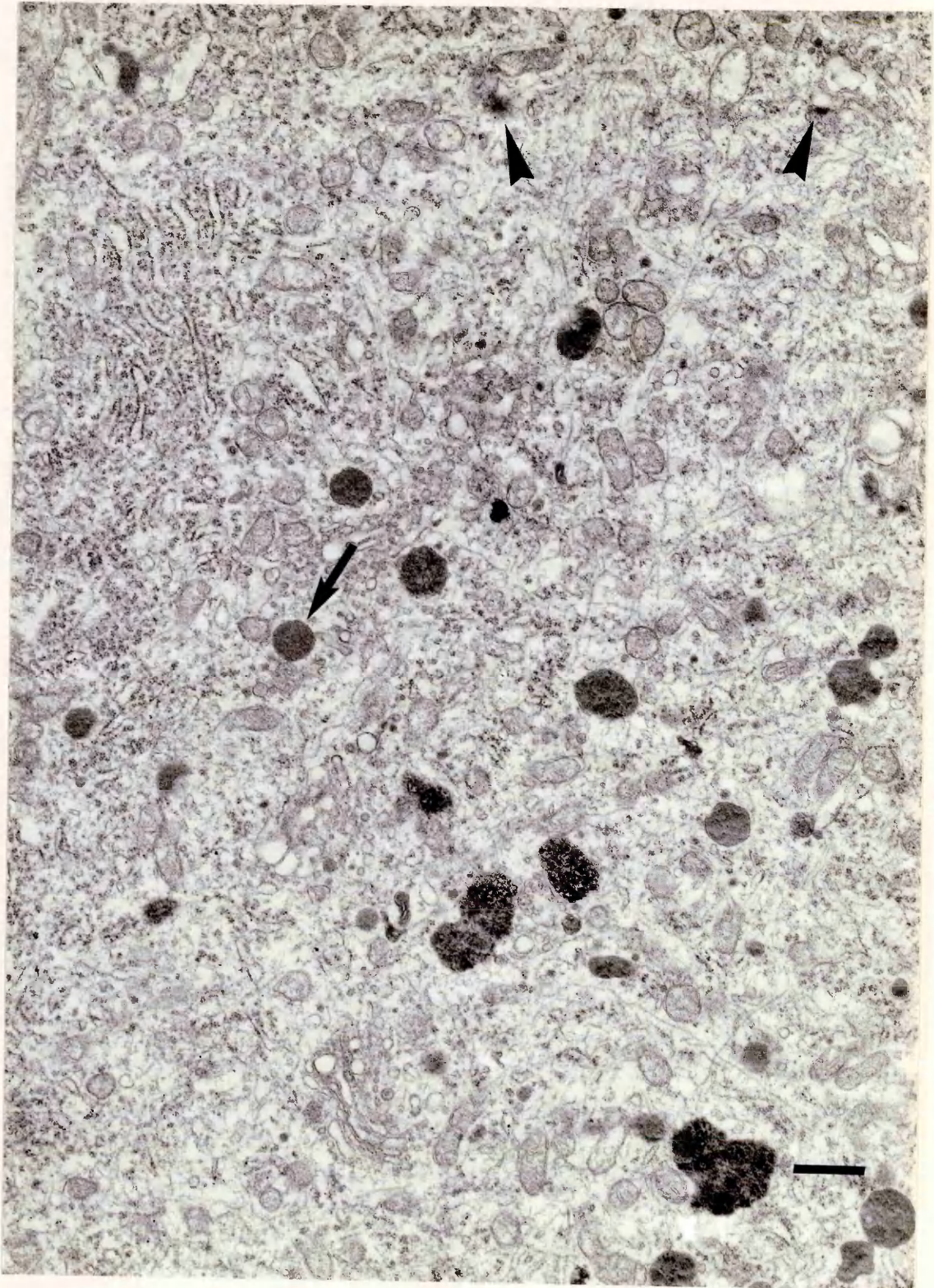


Figure 53

Normal horse, Stellate ganglion, AcPase

Only one dense body in this field clearly shows evidence of AcPase activity (arrows) but there are occasional deposits of reaction product along membranes closely associated with the trans-most cisterna of the Golgi complex. These are areas of GERL (Novikoff and Yam, 1978) which demonstrate AcPase, but not TPPase activity.

Stained with uranyl acetate and lead citrate.

Bar = 0.5 μ m.

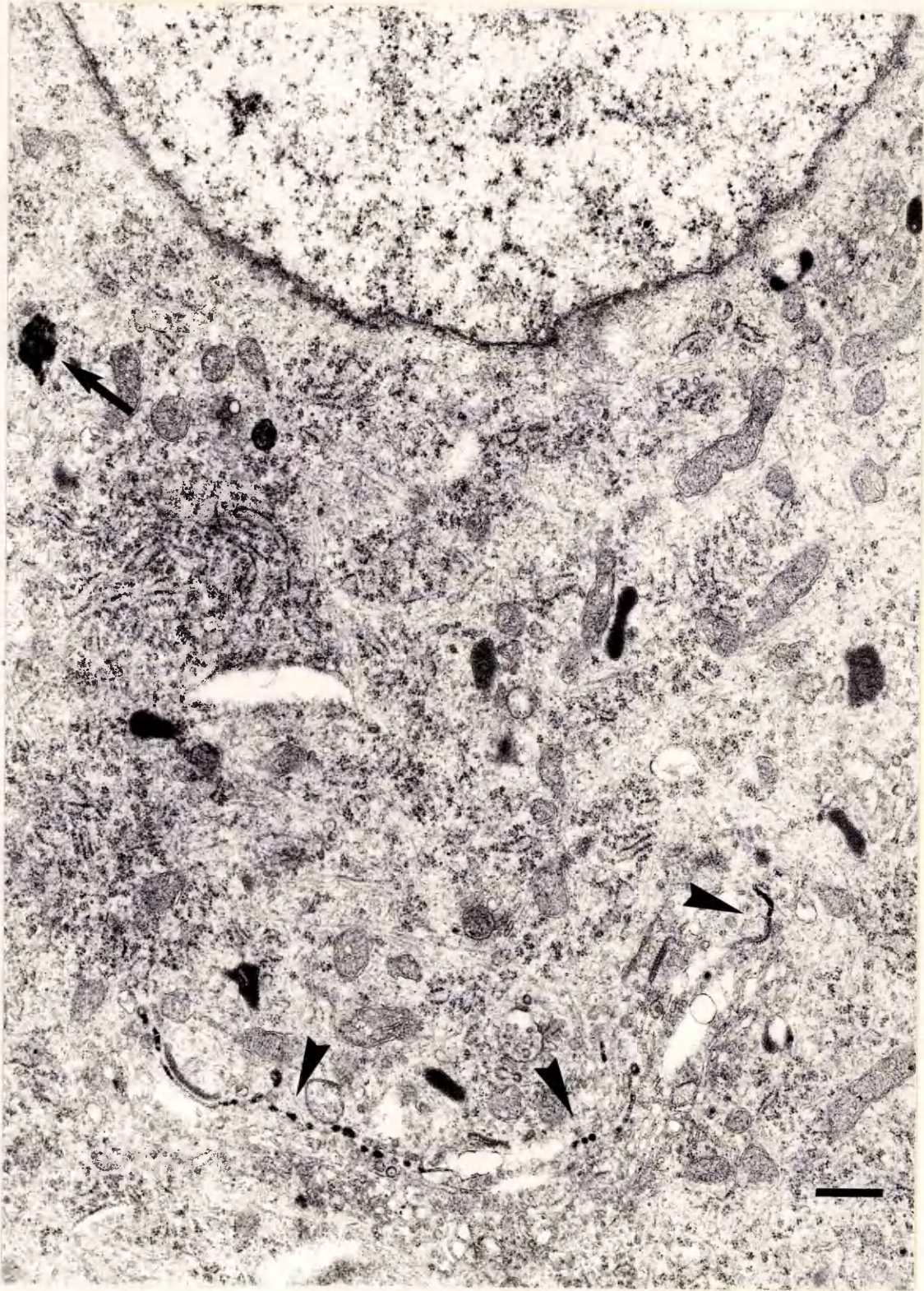


Figure 54

Affected horse (20 hours duration) Stellate ganglion,

TPPase lead capture

The cytoplasm of two affected neurones, demonstrating cytoplasmic vacuoles, increased numbers of mitochondria, no recognisable Nissl substance or Golgi complexes and an increase in smooth membranous and tubular profiles.

There is some non-specific intercellular staining (arrows), but no evidence of any particular structure staining specifically for TPPase.

Stained with uranyl acetate.

Bar = 1 μ m.

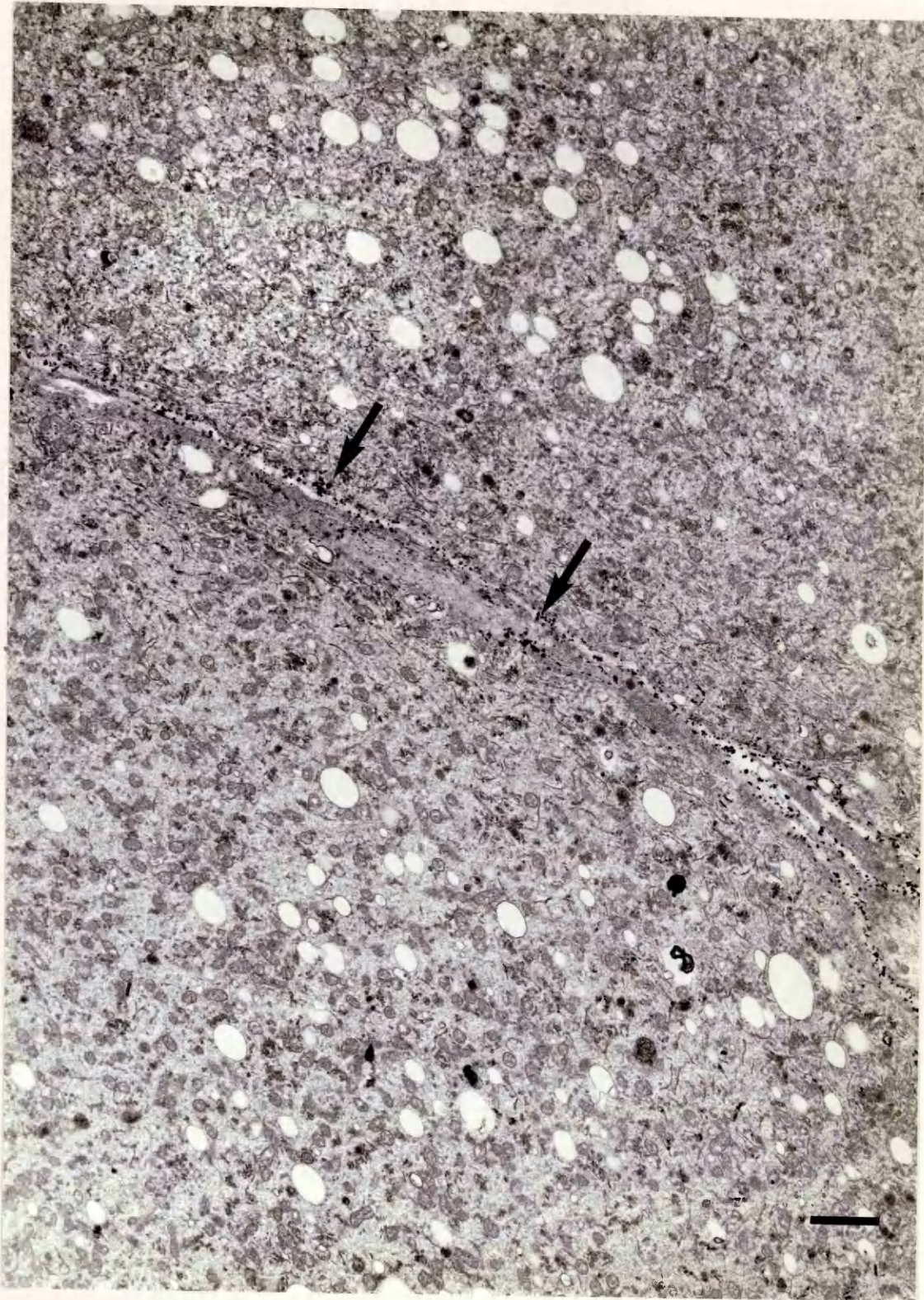


Figure 55

**Affected horse (30 hours duration), Stellate ganglion,
TPPase lead capture**

No normal cytoplasmic structures can be seen. The cytoplasm is packed with numerous small vesicles and vacuoles, proliferated SER and 'blown' mitochondria. Membranous secondary lysosomes are also present (L).

There is some slight non-specific staining of the cell membrane (arrow) but no structures are stained specifically for TPPase activity. Stained with uranyl acetate.

Bar = 1 μ m.

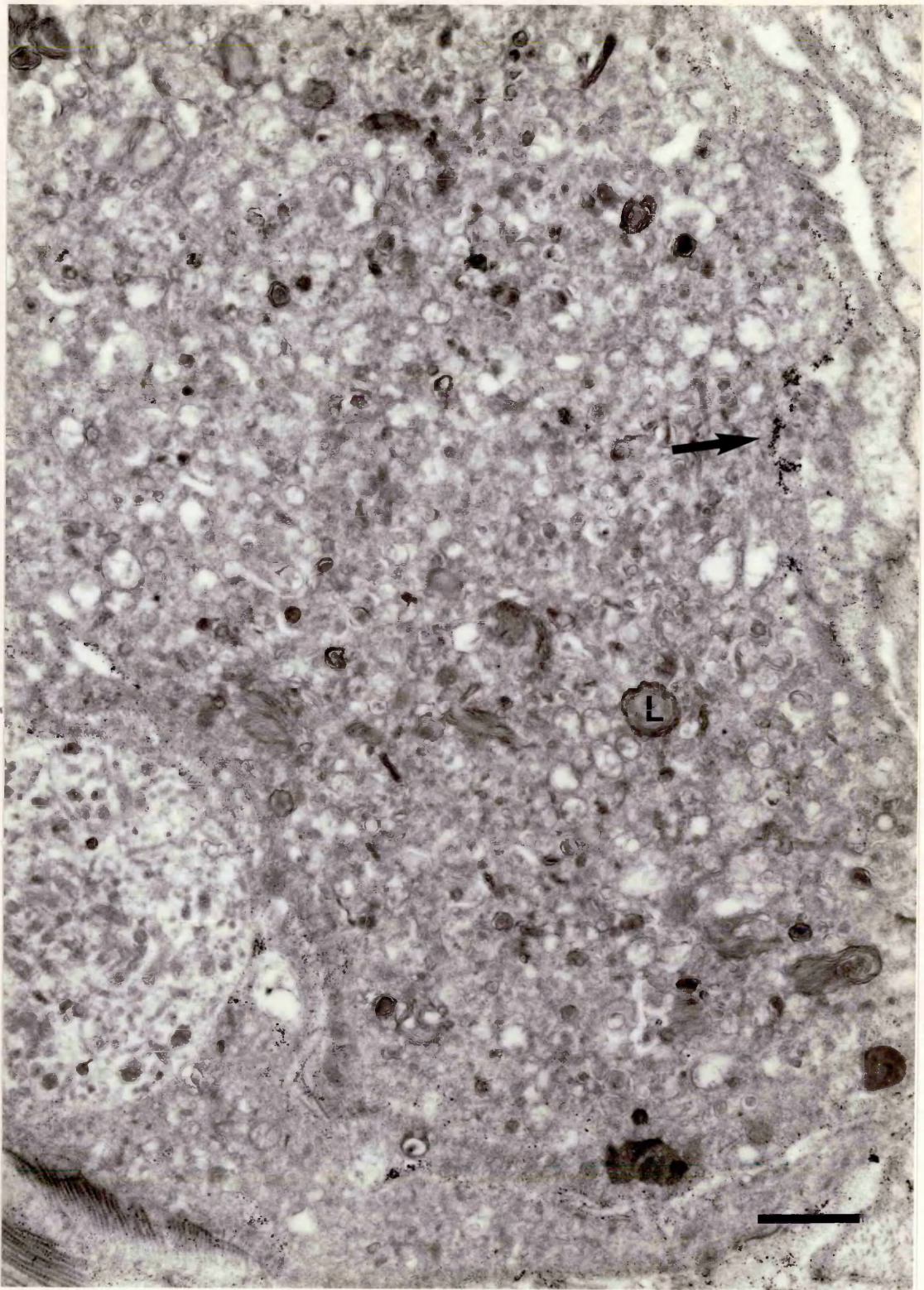


Figure 56

Affected horse (7 days duration) Stellate ganglion,

TPPase cerium capture

Specific cytoplasmic structures are not discernable in this abnormal cell, but there does not appear to be any indication of TPPase activity (see for comparison Figure 59). A few dense non-specific deposits are present at the bottom of this field.

Stained with uranyl acetate and lead citrate.

Bar = 1 um.

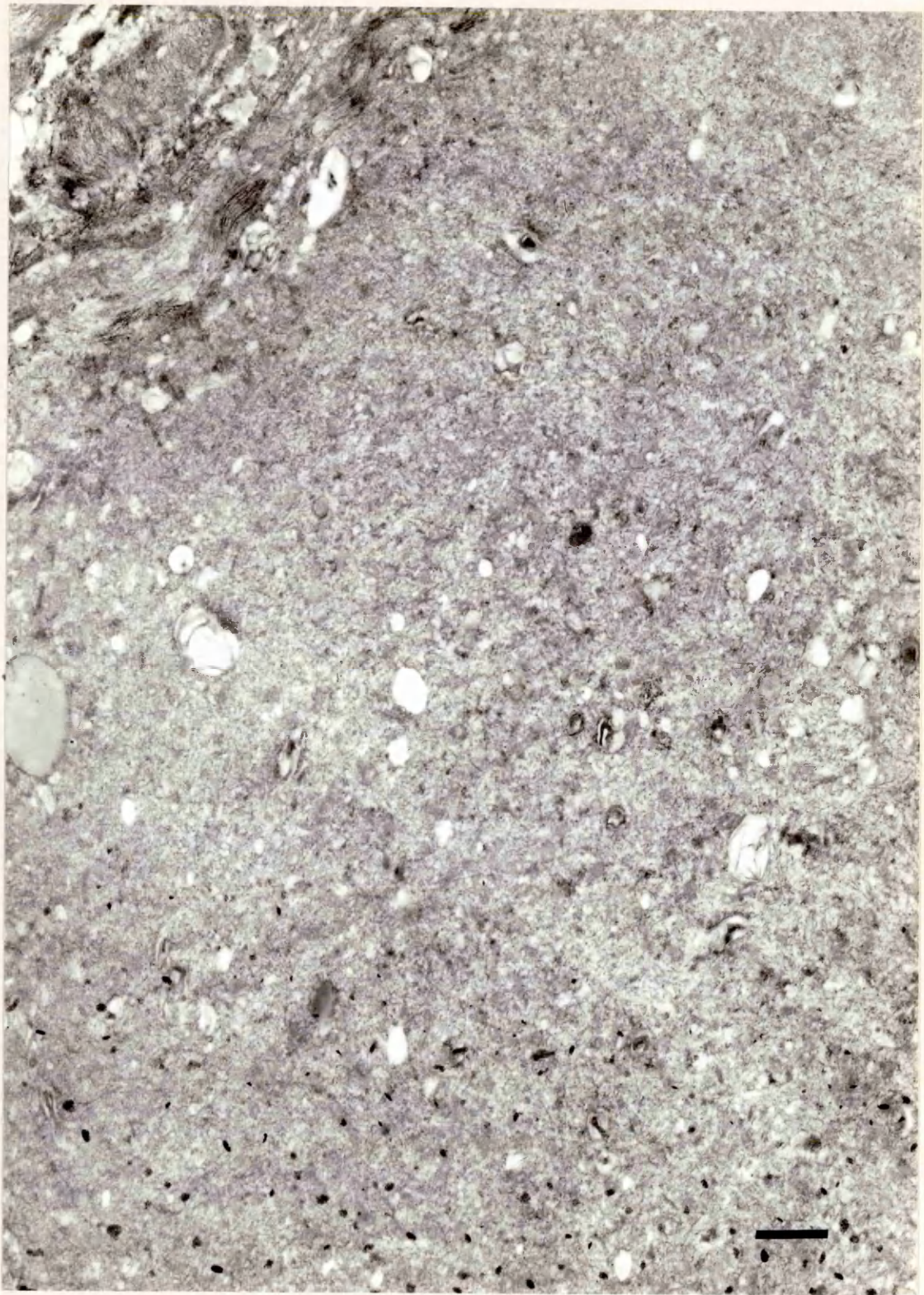


Figure 57

Affected cat (7 days duration) cranial cervical ganglion,

TPPase lead capture

Abnormal stacks of smooth membranous cisternae (SM) are present in this neurone, and although these cisternae contain small amounts of deposit, similar concentrations of deposit are also present in the nucleus (N) and a lysosome (L) suggesting that this is all non-specific.

Stained with uranyl acetate.

Bar = 0.5 μ m.

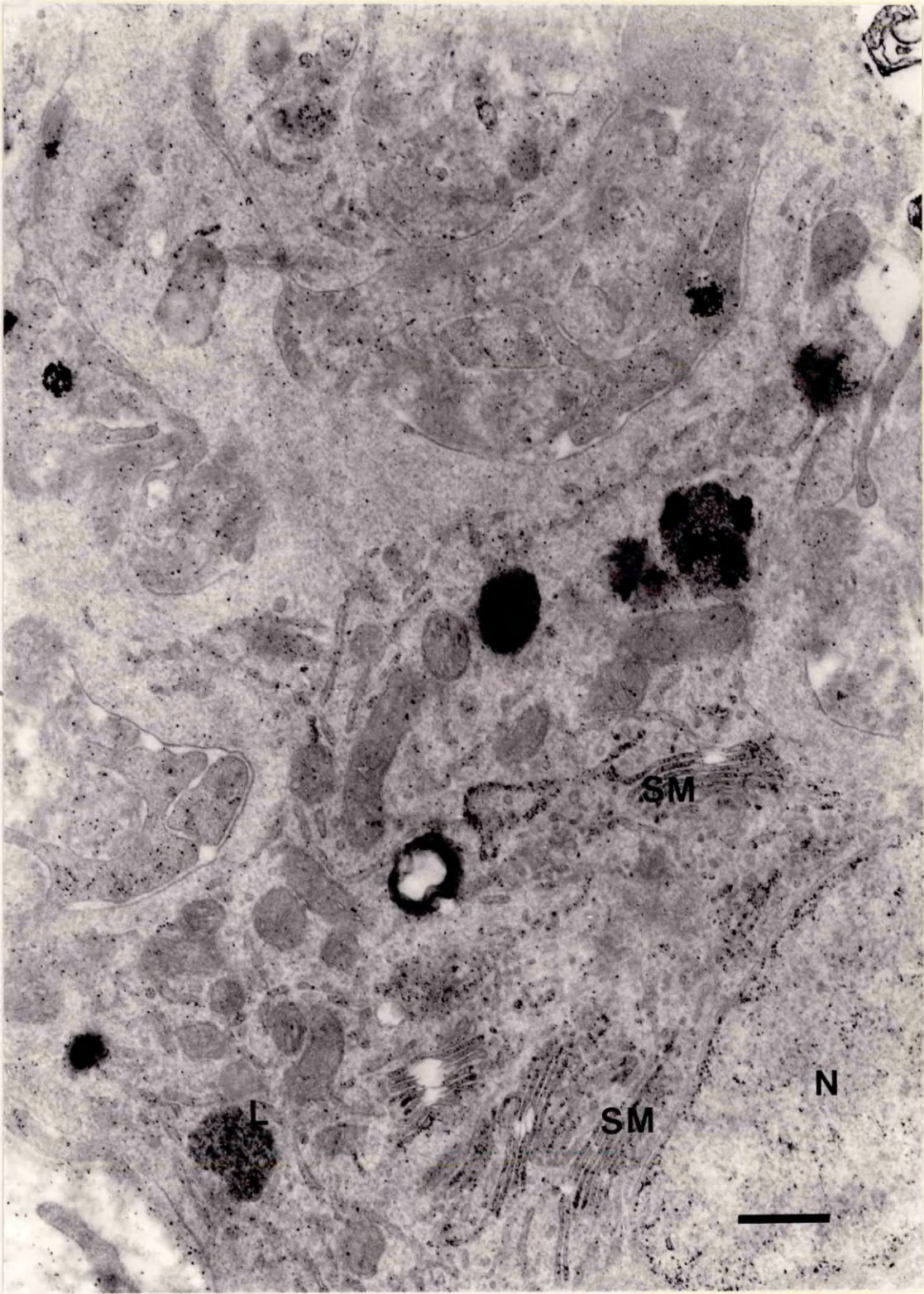


Figure 58

**Affected cat (7 days duration) cranial cervical ganglion,
TPase lead capture**

Lysosomes are the only structure easily defined in the cytoplasm of this neurone, but a small smooth membranous stack (SM) is also present. Several of these lysosomes appear very dense, but this does not seem to be due to any significant stain deposit. The whole section is covered by a fine, non-specific deposit, and no structure seems to be demonstrating specific TPPase activity. Stained with uranyl acetate.

Bar = 0.5 μ m.

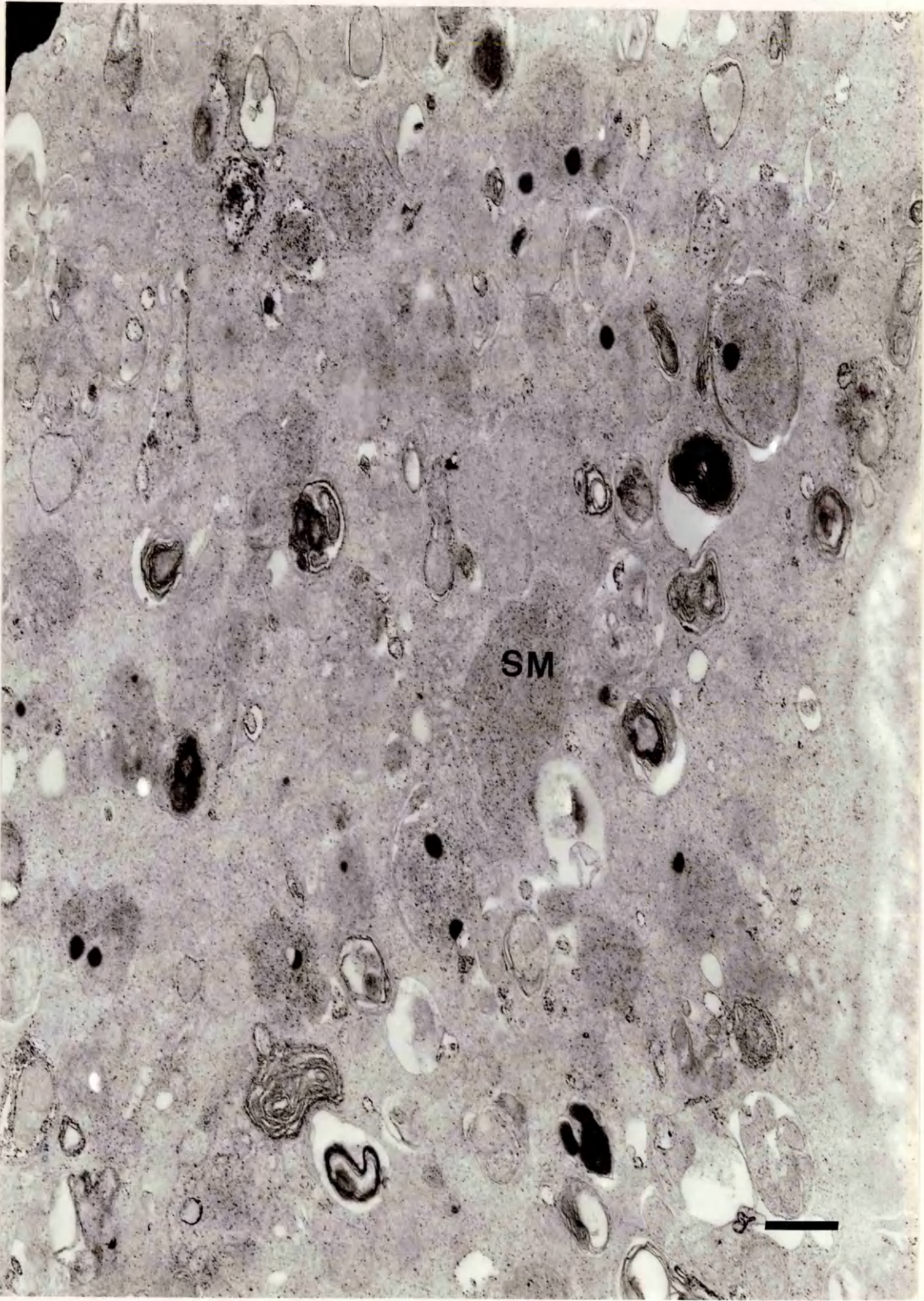


Figure 59

Affected cat (6 weeks duration) Stellate ganglion,

TPPase lead capture

Lysosomes are easily recognisable and mitochondria can be seen (M), but cytoplasmic detail is very poor. The cell contains several discrete accumulations of dense reaction product in approximately single, slightly curved configurations (arrows).

Their appearance is strongly suggestive of Golgi cisternae demonstrating specific TPPase activity. Stained with uranyl acetate.

Bar = 2 μ m.

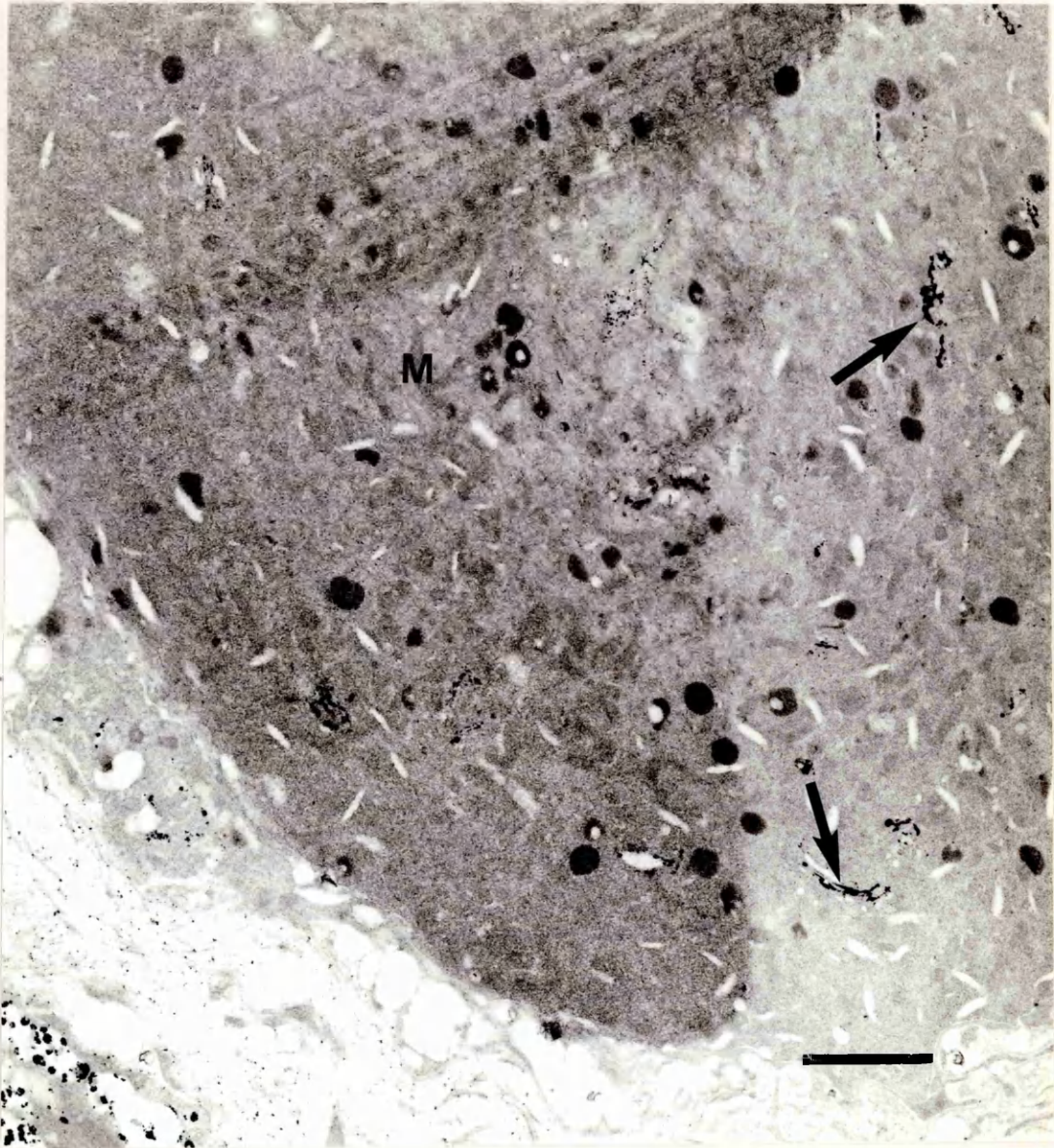


Figure 60

Affected horse (30 hours duration) Stellate ganglion, AcPase

The cytoplasm contains numerous mitochondria, vacuoles of various size and lysosomes, other structures being poorly defined in this example. The only specific stain deposit is associated with the lysosomes (arrows). No other structures show signs of AcPase activity.

Stained with uranyl acetate.

Bar = 2 μ m.

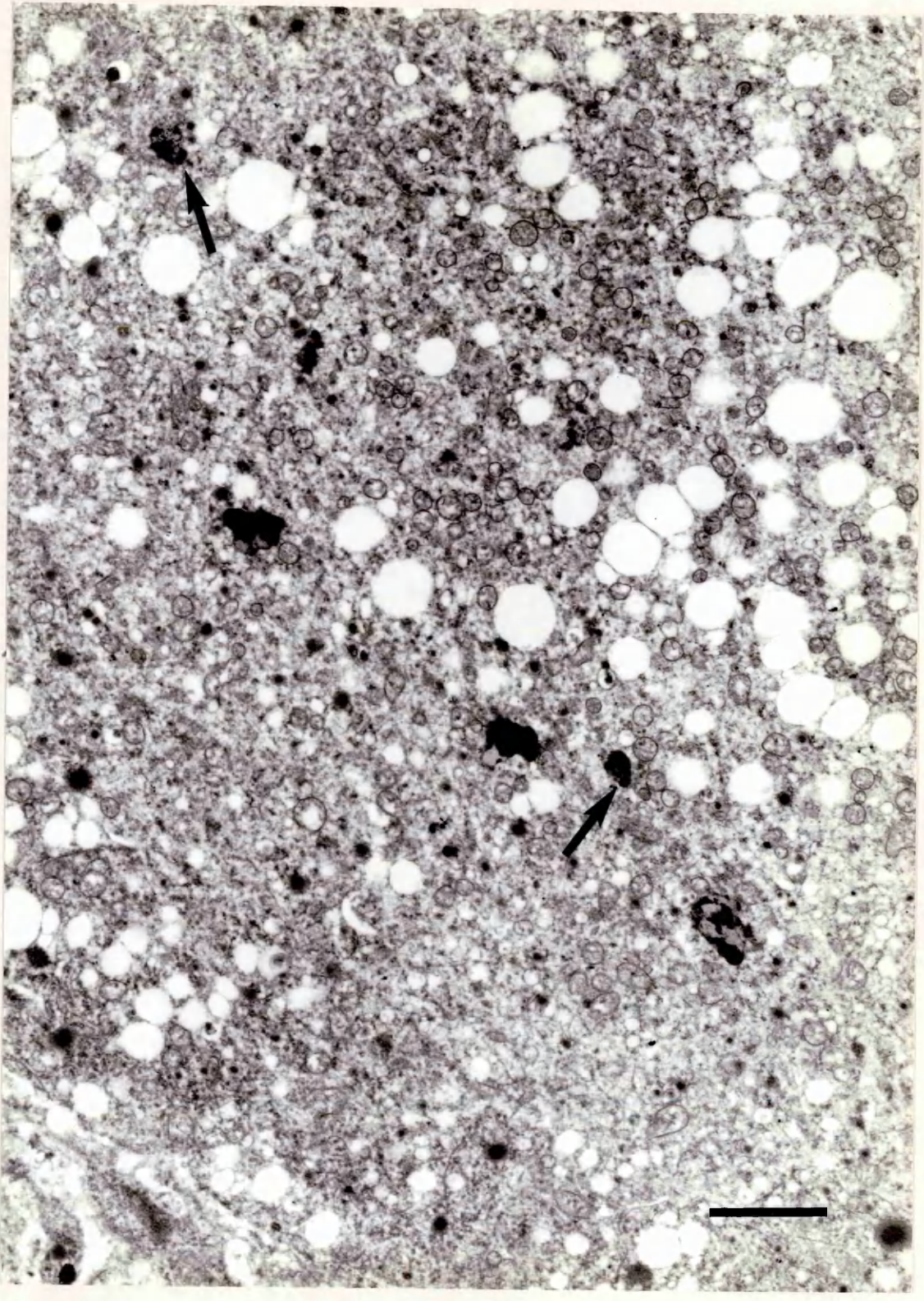


Figure 61

Affected cat (6 weeks duration) Stellate ganglion, AcPase

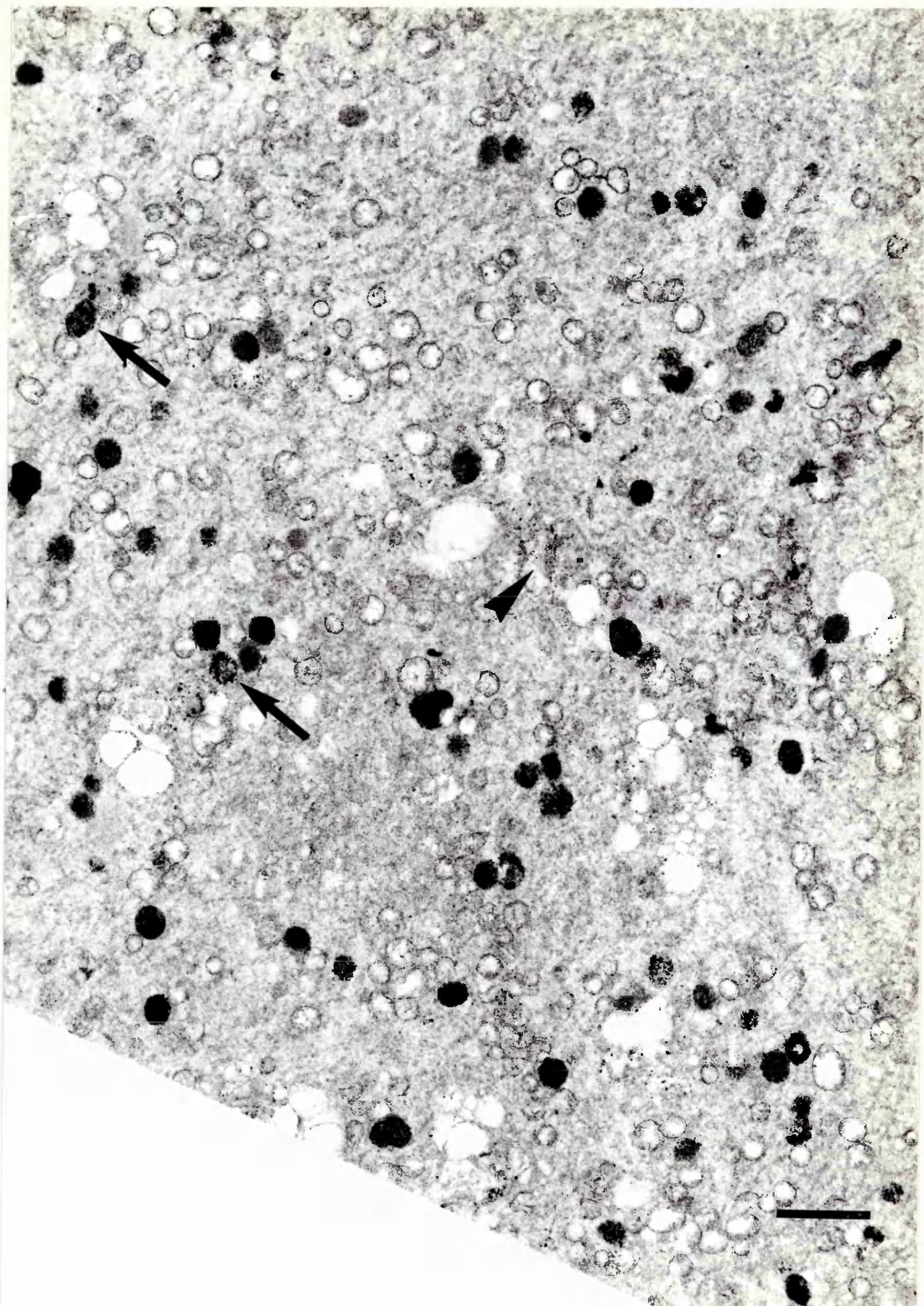
The only structures readily identifiable in this cell are the lysosomes. They are all densely stained with reaction product as a result of AcPase activity (arrows).

A few small non-specific deposits are also present (arrowhead).

No other structures appear to be significantly stained.

Stained with uranyl acetate.

Bar = 1 μ m.



ISOTOPE INCORPORATION in vitro

INTRODUCTION

The ultrastructural examination of dysautonomic neurones has revealed structural changes suggestive of primary damage to the cytoplasmic components of the protein synthetic pathway, notably the RER and Golgi complexes.

The following experiments sought to assess semi-quantitatively any concomitant functional derangement of protein synthesis by examining the ability of autonomic neurones from both normal and dysautonomic animals to incorporate radiolabelled precursors into glycoprotein in vitro.

BACKGROUND TO METHODS

The ability of tissue slices, maintained in vitro, to incorporate labelled compounds is an established means of enabling the well-controlled measurement of metabolic function in specific cell populations under reproducible conditions.

Cerebral cortex slices are frequently used, but DRG preparations have also been described (Miani et al., 1961; Cavanagh and Chen, 1971) to study protein synthesis in detail both in normal cells and in the presence of toxic agents (Miani et al., 1961; Mase et al., 1962; Yoshino et al., 1966; Blomstrand and Hamberger, 1970; Cavanagh and Chen, 1971; Syversen, 1977). Using radiolabelled precursors, function can be quantified biochemically by protein extraction and liquid scintillation counting, or autoradiographically.

No reports have been found in which autonomic tissue is used, nor any methods relating to post-mortem material, as opposed to tissue from experimental animals killed specifically

for its provision. In order to examine the autonomic nervous system, the method used in this study was a modification of those for cerebral cortex slices, as a preliminary, semi-quantitative comparison of glycoprotein synthesis in normal and dysautonomic neurones.

MATERIALS AND METHODS (Summarised in Fig. 62)

The following radiolabelled glycoprotein precursors were obtained from Amersham:

- 1 mCi L [4,5-³H] leucine (140 Ci/mmol) (TRK 683)
- 1 mCi D [2,6-³H] mannose (54 Ci/mmol) (TRK 675)
- 1 mCi L [6-³H] fucose (70 Ci/mmol) (TRK 768)

These were each made up to 2 ml with distilled water, giving a final activity of 100 uCi/200 ul. The leucine and fucose were stored entire at 4°C. The mannose was divided into 200 ul aliquots, stored at -20°C and thawed on the day of use.

HEPES buffered salt solution (HBSS) either with or without amino acids and glucose, was made according to Mata et al. (1980) and is fully described in Appendix 5.

Tissue was available for these studies from two dysautonomic horses, and six non-dysautonomic horses.

As can be seen in Table 2, some horses were shot, others killed by barbiturate overdose. The shot controls were experimental ponies from another department which were being killed, and from which normal autonomic tissue was obtained by kind permission of Mr. S. Love, Veterinary Parasitology. The remaining control tissue was from a surgical case destroyed with

barbiturate on the operating table before being transported to post-mortem facilities. All the control animals were available at the Glasgow University Veterinary School.

The stellate ganglion, which was exposed and removed by opening the thorax, was immediately cut into 3 - 4 mm cubes using a razor blade, and the tissue mounted on the specimen tray of a Polaron DSK Microslicer in a drop of cyanoacrylate adhesive. Once the glue had set (60 - 120 seconds) HBSS was added to cover the tissue. (The tissue was not introduced to buffer earlier than this since problems were encountered with the adhesive if the tissue was wet, and several minutes were required to blot it sufficiently for mounting).

Affected horses were killed by barbiturate overdose, the method chosen by their owners. The vagus nerve was exposed in the cervical region, and the stellate ganglion located and removed by following this nerve manually through the thoracic inlet. Slices were cut directly by hand, using a razor blade. Tissue from both these horses was obtained through the Royal (Dick) Veterinary School.

A minimum of fourteen 300 - 500 μ m sections were cut through the stellate ganglion as soon as possible after death, using one of the above methods, and collected into pre-oxygenated HBSS with amino acids and glucose at room temperature (RT). The sections were allowed to stand at RT for five minutes, transferred to the same medium at 37°C in a Grant shaking waterbath and incubated for a further five minutes prior to labelling. Two slices were then removed into distilled water and homogenised, as described below, as negative controls.

The remaining slices were divided into three groups each containing a minimum of four slices, and placed in 5.2 ml of one of the following three pre-oxygenated labelling media in a 25 ml conical flask in a Grant shaking waterbath at 37°C:-

- (a) HBSS containing leucine-, lysine- and methionine-deficient amino acids (Sigma), to which 100 uCi of ^3H -leucine had been added.
- (b) HBSS with complete amino acids, without glucose to which 100 uCi ^3H -mannose had been added.
- (c) HBSS with complete amino acids, without glucose to which 100 uCi ^3H -fucose had been added.

After fifteen minutes incubation in these media, half of the slices were removed from each flask, washed and homogenised as described below. The remaining sections were incubated for a further fifteen minutes.

All sections removed from the labelling media were given three one minute washes in distilled water, then homogenised by hand in 2 ml distilled water using a Griffiths tube. Each slice was treated individually. The homogenate was transferred to a test-tube to which 2 ml of 20% trichloroacetic acid (TCA) was added. These tubes were kept overnight at 4°C to allow precipitation of protein, and then centrifuged at 2000 rpm for 30 minutes. The supernatant was discarded and the resultant precipitate resuspended in 1 ml distilled water. Some samples could not be homogenised immediately after labelling, and these were placed in 20% TCA for 2 - 4 hours prior to homogenisation as above.

This protein suspension was then divided, 0.1 ml being used for estimation of the protein content and 0.5 ml being processed for liquid scintillation counting (see below):

Protein estimation

The amount of protein in each sample was estimated using the BCA Protein Assay Kit (Pierce Chemical Co. Ltd.) which operates on the following principle. Proteins react with alkaline Cu^{++} to produce Cu^+ , and the BCA protein assay reagent reacts with Cu^+ to form an intense purple colour which can be measured spectrophotometrically.

For each group of samples assayed a set of protein standards were prepared immediately prior to use, from a commercial stock solution of 2 mg/ml bovine serum albumin (BSA) (Pierce Chemical Co. Ltd.). Six concentrations of BSA were used as controls: 0 mg/ml, 0.05 mg/ml, 0.1 mg/ml, 0.15 mg/ml, 0.2 mg/ml, 0.25 mg/ml.

2 ml BCA reagent was added to 0.1 ml of each of the standards and samples in test-tubes, and incubated in a waterbath at 60°C for 30 minutes. The absorbance of each of these samples was then read against distilled water at 562 nm in a Cecil CE 393 digital grating spectrophotometer.

The values for the standards were plotted on a graph as absorbance at 562 nm against protein concentration, and the protein concentration of each unknown sample determined from this standard curve, expressed in mg/ml.

Liquid scintillation counting

0.5 ml of each homogenate was placed in a liquid scintillation vial to which 0.1 ml Soluene 350 (Packard) was

added, and allowed to stand overnight. 10 ml of scintillant (Ecoscint, National Diagnostics) was then added and the sample counted for tritium in a Phillips PW 4540 liquid scintillation analyser for four minutes. The counts were automatically adjusted within the analyser by an external standard channels ratio, and the readings printed out as disintegrations per minute (dpm).

Each sample was counted a minimum of six times, and the results meaned. The final values for all the non-labelled control samples from each animal were also meaned, and this value subtracted from the figures for all other samples before any further calculations were performed. The net dpm for each sample was then doubled and the radioactivity present expressed as dpm/ml.

Data handling

Values for each sample were expressed as dpm/mg protein. As described earlier, a minimum of two samples were processed from every animal for each labelling time in each label. These results were meaned, giving a final single value for each time/label combination.

The rate of precursor incorporation in each animal was then calculated thus:-

$$\text{rate (dpm/mg/min.)} = \frac{(\text{dpm/mg over 30 mins}) - (\text{dpm/mg over 15 mins.})}{15}$$

Statistics

The line of best fit for the shot control horses was calculated by the "least squares" method of fitting a trend line to a distribution (Reichmann, 1964):-

$$r = \frac{\frac{1}{N} \sum (x-\bar{x})(y-\bar{y})}{\sigma_x \sigma_y}$$

Where r = correlation coefficient; \bar{x} and \bar{y} are the respective arithmetic means of the x and y values, and σ_x and σ_y are the standard deviations of the x and y distributions respectively. \sum indicates that all the separate products $(x-\bar{x})(y-\bar{y})$ for all values of x and y are to be summed.

Validation of method

Cycloheximide is a well-documented inhibitor of protein synthesis (see page 115).

To establish that the method employed in this study yielded results representative of synthetic function, normal autonomic tissue was pre-incubated and labelled with radiolabelled amino acid, in the presence of 0 ug/ml, 20 ug/ml or 80 ug/ml cycloheximide.

The results (Table 3) indicate that the uptake of amino acid decreased with increasing concentration of cycloheximide i.e. synthesis was specifically inhibited in a dose-dependent manner.

RESULTS

Samples of autonomic tissue from both control and affected horses showed a great variation in the rate at which incorporation of radiolabelled glycoprotein precursors occurred in vitro.

The variation in absolute values for isotope incorporation rates for normal horses (Tables 4 and 5) was so great as to preclude direct comparison with affected animals.

The protocol (page 81) states that tissue was taken from each animal, sections cut and collected into buffer "as soon as possible after death", and thereafter the timing of each incubation stage was precise. For several reasons, the time taken from the death of the animal to the labelling of the slices varied from less than 30 minutes to more than 60 minutes, this period being estimable to within ten minutes in each case, but not precisely recorded. The reasons for this are fully outlined in the discussion.

The control horses were grouped according to the approximate interval between death and labelling, and the means of death - shooting, or barbiturate overdose - taken into consideration (Table 2). When the rates of incorporation were compared relative to these, a significant correlation became apparent (Figure 63, Table 6).

In control horses which had been shot, the rate of incorporation of each precursor increased in direct proportion to the time taken from the death of the animal to the labelling of the tissue in the time range 0 to 15 minutes. In the case of leucine and fucose the correlation was highly significant, being greater than 0.95 for both precursors, but non-significant for mannose (Table 6).

The incorporation rates of each precursor in the five shot, non-dysautonomic animals, and the calculated line of best fit for

these values were plotted, together with the rates of incorporation achieved in the dysautonomic horses, and the control horse killed by barbiturate overdose. The following comments were then made from visual inspection of these graphs.

The incorporation of leucine in the normal horse killed by barbiturate overdosage was considerably less than that by the horses which had not received barbiturate. The affected horses, however, both of which were killed by barbiturate, appeared to assimilate leucine at a rate equal to, or greater than, those normal horses which had been shot.

A similar pattern was evident for mannose incorporation but, given the poorer correlation between the rate of incorporation in the shot controls, the depressant effect of barbiturate on the normal horse was less clearly defined. One affected horse appeared to have a very greatly increased rate of incorporation.

Barbiturate overdose did not appear to have any marked effect on the incorporation of fucose, all the normal values lying close to the line of best fit for the shot controls. The only affected tissue incubated with fucose was unable to sustain a linear incorporation over 30 minutes, and a negative value for incorporation rate resulted when calculated in the same way as all the other values (Tables 4 and 5). It could not, therefore, be plotted meaningfully on this graph.

DISCUSSION

Several major problems were encountered in this study which made subsequent interpretation of the data extremely difficult.

The most obvious shortfall is the extremely small number of animals examined - especially those with dysautonomia. As will

be discussed more fully below, several other cases were labelled, but not included in these results. A further difficulty was the limited amount of autonomic tissue available from each horse. Both the affected horses were referred to the Royal (Dick) Veterinary College in Edinburgh, and my colleagues there also required tissue from these animals. It was not, therefore, possible to perform in each case all the various investigative methods, reducing further the numbers of affected animals in each section.

The very small sample sizes resulting from this experiment mean that any statistical comparison of the groups would be meaningless, so this has not been attempted. The presented interpretation of the data is therefore qualitative.

The techniques for this investigation had not been previously used by this laboratory and numerous variables, some of which were unavoidable, occurred in the methods, the significance of these not being appreciated until the data were examined retrospectively.

Method of killing

As described in the methods, control tissue was mostly obtained from experimental ponies which were shot. The other non-affected animal was destroyed with barbiturate on the operating table for transportation to the post-mortem facilities, and in the case of the affected animals, the owners opted for euthanasia by means of barbiturate overdose, i.e. the means of death in each case was determined not by me but by the people directly responsible for the animal.

Time from death into label

The very significant effects on isotope incorporation of the length of time taken from the death of the animal to the introduction of label only became apparent retrospectively. Literature regarding such experiments frequently does not define this interval at all (Mase et al., 1962; Cavanagh and Chen, 1971) or uses phrases such as "rapidly" (Blomstrand and Hamberger, 1970), "as soon as possible" (Miani et al., 1961) and "as rapidly as possible" (Lipton, 1985). Unfortunately in this study, reliance on clinical material led to the variation from one animal to another being considerably greater than would be expected under controlled experimental conditions. The sampling requirements of colleagues also affected the time taken for removal of the stellate ganglion following death.

It was not always possible for me to be present at the precise time of death of the animals, and therefore the pre-labelling period had to be estimated (as mentioned earlier). For the purposes of plotting the graphs, each point was considered as the median value for the time "group" into which it fell.

Material obtained from Edinburgh horses was hand-sliced using a razor blade, whereas Glasgow samples were sectioned on a microslice. While this latter method gave more consistent slice thickness, it proved considerably more time consuming than cutting by hand, thus adding further to the variability in the time interval from death to labelling.

Protein precipitation

The non-specificity of protein precipitation is another area introducing potential variables. Neuronal protein synthetic mechanisms were our specific interest, but incorporation by both neuronal and non-neuronal cell populations is measured by this method, and non-labelled connective tissue protein is also included in the TCA precipitate.

The cranial mesenteric and coeliac ganglia are fused in the horse, and enmeshed in the coeliacomesenteric plexus, resulting in a diffuse mass of ganglionic, axonal and connective tissue components (Ghoshal, 1975). The stellate ganglion, however, is much more compact, so the study was confined to slices from the centre of stellate ganglia which had been pre-trimmed to remove all the encapsulating connective tissue.

No morphological abnormalities have been reported in the non-neuronal cell population; these cells in normal animals incorporate label at a much lower rate than the neurones. Other workers have divided labelled tissue post-labelling to demonstrate that neuronal-enriched fragments were six times more active in incorporating ^3H -leucine/mg than were glial fractions, and they were also more sensitive to antimetabolites such as cycloheximide (McIlwain and Bachelard, 1985). This can also be demonstrated autoradiographically (Figure 64). Any abnormal findings in affected slices can therefore be considered mainly representative of changes in the function of the neuronal population.

Preliminary autoradiographic studies on an affected horse have confirmed this selective involvement of neuronal protein

synthesis by demonstrating the continuing incorporation of labelled leucine and mannose in non-neuronal cells, concurrent with a very marked depression of this function in dysautonomic neurones (Fig. 65).

Thickness of the slice

Slices have a zone of 50 - 100 μm at the cut edge in which cells are badly damaged, and these regions should therefore be considered dead tissue (Lipton, 1985). Hand-held razor blade and vibratome slicing methods appear to inflict similar damage on the tissue (Lipton, 1985). Pre-existing protein will still be precipitated from these regions, but the cells would not be capable of synthesising new protein. Since slice thickness was not precisely measured, the proportion of the protein precipitate which originates from these damaged peripheral cells will vary.

The extent to which this affects the results cannot be gauged precisely, but the sensitivity of the results to this variable can be tested on the basis of the following assumptions:-

- Handslicing generally resulted in thicker slices than Vibratome slicing, therefore assume handslices 500 μm thick, Vibratome 300 μm thick.
- Assume the area of damage on either side of the slice was a constant regardless of the slicing method (see above). Assume this was (a) 50 μm (b) 100 μm .

The proportion of the slice assumed to be functioning can then be estimated as follows:-

100 μ m damage each side of 300 μ m slice = 33% functioning

50 μ m damage each side of 300 μ m slice = 66% functioning

100 μ m damage each side of 500 μ m slice = 60% functioning

50 μ m damage each side of 500 μ m slice = 80% functioning

The rate of incorporation of isotope is then adjusted accordingly (Table 7, Figure 66). The examples are based on the results for ^3H -leucine incorporation.

As would be expected, this alteration increases the absolute rate of incorporation in all slices, in proportion to the amount of damage, but by a greater proportion in the thinner (normal) slices than in the thicker ones. Thus, if cutting damage is assumed to be maximal, the affected animal which showed the apparently markedly increased rate of incorporation, as compared to the normals, no longer does so.

It must be remembered that this is an extreme simplification of the data. Slice thickness is an approximate measurement which can be considered relatively accurate for Vibratome slices but much more variable for slices cut by hand, and while the damaged area should be fairly consistent for either method (Lipton, 1985) it can only be assumed that there is no major difference between the two cutting methods, and that there is a minimum of operator error in each case.

This variable is of greater potential significance in the affected animals, where less consistent slice thickness was achieved.

Interpretation of data

It can be seen from Figure 63 that for the normal horses destroyed by shooting, the greater the time interval before labelling, the greater the rate at which labelled precursor is incorporated.

The correlation of these factors is highly significant (Table 6) for both leucine and fucose, but not for mannose. This could possibly be due to the presence of an apparently "rogue" result (C1) which is much higher than would be expected from the values of the other shot controls, given that they are all functions of one synthetic pathway.

Why does this apparently contradictory trend occur? There is no data on the in vivo synthetic rates in these horses, but it could be hypothesised that following death, and the subsequent severing of axons, the neurones show a temporary decrease in synthetic activity, a period of "shock" from which, if the correct environment (incubation medium) is provided they will gradually recover, at least partially. This period of recovery would seem feasible given the good structural preservation of tissue after six hours in vitro (see page 124) in the appropriate milieu.

While accounting for the correlations over the 30 - 60 minute period, this hypothesis does not allow extrapolation into either longer or shorter time intervals.

The lines marked in Figure 63 are linear (Table 6). Negative rates are not possible, so therefore they cannot continue as straight lines.

Should the lines go through the origin? If they did, it would mean that tissue introduced to labelling medium immediately upon death would not synthesise at all over the subsequent 30 minute period. While it is reasonable to expect reduced function, cessation of synthesis is unlikely.

It is probable that the rates at 'time 0' would in fact be greater than those found over the subsequent 10 - 15 minutes, and thus the shape of the initial part of the graph would be that of a falling rate.

Other workers have calculated that the rates of incorporation of labelled amino acid in vitro represent less than 0.1% of the amino acid content of the protein per hour, which is considerably lower than the 0.5% calculated to occur in vivo (McIlwain and Bachelard, 1985).

It is therefore impossible to make any comment on the values obtained from affected tissue.

The normal horse killed by barbiturate does however fall within the time span for the shot controls. It would appear that leucine uptake is very greatly reduced in this case, while mannose is less obviously affected and incorporation of fucose is similar to that found in horses receiving no barbiturate. This would suggest that different levels of the protein synthetic pathway have a differing susceptibility to the depressive effects of barbiturate. Whether this represents an absolute difference or a variation in the recovery time of each metabolic 'step' cannot be commented on, on the basis of values from one animal. It is a well-recognised fact that barbiturate depresses cellular metabolism in vivo in a dose dependent manner, the maximal

reduction being about 50% of normal. Metabolism is also depressed in vitro (Siesjo, 1978).

The rates of uptake in each case were calculated over the second 15 minute period in labelling medium. This allowed for any accommodation of the tissue to the new environment before measurements were made and was considered more representative of function than a measurement made over either the first 15 minutes or the whole 30 minute labelling period.

This resulted in a negative value for fucose incorporation in affected tissue. It cannot be determined whether the failure of the 30 minute slices to sustain a rate equivalent to that of the 15 minutes samples was due to one of the many experimental variables discussed above, or some other experimental error.

Choice of label

In preliminary experiments ^{35}S -methionine was used to assess polypeptide synthesis. However this has a radioactive half-life of 87 days and requires a separate calculation on each occasion of use to determine the specific activity of the label.

In absolute terms, very small amounts of label are present in the precipitate, and so as the isotope decayed, liquid scintillation counting efficiency decreased leading to more potential inaccuracies.

As the supply of clinical material was unpredictable, it was decided to change to a ^3H -labelled compound since this is much more stable ($t_{1/2}$, 11.3 years) and has a longer shelf-life. Tritiated mannose and fucose were then introduced to enable assessment of different levels of the synthetic pathway.

An affected cat and a case of EGS which was shot were both labelled with ^{35}S -methionine, but no normal tissue from either species was available for comparison with these, prior to expiry of the label. A normal cat was then labelled with the tritiated precursors, but no affected cat was subsequently presented.

The validation of this method as an assessment of protein synthesis using the inhibitor cycloheximide (see Materials and Methods) was carried out with ^{35}S -methionine, and since direct comparison with the results from the clinical material was not required, this study was not repeated with the tritiated precursor.

Conclusions

It is the conclusion of this study that due to the unforeseen significance of certain experimental variants and the small number of affected horses no conclusive comments can be made on possible functional differences of the autonomic neurones in normal and affected animals.

This method would enable a valid semiquantitative assessment of any functional derangement of protein synthesis provided the following alterations to protocol were observed:-

(1) The time interval from death to the introduction of label should be constant, and if this was not possible a time delay versus incorporation rate control graph should be established for all possible time intervals [see (3)]. (This would be possible using only one animal by staggering the labelling time of the slices).

(2) The functional slice thickness should be constant, and therefore also the slicing method, to minimise possible differences in the amount of damage sustained by the cells during slicing.

(3) The means of death should be consistent, or relevant control material obtained [see also (1)].

It must be remembered that affected animals will not have been ill for the same period of time when killed, and this must also be taken into consideration when assessing any variation of the data.

TABLE 2

Variations in method prior to labelling

Number	Method of Destruction		Time from Death --> Label (mins)			
	Shot	Barbiturate	15-30	30-45	45-60	60-75
Control 1	1				1	
2	1			1		
3	1			1		
4		1				1
5	1					1
6	1					1
Affected 1		1			1	
2		1			1	

TABLE 3

Rate of incorporation of labelled amino acid
in the presence of cycloheximide

Cycloheximide (ug/ml)	Rate of Incorporation (cpm/mg/min)	Rate as % of non- inhibited rate
0	15136	100
20	372	2.46
80	136	0.89

TABLE 4

Calculation of incorporation rates of tritiated glycoprotein precursors
in normal and dysautonomic animals

Number	LEUCINE			MANNOSE			FUCOSE					
	Incor- poration 30' (dpm)	Incor- poration 15' (dpm)	Incor- poration per minute	Incor- poration 15' (dpm)	Incor- poration 30' (dpm)	Incor- poration per minute	Incor- poration 15' (dpm)	Incor- poration 30' (dpm)	Incor- poration per minute			
CONTROL 1	48216	19971	28245	1883	38960	4140	34820	2321	4827	955	3872	258
2	23680	12945	10735	716	4846	370	4476	298	1908	0	1908	127
3	18992	4230	14762	984	3235	2358	887	58.5	3466	1096	2370	158
4	31880	22302	9578	638	20399	9224	11175	745	22870	16772	6098	406
5	76004	19784	56220	3748	36928	13157	23771	1585	14844	6836	8008	534
6	28588	5014	23574	1572	30909	13075	17834	1189	8672	5208	3464	231
AFFECTED												
1	9321	3479	5842	389	5136	1555	3581	239	-	-	-	-
2	28693	5407	23286	1552	54518	9849	44669	2978	5101	5738	- 637	- 42

TABLE 5

Summary of incorporation rates (absolute values) of tritiated
glycoprotein precursors in normal and dysautonomic animals

Label	Control/ Affected	Number	Mean \pm S.D. rate of incorporation	Range
Leucine	Control	6	1590 \pm 1063	716 - 3748
	Affected	2	970.5 \pm 581.5	389 - 1552
Mannose	Control	6	1033 \pm 770	58.5 - 2321
	Affected	2	1608.5 \pm 1369.5	239 - 2978
Fucose	Control	6	286 \pm 141.5	127 - 534
	Affected	1	-42	-

TABLE 6

Correlation of rate of isotope incorporation in relation to the time taken between the death of the horse and the labelling of the tissue. (Shot control horses only).

Precursor	N	Correlation coefficient	Sign. (P)	Line of best fit
Leucine	5	0.959	< 0.001	$y = 1367 x - 2048$
Mannose	5	0.654	NS	$y = 828 x - 1228.5$
Fucose	5	0.959	< 0.001	$y = 182 x - 249$

NS = not significant

TABLE 7

Effects of slice thickness and cutting damage on the rate of incorporation of ^3H -leucine

Number	Slice Method	Assumed Thickness (μm)	Incorporation of ^3H -leucine (dpm/mg (min)^{-1})		
			Unadjusted rate	Corrected rates	
			50 μm damage	100 μm damage	
Control 1	Vibratome	300	1883	2853	5706
2	Vibratome	300	716	1085	2170
3	Vibratome	300	984	1491	2982
4	Vibratome	300	638	967	1933
5	Vibratome	300	3748	5679	11358
6	Vibratome	300	1572	2382	4764
Control 1	Hand	500	389	486	648
2	Hand	500	1552	1940	2587

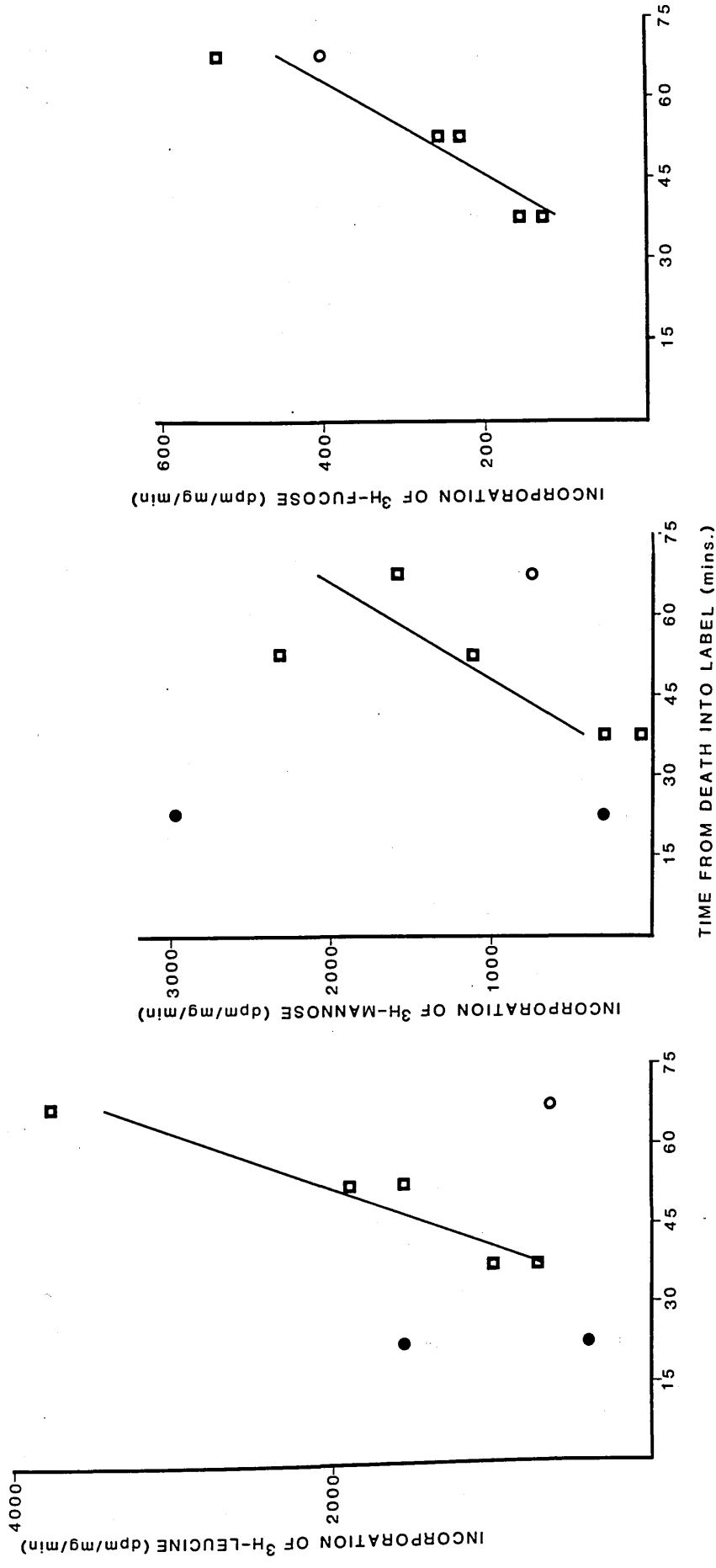


Figure 63. The effect on synthetic function in vitro of a delay between the death of the tissue donor and the onset of labelling

KEY: □ - Normal horse, shot
 ○ - Normal horse, barbiturate
 ● - Affected horse, barbiturate

Figure 64

**Stellate ganglion, Normal horse, ^3H -leucine, 30 minutes
labelling**

Note the high density of grains over the neuronal cytoplasm (arrowhead) as compared to the rest of the section. Where neuronal nuclei are present, grain density is lower over these areas. Smaller numbers of grains are present over the glial cells surrounding the neurones, and very few grains (background count) are found over peripheral regions (*).

Bar = 10 μm .

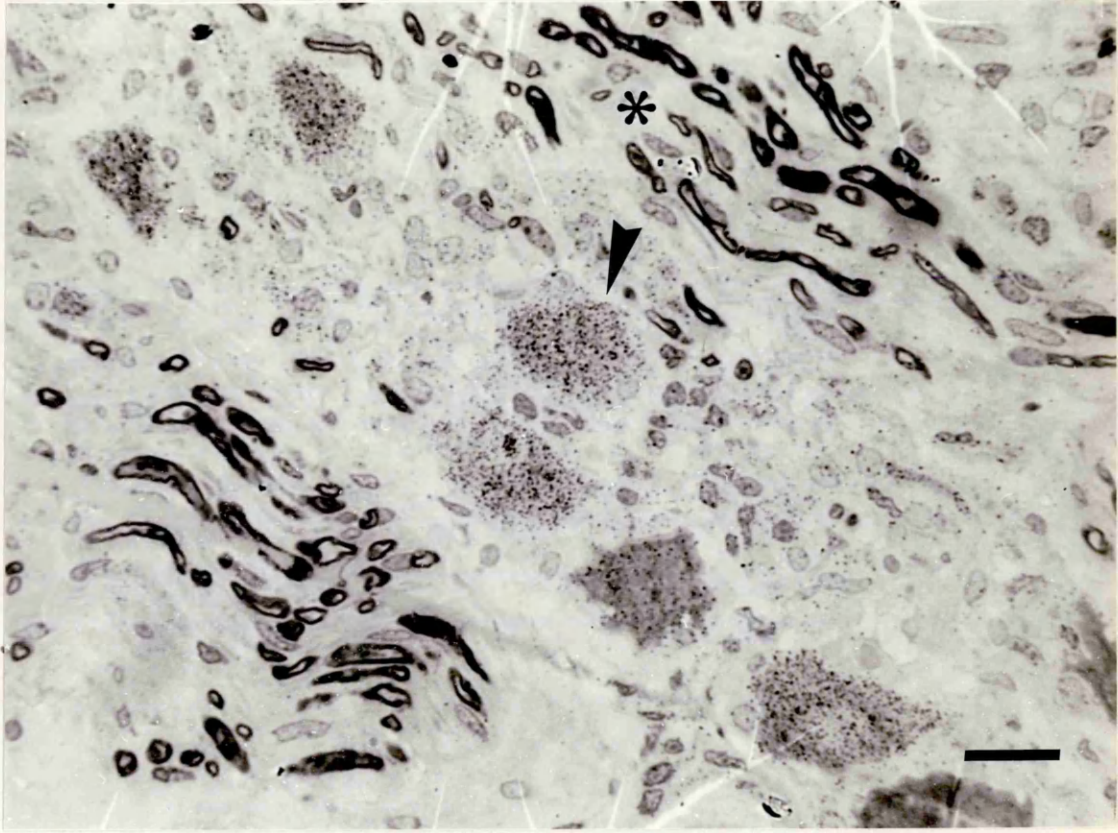


Figure 65

Stellate ganglion, affected horse (6 days duration)

30 minutes labelling

This tissue (and the normal ganglion in Figure 64) were labelled as described earlier (page 80) for 30 minutes, washed in 0.1M sodium cacodylate buffer (Appendix 3) and fixed in 3% paraformaldehyde, 1.25% glutaraldehyde (final concentrations) in 0.1M sodium cacodylate buffer, before being dehydrated through alcohols and embedded in Araldite (Appendix 1).

1.5 μm sections were mounted in gelatin/chrome alum "subbed" slides, coated with Kodak AR10 stripping film and exposed for four weeks prior to development with Kodak D19 developer and counterstaining with toluidine blue.

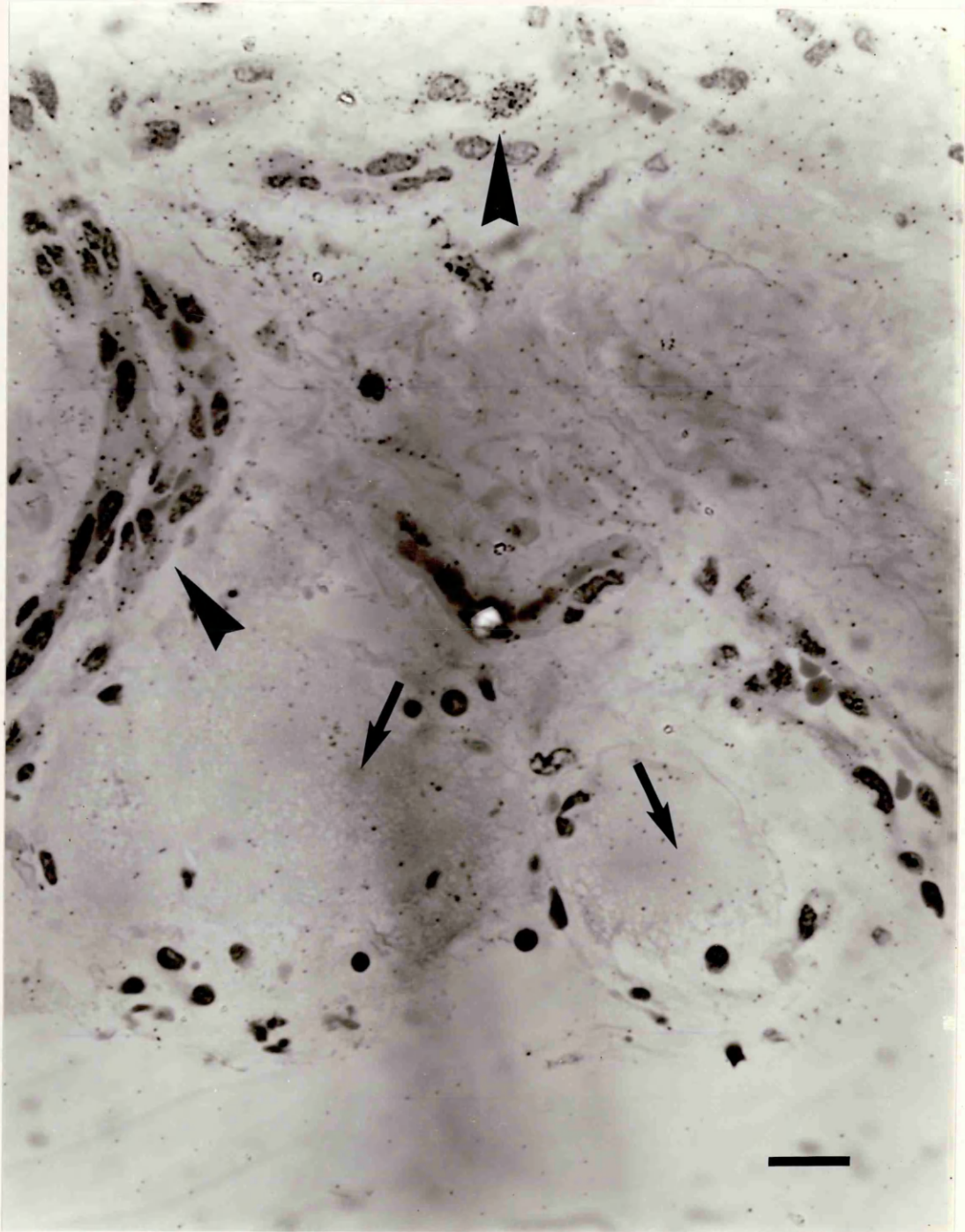
(a) ^3H -leucine

(b) ^3H -mannose (on following page)

While mannose incorporation into neurones (b) is variable, it can be clearly seen that incorporation of both isotopes by the neurones (arrows) is greatly decreased, compared with the non-affected non-neuronal cells (arrowheads).

(a) Bar = 15 μm .

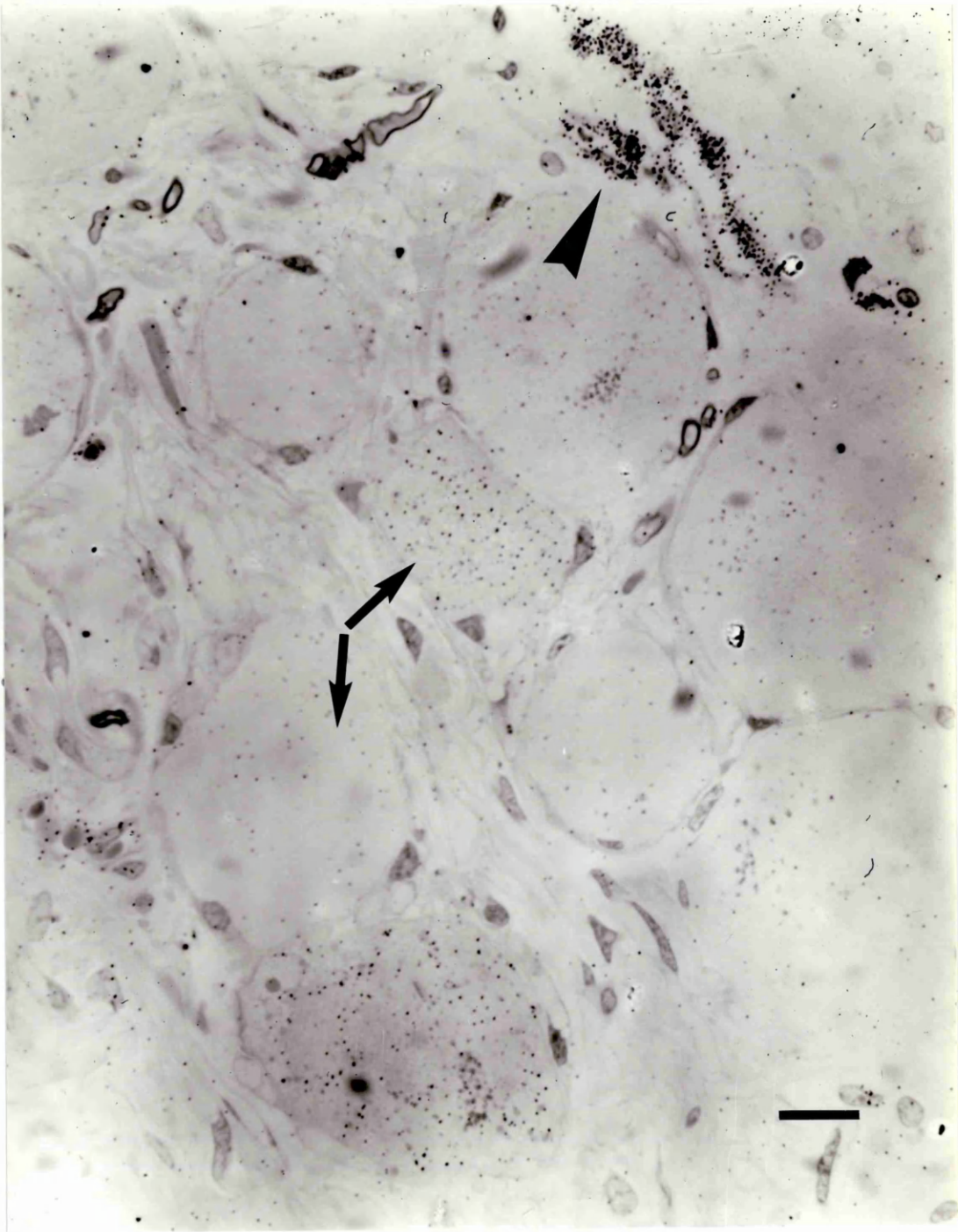
(b) Bar = 15 μm .



Journal of Microscopy

Figure 65b

See previous caption



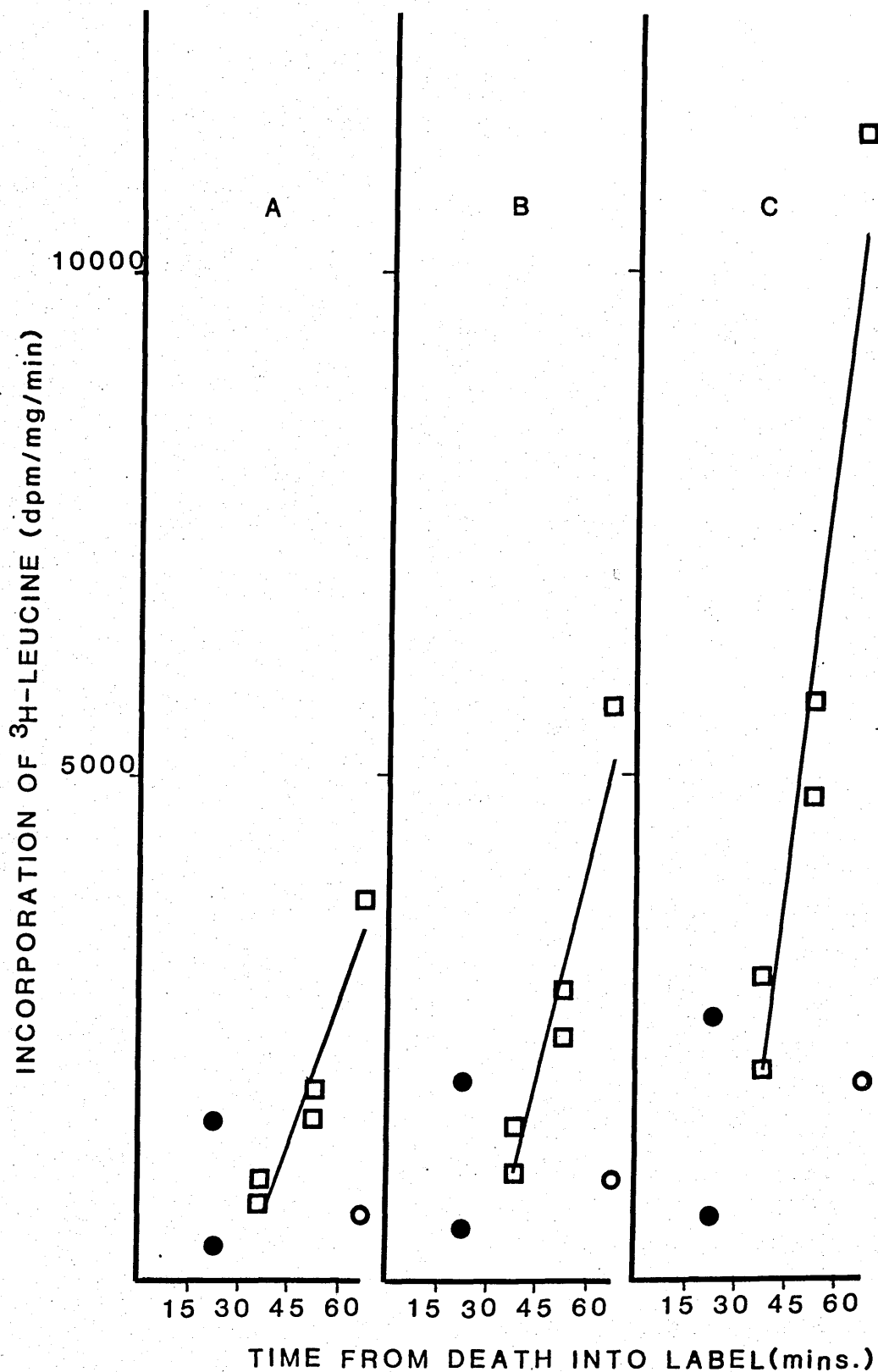


Figure 66. The calculated effects of cutting damage on the semi-quantitative assessment of ^3H -leucine incorporation in vitro

A - experimental results
 B - assume 50 um damage
 C - assume 100 um damage

KEY: \square - normal horse, shot
 \circ - normal horse, barbiturate
 \bullet - affected horse, barbiturate

DISRUPTION OF GLYCOPROTEIN SYNTHESIS

The morphological consequences : A summary

Numerous naturally occurring and synthetic compounds have known disruptive effects on cellular synthetic function. The morphological consequences of these disruptions are less well documented, and not necessarily studied in a variety of different cell types. The following summary outlines the structural changes resulting from damage at several different cellular levels, and refers to neurones unless otherwise stated.

The nucleus

Class 1 anthracycline antibiotics, such as Adriamycin, inhibit nucleolar RNA synthesis and DNA synthesis at equivalent concentrations by binding preferentially to double-stranded DNA via strong intercalative bonds (Crooke, 1979). Substances which bind, intercalate with or cross-link DNA (e.g. Actinomycin D or ethidium bromide (Daskal, 1979)), cause nucleolar segregation with loss of the normal honeycomb structure and a separation of the pars fibrosa and pars granulosa. Nucleolar segregation as a result of Adriamycin toxicity is present within 24 hours of intraperitoneal administration, fragmentation and enlargement occurring over the next 3-6 days (Cavanagh et al., 1987). Featureless cleared areas also occur in the karyoplasm, apparently at random, and this did not change over the period studied. The significance of these areas is unknown. The nucleolar segregation, however, indicates diminished synthetic activity and reduced ribosome production (Cavanagh et al., 1987). Membranous structures are also reported in the karyoplasm as a result of Adriamycin retrogradely transported along the axon

following direct application of this compound to the nerve 'stump' (Kondo et al., 1987).

Distinct cytoplasmic changes are also reported in Adriamycin toxicity. The Nissl substance is reduced in volume and some portions are partially denuded of ribosomes. This progresses over several days to a profound depletion of RER (Cavanagh et al., 1987). Bigotte and Olsson (1983) report peripheral loss of ribosomes and RER after retrograde transport of Adriamycin from the tongue, and the occurrence of peripheral membrane-bound vesicles and cisternae possibly derived from rough or smooth ER is also described (Cho, 1977; Eddy and Nathaniel, 1982). Some authors report central chromatolysis (Cho, 1977; Kondo et al., 1987).

There is an abundance of neurofilaments. Mitochondria are also increased in number, and have been described as vacuolated or "balloon mitochondria" (Bigotte and Olsson, 1983).

The small dark neurones of dorsal root ganglia would appear to be more susceptible to these changes than the large light neurones (Kondo et al., 1987) and younger rats show greater changes than older ones (Eddy and Nathaniel, 1982).

The ribosomes and rough endoplasmic reticulum

Several lectins, which are 'suicidally transported' to the perikaryon along the axon (e.g. ricin) inhibit protein synthesis at a ribosomal level by inactivating the 60S subunit. They have similar actions, but different potencies; it has been reported that a single molecule of ricin free in the cytoplasm is sufficient to kill a cell (Wiley and Stirpe, 1987). These lead

to a marked chromatolytic appearance of neurones at light microscopic level, and within five days there is marked neuronal loss.

The toxin of Shigella dysenteriae also acts at this level (Wiley and Stirpe, 1987). In nodose ganglion neurones, retrograde transport of the toxin causes incomplete loss of RER, numerous cytoplasmic vacuoles and early nucleolar disruption, with mitochondria, Golgi complexes and lysosomes less affected. By day 8, many neurones have disappeared. Very small quantities are required to achieve this - cells can die as a result of a concentration of toxin too small to be detected by immunocytochemistry (Wiley et al., 1985). However, minimal damage was sustained by neurones in the dorsal motor nucleus of the vagus, and no effects are seen in the perikarya of the XII nucleus, therefore these effects appear to be specific for sensory rather than motor neurones (Wiley et al., 1985).

Cycloheximide and emetine both disrupt the synthetic function of bound ribosomes specifically. The morphological changes resulting from this have been described in great detail in hepatocytes (Hwang et al., 1974).

The earliest changes are seen after six to twelve hours, when the cytoplasm contains various-sized vacuoles which are dilations of partially denuded RER. Paired smooth membranes are seen in stacks or whorls; these are flattened cisternae, which end in distended bulbs resembling the Golgi complex. One end of the whorls is reported to be apparently continuous with RER, the other end generally surrounded by the other cytoplasmic organelles. These membranes are free of ribosomes and frequently

form around mitochondria, SER or lipid. They are found most commonly perinuclearly, the frequency increasing progressively with time, but after 24 hours they decrease in size and frequency, and are gone within 36 hours.

Puromycin, which disrupts both free and bound ribosome synthetic function, shows similar effects regarding dilated RER and clusters of free ribosomes, but no whorls have been reported.

These authors (Hwang et al., 1974) hypothesise that the whorls which accumulate after cycloheximide treatment are formed by free ribosomes due to a lack of some component normally supplied by RER. Concurrent functional studies show that when protein synthesis decreases, phospholipid synthesis increases, and this is associated with the accumulation of the membranes. As the whorls disappear, protein synthesis increases and phospholipid synthesis decreases, thus suggesting that the membranes arise from some desynchronisation of protein and lipid synthesis. No comments are made regarding the appearance of the Golgi complexes in these cells.

Since glycoprotein synthesis is arrested by cycloheximide, histone production ceases, thereby impairing subsequent DNA synthesis (Pospelov et al., 1982). Perichromatin granules, the function of which is unknown, increase in number after exposure to cycloheximide (Daskal, 1979).

Tunicamycin inhibits the first enzyme of glycosylation, located in the RER (see also page 116). In cultured lymphocytes initial dilation of the RER is followed by swelling of the Golgi complex after 24 hours (Glassy and Ferrone, 1981).

In rat supraoptic nuclei, tunicamycin resulted in dilated RER cisternae containing filamentous material, and at higher doses (50 ug intracisternally) the Golgi complexes consisted of short, dilated but empty cisternae (Gonzalez et al., 1981). These authors also describe RER vesiculation resulting from treatment with puromycin, with empty cisternae.

Tartakoff (1980) describes arrest of the exit of secretory protein from RER as a result of chemicals which uncouple oxidative phosphorylation (no specific examples given). The Golgi cisternae persist despite lack of apparent input from the RER, suggesting that any distal progression of the cisternae themselves is also blocked.

The Golgi complex

Tunicamycin is previously described as having its effect at the level of the RER. Work in isolated hepatic Golgi fragments shows that tunicamycin also inhibits synthesis at the level of the Golgi. It only has this inhibitory effect, however, if the membranes are not disrupted (for example by detergents). This suggests that it is not the transferase itself which is inhibited, but carrier-mediated transport of nucleotide sugars across membranes (Yusuf et al., 1983).

Several compounds have been shown to fragment Golgi complexes in various cell types, for example the antimetabolic drugs colchicine, colcemid and vinblastine (Lin et al., 1982), but undoubtedly the most frequently used substance is the ionophore monensin, which disturbs monovalent cation homeostasis (Tartakoff, 1983). It interferes with the transport of secretory products and membrane proteins at the level of the Golgi complex,

and the carbohydrate composition of the resultant accumulated proteins suggests that the site of action is before the distal Golgi elements (Pohlmann et al., 1984). It appears to depress the synthesis of all glycoproteins to a similar extent (Hammerschlag et al., 1982).

Low (10^{-9} M) concentrations of monensin added in vitro to spinal ganglion leads to marked swelling of the intermediate Golgi sacs specifically (Lindsey and Ellisman, 1981). The intensity of staining by prolonged osmification or for TPPase is sometimes decreased, but of normal distribution. Higher concentrations (10^{-7} M) lead to extensive disruption of the Golgi complexes. Many of the resulting vacuoles stain to a varying degree with prolonged osmification, and a few cisternae in each clump are weakly TPPase positive, confirming the origin of these vacuoles as the Golgi complex.

A similar study using intraluminal administration of monensin (5×10^{-6} M) to intestinal absorptive cells, shows vacuolation of the Golgi occurring within five minutes (Ellinger and Pavelka, 1984). The AcPase positive GERL is vacuolated when the Golgi saccules are merely dilated, but after a few minutes all stack cisternae are strongly positive for both AcPase and TPPase. In the proximal small intestine all the resulting vacuoles are also positive for both these enzymes, but in the distal small intestine staining is restricted to a proportion of the vacuoles. This response to monensin, which affects the Golgi and GERL, but not the RER, is interpreted as indicating more common properties between the Golgi and GERL than the GERL and

the ER (Ellinger and Pavelka, 1984).

The plant toxin swainsonine is a potent inhibitor of Golgi mannosidase II and influences glycoprotein processing (Novikoff et al., 1985). In hepatocytes however, it is shown to have no discernible effects on the Golgi complex, which retains its conformation and TPPase reactions, but results in numerous AcPase positive, lysosomal-derived vacuoles.

The transport of glycoproteins from the Golgi to the fast axonal transport system is calcium-dependent. This can be inhibited by the absence of calcium, the presence of cobalt or a combination of the two, this latter being the most potent inhibitor (Hammerschlag and Lavoie, 1979; Lindsey and Ellisman, 1981). The volume of the cell occupied by SER is greatly increased by these disruptions, this consisting mainly of a specific, gross distension or vacuolation of the Golgi complexes.

The axon

Mechanical damage resulting in severance of the axon leads to a number of specific perikaryal changes known collectively as the axonal or retrograde reaction.

The nucleus is eccentric and crenated (Flumerfelt and Lewis, 1975; Aldskogius, 1978). Nissl granules in the central cytoplasm are disrupted forming dispersed, short segments and free ribosomes, the remaining RER mostly accumulating peripherally, although some RER (mostly ribosomes) persists round the invaginated nuclear envelope (Holtzman et al., 1967; Flumerfelt and Lewis, 1975; Torvik, 1976). The total volume of RER may or may not be reduced.

A similar disruption and decrease in volume of the RER is

the only qualitative change resulting from crush, but not severance, of the axon. This begins to resolve after one week (Torvik and Skjorten, 1971) as compared to the timecourse of the response to axotomy, where damage may increase over several weeks, and take months to fully resolve.

A proliferation of SER and tubular profiles is sometimes reported (Lieberman, 1971; Aldskogius, 1978) and neurofilaments are also increased (Flumerfelt and Lewis, 1975; Aldskogius, 1978).

The Golgi complexes show no consistent pattern of change. They are variously reported as increased (Price and Porter, 1972; Flumerfelt and Lewis, 1975) and displaced (Barron et al., 1971; Aldskogius, 1978) and in motor neurones there appears to be a transient decrease in TPPase staining (Lazlo and Knyihar, 1975; Torvik, 1976) but are otherwise unchanged.

Mitochondria are more slender and elongated than normal, and may be found accumulated perinuclearly (Holtzman et al., 1967) and at the base of processes in axotomised DNV neurones (Aldskogius, 1978). Lysosomes may also accumulate centrally (Holtzman et al., 1967) and these together with autophagic vacuoles are increased in number (Torvik, 1976).

The perikaryal response to axotomy varies in different neuronal populations (Torvik, 1976), within some populations (Flumerfelt and Lewis, 1975; Aldskogius, 1978) and also in relation to species (Torvik, 1976). The response to injury is more rapid and severe the more proximally the damage occurs, and identical lesions result in a greater degree of damage in younger

animals.

"Chromatolysis" is considered to be an indication of regenerative effort by the perikaryon and, in general, the extent of chromatolysis appears to be a measure of the initial injury. Certain neurones however, regenerate with no obvious chromatolysis, and others fail to regenerate despite extensive chromatolysis. The precise significance of these morphological changes in terms of cell function is not yet fully understood.

Some toxins are thought to have a primary effect on the axon.

Acrylamide causes no identifiable morphological change for five days subsequent to administration, but on the sixth day the nucleus is eccentric and crenated, and the RER, which is quantifiably decreased in volume, and fragmented centrally, occurs mainly peripherally. The perinuclear zone contains numerous hypertrophic mitochondria, and the Golgi complexes are frequently increased in size and complexity. In some neurones which look normal by light microscopy, subtle ultrastructural changes can be detected; often just a small portion of the cytoplasm is affected, containing an increased number of ribosomes and short cisternae of RER and SER (Sterman, 1982; Sterman, 1983).

Isoniazid is also a well-recognised cause of 'dying-back' neuropathy, causing dispersion and degranulation of RER and an increase in the number and size of mitochondria (Jacobs et al., 1979). In DRG neurones, the nuclei which are frequently displaced become crenated in large light cells by 48 hours and by day 4 in small dark cells. By this stage, margination of the

Nissl substance is marked in both types of neurone, and dense bodies are larger and more numerous than normal (Jones and Cavanagh, 1981).

Changes have also been reported in Schwann cells exposed to isoniazid (Jacobs et al., 1979). Within 24 hours there is an increase in microtubules, proliferation of SER, an increase in the size of the Golgi complexes and enlarged RER cisternae, especially at low doses. Although both isoniazid and acrylamide cause axonal damage the described perikaryal responses occur before any expected retrograde reaction from the axonopathy.

It can be seen from this brief summary that even very slight variations in the precise level of the synthetic pathway at which disruption occurs can lead to obvious differences in sub-cellular morphology.

ANTIMETABOLITES

INTRODUCTION

Morphological studies of affected autonomic and CNS neurones in the dysautonomias have shown marked changes in the RER and Golgi complexes. These organelles are concerned with aspects of protein biosynthesis i.e. the formation and elongation of the polypeptide chain, its glycosylation and trimming and modification of the oligosaccharides to produce the mature glycoprotein. It is, therefore, highly probable that the agent(s) causing dysautonomias interfere with protein biosynthesis although the exact location within the pathway is unknown.

There are numerous reports in the literature in which antimetabolites have been used to inhibit or modify protein synthesis. These compounds act in specific ways at various locations along the pathway, and although their biochemical effects are well known, the morphological correlates have been less well studied, and then seldom in neurones.

The aim of this study was to examine the disruptive effects of such drugs on the protein synthetic pathway of neurones and to compare these morphological changes with those in dysautonomias.

Dorsal root ganglion was chosen for these investigations, being susceptible to the natural disease, plentiful and readily sampled under experimental conditions. Also, vascular permeability in this region exposes its neuronal population to many circulating compounds in vivo (Jacobs et al., 1976; Olsson, 1984).

It was decided to study the effect of four antimetabolites

acting at different levels of the protein synthetic pathway.

(1) Adriamycin

Doxorubicin (Adriamycin; Farmitalia), is an anthracycline antibiotic, isolated from Streptomyces peucetius var. caesius. It is a 14-hydroxy derivative of daunorubicin, and exerts its effect by forming a complex with DNA. As judged from a model of the DNA-daunorubicin complex, the predominant mode of interaction appears to be intercalation of the drug between adjacent base-pairs of double-helical DNA molecules. To provide the intercalation with the antibiotics, the closed circular DNA may undergo supercoiling and uncoiling leading to configurational abnormalities. Alteration of the nuclear chromatin pattern has been reported in the neurones of DRG in rats (Cho et al., 1977; Cavanagh et al., 1987). There are indications that the cytotoxic effect may be a result of selective damage to chromosomal DNA molecules rather than to a quantitative reduction in DNA synthesis.

(2) Cycloheximide

This is a glutarimide antibiotic from Streptomyces griseus. It inhibits polypeptide chain initiation and elongation by interaction with 60S ribosomal subunits. Initiation is blocked at lower concentrations than is chain extension. It interferes with chain elongation by inhibiting entry of peptidyl tRNA from the A to the P site through interference with the release of deacylated tRNA from the donor site. It may interfere with initiation by inhibiting the binding of initiator tRNA to ribosomes or binding of 60S subunits to form an initiation

complex (Pestka, 1971).

(3) Tunicamycin

This drug is derived from Streptomyces spp. The inhibitory activity of tunicamycin is due either to its activity as a multi-analogue, competitive inhibitor, or a non-competitive inhibitor of the UDP-GlcNAc:dolichol phosphate-GlcNAc-1-phosphate transferase that catalyses the first step in lipid carrier dependent protein glycosylation.

Several homologues differ in their fatty acid side chains. Homologues with different side chain structures exert similar inhibition of protein glycosylation. This might also be important in the inhibition of protein synthesis, an activity which is shared by only a few homologues. The side chain structure also contributes to the lipophilicity of the molecules, which may be responsible for solubility differences of the various homologues in the lipid bilayer of the cell membrane, and thus affecting the overall activity in cells.

In summary, tunicamycin is thought to act by inhibiting the first glycosyltransferase in the dolichol cycle, an enzyme that is probably located in the lipid bilayer entity of the RER membranes, but there are some functional differences between the various homologues, and the composition of purchased tunicamycin may vary from batch to batch (Duskin and Mahoney, 1982; Sigma catalogue, 1986). Yusuf et al. (1983) have produced evidence, however, to suggest that it is not transferase itself which is inhibited, but the carrier-mediated transport of nucleotide sugars across membranes.

(4) Monensin

This is derived from Streptomyces cinnamomensis. It is a carboxylic ionophore, which disrupts intracellular vesicular transport, including transport across the Golgi stack, and prematurely terminates Golgi-associated processing of the oligosaccharides on many exported proteins (Dunphy and Rothman, 1985).

MATERIALS AND METHODS

(a) In vivo

Adriamycin (doxorubicin INN; Farmitalia) was reconstituted to a concentration of 2 mg/ml in sterile saline, and administered to Lou rats (weighing 100-150 g) by one of two routes.

(i) Five rats received 10 mg/kg intravenously, and were subsequently killed 6 hrs., 1, 3, 5 and 7 days post-injection.

(ii) Four rats received 10 mg/kg intraperitoneally and were killed 1, 3, 5 and 7 days post-injection.

Two rats which received no Adriamycin were also used as controls.

Each rat was killed by perfusion-fixation (see Appendix 4) under anaesthesia induced by 1 ml pentobarbitone administered intraperitoneally.

150 ml of a fixative containing:

(Final concentrations)

8% paraformaldehyde	75 ml	(5%)
2.5% glutaraldehyde	30 ml	(4%)
calcium chloride	75 mg	(4.5 mM)

made up in 0.08M sodium cacodylate buffer (see Appendix 3) was used for each perfusion.

Following perfusion, cervical DRG were removed. Autonomic ganglia (coeliaco-mesenteric ganglion, stellate ganglion and cranial cervical ganglion) were also removed, but not labelled individually. These ganglia were further fixed in the same fixative for a variable period of up to one week prior to routine processing for electron microscopy (see Appendix 1).

(b) Short term in vitro

The following stock solutions were made:-

(i) Cycloheximide, 1 ug/ul

2 mg cycloheximide (Sigma) was dissolved in one drop of absolute alcohol from a Pasteur pipette (approximately 50 ul), and made up to 2 ml with HBSS complete with amino acids and glucose (Appendix 5). This was made fresh on the required day, and any surplus discarded.

(ii) Tunicamycin 1 ug/ul

1 mg tunicamycin (Sigma) was suspended in 800 ul distilled H₂O. A 10% solution of concentrated ammonia was then added in 5 ul amounts, and the suspension agitated each time until the tunicamycin was fully dissolved (approximately 20 ul ammonia usually required). This solution was then made up to 1 ml with distilled H₂O, divided into ten 100 ul aliquots and stored at -

20°C until required.

(iii) Monensin, 1 mM

3.5 g monensin (Sigma) was dissolved in 5 ml absolute alcohol and refrigerated (4°C) until required.

The final concentrations used (see below) were obtained by making the following dilutions in HBSS with amino acids and glucose (Appendix 5).

- (a) 1 : 100 of stock solution (10 μ M).
- (b) 1 : 100 of 10 μ M solution (0.1 μ M).
- (c) 1 : 1000 of stock solution (1 μ M).

Adult White Wistar rats of both sexes were used. Each rat was anaesthetised with Halothane by inhalation and 1 ml pentobarbitone administered intraperitoneally, then killed by perfusion with 120 ml chilled saline (see Appendix 4).

Cervical DRG were removed, the capsules incised and whole ganglia placed in 5 ml incubation medium (HEPES buffered salt solution with amino acids and glucose (Mata et al., 1980) (see Appendix 5) in 25 ml flasks in a shaking waterbath at 37°C within 25 mins. of death.

- (i) Ganglia were incubated for varying periods of up to 24 hours, to determine the period for which neurones remained morphologically normal.
- (ii) Cycloheximide was added to the incubation medium at concentrations of 0, 20 μ g/ml and 80 μ g/ml and ganglia incubated for three or six hours.

(iii) Tunicamycin was added to the incubation medium at concentrations of 0, 10 ug/ml and 25 ug/ml and 50 ug/ml and ganglia incubated for three or six hours.

(iv) Monensin was added to the incubation medium at concentrations of 0, 0.1 uM, 1uM and 10uM and ganglia incubated for three or six hours.

The control solution with no monensin contained 1% alcohol.

All ganglia were fixed for a minimum period of 16 hours in the following fixative:-

	(Final concentrations)
paraformaldehyde	3%
glutaraldehyde	0.5%

made up in 0.1M sodium cacodylate buffer (pH 7.4) (Appendix 3).

They were then rinsed in 0.075M isotonic cacodylate buffer (pH 7.3) (Appendix 3) and processed for electron microscopy (Appendix 1).

Following embedding in Araldite resin (Appendix 1) 1 um sections were cut on a Reichert OmU3 ultratome, and stained with methylene blue. Grids were then cut (600-800 A) from selected areas of these sections.

All grids were stained with uranyl acetate and lead citrate (Appendix 2) and examined under a Philips 301 electron microscope.

RESULTS

Dorsal root ganglia are generally considered to contain two main neuronal populations; the large light cells, and the small dark cells. However, several authors working with rodent DRG

have subdivided these categories into six or seven distinct neuronal populations on the basis of their ultrastructural appearance and histochemical properties (Duce and Keen, 1977; Rambourg et al., 1983; Sommer et al., 1985; Malchiodi et al., 1986).

These authors subdivided the two main classifications of large light and small dark neurones according to the volume of their Nissl substance and the distribution of this and the other organelles within the cytoplasm. The differing affinity of the Golgi complexes for various histochemical markers also contributed to their classifications.

For the purposes of this study only the two main groupings, based on the nuclear : cytoplasmic volume ratio were used.

(a) In vivo Studies

Normal DRG

Under the light microscope, all the neurones had large, centrally placed nuclei with prominent nucleoli, and the cytoplasm was granular, due to the presence of RER (Nissl granules) (Fig. 67).

Ultrastructurally the cytoplasm contained numerous areas of RER throughout its volume, varying in size from stacks of 5-6 parallel cisternae, to smaller vesiculo-tubular arrays. The bigger stacks tended to be more clearly defined, and the volume of cytoplasm separating these discrete Nissl granules varied from one neurone to another.

Golgi complexes generally consisted of 3-4 cisternae and numerous associated small vesicles, found close to areas of RER

but not closely related to either the cell membrane or the nuclear envelope. They were more prominent in the smaller, darker neurones than in those cells with a greater volume of cytoplasm and larger Nissl granules.

Lysosomes and mitochondria were evenly distributed throughout the cytoplasm, the remainder of which contained numerous neurofilaments and tubules.

Adriamycin DRG

No differences could be found between rats receiving intravenous Adriamycin and those which were treated by intraperitoneal administration. The following comments therefore apply equally to both sets of animals.

Many DRG neurones remained normal throughout exposure to Adriamycin.

The earliest changes, after six hours, were seen in the nucleus, with some separation of the pars fibrosa and pars granulosa in the nucleolus, and clear areas in the karyoplasm (Fig. 68a). These abnormalities were found in some neurones in every rat treated with Adriamycin.

Cytoplasmic changes were not seen at this stage, but after one day, one neurone showed a discrete area of cytoplasm with a loss of Nissl substance and an accumulation of tubular profiles (Fig. 68b).

More commonly, however, even cells with nuclear abnormalities showed no cytoplasmic change up to three days after the administration of Adriamycin (Fig. 69a).

After 3-5 days a few neurones did demonstrate subtle changes in the intracellular distribution of RER, and an increase in the

number of mitochondria was occasionally found (Figs. 69b and 70). In these cells, RER tended to accumulate around the periphery of the cell leaving smaller fragments centrally, but this redistribution of RER was not necessarily concurrent with a change in mitochondrial numbers (Fig. 71a).

A reduction in the amount of RER and an increase in neuro-filamentous structures could be seen by one week after treatment (Fig. 71b). Nuclear structure was little different from that in the earliest examples (Fig. 68a).

No gross structural abnormalities of any of the cytoplasmic organelles were found as a result of Adriamycin.

Normal autonomic neurones

Normal autonomic neurones (Fig. 72) were generally rounded or oval with a prominent nucleus containing a typical "honeycomb" nucleolus. RER was well-formed and distributed throughout the entire cytoplasm. At lower magnifications, a tendency for the RER to occur in Nissl granules could be detected, but this was not well-defined at higher powers. Golgi complexes were well-formed and numerous, being found most frequently in the central band of cytoplasm not closely associated with either the cell or the nuclear membranes.

Mitochondria and lysosomes were randomly distributed throughout the cytoplasm.

Adriamycin-affected autonomic neurones

Six hours after treatment, the neurones looked relatively normal (Fig. 73), but small cleared areas were present in some nuclei. RER did not occur at the periphery of the neurone, but

looked otherwise normal. Close to the nucleus RER was very dense, with no clear boundary between it and the other organelles.

Occasional neurones contained single bundles of neurofilaments found close to the nucleus within areas of RER (Fig. 73).

The neurones of animals killed 1-3 days after the administration of Adriamycin had profuse quantities of RER distributed throughout the cytoplasm from the nuclear envelope to the cell membrane. This profusion of RER made the identification of Golgi complexes difficult, but when observed, they appeared normal. Some nuclei contained 'cleared' areas. These reflected the changes already described in the earlier example (Fig. 73). The other organelles appeared normal.

By five days after the injection, some nuclei were more dense than normal, with poorly-defined boundaries. RER was beginning to accumulate at the neuronal margins, leaving the Golgi complexes central to it.

One week after the administration of Adriamycin, the neurones showed marked margination of normal-looking RER, and resulting central chromatolysis. Golgi complexes, mitochondria and lysosomes were normal (Fig. 74).

(b) Short term in vitro studies

(i) Cell survival

Ganglia were incubated for periods of up to 24 hours, and examined at two hour intervals.

With the exception of the control ganglion, fixed immediately after removal from the rat, degeneration was seen in a number of the neurones in the centre of the ganglion (Fig. 75).

This number increased in direct proportion to the incubation time.

In the first 6-8 hours, the large majority (80-90%) of neurones lying in the peripheral areas of the ganglion remained morphologically normal (Figs. 76 and 77). After this time large numbers of neurones degenerated, and it was decided to confine the assessment of antimetabolite-related morphological change to within the first six hours of incubation.

(ii) Cycloheximide

Nothing remarkable was noted on light microscopic examination of DRG incubated with cycloheximide for three hours. After six hours the cells showed generalised cytoplasmic vacuolation. These vacuoles were small in every case, and evenly distributed.

Ultrastructural changes after three hours' incubation were inconsistent, with some neurones showing no abnormalities at all (Fig. 78a) while others displayed slightly dispersed RER and occasional small accumulations of free ribosomes (Fig. 78b).

A six hour incubation period resulted in much more definable change with both the concentrations examined (Fig. 79). RER became distended, sometimes by an obvious electron-dense floccular material, and the surrounding cytoplasm looked granular as a result of increased numbers of free ribosomes.

Golgi complexes were not seen in their usual configuration of curved stacks of parallel cisternae, but there were occasional areas of cytoplasm containing closely associated vesicular profiles which were thought to be unusual Golgi complexes. The

other organelles appeared normal.

(iii) Tunicamycin

Light microscopic examination of ganglia exposed to tunicamycin revealed small, discrete perinuclear cytoplasmic vacuoles which were much more readily seen in the preparations incubated for six hours (Fig. 80).

On ultrastructural examination such vacuoles were found to be distended elements of the Golgi complex which retained the expected cytoplasmic orientation, but no normal Golgi complexes could be seen (Figs. 81 and 82). All other organelles appeared normal.

No variations were seen in relation to the differing concentrations of tunicamycin, and very slight distension of the Golgi elements was the only change discernible after three hours incubation (Fig. 81).

Six hours' incubation resulted in markedly distended Golgi cisternae, with the appearance of clumps of cytoplasmic vacuoles (Fig. 82). No recognisable Golgi elements remained, but there was no visible involvement of the surrounding organelles.

(iv) Monensin

Incubation of DRG in the presence of monensin resulted in a "foamy" appearance of the cytoplasm at light microscope level, caused by clusters of vacuoles which tended to be perinuclear (Fig. 83). Both light and dark neuronal populations were affected to approximately the same degree, although a moderately larger proportion of cytoplasm in small dark cells tended to be vacuolated. The nuclei remained prominent and centrally positioned.

Ultrastructurally, after three hours' incubation with all three concentrations of this antimetabolite, the cytoplasm contained many vacuoles which were commonly round or oval, bounded by a single limiting membrane, apparently empty, and occurring in discrete groups (Figs. 83-85). They were generally closely associated with areas of normal RER in a similar orientation to that of Golgi complexes in the normal neurone. No Golgi complexes could be seen, and mitochondria tended to be more dense and slender than normal.

With all concentrations, six hour incubations led to greater and apparently more random vacuolation. RER was difficult to identify and the mitochondria were more varied in shape and size, denser than usual, and in some cells increased in number (but this was not quantified) (Fig. 86).

While the 0.1 μ M concentration did not result in such devastation of the RER as was apparent with higher concentrations, it can be seen (Fig. 87) that increasing incubation time has a very marked effect on the degree of vacuolation when assessed in proportion to cytoplasmic volume.

DISCUSSION

The results obtained by these experimental techniques are discussed in detail in the second part of this section. However, there are several methodological factors which must first be taken into account regarding interpretation of these findings.

Methodological considerations

The in vivo administration of an antimetabolite enables its effects to be examined over a period of several days, or longer if required. When neuropathological changes are of specific

interest, however, two problems arise.

Exposure of the majority of the nervous system to circulating antimetabolite may be poor, due to the effects of the blood-brain barrier. There is vascular leakage into DRG however, as demonstrated by tracers (Jacobs et al., 1976) but this does not ensure comprehensive exposure of neurones.

Also, administration of antimetabolites which are not specifically neurotoxic in concentrations high enough to enable good exposure of neurones, can lead to generalised toxicity and death before the specific effects within neurones can be visualised.

Both of these problems were encountered to some degree in this study with Adriamycin. Several neurones showed no effects at all in each rat examined, and a rat given Adriamycin (intravenously) for examination on day 11 post-treatment, died on day 3.

The morphological effects of the other antimetabolites were examined in vitro in whole ganglion preparations. This method was chosen for several reasons:-

- (i) Numerous ganglia could be obtained from one rat, greatly reducing both the total number of rats required for the study, and the potential differences introduced by individual variation.
- (ii) Direct exposure of neurones to the antimetabolite was possible.
- (iii) There were no complications resulting from systemic toxicity.

(iv) The earliest changes resulting from disturbance of synthetic function were anticipated to be of the greatest interest, therefore sufficient time was available within the limits imposed by cell survival in vitro.

This system does have some inherent problems which must be considered in the interpretation of the results. Given that cellular degeneration is marked after eight hours, and that metabolic functions are depressed in vitro (see page 94) it should be remembered that, even in the controls, function will be altered in comparison to the situation in vivo.

Provided that non-treated controls are included for each incubation time in every experiment and perfusion-fixed normal material is available, any antimetabolite-specific changes are readily discernible. This allows comparison with the non-specific degeneration present in the controls.

It is possible that cellular susceptibility to a specific disruptive agent will increase as the cell approaches the stage at which internal compensatory mechanisms fail, and non-specific degeneration occurs. Care must therefore be taken when interpreting the differences described earlier between the three and the six hour incubations.

The purpose of this study was to determine qualitative and not quantitative change, however, and the experimental design was considered both simple and adequate. Varying concentrations of each antimetabolite were used because no reference could be found regarding concentrations known to cause morphological change within such a short time-period.

The effects of Adriamycin were examined in vivo rather than in this system since retention of nuclear function is reputedly poor in short-term in vitro preparations (I.R. Freshney, personal communication), and no longer-term in vitro model was available (see below). Only one concentration was used, since this (10 mg/kg) has been shown to result in distinct cytoplasmic changes (Cho, 1977; Cavanagh et al., 1987).

Tissue culture offers all the advantages of the in vitro model used here, without the drawbacks of superimposed cell death and the subsequent restrictions on time. While being outwith the scope of this study, preliminary work was undertaken with the aim of establishing neurones in culture for future, more detailed examination of the ultrastructural effects of antimetabolites. The methods and results of this are briefly summarised later in this discussion.

Consideration of Results

The morphological consequences of inhibiting protein synthesis using these specific antimetabolites have been studied by other authors, using various cell-types, and their findings have been described in detail earlier. This discussion compares these previously reported findings with the present results in neurones.

(i) Adriamycin

Nucleolar segregation and cleared areas within the karyoplasm were early changes in both DRG and autonomic neuronal populations in this study, and correspond to those described by Cavanagh et al. (1987). Cytoplasmic changes in the DRG also correlate to those authors' findings, with a disruption of RER

and a relative increase in neurofilaments. These alterations were much less severe than those described by Kondo et al. (1987) where a much greater proportion of neurones were involved, and cytoplasmic structures were more markedly affected.

This difference can be accounted for by the route of administration. The Kondo et al. (1987) method involved direct access to a nerve stump, thus ensuring that each neurone was exposed to a relatively high concentration of the drug. The other routes of administration relied on vascular permeability of the ganglia which results in much lower concentrations at the cellular level, and a more uneven exposure of the ganglionic population.

The margination of RER and central chromatolysis was more pronounced in the autonomic ganglia than the DRG, but the overall effect of net loss of the RER was the same, and other organelles remained unaffected in both populations.

Adriamycin depresses RNA synthesis in the nucleus, therefore fewer new ribosomes will be available to replenish the cytoplasmic population and a gradual depletion occurs. mRNA will also be decreased, and therefore the synthetic demand on the existing ribosomes lessened. The increase in neurofilaments is an apparent anomaly since neurofilament proteins, like other proteins, require an mRNA signal and ribosomes for their synthesis. Depending on the concentration of Adriamycin in the cell, however, synthesis is likely to be depressed rather than totally inhibited, and as the volume of RER gradually decreases there will be a need for neurofilaments to maintain the cellular

volume, and therefore no internal negative feedback on neurofilament production.

(ii) Cycloheximide

Dilated, partially denuded cisternae of RER are a documented change in cycloheximide toxicity, and were reproduced in this study after six hours' incubation.

Since cycloheximide inhibits the synthetic function of bound ribosomes specifically, its only primary effect is the cessation of glycoprotein polypeptide-backbone production once ribosomes are attached to the RER membrane. Since the "signal sequence" of the polypeptide is synthesised on free ribosomes and inserted into RER when the ribosome binds, these short polypeptides must remain in the RER and accumulate in the absence of any chain elongation. Any polypeptides incompletely elongated at the start of exposure to the drug will also remain in the cisternal lumen.

Polypeptide synthesis is depressed in a dose-dependent manner by cycloheximide (see page 99), therefore it is probable that at lower doses there are insufficient molecules of drug in the cell to inhibit every ribosome the moment it attaches to RER but enough to do so at some subsequent stage, and therefore more incomplete chains would accumulate in the cisternal lumen.

Depression of synthesis means reduced protein is available for glycosylation and transportation from the RER to the Golgi. Vesicular transport will be decreased between these organelles. Since membrane proteins are also supplied to the Golgi in this way it is conceivable that the abnormalities of the Golgi complexes seen in this study arise as a result of inadequate membrane replenishment.

The peculiar membrane configurations reported in hepatocytes (Hwang et al., 1974) were seen after a longer period, and the function and architecture of these cell-types so different from neurones that any direct comparison is, at best, speculative. The membranes were transient in the hepatocytes, so a longer time-course in neurones may have revealed similar abnormalities in response to the cycloheximide. Alternatively the cells are so different that a similar lesion has markedly different morphological consequences. There was no comment on the fate of the Golgi complex in those treated hepatocytes.

(iii) Tunicamycin

There is some uncertainty regarding the precise mode of action of this antimetabolite. It is generally recognised to inhibit core glycosylation at the level of the first enzyme in the RER, but as mentioned earlier cell-fraction work has demonstrated that it may be less specific and exert an influence over a wider section of the glycosylation process by inhibiting the transport of sugars into the relevant organelles. The functional effect is still the same, however, an inhibition of the glycosylation of polypeptides.

The dilation of RER reported to occur initially (in lymphocytes) was not observed in the ganglion preparations, but the subsequent dilation of the Golgi elements was comparable. This is most likely due to incompletely-glycosylated glycoprotein being transported to the Golgi complexes where terminal glycosylation of these abnormal molecules cannot occur and they accumulate in the Golgi cisternae, unsuitable for export.

Failure of glycosylation affects various proteins differently but in some, the oligosaccharide moiety is necessary for structural stability or for transport.

(iv) Monensin

This well documented antimetabolite is reported to produce disruption of the Golgi complex and the formation of multiple cytoplasmic vacuoles, as described in this study, in all cell-types in which its effects have been examined.

The precise level at which monensin disrupts intracellular transport is not known, but is thought to be in the region of the intermediate Golgi saccules, which are particularly sensitive to this ionophore in ganglionic neurones (Lindsey and Ellisman, 1981). Swelling of the vacuoles could be attributed to water influx occurring as a result of the disturbed monovalent cation homeostasis.

It is interesting to note that there is no concomitant disruption of RER, suggesting that either the exit of newly-formed protein from the RER is not inhibited, and more vacuoles are formed by this process, or that there is a feedback inhibition of synthesis when transport is disrupted.

The overall significance of this antimetabolite study in relation to the pathogenesis of dysautonomias will be evaluated in the General Discussion.

As mentioned at the beginning of this section, the use of an in vitro model which would allow the study of antimetabolite-induced morphological change over longer time periods, without the complication of superimposed slow cell-death, would greatly enhance the understanding of the neurones' responses to specific

insult. One such possible system is outlined below.

Tissue culture as an alternative in vitro model

(i) Methods

Sterile glass coverslips (22 mm diameter) were coated with an aseptically prepared, dialysed, acetic acid extract of rat-tail tendon collagen subsequently reconstituted by exposure to concentrated ammonia vapour for two minutes, and stored in Eagles MEM containing foetal calf serum, glucose and penicillin/streptomycin for 3-12 days prior to use.

Mouse embryos (18 days or older) or neonates less than 24 hours old were used for the provision of ganglia. DRG were removed using sterile techniques, collected into Hank's Buffered Salt Solution (BSS), their capsules carefully broken by teasing the ganglia gently with fine forceps, and placed on the collagen-coated coverslips at a rate of six per coverslip. Each coverslip was then placed in one of the wells of a 6-well multiwell plate. After one hour at room temperature, 1 ml of Eagles MEM containing glucose, foetal calf serum and chick embryo extract (made from nine-day old chick embryos) was added to each well, and the ganglia incubated at 37°C in a CO₂-enriched (approx 5%) atmosphere for seven days. Exhausted medium was removed, replaced with fresh medium and the cultures incubated for a further five days prior to the addition of antimetabolite.

After 48 hours, the cultures were washed in Hanks BSS and fixed for one hour in either 4% paraformaldehyde or 2.5% glutaraldehyde (both in 0.1M phosphate buffer [pH 7.3]) for either light or electron microscopy respectively.

Cultures for electron microscopy were washed in buffer, post-fixed in osmium tetroxide and dehydrated as in Appendix 1 until 70% alcohol was reached. The collagen-based cultures were then cut away from the rest of the collagen using a razor-blade fragment, and placed flat on a thin layer of agar. Another thin layer of agar was added on top of the culture and an agar block containing the resultant culture "sandwich" then underwent the remaining processing as a free-floating block, thus keeping the culture flat. These blocks were embedded in a drop of Araldite between two silicone-coated slides, and the resulting thin sample mounted on a blank Araldite block with cyanoacrylate resin to present the culture parallel to a flat cutting surface for easy orientation. Thin sections were cut with no prior reference to 1 μ m sections.

Cultures for light microscopy were washed in buffer post-fixing, then stained by the combined Karnovsky and Roots cholinesterase and Tsuji and Tobin-Gros' method for axons, and counterstained with 0.02% methylene blue.

(ii) Results

Some problems were encountered initially due to unfamiliarity with dissection techniques, and subsequently as a result of occasional contamination and the variable age of the neurones. The difficulties in maintaining a constant CO₂ supplement with limited facilities, sometimes caused a physiologically quite marked pH fluctuation (as indicated by the phenol red in the medium).

In cultures which grew healthily in vitro, Schwann cells and fibroblasts migrated away from the ganglion to form a monolayer,

leaving the original population of neurones stationary at the original site of the transplanted ganglion. The forces arising from the migration of the non-neuronal cells caused a flattening of the neuronal clumps and the resultant surviving neuronal population closely resembled a monolayer. Individual perikarya could therefore be readily examined either in culture, or following fixation and staining for light microscopy (Fig. 88) or electron microscopy.

The ultrastructural appearance of cultured DRG neurones is basically the same as that of neurones in more conventional DRG preparations (M. Ecob, personal communication).

Because of contamination problems no examples of normal neurones at ultrastructural level were available, but Fig. 89 shows a neurone which had been in vitro for 14 days and exposed to tunicamycin for the final 24 hours. As described earlier, tunicamycin results in a distension of the Golgi complex, but no other specific structural abnormalities.

The preliminary results were therefore very promising in general, suggesting that once all the methodological inconsistencies were removed, this would indeed be a valid in vitro model for studying the morphological effects of the disruption of neuronal protein synthesis.

Figures 67 – 89

Figure 67

Large light cell, non-incubated dorsal root ganglion,
perfusion-fixation

Extensive areas of RER (RER) are present in this neurone, with no pronounced demarcation between one area and another. The Golgi complex (G) is large, and closely related to the RER. It has many associated small vesicles. Mitochondria (M) are frequent, and occasional dense lysosomes (L) can be seen. One small Golgi complex (*) is present, uncommonly close to the nucleus (N).

Bar = 0.5 μ m.

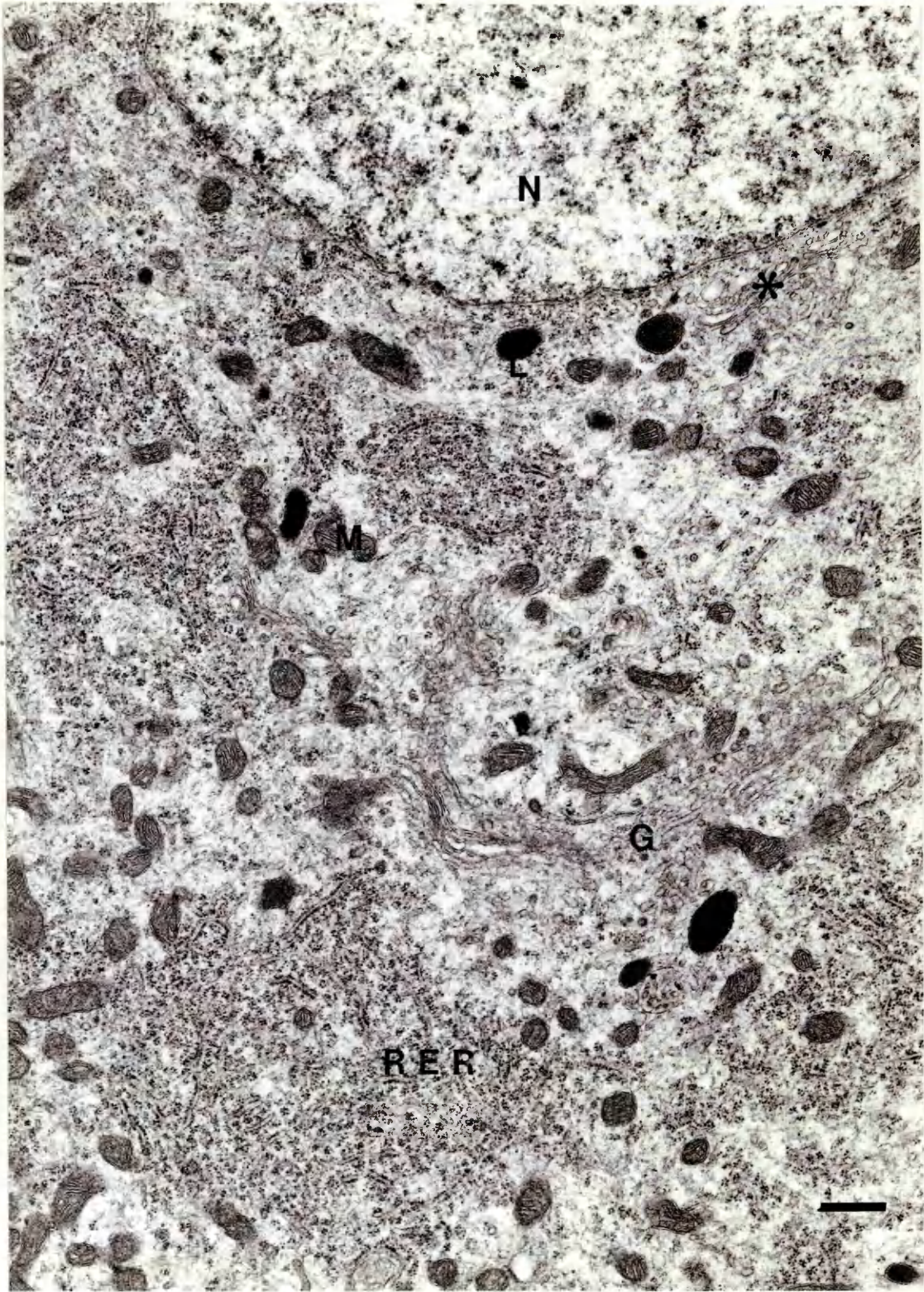


Figure 68

Dorsal root ganglion, Adriamycin (intravenous)

(a) 6 hours

Several 'cleared' areas (arrowhead) can be seen within the nucleus, and the nucleolus contains small areas where there has been separation of the pars fibrosa and the pars granulosa (arrow).

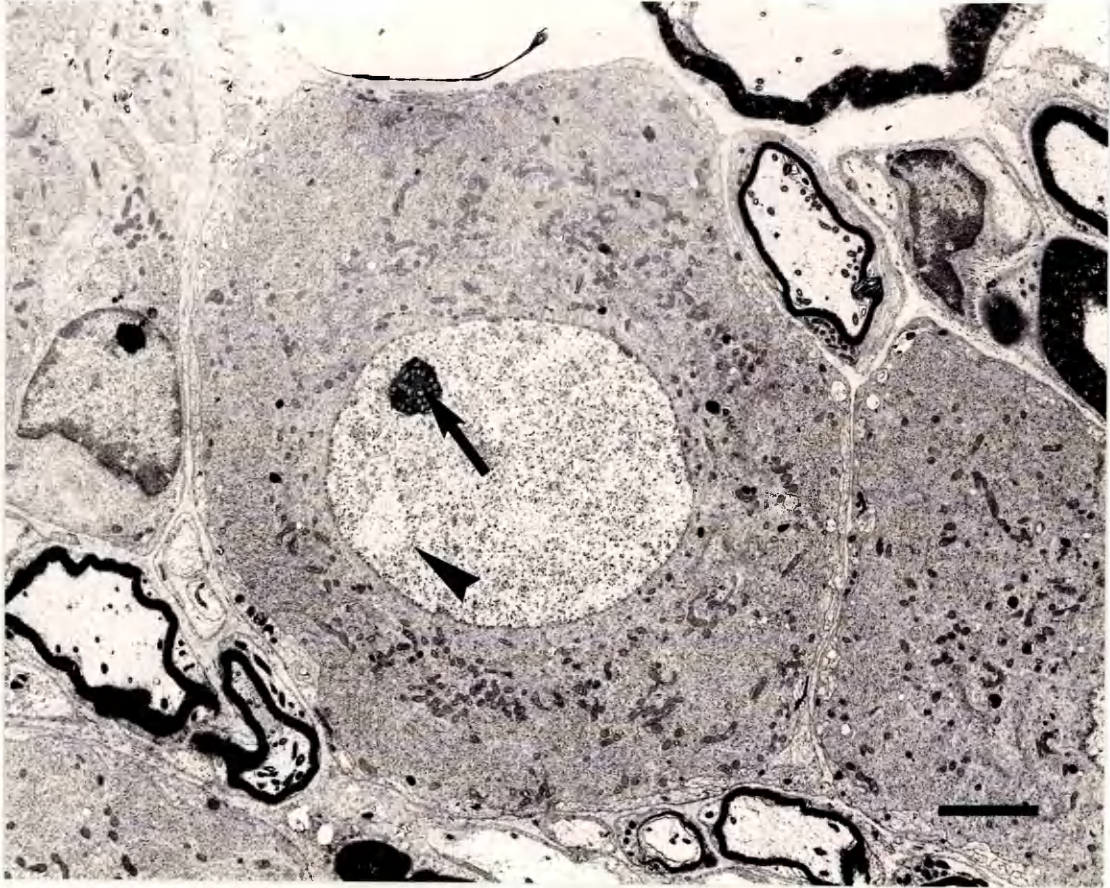
No cytoplasmic abnormalities can be detected.

(b) 1 day

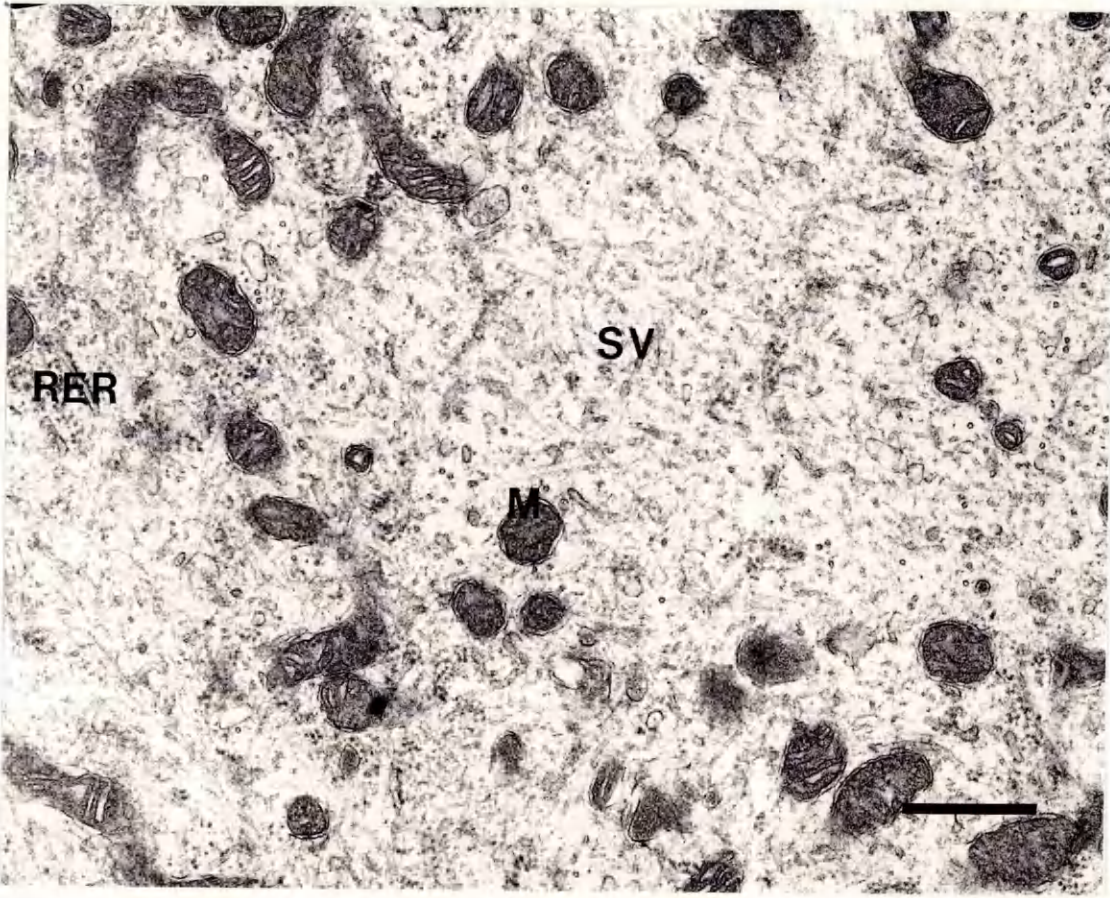
One neurone contains increased amounts of smooth vesiculo-tubular material (SV) one area of which is exclusive of the other organelles. This area is bounded by mitochondria (M) and fragments of RER (RER). This is the only neurone showing these changes.

(a) Bar = 3 μ m.

(b) Bar = 0.5 μ m.



a

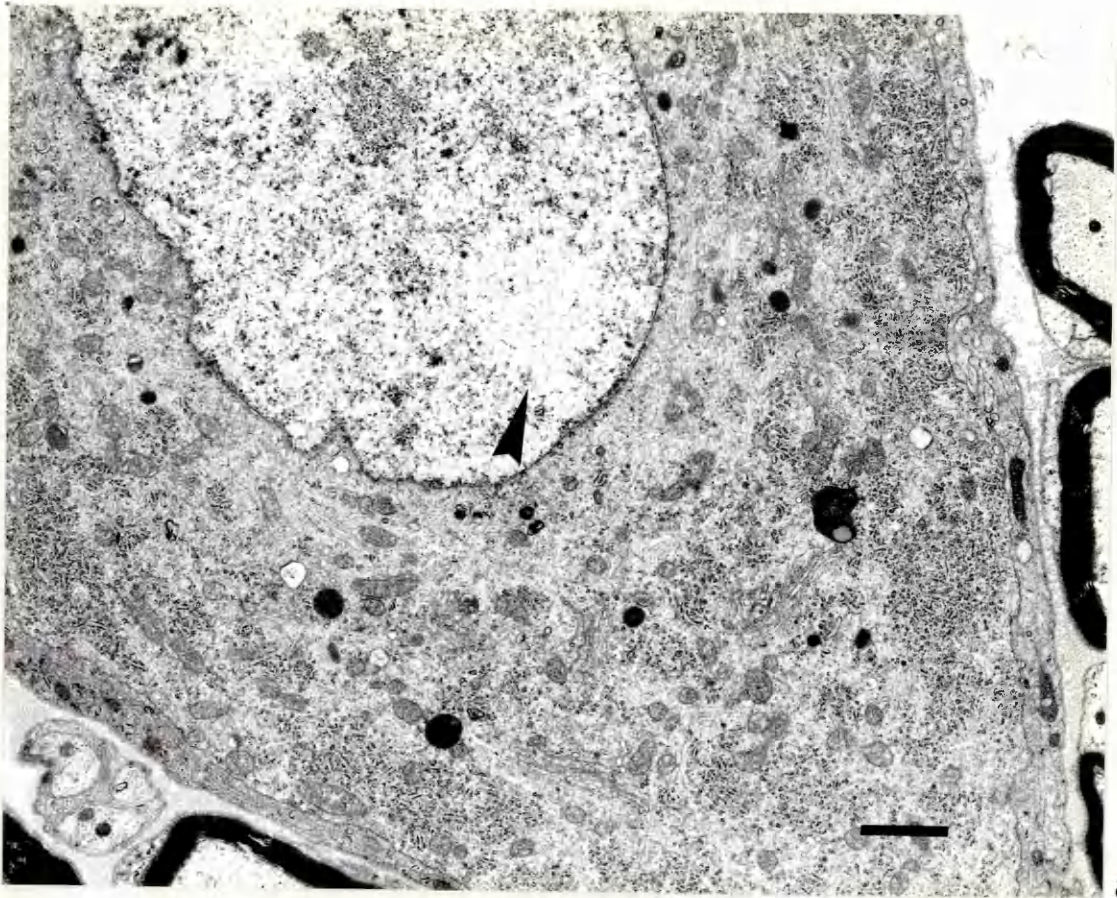


b

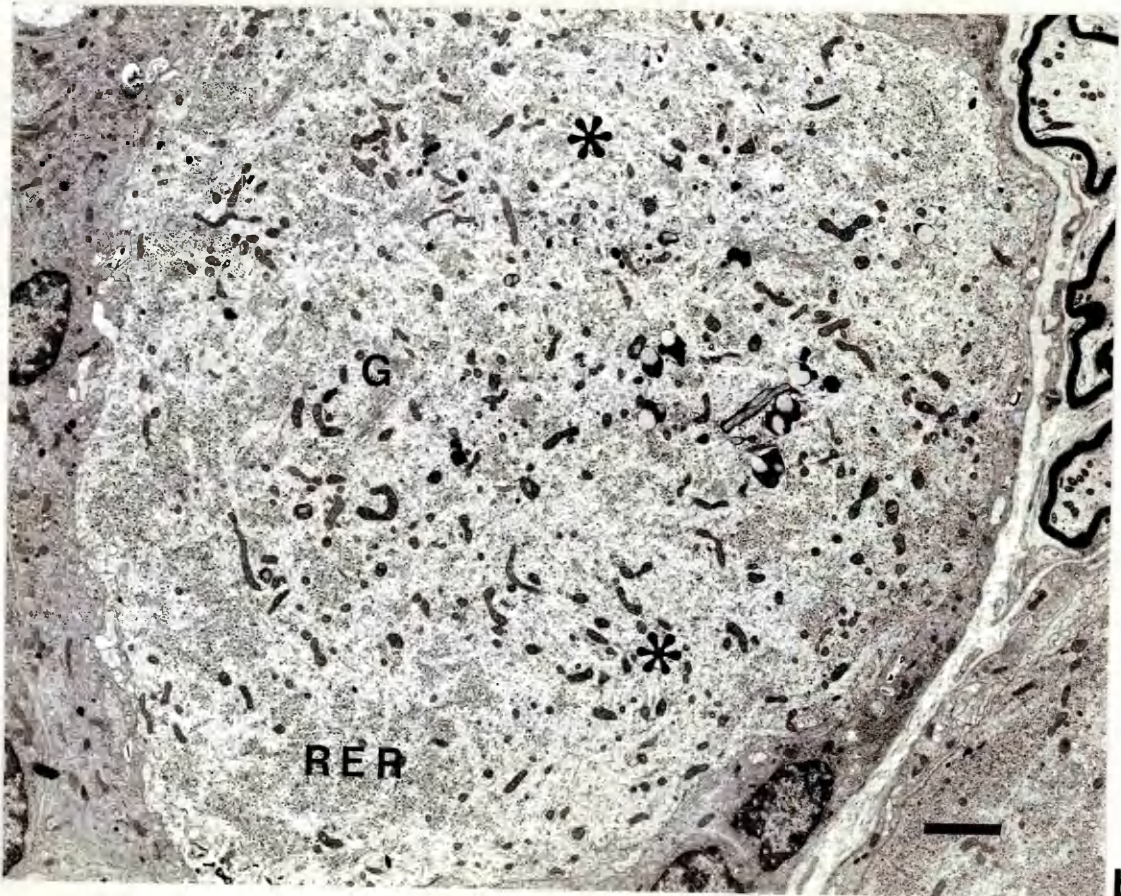
Figure 69

Dorsal root ganglion, Adriamycin (intravenous) 3 days

- (a) Frequently, no cytoplasmic abnormalities can be found even in neurones showing abnormal nuclear 'cleared' areas (arrowhead).
 - (b) Some neurones appear to have slightly less RER than normal, with any larger Nissl granules (RER) occurring peripherally, the more centrally placed RER being more fragmented. Some areas (*) contain hardly any RER. Mitochondria appear more dense and slender than usual. Golgi complexes (G) and lysosomes look normal.
- (a) Bar = 1 μ m.
- (b) Bar = 2 μ m.



a

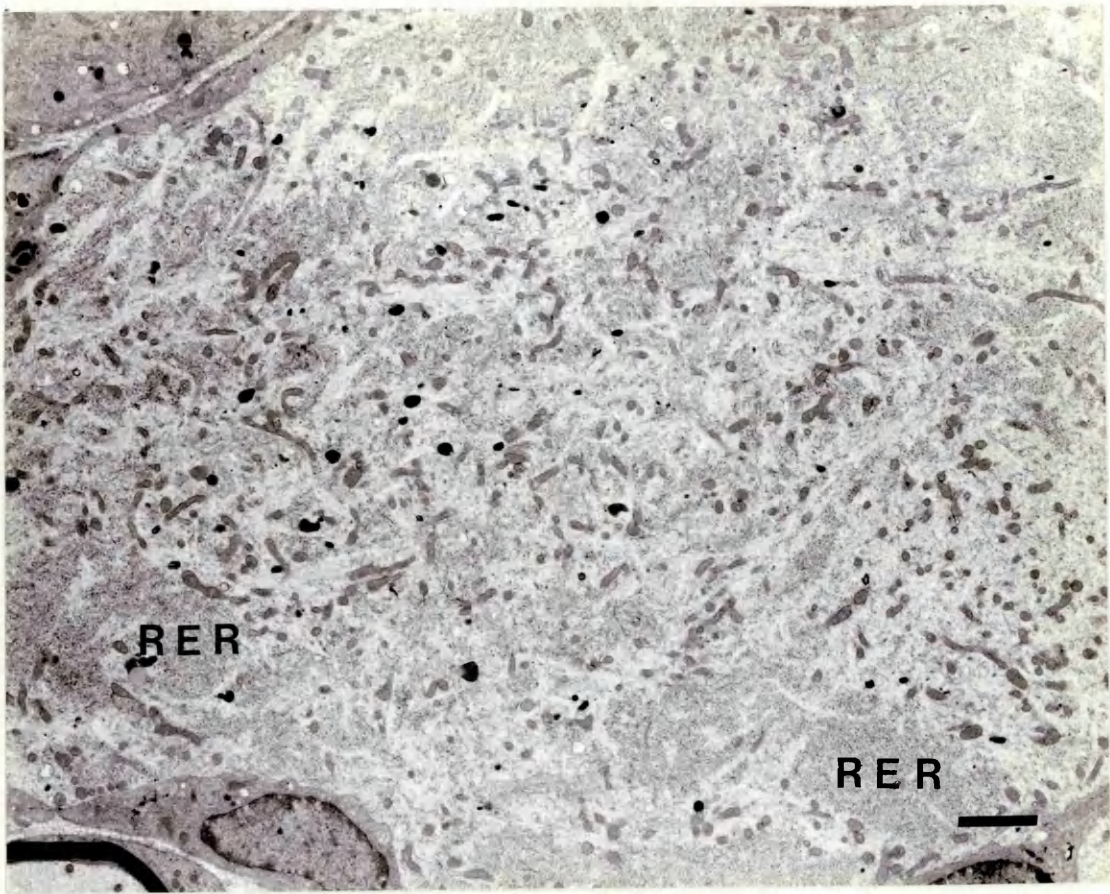


b

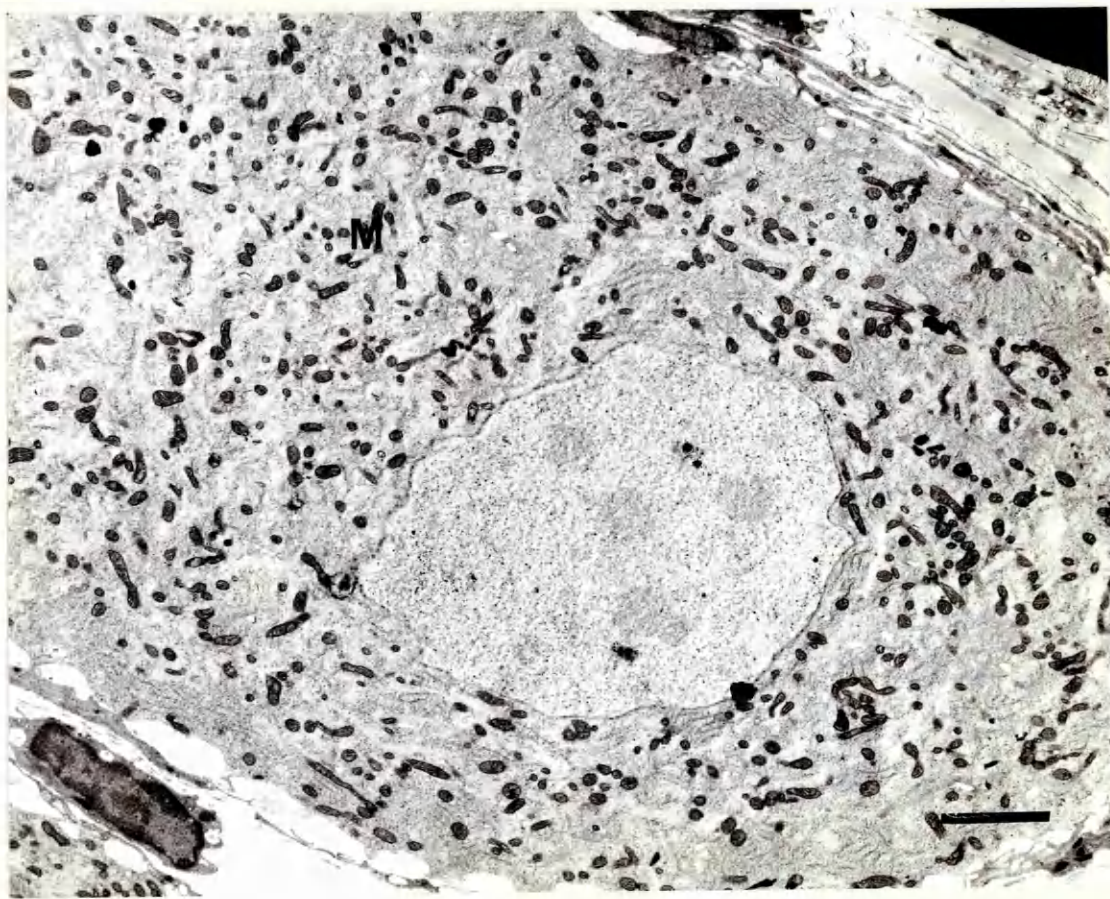
Figure 70

Dorsal root ganglion, Adriamycin (intraperitoneal) 5 days

- (a) Much of the RER in this neurone is found peripherally (RER) with smaller fragments occurring centrally. One area (*) is devoid of RER; it appears to contain mostly smooth tubular and filamentous structures and mitochondria, but definition is not good at this magnification.
- (b) Cytoplasmic detail is not good in this neurone. The most striking feature is the large number of dense mitochondria (M) present.
- (a) Bar = 2 μ m.
- (b) Bar = 2 μ m.



a



b

Figure 71

Dorsal root ganglion, Adriamycin, 7 days

(a) Intravenous

Golgi complexes (G) and RER (RER) look normal, although the volume of RER appears to be reduced, with some areas of the cytoplasm containing only occasional fragments (*). Mitochondria are dense and slender, but appear otherwise normal.

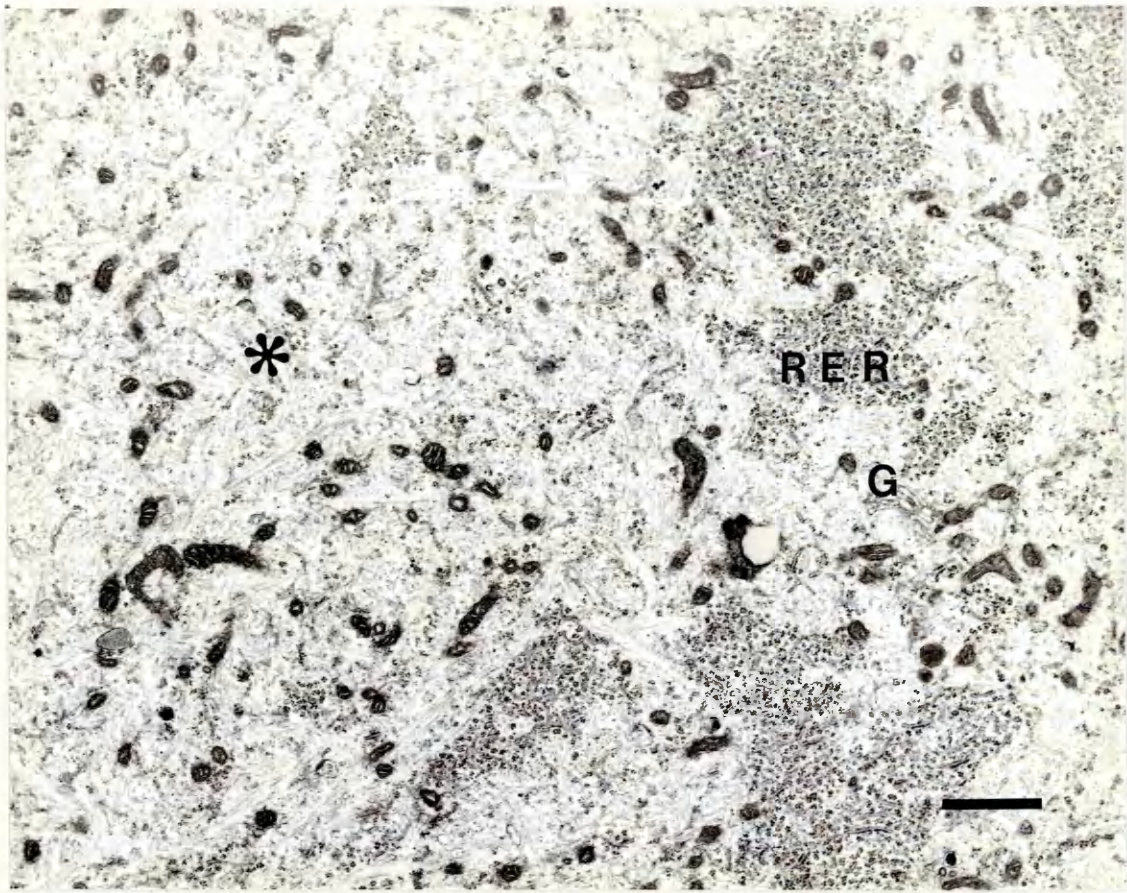
(b) Intraperitoneal

This small dark neurone contains a greatly increased number of neurofilaments (NF) coursing between areas of normal-looking RER (RER) which is reduced in volume, and small Golgi complexes (G).

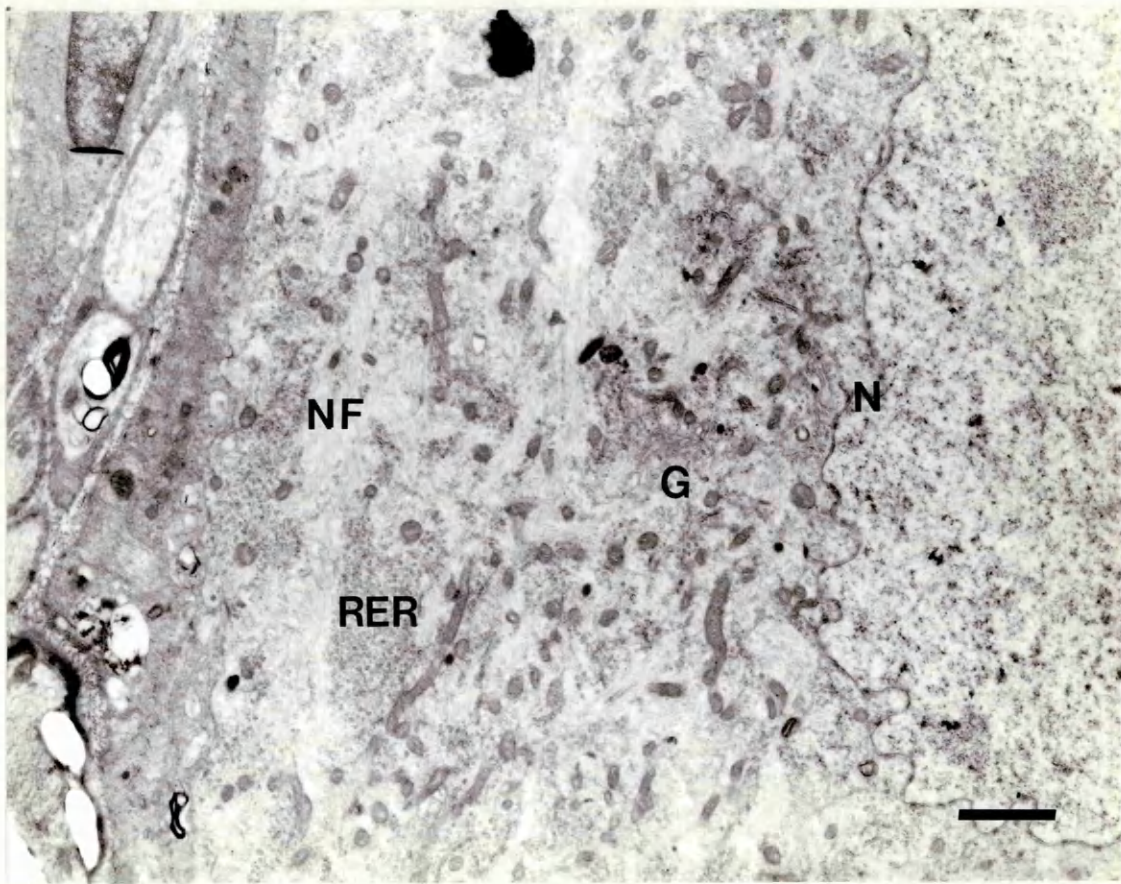
Mitochondria appear normal, and the nuclear envelope (N) is intact, although crenated.

(a) Bar = 1 μ m.

(b) Bar = 1 μ m.



a



b

Figure 72

Normal autonomic neurone, rat, perfusion-fixation

(a)&(b)

Different magnifications of the same neurone.

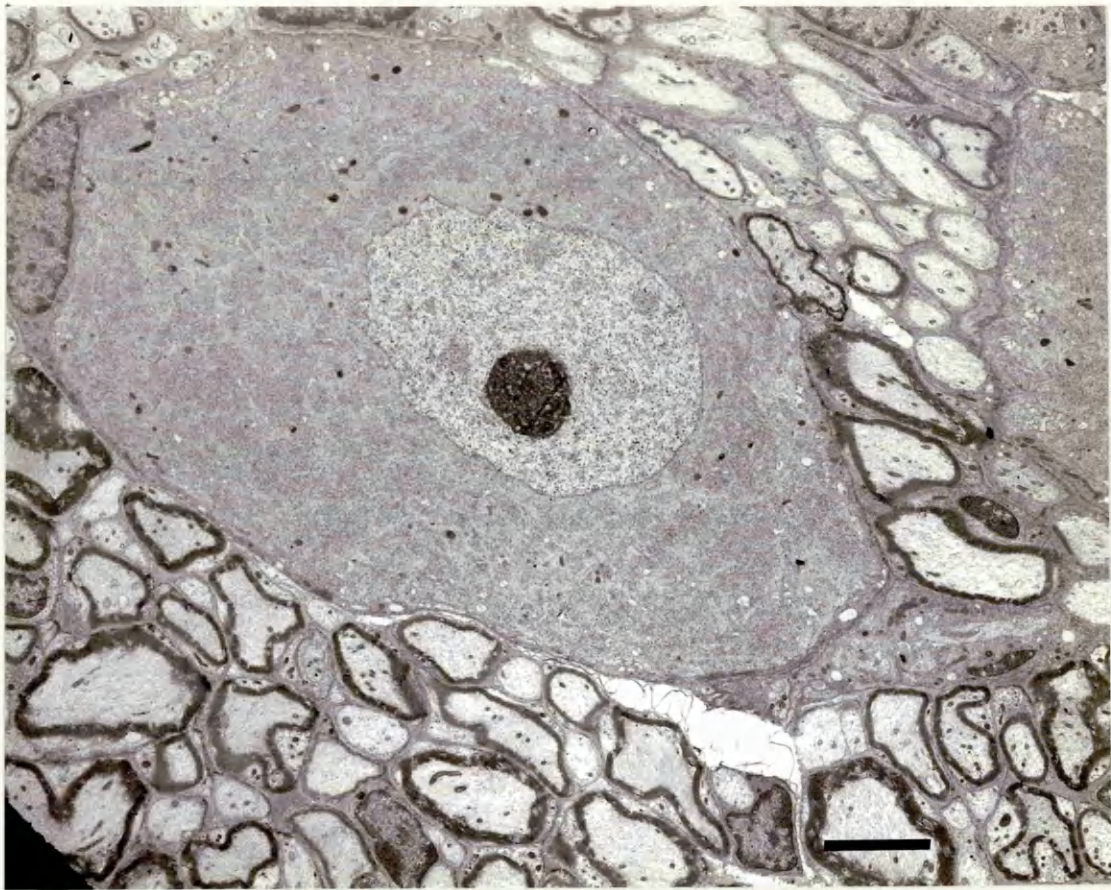
RER (RER) is plentiful and, although its division into discrete areas is not clear at high magnifications, the lower power field (a) demonstrates the 'patchy' effect attributable to Nissl granules.

Golgi complexes (G) are prominent and frequent, and mitochondria (M) and lysosomes are distributed at random throughout the cytoplasm.

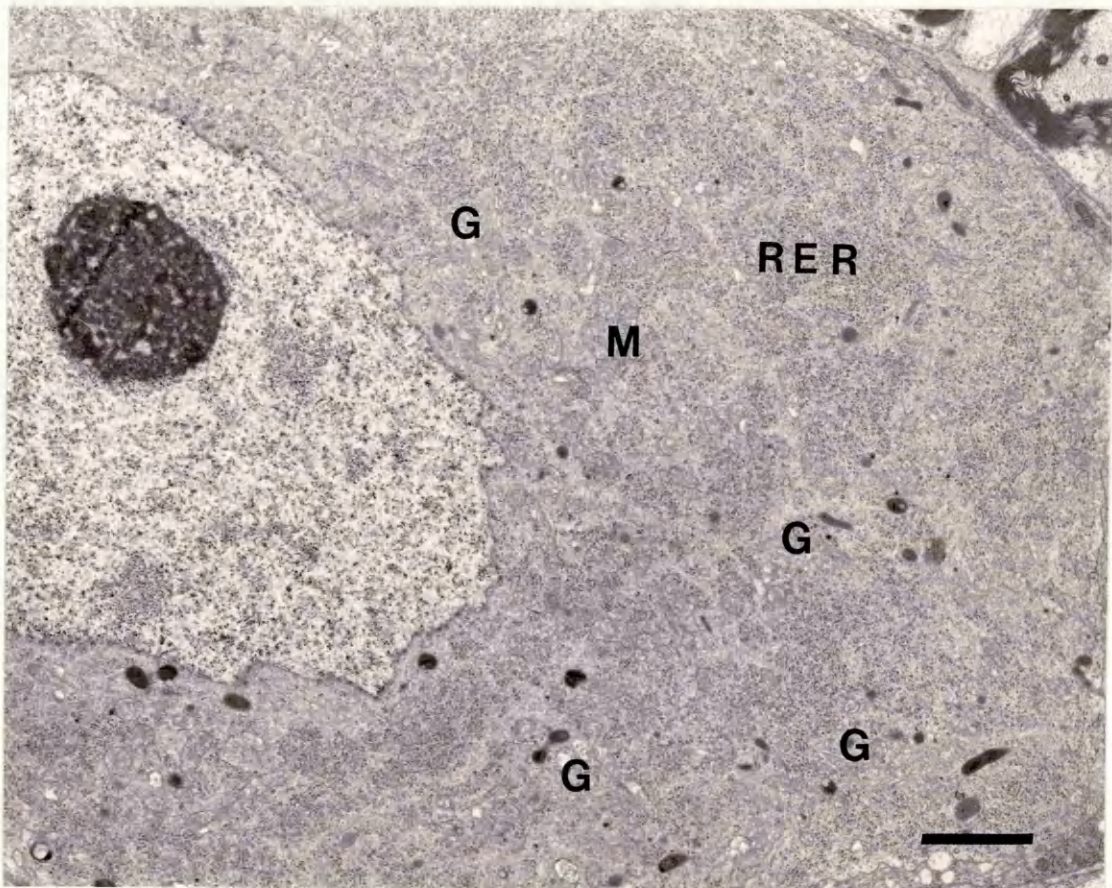
The nuclear shape reflects the shape of the perikaryon, and the nucleolus is large and prominent with a honeycomb appearance.

(a) Bar = 5 μ m.

(b) Bar = 2 μ m.



a



b

Figure 73

Autonomic ganglion, Adriamycin (intravenous) 6 hours

(a) Small cleared areas are present in the nucleus (arrowheads). The cytoplasm appears relatively normal, although the RER (RER) is found perinuclearly, leaving a 'clear' area next to the cell membrane.

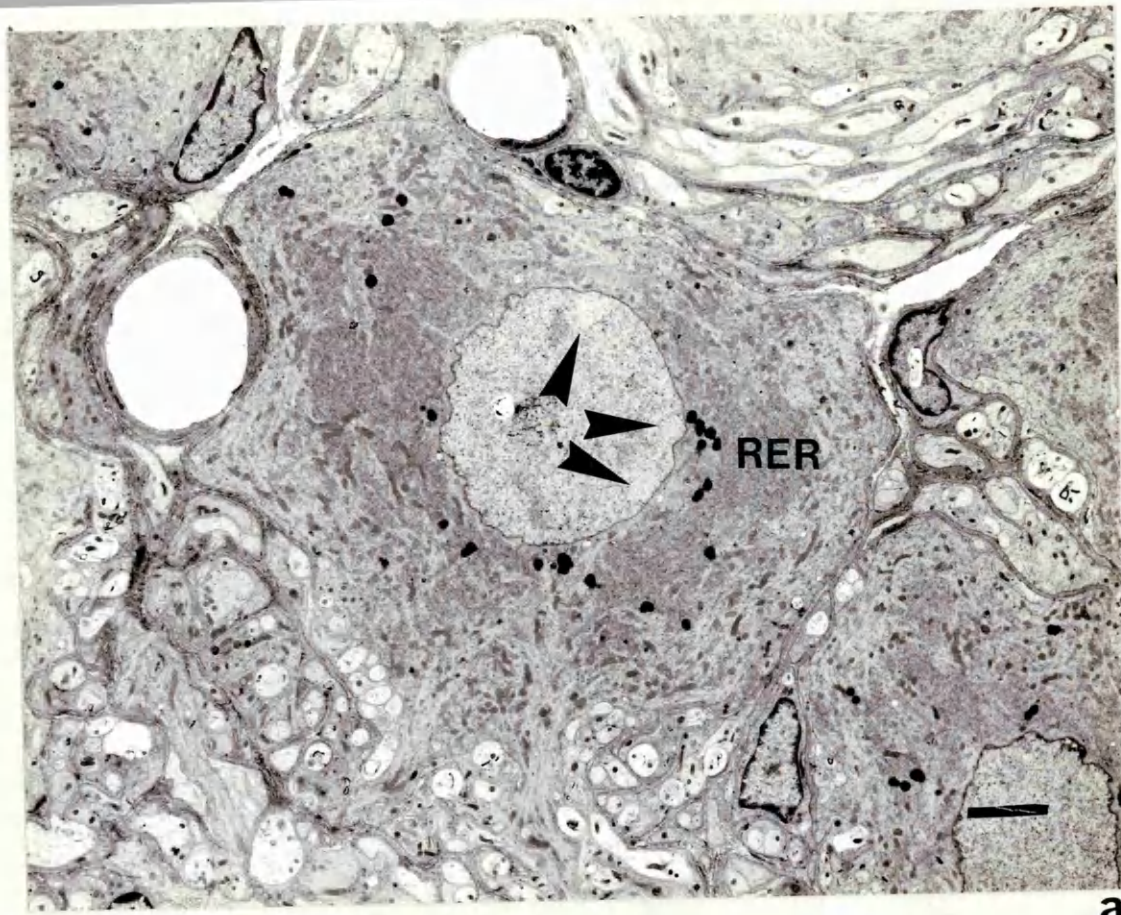
(b)&(c)

Two isolated bundles of neurofilaments (NF) are found close to the nucleus in adjacent cells. The RER is centrally positioned in these cells, as in (a). Other organelles appear normal.

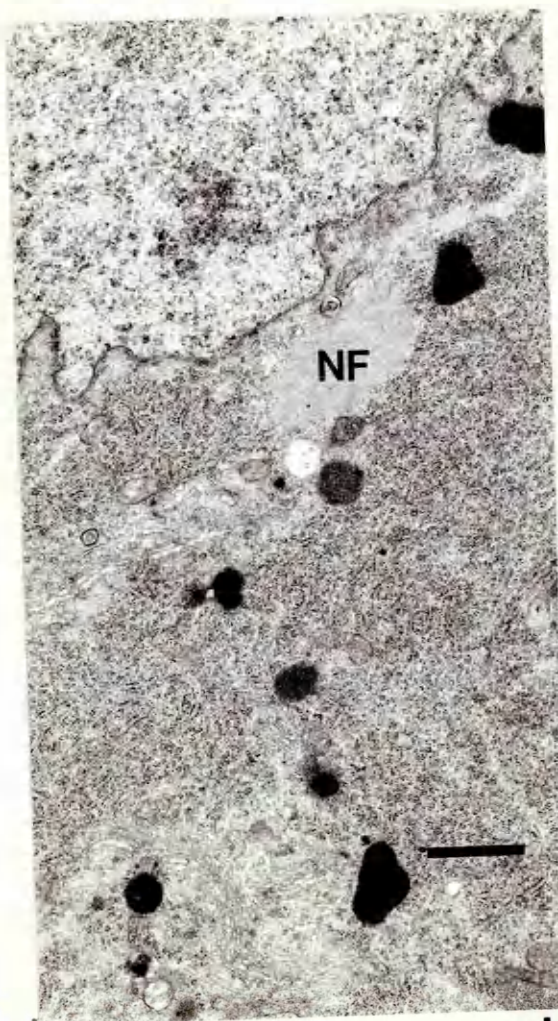
(a) Bar = 3 μ m.

(b) Bar = 1 μ m.

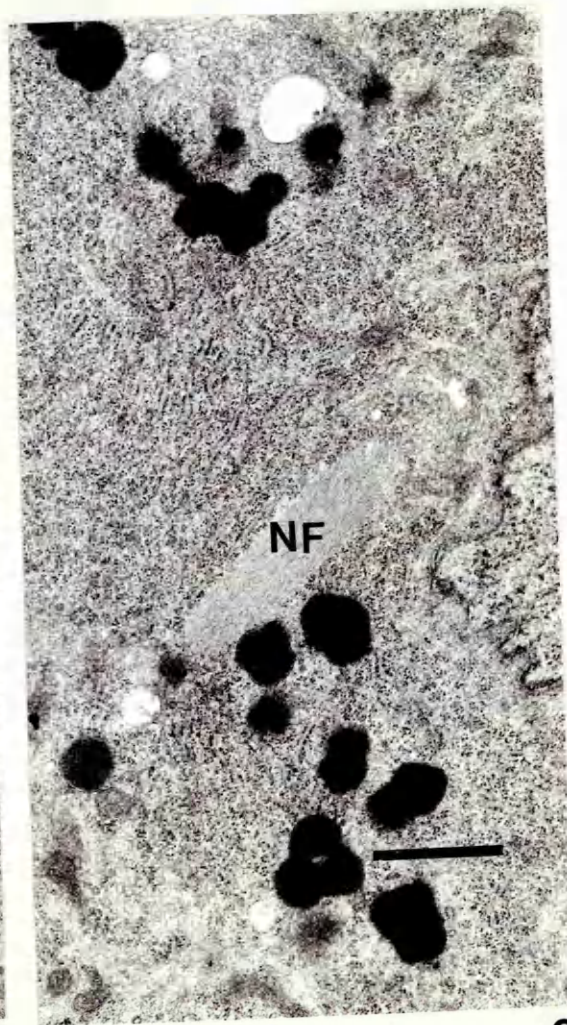
(c) Bar = 1 μ m.



a



b



c

Figure 74

Autonomic neurone, Adriamycin (intravenous) 7 days

Large quantities of RER (RER) are found in a band round the periphery of the cell. Golgi complexes (G) appear to be associated with the inner border of this band, but apart from occasional mitochondria (M), lysosomes and small areas of RER, there is little cytoplasmic definition in the more central areas of this neurone.

Bar = 1 μ m.

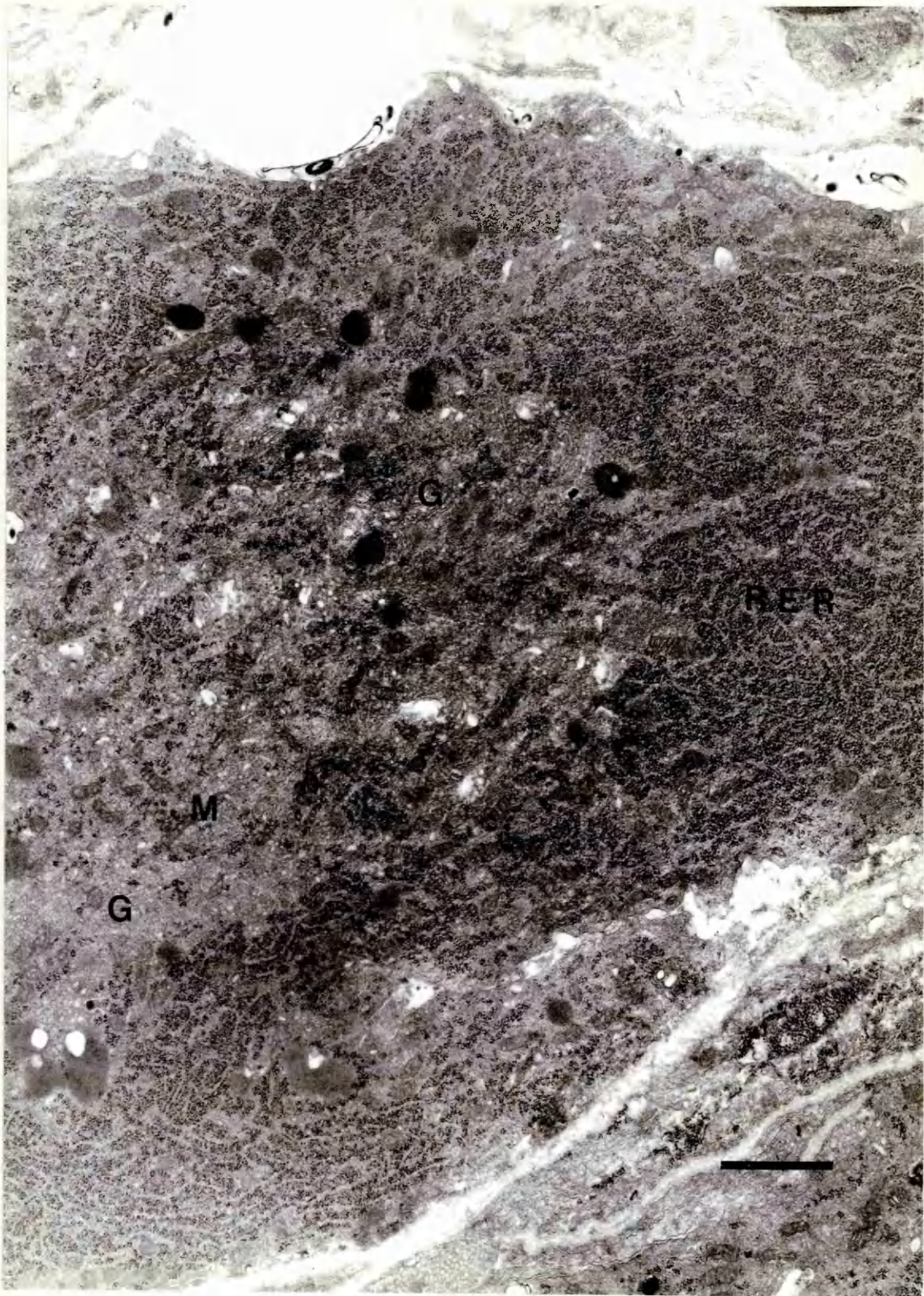


Figure 75

Dorsal root ganglion, control incubation, 3 hours

Normal neurones (arrow) have a large, centrally placed nucleus with a prominent nucleolus, and the cytoplasm is granular in appearance due to the presence of RER.

Large light neurones (arrow) and small dark neurones (arrowhead) can be clearly distinguished.

The perikarya more centrally placed in the ganglion are showing signs of degeneration (*).

Bar = 10 μ m.

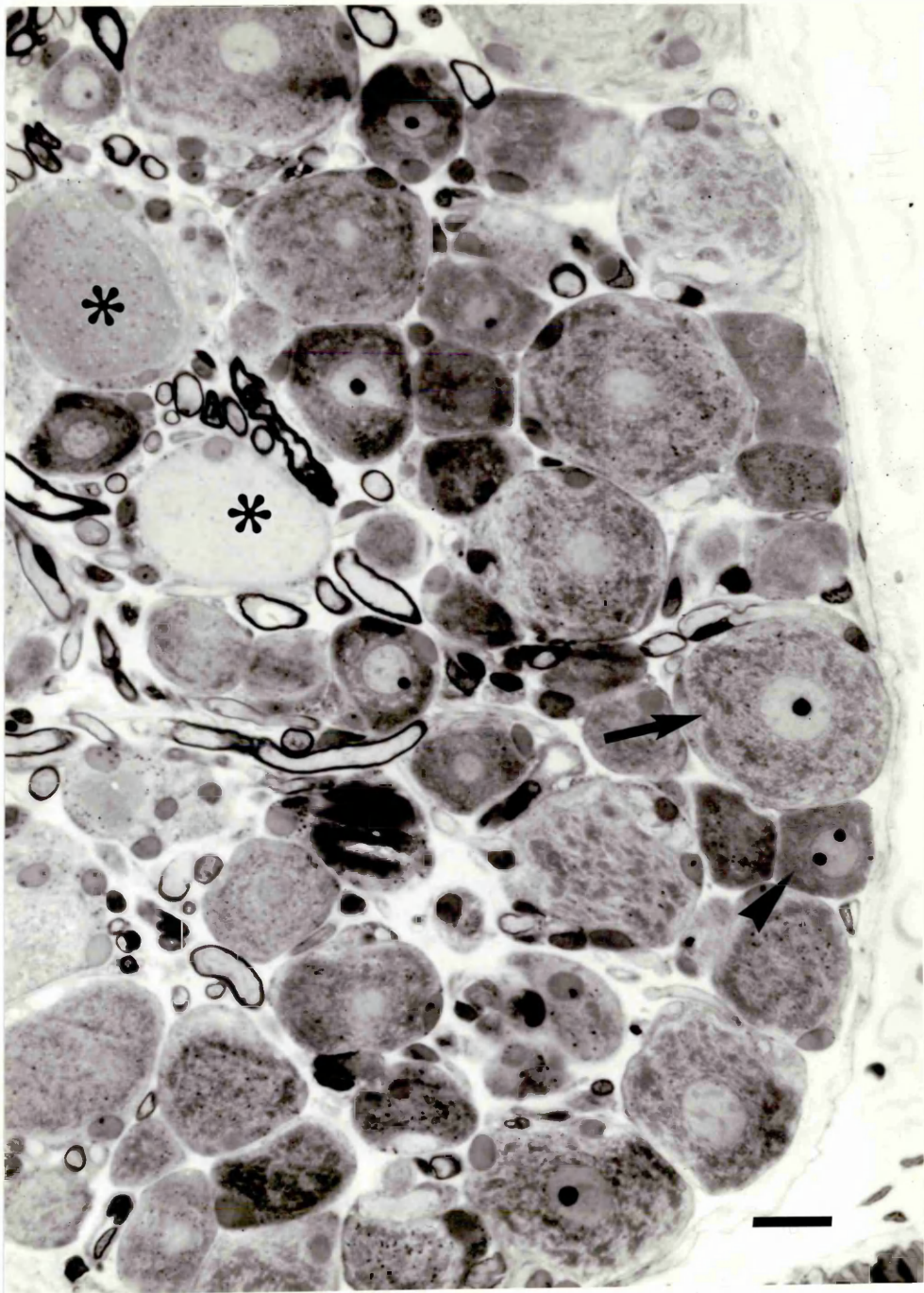


Figure 76

Small dark neurone, dorsal root ganglion, control incubation,

3 hours

RER (RER) is pronounced, tending to occur more profusely towards the periphery of the cell. The perinuclear orientation of the prominent Golgi complexes (G) can be clearly seen. Mitochondria and lysosomes occur at random and there are no clear divisions between the organelles. Structural preservation is very good.

Bar = 1 μ m.

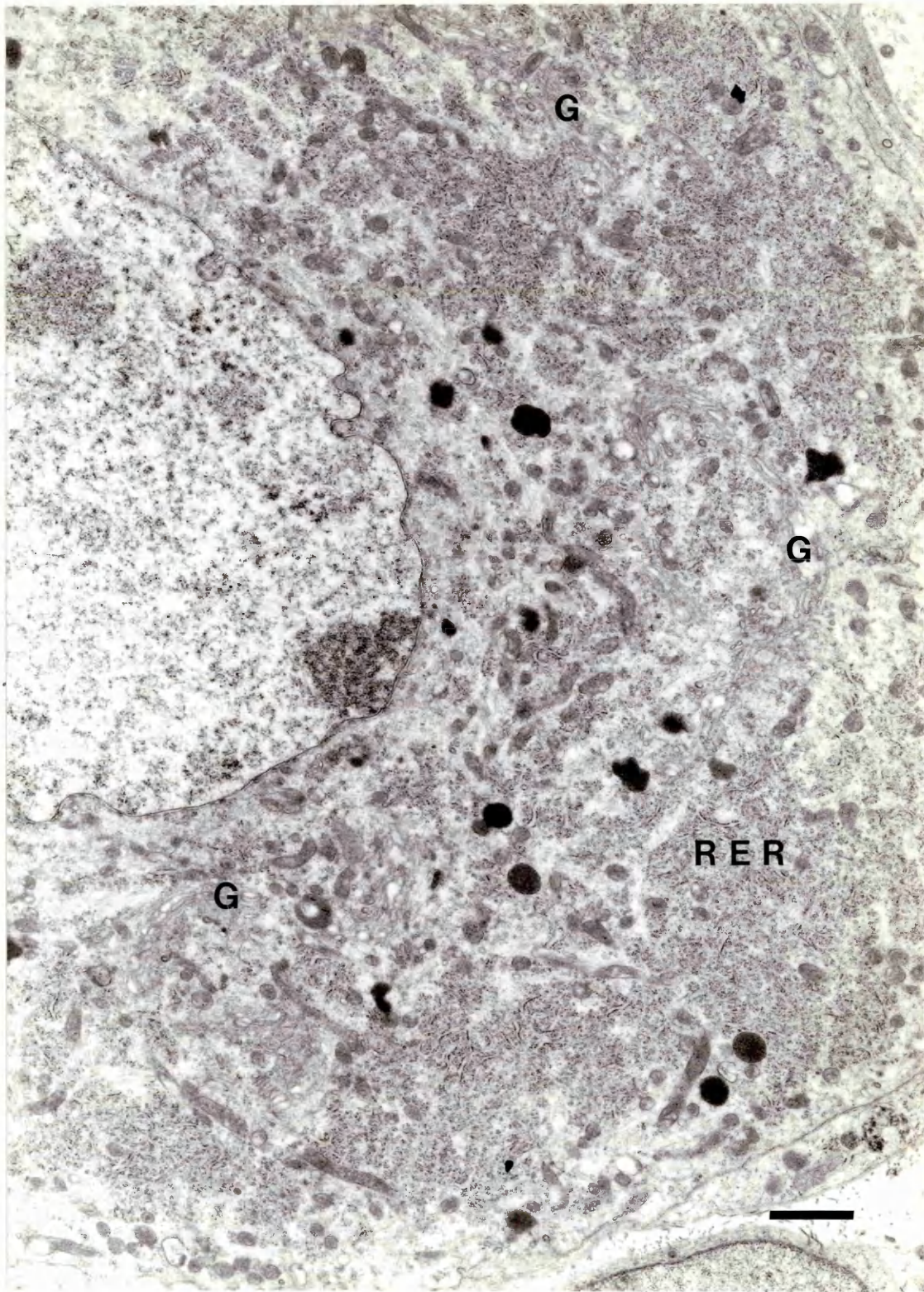


Figure 77

Large light cell, dorsal root ganglion, control incubation,
6 hours

The Nissl substance in this neurone is in much smaller arrays than in Figure 67, and single cisternae are seen. It is well dispersed throughout the cytoplasm and small bands of neurofilaments (F) can be seen separating some of these areas. Golgi complexes (G) are relatively small, but frequent, and the cisternae appear slightly dilated. This is possibly an early sign of cytoplasmic degeneration, since occasional mitochondria are also showing some degenerative vacuolation (arrows).

Bar = 1 μ m.

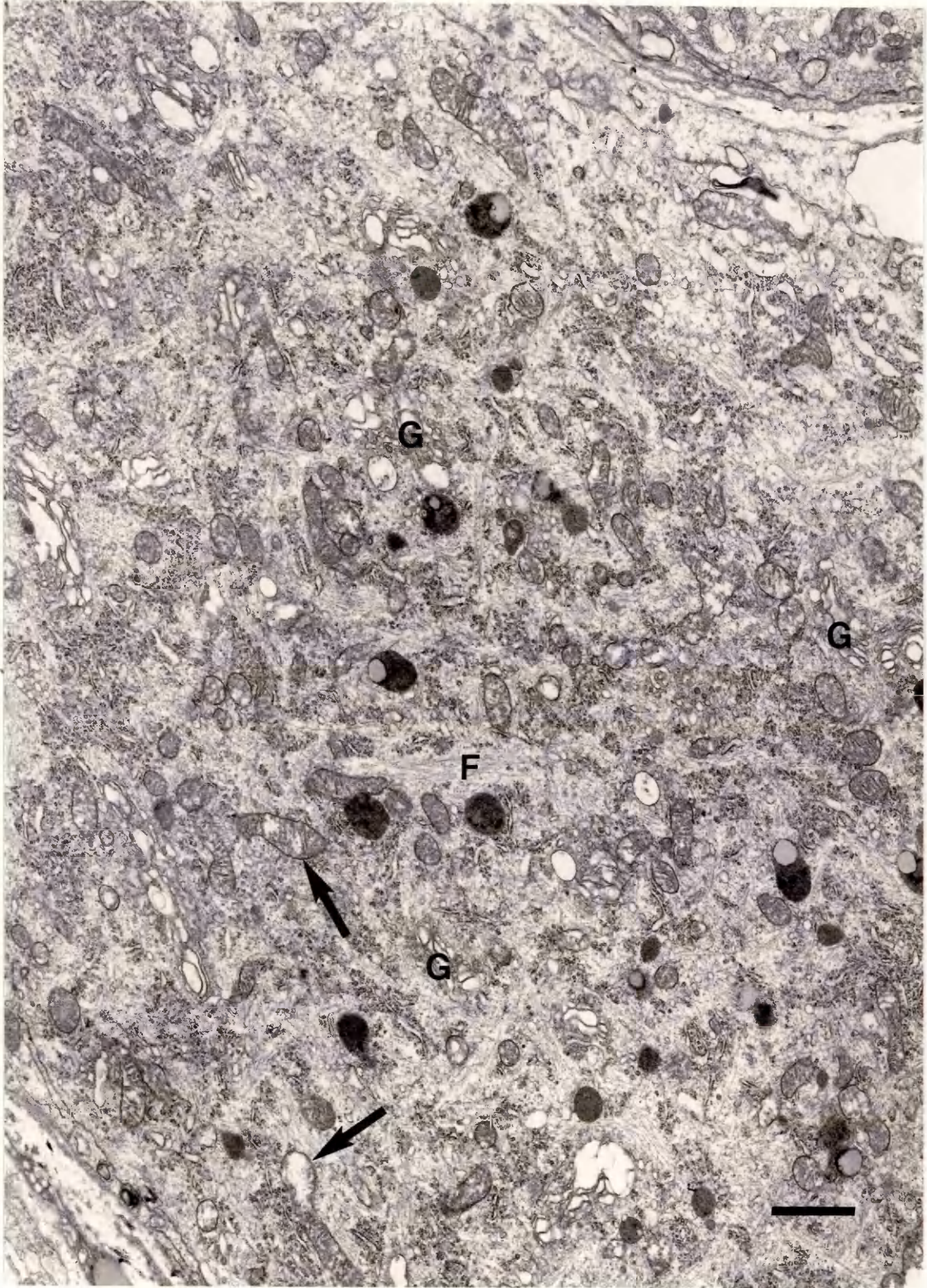


Figure 78

Dorsal root ganglion, 3 hours incubation, Cycloheximide

(a) 80 ug/ml

No abnormality can be seen.

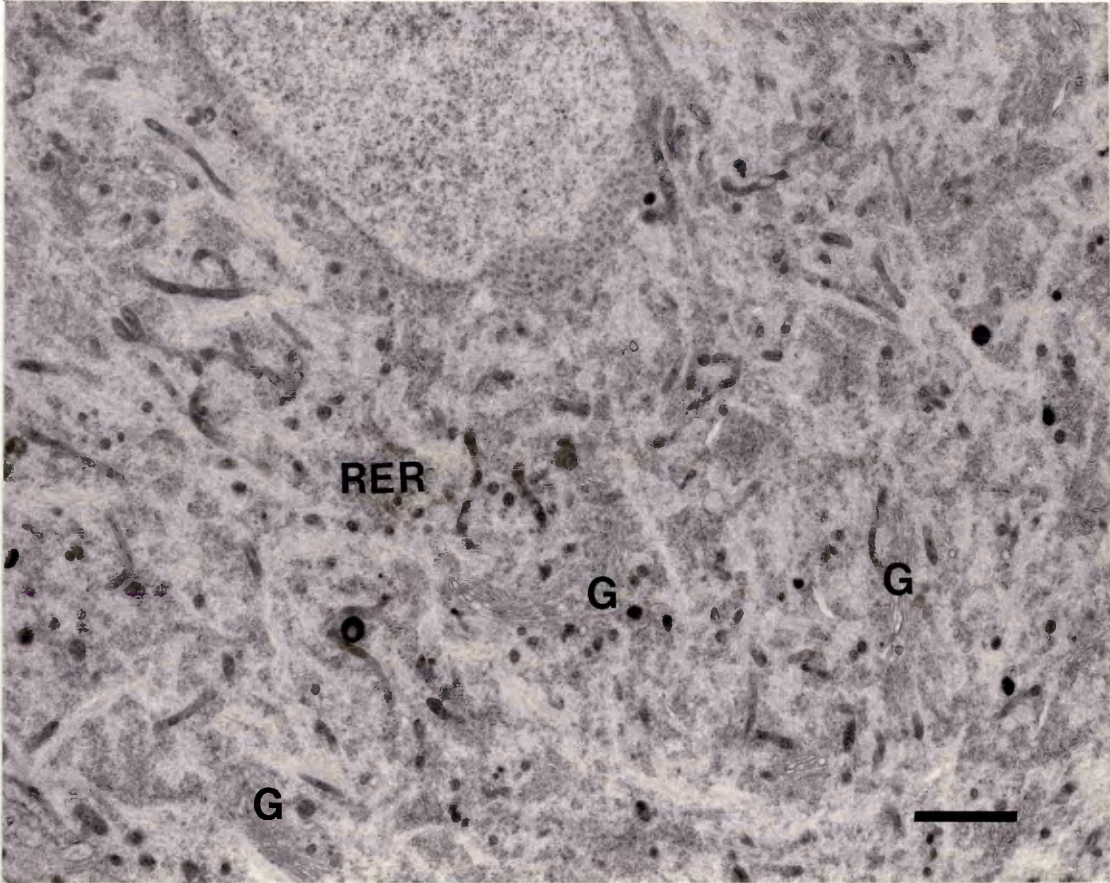
There are large, well-formed Golgi complexes (G), clumps of RER (RER), mitochondria and lysosomes separated by bands of neurofilaments.

(b) 20 ug/ml

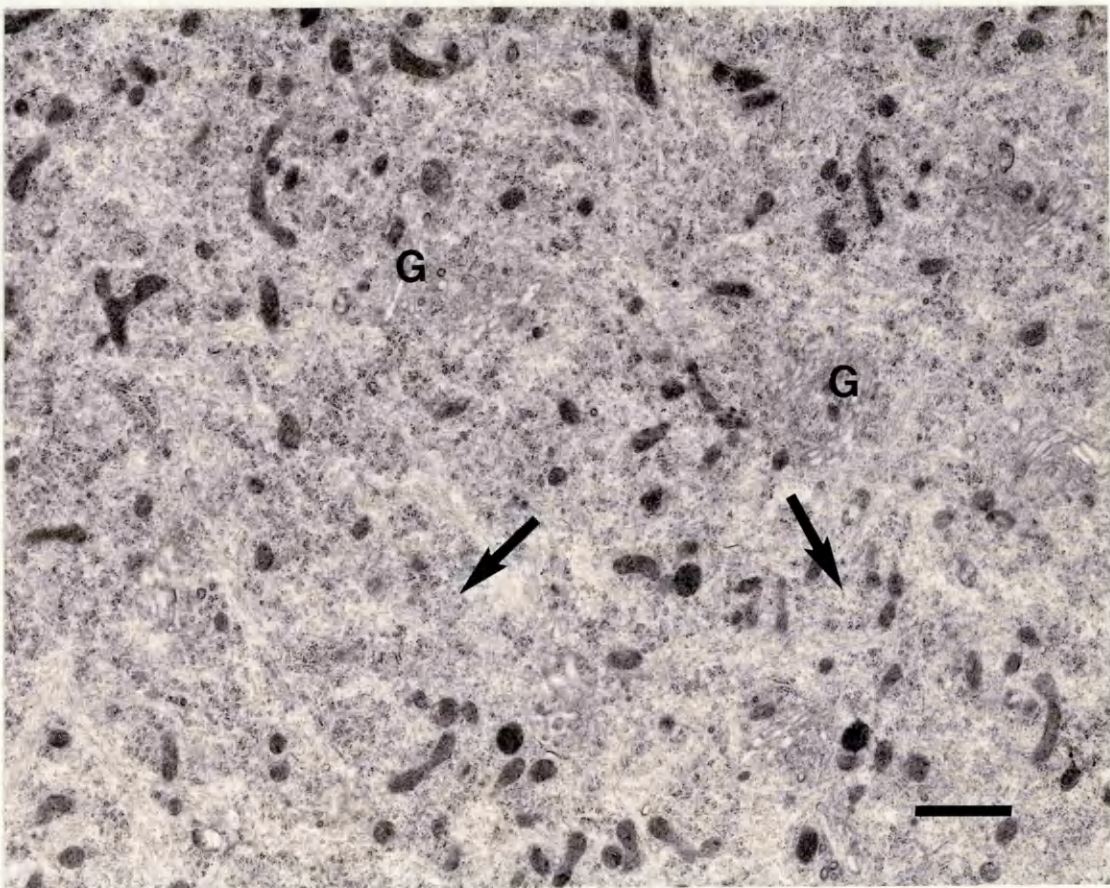
Golgi complexes (G) appear normal, and RER is present, but seems slightly more dispersed than usual with profiles tending to be vesicular rather than tubular, and there are several areas with numerous free ribosomes (arrows). Other organelles appear normal.

(a) Bar = 2 um.

(b) Bar = 1 um.



a



b

Figure 79

Dorsal root ganglion, 6 hours incubation, cycloheximide

(a) 20 ug/ml and

(b) 80 ug/ml

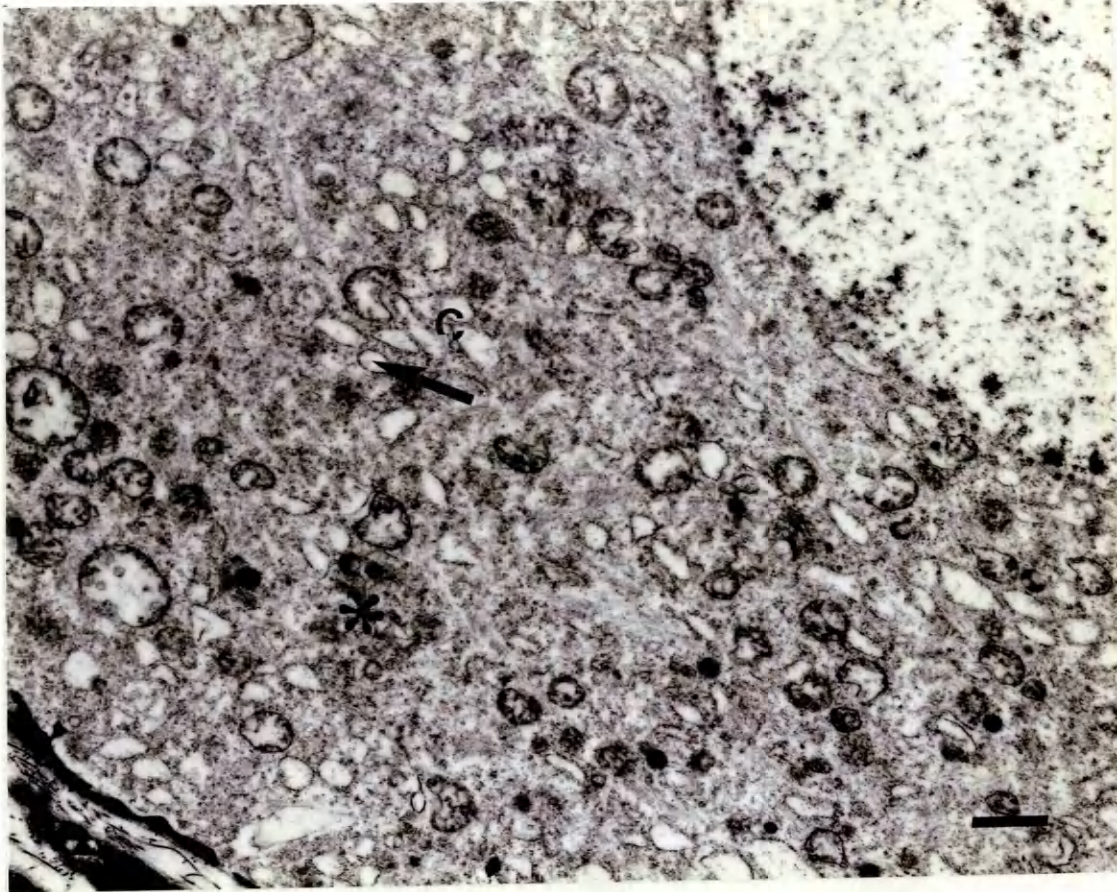
Normal RER is not present in these neurones. Instead there are dilated cisternae (C) which in a appear empty and in b contain electron-dense floccular material. Ribosomes adherent to their limiting membranes (arrows) identify them as RER cisternae.

Normal Golgi complexes also cannot be seen, although there are smooth membranous vesicular profiles (*) which could be unusual Golgi configurations.

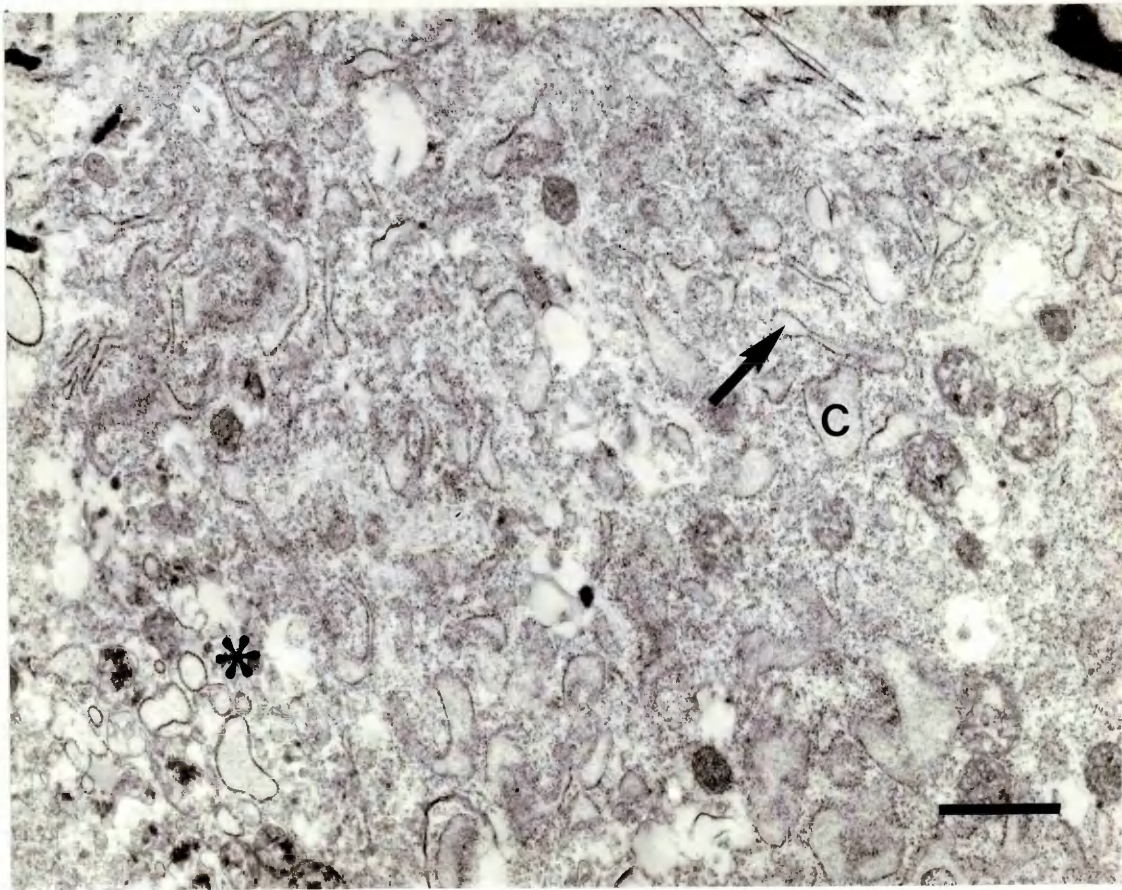
The general appearance of the remaining cytoplasm is 'grainy' due to the presence of many free ribosomes.

(a) Bar = 1 um.

(b) Bar = 1 um.



a



b

Figure 80

Dorsal root ganglion, tunicamycin 25 ug/ml, 6 hours incubation

The six hour incubation period has resulted in occasional neurones showing non-specific degeneration (*), but the great majority of both light and dark neurones show specific 'pin-hole' type perinuclear cytoplasmic vacuoles.

Bar = 10 um.

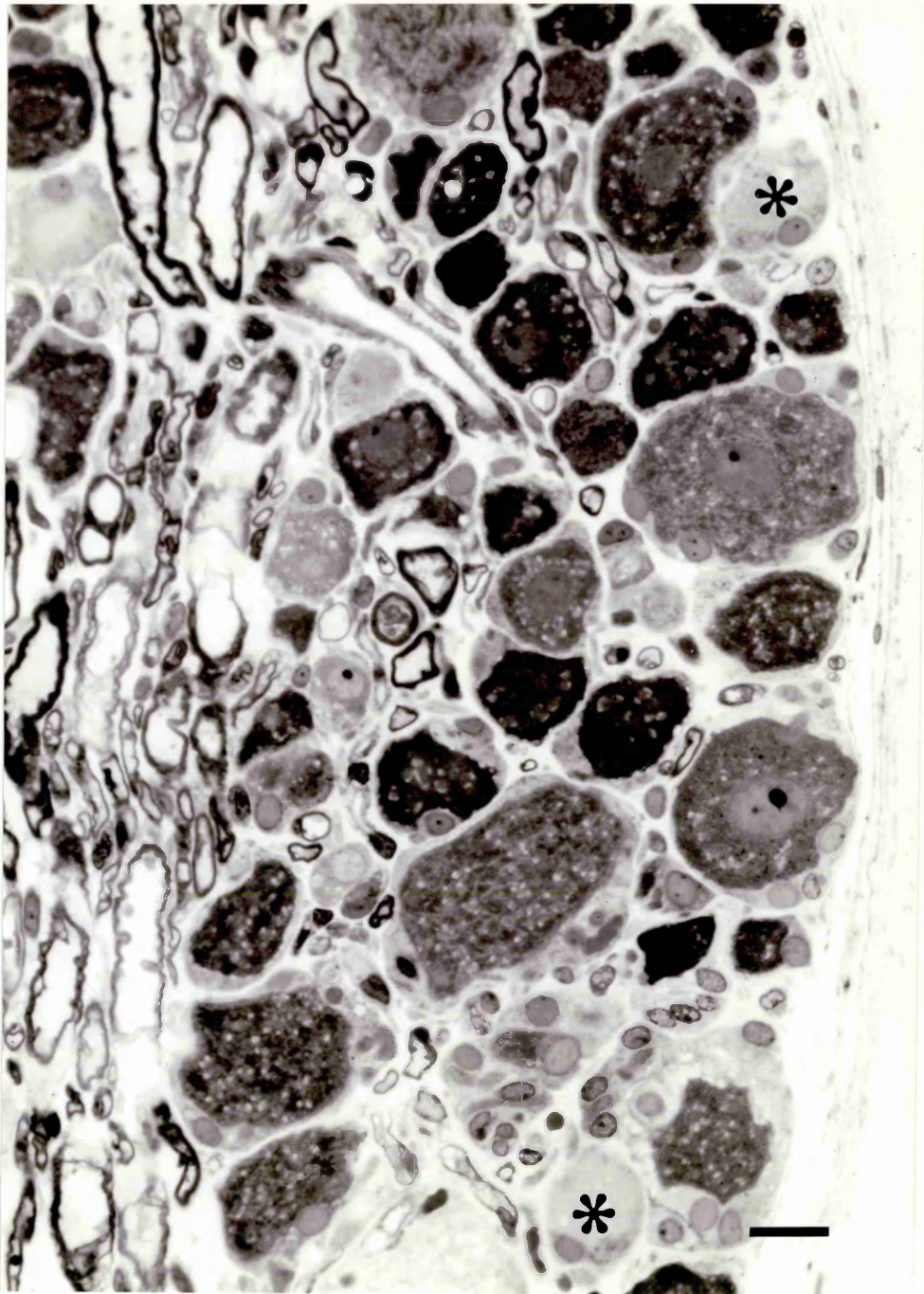


Figure 81

Dorsal root ganglion, 3 hours incubation, tunicamycin

(a) 10 ug/ml

The only abnormality detectable in this neurone is a slight distension of the Golgi cisternae (arrows), the other organelles appearing normal.

These comments are equally applicable to,

(b) 25 ug/ml and

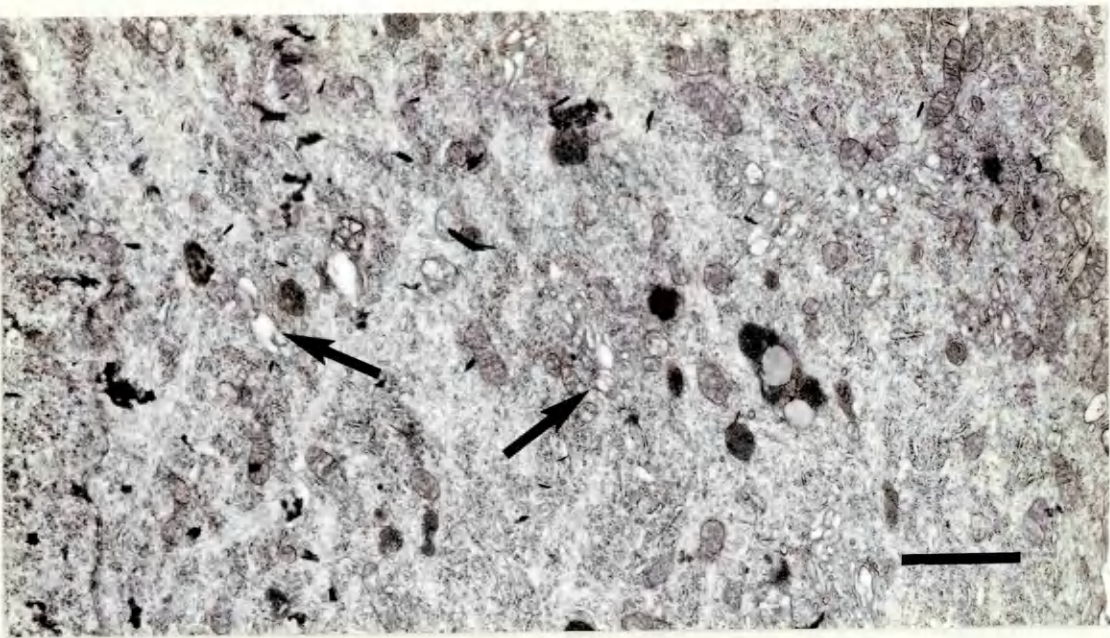
(c) 50 ug/ml

The differences in distribution of the various organelles in these examples can be accounted for by the existence of distinct neuronal sub-groups (see discussion).

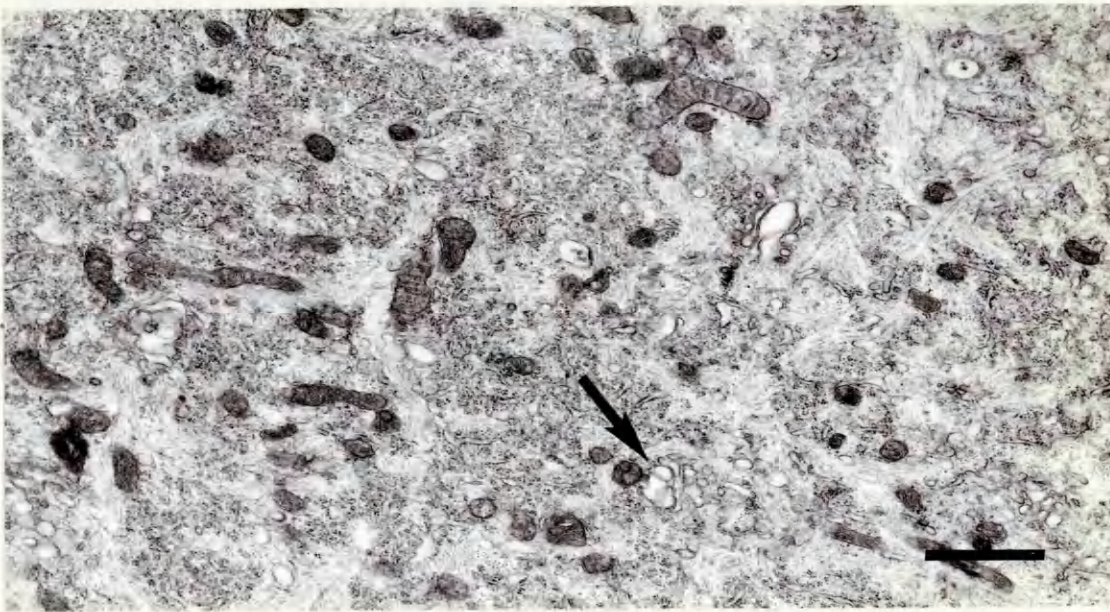
(a) Bar = 1 μ m.

(b) Bar = 1 μ m.

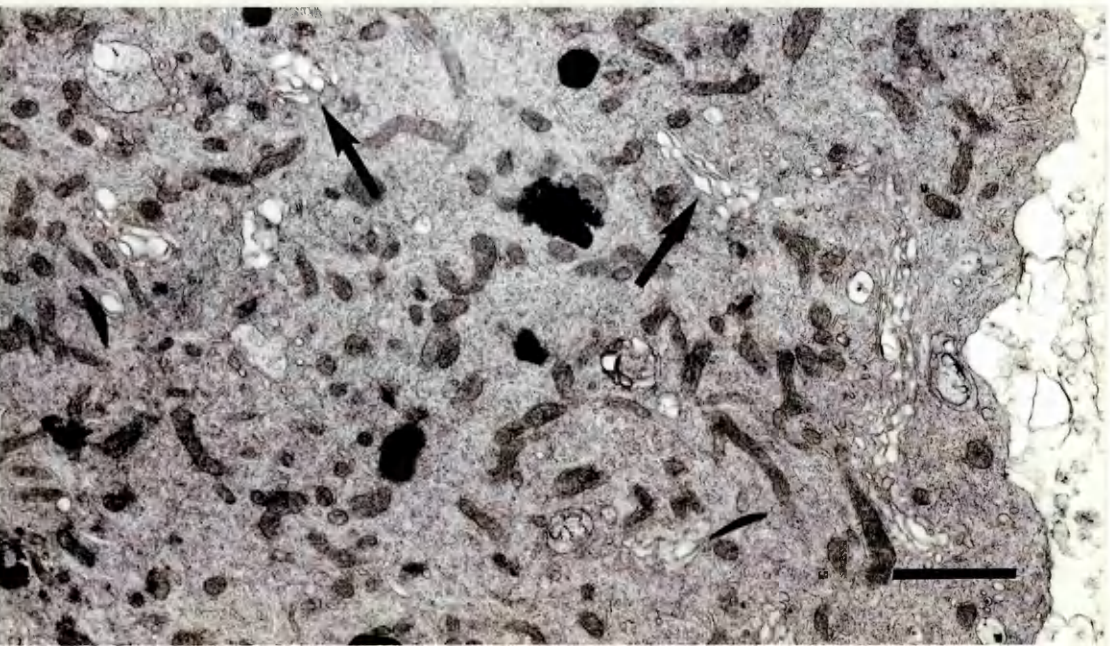
(c) Bar = 1 μ m.



a



b



c

Figure 82

Dorsal root ganglion, 6 hours incubation, tunicamycin

(a) 10 ug/ml

Well-formed, normal areas of RER (RER) are prominent in this neurone, separated by bands of neurofilaments. Normal Golgi complexes cannot be seen; instead there are discrete groups of vacuoles (V). The other organelles appear normal.

(b) 25 ug/ml and

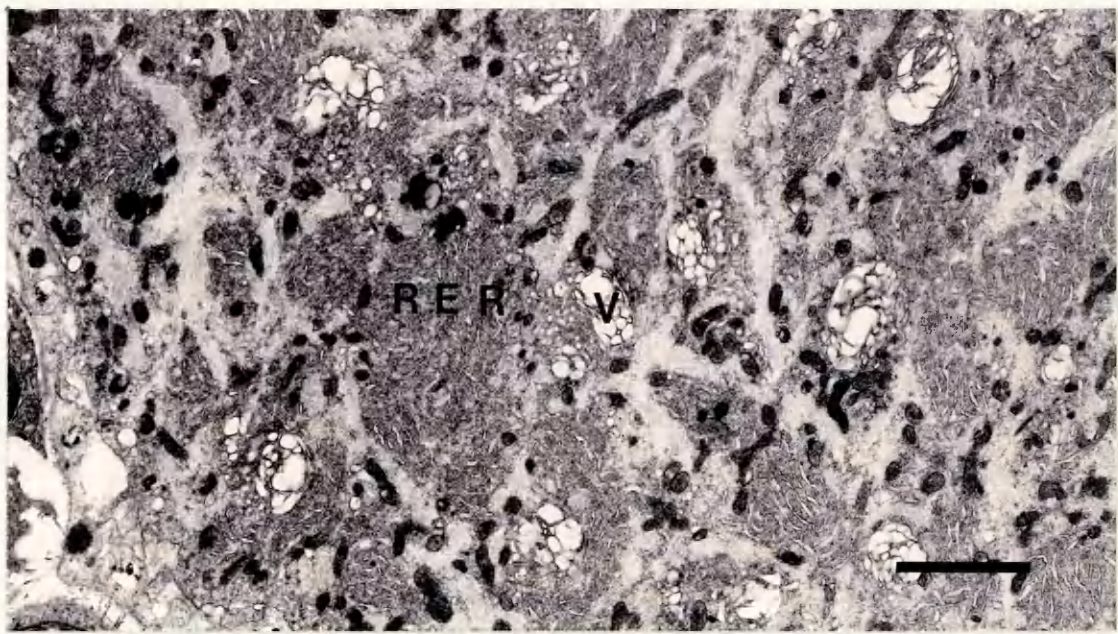
(c) 50 ug/ml

These both show changes similar to (a), with vacuolation of the Golgi complexes (V), but normal RER (RER), mitochondria (M) and lysosomes (L).

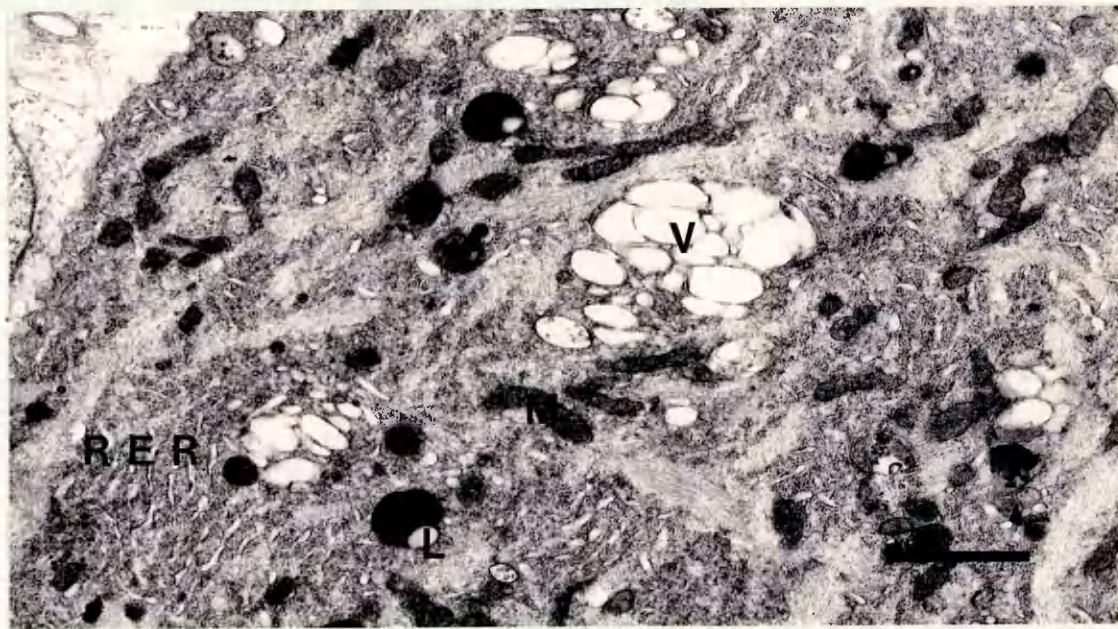
(a) Bar = 2 um.

(b) Bar = 1 um.

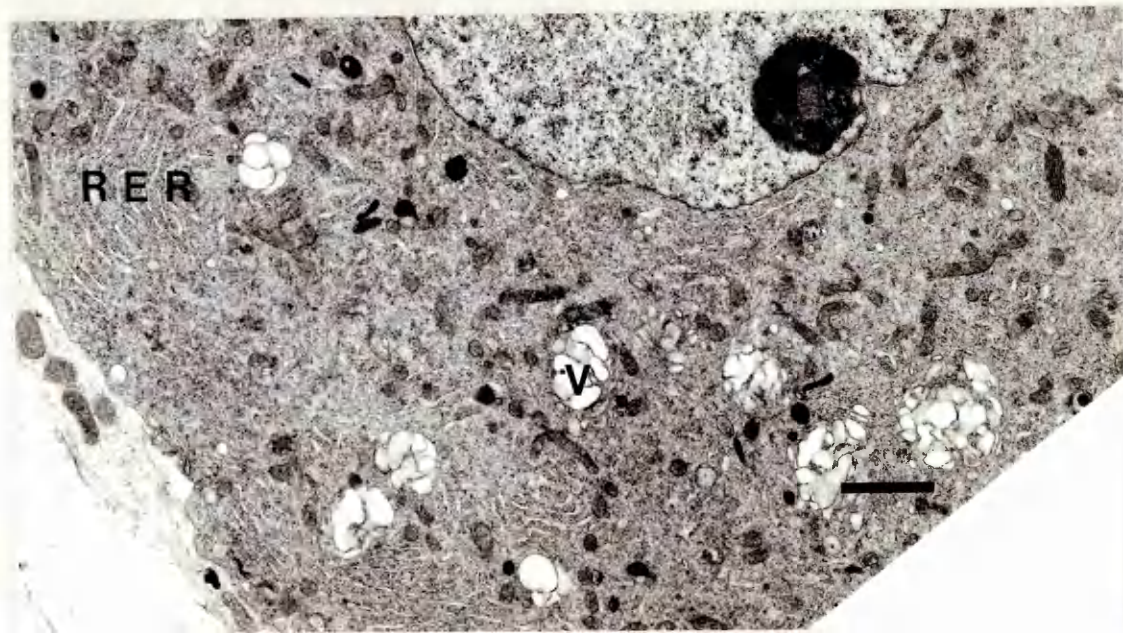
(c) Bar = 1 um.



a



b



c

Figure 83

Dorsal root ganglion, monensin, 10 μ M, 3 hour incubation

Numerous clumps of approximately perinuclear cytoplasmic vacuoles give the neurones a 'foamy' appearance. The large light (LL) and small dark (SD) neurones appear to be affected to a similar degree, although there is proportionately less cytoplasm separating these clusters in the smaller, darker neurones.

Bar = 10 μ m.

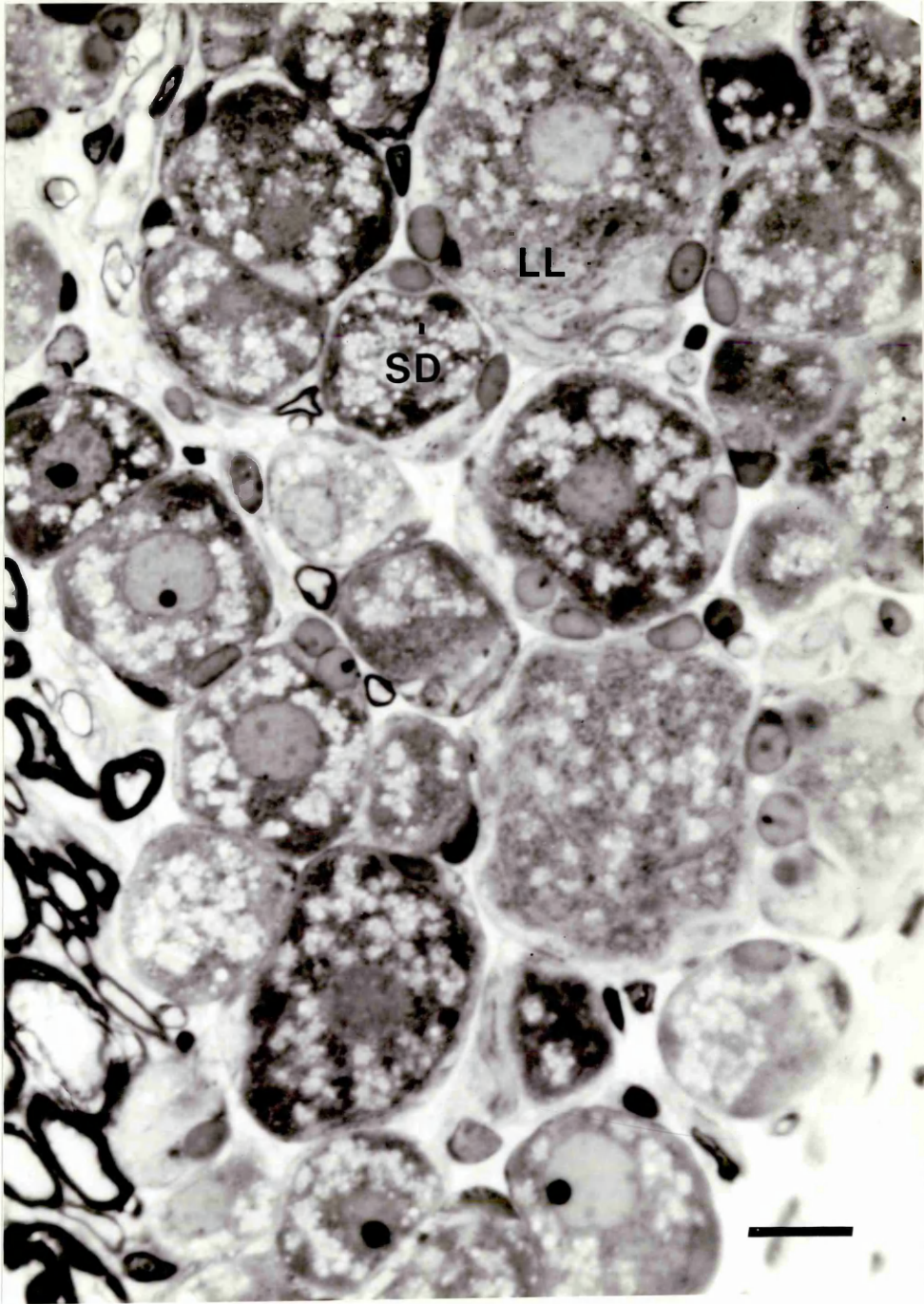


Figure 84

Dorsal root ganglion, monensin 1 μ M, 3 hours incubation

The prominent abnormality in this neurone is the discrete cytoplasmic vacuolation (V). This occurs close to areas of RER but not within them, in a similar orientation to that which would be expected of Golgi complexes. No Golgi complexes can be seen. RER, mitochondria, lysosomes and neurofilaments appear normal. There is slight crenation of the nuclear envelope (N).

Bar = 2 μ m.

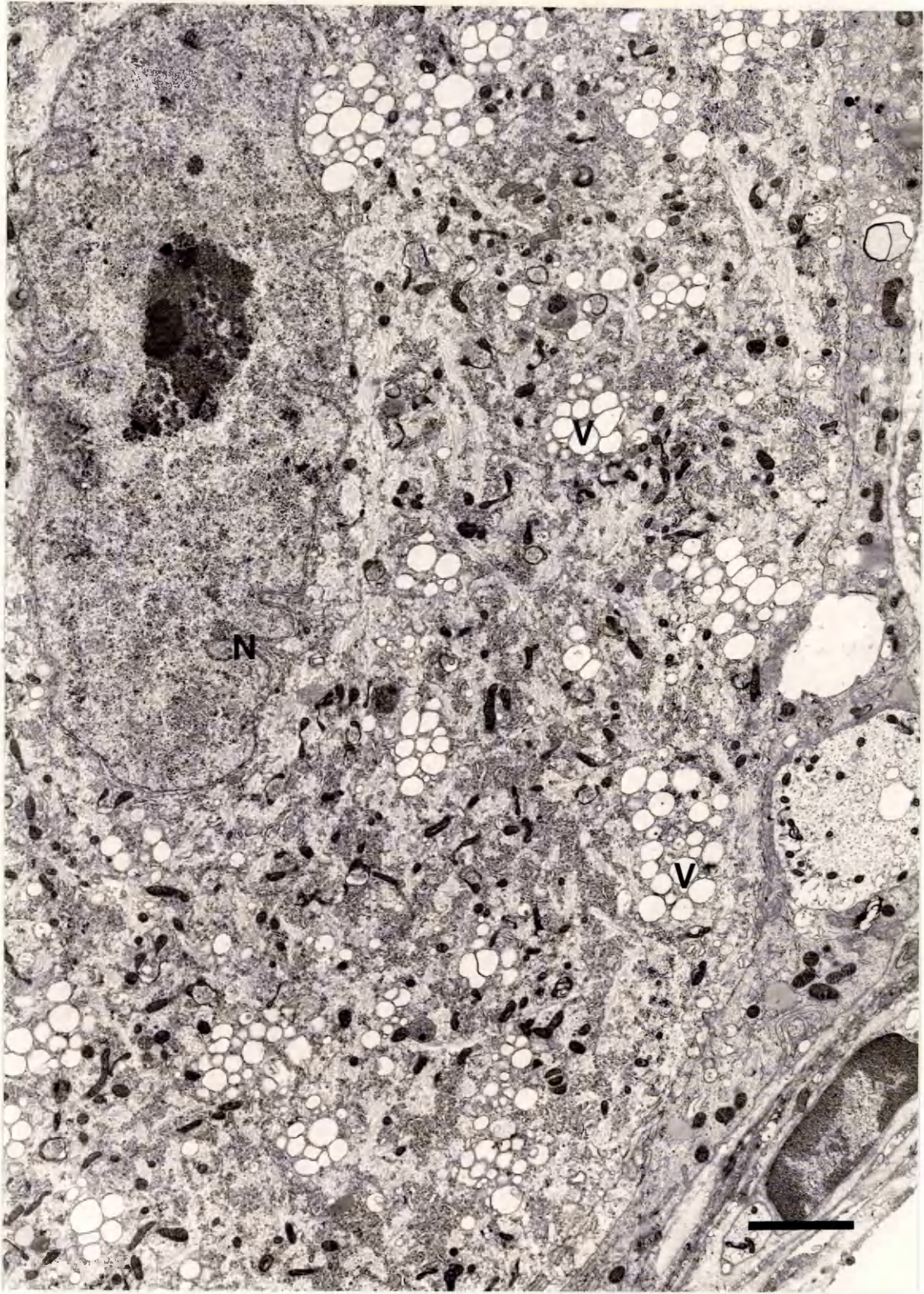


Figure 85

Dorsal root ganglion, 3 hours incubation

(a) Monensin, 1 μ M

Clumps of single-membrane-bound vesicles (V) can be seen in cytoplasm which is otherwise relatively normal-looking apart from the absence of Golgi complexes. Most of these vesicles are of fairly uniform size, but much smaller vesicles can also be seen, and they tend to occur outwith these areas of RER, although some close associations can be seen (arrow).

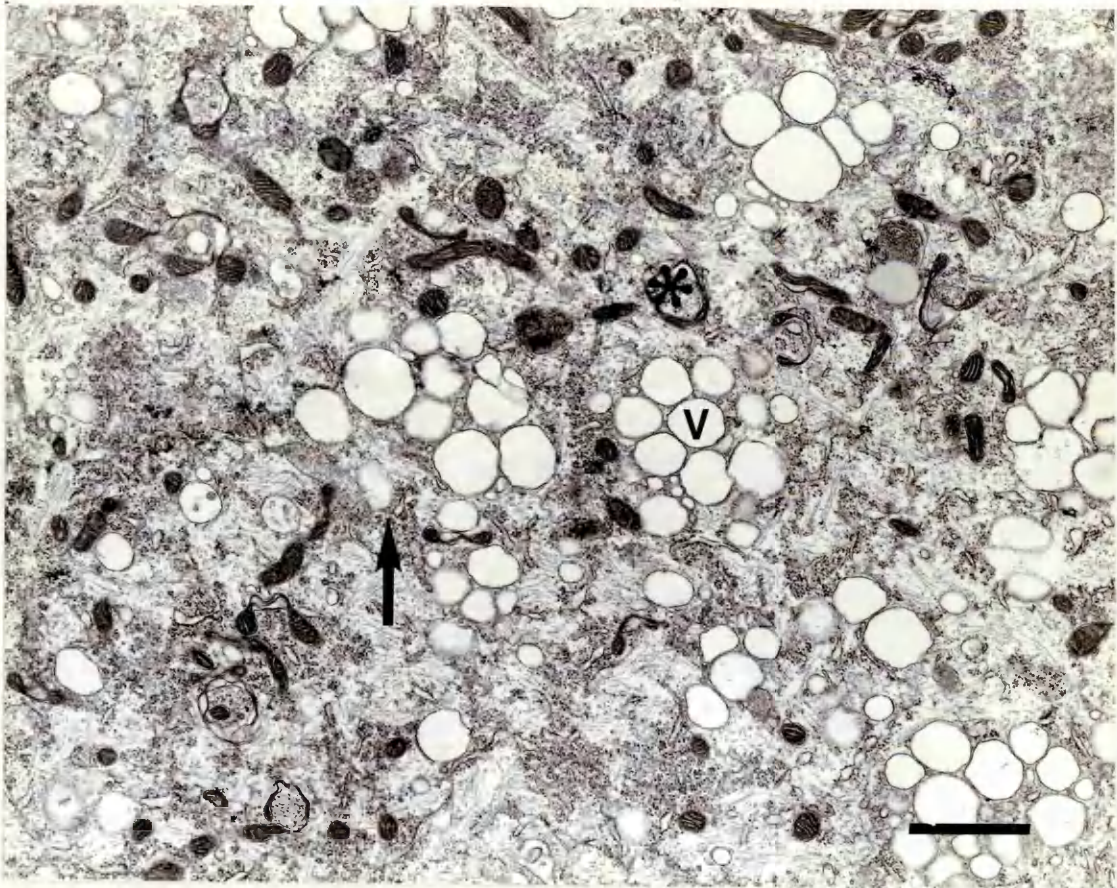
Occasional autophagic vacuoles (*) can be seen, apparently associated with mitochondria.

(b) Monensin 10 μ M

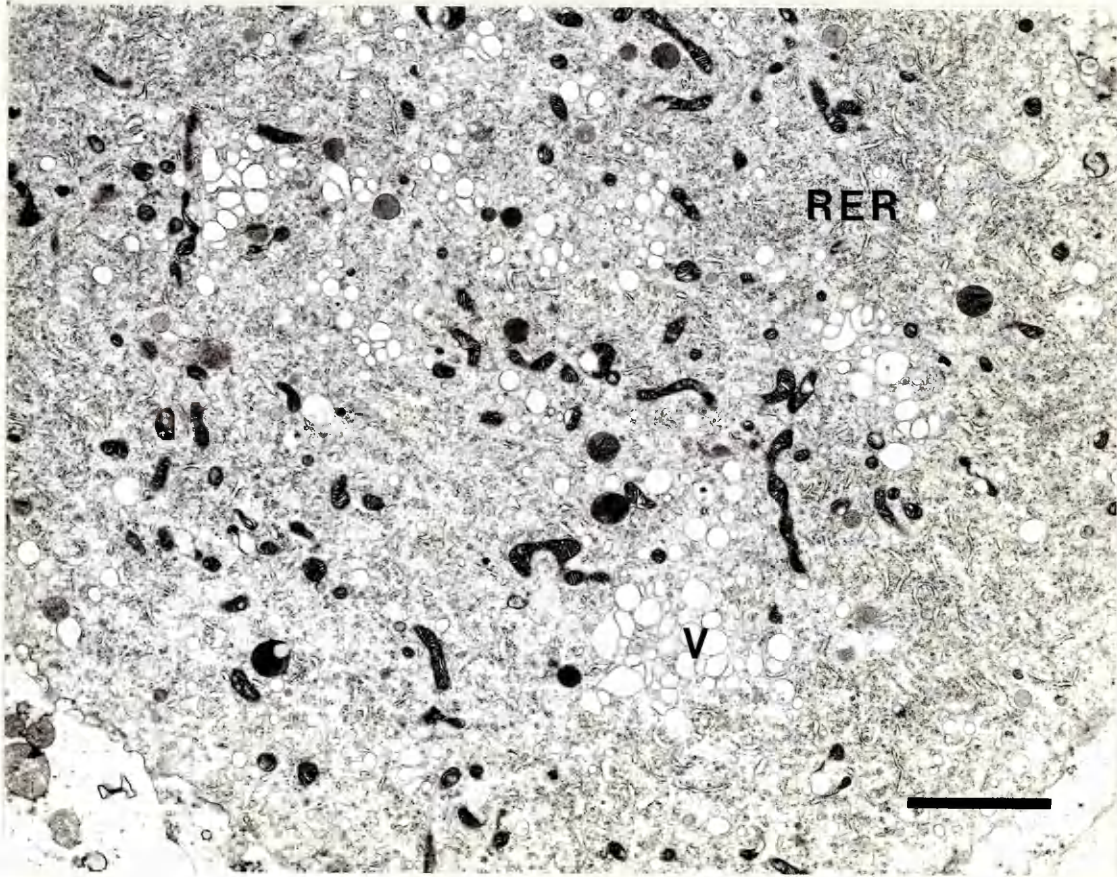
A very similar appearance to that of (a) is seen with the higher concentration of monensin. RER (RER) appears normal. No Golgi complexes are present.

(a) Bar = 1 μ m.

(b) Bar = 2 μ m.



a



b

Figure 86

Dorsal root ganglion, monensin 1 μ M, 6 hours incubation

This neurone was exposed to the same concentration of monensin as the cells in Figs. 84 and 85a, but for twice as long. The vacuoles are more varied in size and the 'clumping' effect is much less pronounced, with vacuoles occurring within a much greater proportion of the cytoplasm. No Golgi complexes are present, and areas of RER are hard to identify (arrow). Mitochondria (M) are more dense than usual, and show a greater variation in shape and size. They also appear to be increased in number (not quantified).

Bar = 2 μ m.

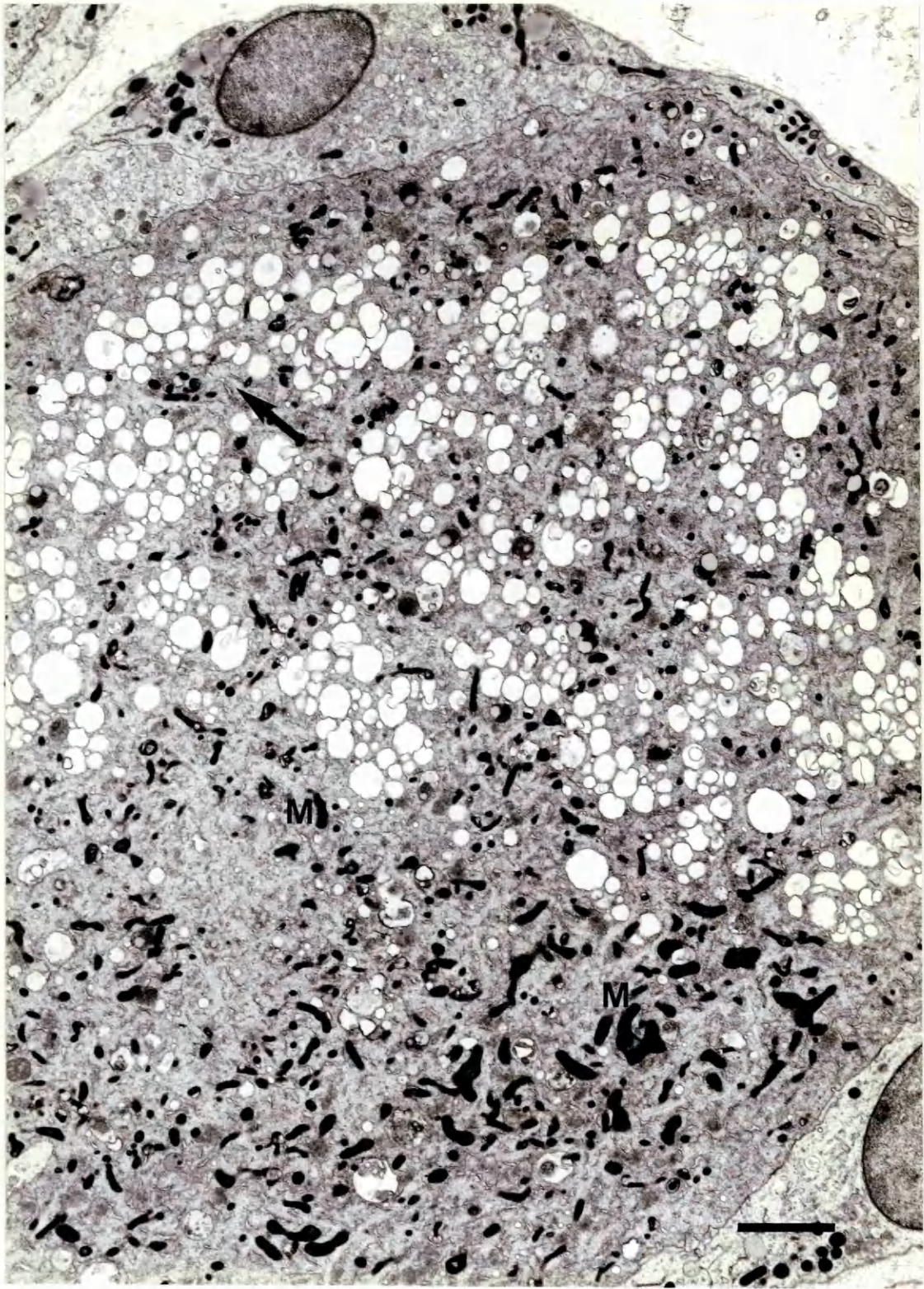


Figure 87

Dorsal root ganglion, monensin 0.1 μ M

(a) 3 hours incubation

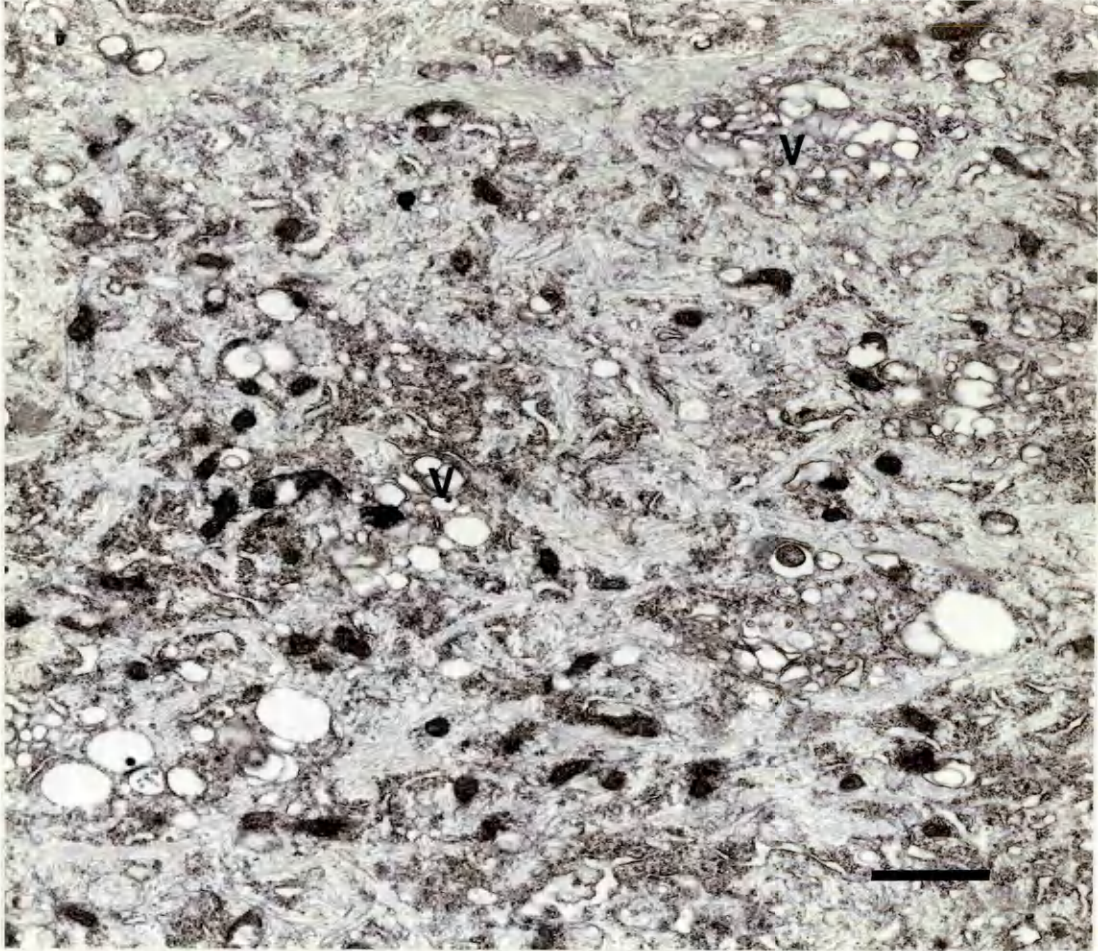
Small discrete areas of vacuolation can be seen (V) closely associated with RER, and separated by bands of neurofilaments as is typical of large, light neurones. No Golgi complexes can be seen. The other organelles appear normal.

(b) 6 hours incubation

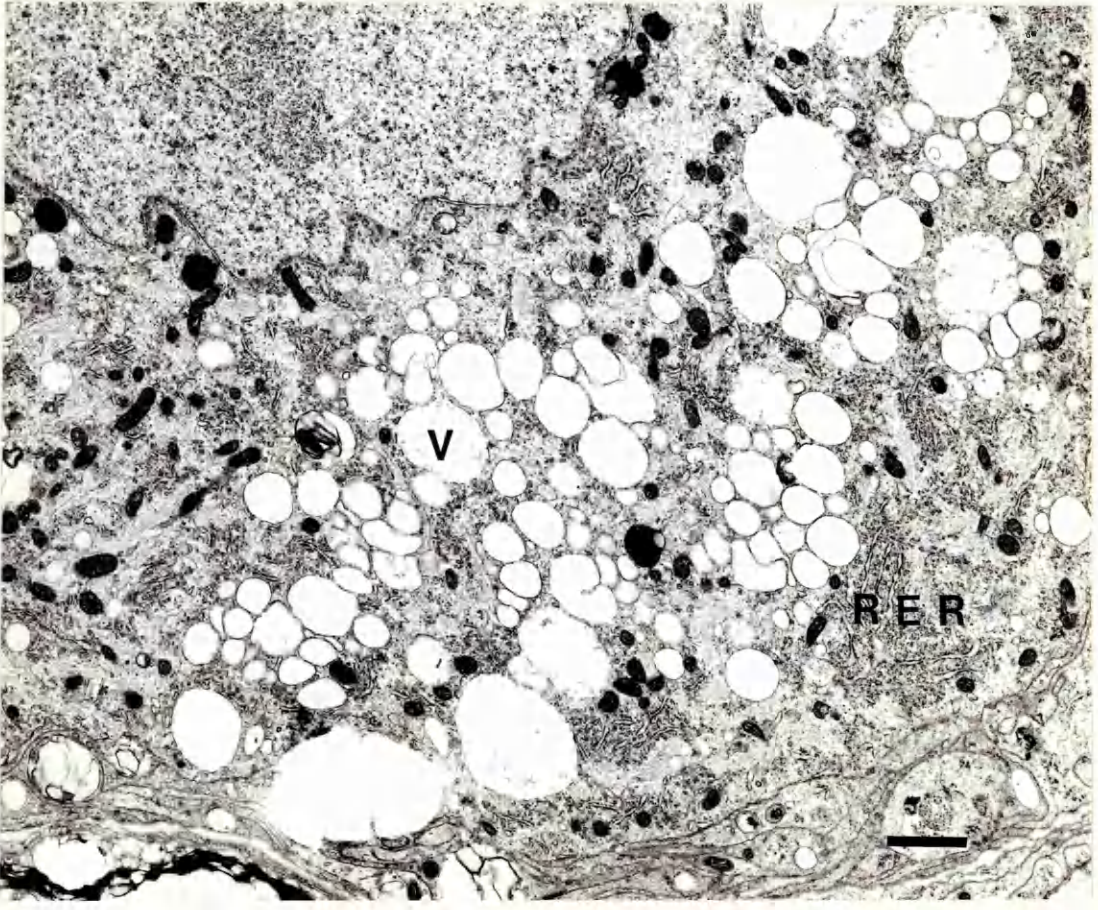
This is a small, dark neurone, and the organelles are therefore closer together normally, but it can still be seen that a large amount of cytoplasm is occupied by variably-sized vacuoles. RER (RER) is still present in organised "granules" and appears normal. There are no Golgi complexes. Mitochondria and lysosomes appear normal.

(a) Bar = 1 μ m.

(b) Bar = 1 μ m.



a



b

Figure 88

Embryonic mouse DRG after 12 days in vitro

Neurones are well-spaced as compared to the original ganglion, and greatly reduced in number. Those that remain form an approximate monolayer ranging over various planes of focus.

Some neurones do not look healthy (arrowhead) with a dark, shrunken outline, eccentric nucleus and poor axon projection.

One neurone is a very good example of a normal, healthy DRG neurone in vitro (arrow) with a rounded granular perikaryon, pale, prominent central nucleus and a single strong axon projecting from it.

There is a general impression of a 'tangle' of newly-formed axons. Stained by the combined Karnovsky-Roots cholinesterase and Tsuji and Tobin-Gros' method for axons (a silver stain).

Bar = 5 μ m.

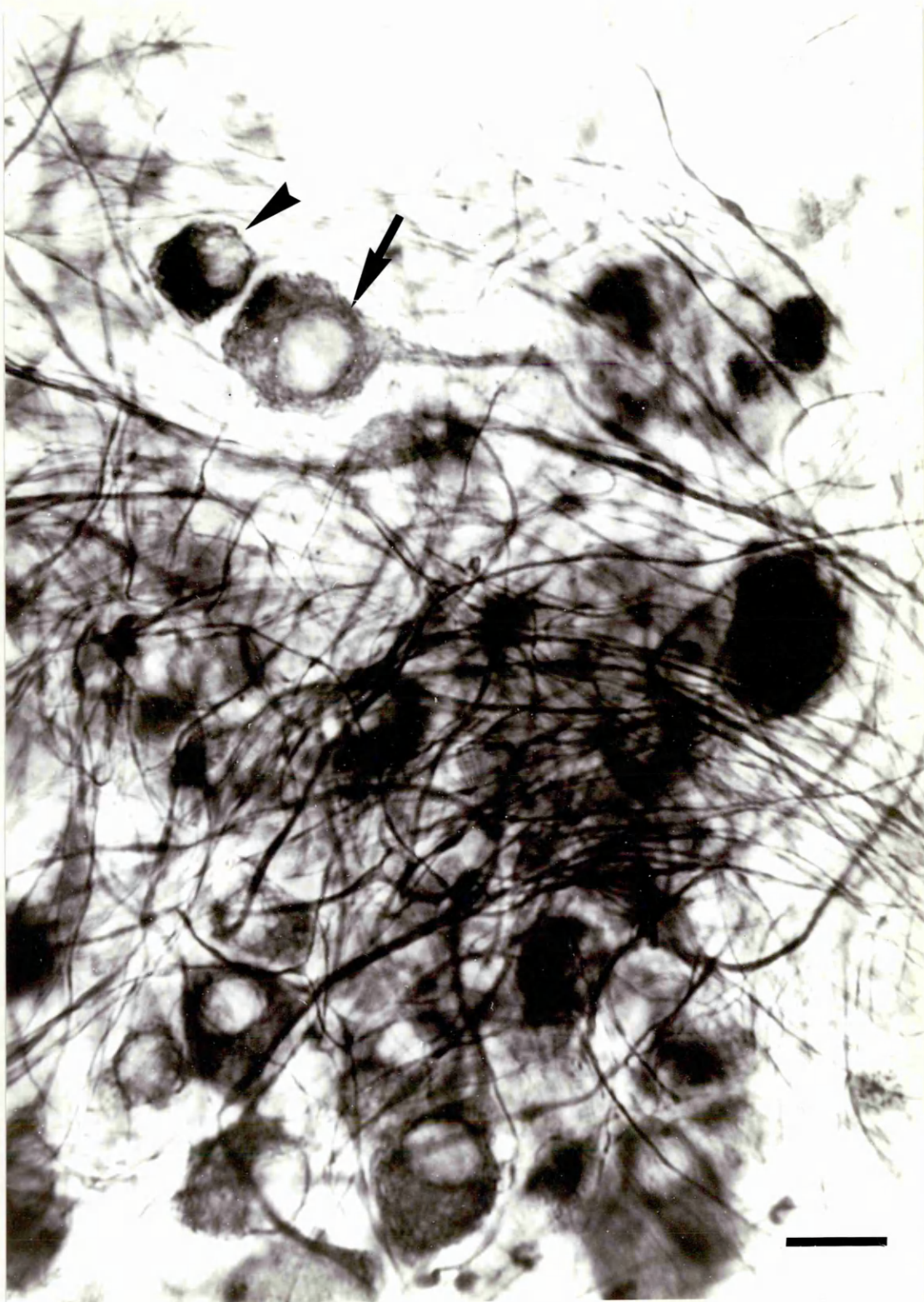


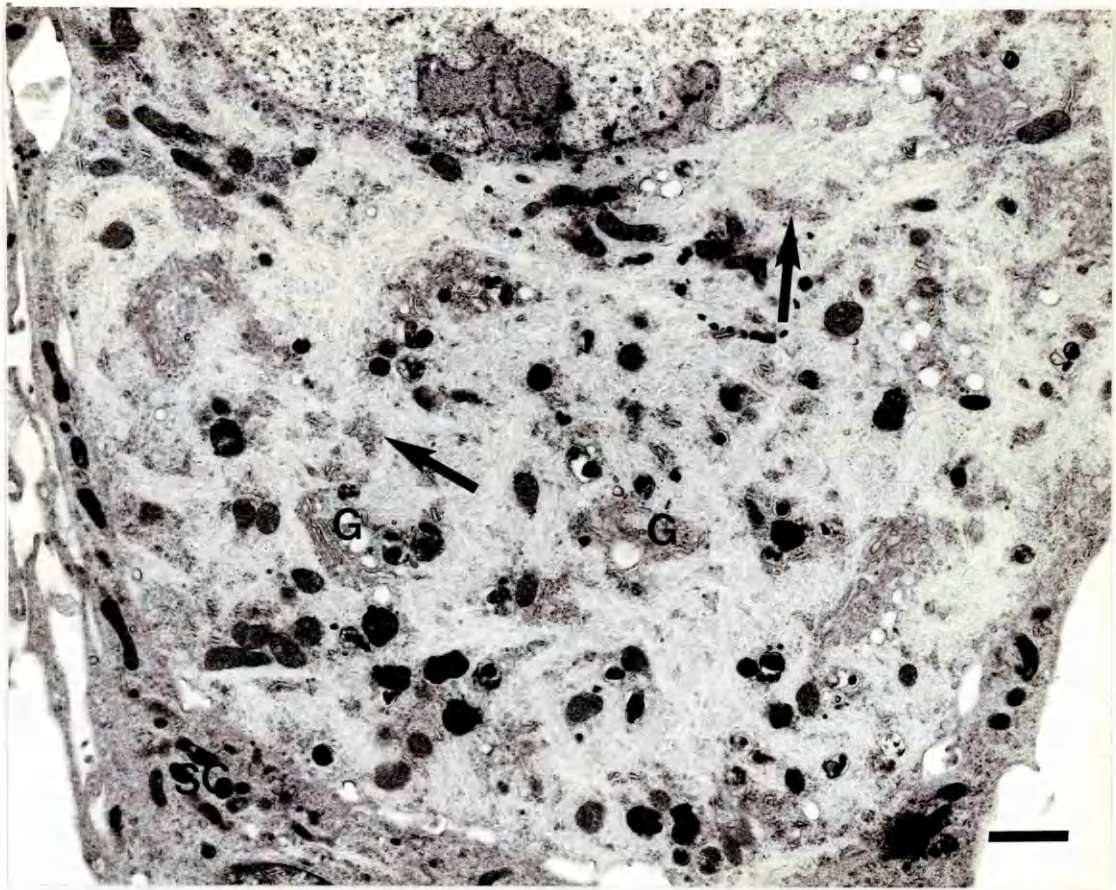
Figure 89

Embryonic mouse DRG neurone, 14 days in vitro

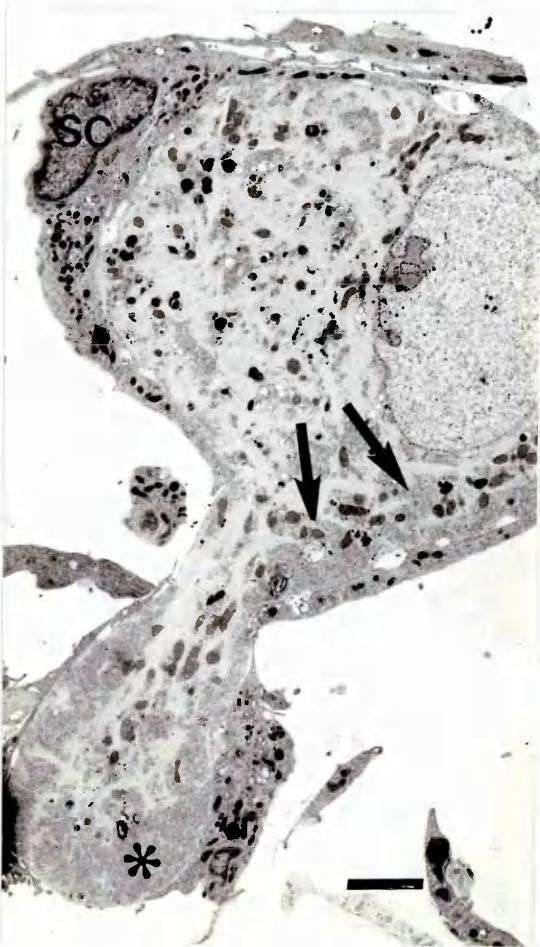
- (a) The cytoplasm contains many neurofilaments and frequent Golgi complexes (G) which sometimes appear vacuolated. This can be attributed to the neurone's exposure to tunicamycin. Mitochondria and lysosomes are hard to differentiate in some cases. There is very little RER (arrows).
- (b) At lower magnification, it can be seen that much of this neurone's RER is found peripherally (arrows) and in the cell process (*). This can be more clearly seen in (c).
- (c) A higher power of the cell process in (b). The RER (RER) is profuse and well-formed. Neurofilaments (NF) course along the long axis of the process. Mitochondria (M) and lysosomes (L) are also present.

It can be seen in all three plates that neurones in organotypic culture retain their intimate association with their satellite cells (SC).

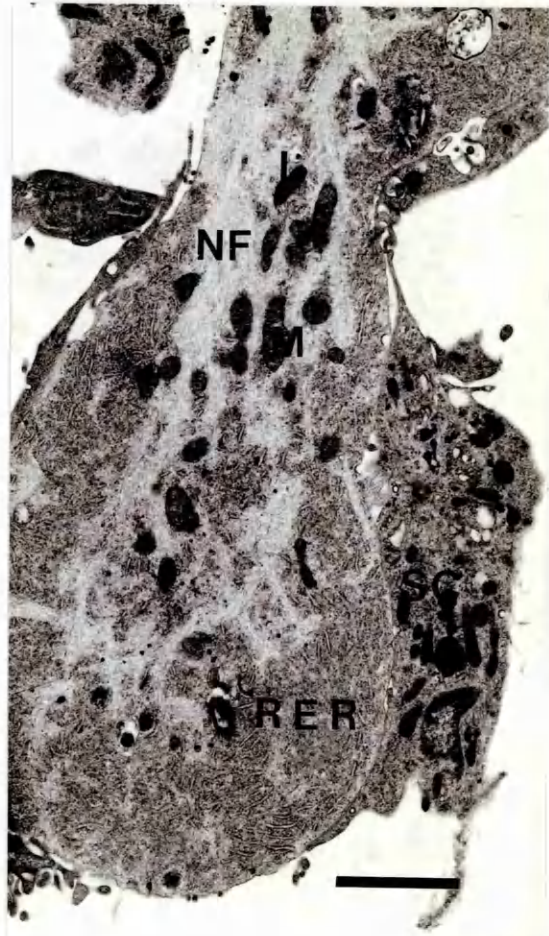
- (a) Bar = 1 μ m.
- (b) Bar = 3 μ m.
- (c) Bar = 2 μ m.



a



b



c

GENERAL DISCUSSION

It has been shown that the consistent changes demonstrable in the primary dysautonomias of domestic animals involve the cytoplasmic glycoprotein synthetic pathway, particularly the RER and Golgi complexes, in certain specific neuronal populations.

The spectrum of morphological damage varies from neurone to neurone within any one population of cells and differences can be seen between one population and another in an individual animal, but these differences are only readily detectable in 1 μ m sections, or ultrastructurally, all affected neurones appearing similarly chromatolytic in haematoxylin-eosin sections.

In general, all affected neurones show a very similar pattern of morphological change. The RER cisternae become distended with electron-dense floccular material, and are denuded of most of their ribosomes, SER profiles proliferate, the Golgi complexes are lost, and the nucleus is frequently eccentric and crenated. Nucleolar changes include segregation of the pars granulosa and pars fibrosa, and ring nucleoli, but these are inconsistent. Mitochondria are often increased in number but appear morphologically normal as do the cytoskeletal elements. Lysosomes show secondary activity as the disease progresses.

The earliest of these changes appears to be a redistribution of the RER, very closely related to the loss of the Golgi complex without any associated abnormal structure becoming apparent. A spectrum of change is visible within a few hours of the onset of clinical signs.

The one major difference morphologically between some feline peripheral autonomic neurones and all other neurones which have

succumbed to dysautonomia in both cats and horses is the presence of membranous stacks. These have been postulated to arise from Golgi complexes (Sharp et al., 1984) and may bear structural resemblances to this organelle in some cases, with smooth flattened cisternae dilated at the rims, and very occasionally a similar cytoplasmic distribution.

In an attempt to determine the fate of the Golgi complexes, and possibly confirm the origin of these stacks, enzyme cytochemical techniques failed to demonstrate any abnormal structure with specific staining for Golgi enzymes. The method used in this study was specific only for the trans Golgi saccules, but two statements can be made on the basis of this work; either there are no abnormal structures derived from the trans Golgi cisternae, or structures derived from this region have not retained their normal enzyme function. Many enzyme and immunocytochemical methods can be used to demonstrate the various membranes of the Golgi complex, as described earlier and further study enabling a comprehensive screen for all Golgi membranes would be of great value. This, however, presupposes that abnormal membranes would retain their normal composition and function. In this regard it would be of most use to examine cells in the very earliest stages of disease.

The synthetic pathways for cytosolic, structural and glycoproteins are common during the transcription of mRNA in the nucleolus, transfer of this mRNA to the cytoplasm, and the synthesis of the initial oligopeptide chain on the ribosomes. Although some nuclear and nucleolar changes are present they are

not consistent, and mitochondrial and neurofilamentous structures appear normal. It can be reasonably concluded on this basis, that these early steps in the synthetic pathway are not primarily involved. The restriction of consistent damage to the RER and Golgi complexes in dysautonomia would suggest a primary lesion of the glycoprotein synthetic pathway within these organelles.

The synthetic pathway in this region of the cytoplasm consists of many complex reactions, which are summarised elsewhere (pages 17-32).

Examination of the morphological consequences of disruption of what is only a very small number of the possible biochemical sites has not revealed any site of damage which results in precisely the same patterns of cellular disruption to those of the naturally occurring disease.

Any compounds acting at the level of the Golgi complex, or disrupting the exit of glycoprotein from the Golgi complex affect the structure of this organelle, causing distension and vacuolation of the cisternae. In the early stages, abnormal complexes can be identified, giving an indication of which deranged structures subsequently result from it. These structures may retain some functional properties of the membranes from which they originate, for example TPPase activity in monensin-induced vacuoles. Many of the reports regarding the Golgi complex do not discuss secondary effects on other organelles. Observations on the in vitro effects of monensin on DRG neurones suggest that while Nissl granules are disrupted and RER dispersed and diminished in volume, no changes are seen resembling the denudation and distension of RER in dysautonomias.

Disturbance of ribosomal or RER function results in a variety of structural changes depending on the specific site of the lesion. Inhibiting protein synthesis at ribosomal level using cycloheximide results in a marked distension of RER cisternae with electron-dense floccular material, and a reduction in the numbers of adherent ribosomes. Golgi complexes have also been observed to be abnormal, occurring in unusual vesiculated profiles, thought to result from inadequate replenishment of membrane proteins from the inactive RER. The occurrence of unusual membrane configurations closely resembling those of natural dysautonomias, are described in hepatocytes but are transient features.

Damage to the protein synthetic pathways outwith these organelles, or generalised cellular damage, can also cause these structural alterations.

Drugs affecting nucleolar function result in a gradual depletion of RER volume and a redistribution of Nissl substance within the cell. Nuclear and nucleolar changes are pronounced and consistent while the Golgi complexes remain relatively unscathed.

Axonal damage (the axonal or retrograde reaction) also results in a redistribution of RER, but in this case the Golgi complexes are frequently hypertrophied, with a concomitant decrease in TPPase activity.

It must be borne in mind that cells from different tissues and even cellular subpopulations may react differently to the same insult, and that these comments can therefore only be

considered in general rather than specific terms.

In no circumstances, however, has complete loss of a recognisable or detectable Golgi complex been described.

It is very difficult to conceive of a situation in which a large structure composed of many heterogeneous membranes could disappear without any degenerate or residual stages being visible. Neuronal lysosomes in the early stages of dysautonomic change are frequently inactive, further suggesting that there is no cytoplasmic debris resulting from the loss of the Golgi complex.

Although the specific level at which damage occurs in these cells is as yet unclear, it is most likely to be within the RER or Golgi complex.

It would seem likely that the causal agent gains access to susceptible neuronal perikarya via the circulatory system, and that clinical signs occur following the neuronal lesion. The specificity of damage within the nervous system can only be accounted for by some as yet unknown inherent structural, metabolic or functional property of these particular neuronal populations. For example, the knowledge regarding the numerous neuropeptides co-existing with classical neurotransmitters, and found in various combinations in different neurones is expanding rapidly; the susceptible neuronal populations in dysautonomias may contain some as yet undefined peptide or combination of peptides which would render them distinct from other neurones in their response to a given insult.

Another possible route of entry is that of retrograde transport along the axons from the gastrointestinal tract.

Several of the affected areas have only tenuous connections with the gut, however, and this could not account for lesions in the ventral horn cells, for example.

The transmission studies carried out in the horse by transference of affected serum would seem to favour the former theory of a neurotoxic agent in the blood (see page 59). This work demonstrated that high molecular weight (M.W.) serum fractions retained the neurotoxic properties observed for whole serum. There were no clinical signs associated with these lesions, however, which raises the question of how badly damaged a neurone has to be before functional deficits are detectable clinically. Other work analysing serum components from affected horses has shown the presence of an unusual compound of low M.W. (Johnson, 1985) but the low M.W. serum fraction of Gilmour caused no apparent lesion. As mentioned earlier the lesions found by Gilmour were only examined in paraffin section, and much more work is needed on this subject, with ultrastructural examination of damaged neurones, to determine whether or not the precise lesion of dysautonomia is indeed transmissible via serum.

The majority of the present evidence would support the hypothesis that the primary lesion occurs within the neuronal perikaryon, affecting the cytoplasmic organelles of glycoprotein synthesis, although the precise biochemical level has not yet been identified.

A possible pathogenesis could involve primary damage to the synthetic function of specific neurones, resulting in decreased production of their secretory proteins, morphological changes at

that time being restricted to the perikaryon. This would account for the loss of peptides seen in the gut plexi, in the absence of morphological change at the same level. The clinical signs would then develop as a result of the specific loss of neuronal function. By the time affected tissue was available for examination, the neurones originally involved would be undergoing the less specific changes leading to cell death, with more recently involved, or less severely affected neurones demonstrating a spectrum of intermediate changes.

More advanced lesions would be commoner in feline tissue since gastrointestinal stasis is less dramatic and, initially, less life-threatening than the equivalent state in horses.

To establish the precise site of the primary lesion, the possible origins of the membrane stacks and the functional disturbances associated with particular synthetic disruptions, further work of a similar nature to that of this thesis would need to be undertaken.

Neuronal tissue culture offers an extremely flexible system in which to study the structural and functional aspects of glycoprotein synthesis. Compounds not specifically neurotoxic in vivo or possessing systemic toxic effects which render them unsuitable for use in vivo could be examined in this way. Several cultures can be established from a single animal reducing the potential difficulties ensuing from individual variation, and the environment in which each culture is maintained can be very precisely defined and controlled.

Tissue culture techniques would also enable the examination of the neurones recovering from 'pulse' exposure to an

antimetabolite, in comparison to the damage resulting from extended exposure. Thus transient structures appearing as the cell attempts to recover could be observed, and lethal and potentially reversible cell change could be differentiated. This would be of great value, since the appearance of a neurone exposed to a toxin, and one recovering from the same insult may be different, and there is no indication at present whether the neuronal change in dysautonomia is potentially reversible in the less extensively damaged neurones.

Ultrastructural, enzyme and immunocytochemical investigations of structure can be readily undertaken, and the autoradiographic tracing of function at both light and electron microscopic levels in normal neurones, and those exposed to antimetabolites, would furnish a very well integrated view of many specific metabolic disturbances.

These techniques in conjunction with tissue culture could also be used as a "screening" system for material from clinical cases. For example, the damaging effects of serum fractions as described earlier, could be assessed using much smaller volumes, necessitating fewer affected 'donor' horses and allowing greater numbers of fractions to be tested. While the related clinical picture would not be available, a large number of samples could be tested for any toxic effect, reducing the number of compounds requiring to be tested in vivo.

If, for example, a serum fraction from affected animals could be demonstrated as consistently and specifically toxic to cultured neurones, then there would be the potential to develop

this as an in vivo diagnostic test for dysautonomia, even in the absence of any known aetiological agent. It is unlikely, however, that this would be either rapid or inexpensive, but would nonetheless prove conclusive in cases where doubt was expressed clinically.

It is the conclusion of this thesis that the dysautonomias of domestic animals are caused by very similar, or common, aetiological agents which have a primary effect on the glycoprotein synthetic pathway of specific neuronal populations at the level of the RER or the Golgi complex.

The development and continued application of the techniques employed in this study to both clinical and experimental material would provide further information on the pathogenesis of this disease and add to the general understanding of neuronal response to injury, both in terms of cellular function and the associated sub-cellular architecture.

Appendix 1

Processing of samples for electron microscopy

(i) Long schedule

Tissue was post-fixed in 1% osmium tetroxide (made up in isotonic cacodylate buffer - Appendix 3) for 1-2 hours, then washed for a minimum of 30 mins. in at least two changes of isotonic cacodylate buffer.

Samples were dehydrated through graded alcohols according to the following schedule:-

50% alcohol	15 mins.
70% alcohol	15 mins.
80% alcohol	15 mins.
90% alcohol	15 mins.
100% alcohol	20 mins. (Repeat once)
Propylene oxide	15 mins. (Repeat once)

These dehydrated samples were placed overnight in a 1 : 1 mixture of propylene oxide and Araldite resin (see below), in a rotator (2 rpm). The following day this was changed to a 1 : 3 mixture of propylene oxide and Araldite resin, and again left overnight in the rotator.

On the third day, the propylene oxide was allowed to evaporate from the bottles, and when the remaining Araldite was viscous, the tissue was removed and embedded in freshly made 100% Araldite, which was then polymerised overnight at 60°C.

(ii) Short schedule

Tissue was post-fixed in 1% osmium tetroxide and rinsed in cacodylate buffer as in (i).

It was then dehydrated through graded alcohols according to the following schedule:-

70% alcohol	3-5 mins. (repeat twice)
90% alcohol	3-5 mins. (repeat once)
100% alcohol	3-5 mins. (repeat twice)
Propylene oxide	30 mins.

These dehydrated samples were placed in a 1 : 1 mixture of propylene oxide and Araldite resin in a rotator (2 rpm) and the propylene oxide allowed to evaporate.

When the remaining Araldite was viscous, the tissue was embedded in Araldite as described above.

(iii) Araldite Resin

Araldite CY212	30 g
DDSA	25.2 g
DMP 30	1.2 ml
Dibutylphthalate	1 ml

Appendix 2

Staining of grids for electron microscopy

(1) Uranyl acetate

20% uranyl acetate in alcohol. Filter before use.

Place grids in stain for 5 mins.

Rinse in 50% alcohol rapidly, six times.

Blot dry.

(2) Lead citrate

1.33 g lead nitrate

1.76 g sodium citrate

Dissolve each salt in 15 ml distilled water, then mix the solutions. Leave for 30 mins. shaking occasionally. Add 8 ml of 1N sodium hydroxide to dissolve precipitate, then make up to 50 ml with distilled water. Filter before use.

Staining is carried out in a sodium hydroxide chamber. Place grids face down on drops of the staining solution for 5 mins. Rinse rapidly in 0.02N sodium hydroxide once. Rinse rapidly in 50% alcohol six times. Blot dry.

Appendix 3

Buffers

(i) Acetate buffer, 0.05M [pH 5.0]

Solution A - 0.285 ml glacial acetic acid made up to
100 ml with distilled H₂O.

Solution B - 0.410 g sodium acetate made up to 100 ml with
distilled H₂O.

Buffer - 14.8 ml of Solution A
35.2 ml of Solution B
made up to 100 ml with distilled H₂O.
Check pH.

(ii) Gomori's TRIS-maleate buffer, 0.2M [pH 7.2]

Solution A - 2.42 g TRIS
2.32 g maleic acid
made up to 100 ml with distilled H₂O.

Solution B - 0.8 g NaOH made up to 100 ml with distilled
H₂O.

Buffer - 25 ml of Solution A
25.5 ml of Solution B
made up to 100 ml with distilled H₂O.
Check pH.

(iii) Sodium cacodylate buffer, 0.025 M

5.35 g sodium cacodylate in 1 litre distilled H₂O.

(iv) Sodium cacodylate buffer, 0.08M [pH 7.2]

17.225 g sodium cacodylate in 1 litre distilled H₂O.

Check pH, and adjust if necessary with hydrochloric acid
(1M).

(v) Sodium cacodylate buffer, 0.1 M [pH 7.4]

2.1403 g sodium cacodylate made up to 100 ml with distilled H₂O.

Check pH, and adjust if necessary with hydrochloric acid (1M).

Add 7.5 g sucrose for use in enzyme cytochemical fixatives.

(vi) Isotonic sodium cacodylate buffer [pH 7.3]

16.0520 g sodium cacodylate

3.8 g sodium chloride

0.111 g calcium chloride

0.202 g magnesium chloride

Check pH, and adjust if necessary with hydrochloric acid (1M).

Appendix 4

Perfusion Fixation

(i) Cats

Prior to perfusion, each cat received 1500 units of heparin sodium (Evans) intravenously, and was then anaesthetised by intravenous administration of 2.5% thiopentone (Intraval Sodium; RMB Animal Health Limited) to effect. Anaesthesia was maintained with O₂, N₂O (70/30) and halothane administered by a respiratory pump via an endotracheal tube.

The thoracic cavity was opened on the left and the heart exposed by incising the pericardium. A cannula for the administration of perfusates was then placed and secured in either the left ventricle or aorta. The right ventricle was cannulated for the drainage of blood and circulated perfusate.

The perfusate was a modification of Karnovsky's method (1965), and consisted of 500 ml of a "weak" fixative,

(final concentrations)

paraformaldehyde (8%)	62.5 ml	1%
glutaraldehyde (25%)	25 ml	1.25%
calcium chloride	250 mg	4.5 mM

made up in 0.08 M sodium cacodylate buffer (Appendix 3) followed by 1500 ml of "strong" fixative,

(final concentrations)

paraformaldehyde (8%)	700 ml	4%
glutaraldehyde (25%)	300 ml	5%
calcium chloride	750 mg	4.5 mM

made up in 0.08 M sodium cacodylate buffer.

Two bottles containing the fixatives were connected to the cannula by a series of tubes and 3-way taps which formed an airtight system (Fig. 90). Air added to the system by means of a 50 ml syringe and a 3-way tap connected to the fixative bottle increased the pressure within the bottle, forcing the perfusate through the apparatus and into the cardiovascular system of the cat. The bottle was emptied by additional volumes of air. The second perfusate was introduced from the other bottle by the same method. Care was taken to ensure that bubbles were excluded from the perfusate entering the cat. The perfusion pressure was not monitored.

(ii) Rats

Prior to fixation, the rats were anaesthetised by intraperitoneal administration of pentobarbitone (Sagatal), and the heart exposed by removal of the thoracic cage and incision of the pericardium. The right atrium was incised to allow drainage of blood and circulated perfusate, and the perfusate (fixative of choice varied; see relevant Methods section) administered via a cannula placed in the left ventricle and retained manually. The perfusate was introduced directly to the cannula by two 50 ml syringes (Fig. 90), care being taken to exclude air-bubbles via a 3-way tap at the top of the cannula. The perfusion pressure was not monitored.

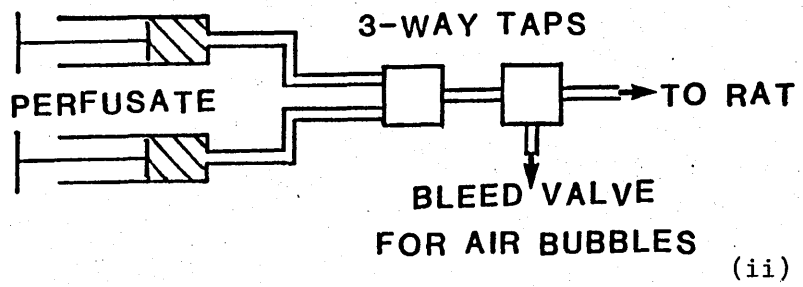
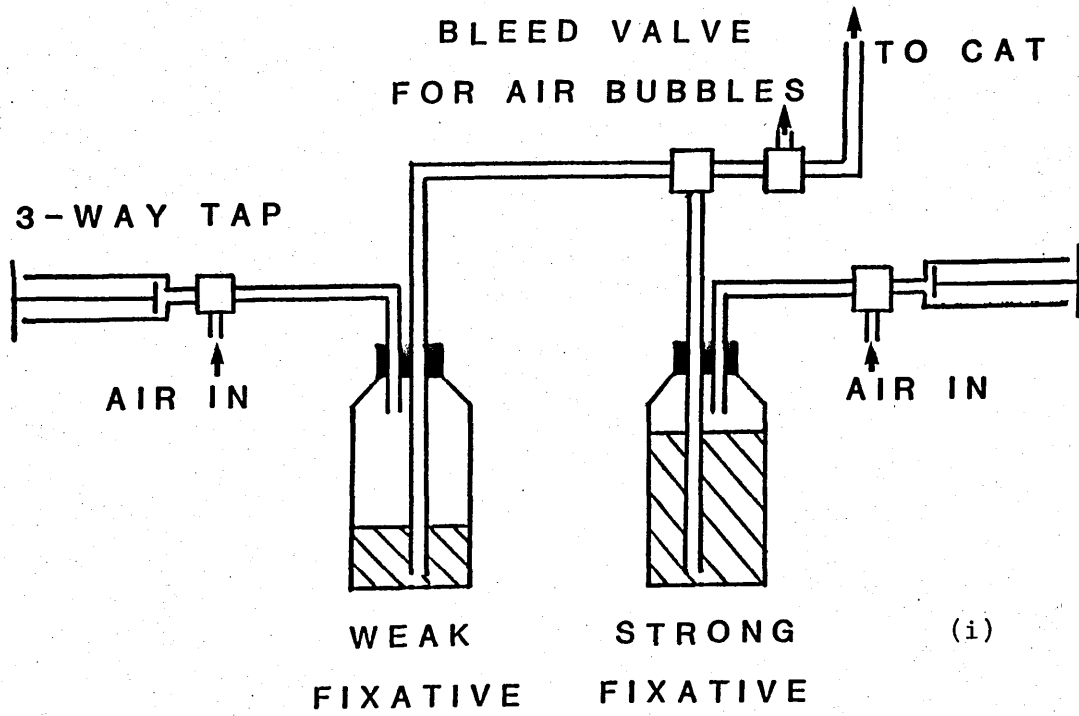


Figure 90. Perfusion apparatus for (i) cats (ii) rats

Appendix 5

HEPES Buffered Salt Solution (HBSS) (Mata et al, 1980)

HEPES	20 mM
NaCl	130 mM
KCl	4.5 mM
CaCl ₂	1.8 mM
MgSO ₄ (7 H ₂ O)	0.9 mM
-D+glucose	11.1 mM

[pH 7.46 - 7.51 at 25°C with 0.1 M NaOH]

L-glutamine (Sigma) 2 mM

MEM (50 x) Amino acids without L-glutamine
(Sigma) 20 ml/l.

MEM (100 x) non-essential amino acids (Sigma)
10 ml/l.

This medium was aliquoted and frozen (-20°C) immediately after being made, and the required amount thawed on the day of use.

Any surplus from a thawed aliquot was discarded.

REFERENCES

- Aldskogius, H. (1978). Fine structural changes in nerve cell bodies of the adult rabbit dorsal motor vagal nucleus during axon reaction. *Neuropathology and Applied Neurobiology* **4**, 323-341.
- Anderson, P.H., Patterson, D.S.P. and Barrett, S. (1978). Selenium deficiency. *Veterinary Record* **103**, 145-148.
- Anderson, W.G.F. (1978). Selenium deficiency. *Veterinary Record* **103**, 102.
- Angermuller, S. and Fahimi, H. (1984). A new cerium-based method for cytochemical localisation of thiamine pyrophosphatase in the Golgi complex of rat hepatocytes. Comparison with the lead technique. *Histochemistry* **80**, 107-111.
- Arechaga, J. and Bahr, G.F. (1985). Nuclear rings - portrait of a new cell organelle. In Smuckler, E.A. and Clawson, G.A. (Eds.). *Nuclear envelope structure and RNA maturation. UCLA symposium on Molecular and Cellular Biology. New Series Vol. 26*, Alan R. Liss Inc. New York.
- Ashton, D.G., Jones, D.M. and Gilmour, J.S. (1977). Grass sickness in two non-domestic equines. *Veterinary Record* **100**, 406-407.
- Bainton, D.F. (1981). The Discovery of Lysosomes. *Journal of Cell Biology* **91**, 665.
- Bannister, R. (Ed) (1983). *Autonomic failure: a textbook of clinical disorders of the autonomic nervous system*. Oxford Medical Publications.

- Barlow, R.M. (1969). Neuropathological observations in grass sickness of horses. *Journal of Comparative Pathology* **79**, 407-411.
- Barron, K.D., Chiang, T.Y., Daniels, A.C. and Doolin, P.F. (1971). Subcellular accompaniments of axon reaction in cervical motoneurons of the cat. *Progress in Neuropathology* **1**, 225-280.
- Begg, G.W. (1936). Grass disease in horses. *Veterinary Record* **48 (21)**, 655-662.
- Bigotte, L. and Olsson, Y. (1983). Cytotoxic effects of Adriamycin on mouse hypoglossal neurones following retrograde axonal transport from the tongue. *Acta Neuropathologica (Berl.)* **61**, 161-168.
- Bishop, A.E., Hodson, N.P., Major, J.H., Probert, L., Yeats, J., Edwards, G.B., Wright, J.A., Bloom, S.R. and Polak, J.M. (1984). The regulatory peptide system of the large bowel in equine grass sickness. *Experientia* **40**, 801-806.
- Blomstrand, C. and Hamberger, A. (1970). Amino acid incorporation in vitro into protein of neuronal and glial cell-enriched fractions. *Journal of Neurochemistry* **17**, 1187-1195.
- Bloom, F.E. (1973). Ultrastructural identification of catecholamine-containing central synaptic terminals. *Journal of Histochemistry and Cytochemistry* **21**, 333-348.
- Bouteille, M. and Dupuy-Coin, A.A. (1979). Nuclear Structure and Function. In Busch, H., Crooke, S.T. and Daskal, Y. (Eds.). *Effects of Drugs on the Cell Nucleus*. Academic Press.

- Broadwell, R.D. and Cataldo, A.M. (1983). The neuronal endoplasmic reticulum : Its cytochemistry and contribution to the endomembrane system. I. Cell bodies and dendrites. *Journal of Histochemistry and Cytochemistry* **31**, 1077-1088.
- Brownlee, A. (1939). Grass disease of horses and game preservation; their possible correlation: an hypothesis and an appeal. *Veterinary Record* **51**, 1404-1407.
- Brownlee, A. (1959). Changes in the coeliaco-mesenteric ganglia of horses affected with grass sickness and of horses affected with some other diseases. *Veterinary Record* **71**, 668-669.
- Brownlee, A. (1985). Neurogenic colic (grass sickness). *Veterinary Record* **116**, 27.
- Cataldo, A.M. and Broadwell, R.D. (1984). Cytochemical staining of the endoplasmic reticulum and glycogen in mouse anterior pituitary cells. *Journal of Histochemistry and Cytochemistry* **32**, 1285-1294.
- Cavanagh, J.B. and Chen, F.C.K. (1977). Amino acid incorporation in protein during the 'silent phase' before organomercury and p-bromophenylacetylurea neuropathy in the rat. *Acta Neuropathologica (Berl.)* **19**, 216-224.
- Cavanagh, J.B., Tomiwa, K. and Munro, P.M.G. (1987). Nuclear and nucleolar damage in adriamycin-induced toxicity to rat sensory ganglion cells. *Neuropathology and Applied Neurobiology* **13**, 23-38.
- Chandler, R.L. and Brownlee, A. (1967). Ultrastructural observations on neurons of the sympathetic ganglia in grass sickness. *Journal of Comparative Pathology* **77**, 339-342.

- Cho, E.S. (1977). Toxic effects of adriamycin on the ganglia of the peripheral nervous system : A neuropathological study. *Journal of Neuropathology and Experimental Neurology* **36**, 907-915.
- Cho, E.S., Jortner, B.S., Schaumburg, H.H. and Spencer, P.S. (1977). A single injection of doxorubicin (adriamycin) induces sensory neuronopathy in the rat. *Neurotoxicology* **1**, 583-591.
- Crooke, S.T. (1979). Biochemical effects of drugs on the cell nucleus. In Busch, H., Crooke, S.T. and Daskal, Y. (Eds.) *Effects of Drugs on the Cell Nucleus*. Academic Press.
- Dancis, J. (1983). Familial dysautonomia (Riley-Day syndrome). In Bannister (Ed) *Autonomic failure*. **Ch.28**, 615. Oxford Medical Publications.
- Daskal, Y. (1979). Drug effects on nucleolar and extranucleolar chromatin. In Busch, H., Crooke, S.T. and Daskal, Y. (Eds.). *Effects of Drugs on the Cell Nucleus*. Academic Press.
- Doine, A.I., Oliver, C. and Hand, A.R. (1984). The Golgi apparatus and GERL during post-natal differentiation of rat parotid acinar cells. *Journal of Histochemistry and Cytochemistry* **32**, 477-485.
- Duce, I.R. and Keen, P. (1977). An ultrastructural classification of the neuronal cell bodies of the rat dorsal root ganglion using zinc iodide-osmium impregnation. *Cell and Tissue Research* **185**, 263-277.

- Dunphy, W.G., Brands, R. and Rothman, J.E. (1985). Attachment of terminal N-acetylglucosamine to asparagine-linked oligosaccharides occurs in central cisternae of the Golgi stack. *Cell* **40**, 463-472.
- Dunphy, W.G. and Rothman, J.E. (1983). Compartmentation of asparagine-linked oligosaccharide processing in the Golgi apparatus. *Journal of Cell Biology* **97**, 270-275.
- Dunphy, W.G. and Rothman, J.E. (1985). Compartmental Organisation of the Golgi stack. *Cell*. **42**, 13-21.
- Duskin, D. and Mahoney, W.C. (1982). Relationship of the structure and biological activity of the natural homologues of Tunicamycin. *Journal of Biological Chemistry* **257**, 3105-3109.
- Eddy, E.L. and Nathaniel, E.J.H. (1982). An ultrastructural study of the effects of Adriamycin on the dorsal root ganglia of young and adult rats. *Experimental Neurology* **77**, 275-285.
- Edney, A.T.B., Gaskell, C.J., Flagstad, A., Hedhammar, A.A. and Presthus, J. (1986). Feline dysautonomia. *Veterinary Record* **117**, 395 (Correspondence).
- Edwards, G.B. (1987). Grass sickness of horses; clinical picture and management. 6th Waltham Symposium. *Journal of Small Animal Practice* **28**, 364-368.
- Ellinger, A. and Pavelka, M. (1984). Effect of monensin on the Golgi apparatus of absorptive cells in the small intestine of the rat. Morphological and cytochemical studies. *Cell and Tissue Research* **235**, 187-194.

- Farquhar, M.G. and Palade, G.E. (1981). The Golgi apparatus (complex) - (1954-1981) - from artefact to center stage. *Journal of Cell Biology* **91**, 77s-103s.
- Feldherr, C.M. (1985). The facilitated transport of proteins across the nuclear envelope. In Smuckler, E.A. and Clawson, G.A. (Eds.). *Nuclear Envelope Structure and RNA Maturation. UCLA Symposia on Molecular and Cellular Biology. New Series Vol.26*, Alan R. Liss Inc. New York.
- Flagstad, A., Dietz, H.H. and Bindsell, E. (1986). Feline dysautonomia. *Veterinary Record* **119**, 483 (Correspondence).
- Flumerfelt, B.A. and Lewis, P.R. (1975). Cholinesterase activity in the hypoglossal nucleus of the rat and the changes produced by axotomy : A light and electron microscopic study. *Journal of Anatomy* **119**, 309-331.
- Forsyth, A.A. (1941). Grass disease in a coal mine. *British Veterinary Journal* **97**, 26-28.
- Fraser, A.F. and Brownlee, A. (1974). Veterinary ethology and grass sickness in horses. *Veterinary Record* **95**, 448.
- Gaskell, C.J. (1987). Epidemiology : some preliminary observations. 6th Waltham Symposium. *Journal of Small Animal Practice* **28**, 343-346.
- Gaskell, C.J. and Edney, A.T.B. (1985). Feline dysautonomia distribution. *Veterinary Record* **117**, 395.
- Geuze, H.J., Shot, J.W., Strous, J.A.M., Hasilik, A. and von Figura, K. (1985). Possible pathways for lysosomal enzyme delivery. *Journal of Cell Biology* **101**, 2253-2262.

- Ghoshal, N.G. (1975). Abdominal, pelvic and caudal autonomic innervation. In Getty, R. (Ed) Sisson and Grossman's The Anatomy of the Domestic Animals. W.B. Saunders Company. Vol. 1, p.697.
- Gilmour, J.S.(1973a). Experimental reproduction of the neurological lesions associated with grass sickness. Veterinary Record 92, 565-566.
- Gilmour, J.S. (1973b). Observations on neuronal changes in grass sickness of horses. Research in Veterinary Science 15, 197-200.
- Gilmour, J.S. (1975). Chromatolysis and axonal dystrophy in the autonomic nervous system in grass sickness of equidae. Neuropathology and Applied Neurobiology 1, 39-47.
- Gilmour, J.S. (1976). Accumulations of nor-adrenaline associated with axonal changes in autonomic ganglia in grass sickness. Neuropathology and Applied Neurobiology 2, 389-394.
- Gilmour, J.S. (1987). Epidemiology and pathology. 6th Waltham Symposium. Journal of Small Animal Practice 28, 373-380.
- Gilmour, J.S. and Jolly, G.M. (1974). Some aspects of the epidemiology of equine grass sickness. Veterinary Record 95, 77-81.
- Glassy, M.C. and Ferrone, S. (1981). Ultrastructural alterations in human lymphoblastoid B cell lines treated with tunicamycin. American Journal of Pathology 103, 1-9.
- Glover, R.A. (1982). Chronological changes in acid phosphatase activity within neurons and perineuronal satellite cells of the inferior vagal ganglion of the cat induced by vagotomy. Journal of Anatomy 134, 215-225.

- Gonzalez, C.B., Swann, R.W. and Pickering, B.T. (1981). Effects of tunicamycin on the hypothalamo-neurohypophysial system of the rat. *Cell and Tissue Research* **217**, 199-210.
- Gordon, W.S. (1934). Enterotoxaemia in herbivorous animals - its possible bearing on grass sickness in horses. *Veterinary Record* **XIV**, 1016-1032.
- Greet, T.R.C. and Whitwell, K.E. (1986). Radiological features of the equine oesophagus in grass sickness. *Equine Veterinary Journal* **18**, 294-297.
- Greet, T.R.C. and Whitwell, K.E. (1987). Studies of oesophageal function. 6th Waltham Symposium. *Journal of Small Animal Practice* **28**, 369-372.
- Greig, J.R. (1928). Acute "grass disease": an interpretation of the clinical symptoms. *Veterinary Record* **VIII (40)**, 31-34.
- Greig, J.R. (1942). Grass sickness in horses. A review of the present knowledge of the disease with particular reference to the nature of the causal agent. *Transactions of the Highland and Agricultural Society of Scotland. Fifth Series* **LIV**.
- Griffiths, G. and Simons, K. (1986). The trans-Golgi network : sorting at the exit site of the Golgi complex. *Science* **234**, 438-443.
- Griffiths, I.R., Nash, A.S. and Sharp, N.J.H. (1982). The Key-Gaskell syndrome - the current situation. *Veterinary Record* **111**, 532-533.

- Griffiths, I.R. and Sharp, N.J.H. (1983). Feline autonomic polyganglionopathy. *Neuropathology and Applied Neurobiology* 9, 336.
- Griffiths, I.R., Sharp, N.J.H. and McCulloch, M.C. (1985). Feline dysautonomia - the Key-Gaskell syndrome: An ultrastructural study of autonomic ganglia and nerves. *Neuropathology and Applied Neurobiology* 11, 17-29.
- Guthrie, W.J. (1940). Grass sickness in horses. *Journal of the Royal Agricultural Society of England* 100 pt 111, 50-59.
- Hammerschlag, R. and Lavoie, P.A. (1979). Initiation of fast axonal transport : Involvement of calcium during transfer of proteins from Golgi apparatus to the transport system. *Neuroscience* 4, 1195-1201.
- Hammerschlag, R., Stone, G.C., Bolen, F.A., Lindsey, J.D. and Ellisman, M.H. (1982). Evidence that all newly synthesised proteins destined for fast axonal transport pass through the Golgi apparatus. *Journal of Cell Biology* 93, 568-575.
- Hodson, N.P., Edwards, G.B., Barnett, S.W., Bishop, A.E., Cole, G.A., Probert, L., Bloom, S.R. and Polak, J.M. (1982). Grass sickness of horses: changes in the regulatory peptide system of the bowel. *Veterinary Record* 110, 276.
- Hodson, N.P. and Wright, J.A. (1987). Electron Microscopy. 6th Waltham Symposium. *Journal of Small Animal Practice* 28, 381-386.
- Hodson, N.P., Wright, J.A., Edwards, G.B., Mescall, P.E. and Suswillo, R.E. (1984). Observations on the coeliacomesenteric ganglion in normal and horses with grass sickness. *Journal of Pathology* 142, A21.

- Holman, H.H., Gordon, W.S. and Pattison, I.H. (1944).
Observations on the pathology of grass sickness in horses.
Journal of Comparative Pathology 54, 97-107.
- Holtzman, E., Novikoff, A.B. and Villaverde, H. (1967).
Lysosomes and GERL in normal and chromatolytic neurons of
the rat ganglion nodosum. *Journal of Cell Biology* 33, 419-
435.
- Howell, J.McC., Baker, J.R. and Ritchie, H.E. (1974).
Observations on the coeliacomesenteric ganglia of horses
with and without grass sickness. *British Veterinary Journal*
130, 265-270.
- Hwang, K.M., Yang, L.C., Carrico, C.K., Schulz, R.A., Schenkman,
J.B. and Sartorelli, A.C. (1974). Production of membrane
whorls in rat liver by some inhibitors of protein synthesis.
Journal of Cell Biology 62, 20-31.
- Inamdar, S., Easton, L.B. and Lester, G. (1982). Acquired post-
ganglionic cholinergic dysautonomia. Case report and review
of the literature. *Pediatrics* 70, 976,
- Jacobs, J.M., Macfarlane, R.M. and Cavanagh, J.B. (1976).
Vascular leakage in the dorsal root ganglia of the rat,
studied with horseradish peroxidase. *Journal of the
Neurological Sciences* 29, 95-107.
- Jacobs, R.M., Miller, R.H., Whittle, A. and Cavanagh, J.B.
(1979). Studies on the early changes in acute isoniazid
neuropathy in rat. *Acta Neuropathologica (Berl.)* 47, 85-92.
- Janz, R. (1982). *Veterinary Record* 111, 401 (Correspondence).

- Johnson, P. (1985). Unusual compound of small molecular weight in the serum of horses with acute grass sickness. *Research in Veterinary Science* 38, 329-333.
- Johnson, R.H. (1983). Autonomic failure and the eyes. In Bannister (Ed) *Autonomic failure* Ch.24. Oxford Medical Publications.
- Jones, H.B. and Cavanagh, J.B. (1981). Comparison between the early changes in isoniazid intoxication and the chromatolytic response to nerve ligation in spinal ganglion cells of the rat. *Neuropathology and Applied Neurobiology* 7, 489-501.
- Karnovsky, M.J. (1965). A formaldehyde-glutaraldehyde fixative of high osmolarity for use in electron microscopy. *Journal of Cell Biology* 27, 137a.
- Key, T. and Gaskell, C.J. (1982). *Veterinary Record* 110, 160 (Correspondence).
- Koch, R. (1982). *Veterinary Record* 111, 469 (Correspondence).
- Kondo, A., Ohnishi, A., Nagara, H. and Tateishi, J. (1987). Neuronotoxicity in primary sensory neurons of Adriamycin administered through retrograde axoplasmic transport in rats. *Neuropathology and Applied Neurobiology* 13, 177-192.
- Lannek, N., Lindberg, P., Persson, F., Obel, A-L. and Sevelius, F. (1961). A grass disease enzootic in stable-fed horses with an investigation of the aetiological role of the food. *Veterinary Record* 73, 601-603.

- Laszlo, I. and Knyihar, E. (1975). Electron histochemistry of thiamine pyrophosphatase activity in the neuronal Golgi apparatus observed after axotomy and transneuronal deprivation. *Journal of Neural Transmission* **36**, 123-141.
- Leblond, C.P. and Bennett, G. (1977). Role of the Golgi apparatus in terminal glycosylation. In Brinkley, B.R. and Porter, K.R. (Eds.). *International Cell Biology 1976-1977*. Rockefeller University Press, N.Y. 326-336.
- Lewis, P.R. (1977). Metal precipitation methods for hydrolytic enzymes. In Lewis, P.R. and Knight, D.P., *Staining Methods for Sectioned Material, Vol. 5, Pt 1* of Glauert, A.M. (Ed) *Practical Methods in Electron Microscopy*. North Holland Publishing Company.
- Lewis, P.R. and Knight, D.P. (1977). Staining methods for sectioned material. *Vol. 5, pt 1* of Glauert, A.M. (Ed) *Practical Methods in Electron Microscopy*. North Holland Publishing Company.
- Lieberman, A.R. (1971). The axon reaction : A review of the principal features of perikaryon responses to axon injury. *International Review of Neurobiology* **14**, 49-124.
- Lin, J-C. and Queally, S.A. (1982). A monoclonal antibody that recognises Golgi-associated protein of cultured fibroblast cells. *Journal of Cell Biology* **92**, 108-112.
- Lindsey, J.D. and Ellisman, M.H. (1981). Histochemical analysis of the effect of monensin on the Golgi apparatus. *Journal of Cell Biology* **91**, 96a.

- Lipton, P. (1985). Brain slices : uses and abuses. In Boulton, A.A. and Baker, G.B. (Eds.). Neuromethods. Series 1, Neurochemistry. Humana Press.
- Louvard, D., Reggio, H. and Warren, G. (1982). Antibodies to the Golgi complex and the rough endoplasmic reticulum. *Journal of Cell Biology* **92**, 92-107.
- McIlwain, H. and Bachelard, H.S. (1985). Biochemistry and the central nervous system. Churchill Livingstone, 5th Edition.
- McLeod, J.G. (1983). Distal autonomic neuropathy. In Bannister (Ed) Autonomic failure. **Ch.25**, 453. Oxford Medical Publications.
- Macpherson, R. (1978). Selenium deficiency. *Veterinary Record* **103**, 60.
- Macholc, E.J.A. and Macholc, L-J. (1985). Key-Gaskell syndrome in burmese kittens. *Veterinary Record* **116**, 83 (Correspondence).
- Madieros, C. (1982). *Veterinary Record* **111**, 540 (Correspondence).
- Mahaffey, L.W. (1959). Ganglionic lesions in grass sickness of horses. *Veterinary Record* **71**, 170-171.
- Malchiodi, F., Rambourg, A., Clermont, Y. and Caroff, A. (1986). Ultrastructural localisation of concanavalin A-binding sites in the Golgi apparatus of various types of neurons in rat dorsal root ganglia : functional implications. *American Journal of Anatomy* **177**, 81-95.

- Martinez-Rodriguez, R., Martinez-Murillo, R., Toledano, A. and Barca, M.A. (1980). A comparative histochemical study of disphosphate nucleosidases and thiamine pyrophosphatase in the mammalian hypothalamus. *Journal of Anatomy* **130**, 173-182.
- Mase, K., Takahashi, Y. and Ogata, K. (1962). The incorporation of [^{14}C] glycine into the protein of guinea pig brain cortex slices. *Journal of Neurochemistry* **9**, 281-288.
- Mata, M., Frick, D.J., Gainer, H., Smith, C.B., Davidson, L., Savaki, H., Schwartz, W.J. and Sokoloff, L. (1980). Activity-dependent energy metabolism in rat posterior pituitary primarily reflects sodium pump activity. *Journal of Neurochemistry* **34**, 213-215.
- Maul, G.G. and Schatten, G. (1985). The nuclear envelope and its associated structures. In Smuckler, E.A. and Clawson, G.A. (Eds.). *Nuclear envelope structure and RNA maturation. UCLA Symposium on Molecular and Cellular Biology. New Series Vol.26.* Alan R. Liss Inc. N.Y.
- Mathias, C.J. (1987). Primary autonomic failure in man. 6th Waltham Symposium. *Journal of Small Animal Practice* **28**, 387-396.
- Miani, N., Rizzoli, A. and Bucciante, G. (1961). Metabolic and chemical changes in regenerating neurons. II. In vitro rate of incorporation of amino acids into proteins of the nerve cell perikaryon of the C8 spinal ganglion of rabbit. *Journal of Neurochemistry* **7**, 161-173.

- Morre, D.J., Mollenhauer, H.H. and Bracker, C.E. (1971). Origin and continuity of Golgi apparatus. In Reinert, J. and Ursprung, H. (Eds.). Origin and Continuity of Cell Organelles. Springer-Verlag.
- Nash, A.S. (1987). Clinical features and management. 6th Waltham Symposium. Journal of Small Animal Practice 28, 339-342.
- Nash, A.S., Griffiths, I.R. and Sharp, N.J.H. (1982). Veterinary Record 111, 564 (Correspondence).
- Novikoff, A.B. (1976). The endoplasmic reticulum : A cytochemists' view (A review). Proceedings of the National Academy of Science U.S.A. 73, 2781-2787.
- Novikoff, A.B. and Essner, E. (1962). Pathological changes in cytoplasmic organelles. Federation Proceedings 21, 1130-1142.
- Novikoff, A.B. and Holtzman, E. (1970). 'Cells and Organelles'. Modern Biology Series. Holt, Rinehart and Winston.
- Novikoff, P.M., Novikoff, A.B., Quintana, N. and Hauw, J-J. (1971). Golgi apparatus, GERL and lysosomes of neurons in rat dorsal root ganglia, studied by thick section and thin section cytochemistry. Journal of Cell Biology 50, 859-880.
- Novikoff, P.M., Touster, O., Novikoff, A.B. and Tulsiani, D.P. (1985). Effects of swainsonine on rat liver and kidney : biochemical and morphological studies. Journal of Cell Biology 101, 339-349.

- Novikoff, P.M. and Yam, A. (1978). The cytochemical demonstration of GERL in rat hepatocytes during lipoprotein mobilisation. *Journal of Histochemistry and Cytochemistry* 26, 1-13.
- Obel, A-L. (1955). Studies on grass disease. The morphological picture with special reference to the vegetative nervous system. *Journal of Comparative Pathology* 65, 334-346.
- Ochoa, R. and de Velandia, S. (1978). Equine grass sickness: serological evidence of association with Clostridium perfringens type A enterotoxin. *American Journal of Veterinary Research* 39, 1049-1051.
- Ochoa, R., Gomez, S., Bustos, F. and Trejos, E. (1974). Enterotoxaemia de los equinos. Reporte inicial sobre la reproduccion de la enterotoxaemia equina (Colico inspecifico infladera o sopladera) *Rev. Inst. Colomb. Agropecu.* 9, 15-49.
- Ogawa, K. and Sakai, M. (1982). Recent findings on ultracytochemistry of thiamin phosphatases. *Annals of the New York Academy of Sciences* 378, 188-214.
- Olsson, Y. (1984). Vascular permeability in the peripheral nervous system. In Dyck, P.J., Thomas, P.K., Lambert, E.H. and Bunge, R. (Eds). *Peripheral Neuropathy (2nd Edtn) Vol.1, Ch.27.* W.B. Saunders Company.
- Pestka, S. (1971). Inhibitors of ribosome function. *Annual Review of Biochemistry* 697-710.
- Pickering, J.P. (1974). Ethology and grass sickness. *Veterinary Record* 95, 474 (Correspondence).

- Pohlmann, R., Kruger, S., Hasilik, A. and von Figura, K. (1984).
Effect of monensin on intracellular transport and receptor-mediated endocytosis of lysosomal enzymes. *Biochemical Journal* **217**, 649-658.
- Pohlmann, R., Waheed, A., Hasilik, A. and von Figura, K. (1982).
Synthesis of phosphorylated recognition marker in lysosomal enzymes is located in the cis part of Golgi apparatus. *Journal of Biological Chemistry* **257**, 5323-5325.
- Pollin, M.M. (1985). Feline dysautonomia: the Key-Gaskell syndrome. A clinical, pharmacological and pathological study. M.V.M. Thesis. University of Glasgow.
- Pollin, M.M. and Griffiths, I.R. (1987). Feline dysautonomia : An ultrastructural study of neurones in the XII nucleus. *Acta Neuropathologica (Berl)* **73**, 275-280.
- Pollin, M.M. and Sullivan, M. (1986). A canine dysautonomia resembling the Key-Gaskell syndrome. *Veterinary Record* **118**, 402-403.
- Pospelov, V., Russev, G., Vassilev, L. and Tsanev, R. (1982). Nucleosome segregation in chromatin replicated in the presence of cycloheximide. *Journal of Molecular Biology* **156**, 79-91.
- Power, J.L. and Temple, J.D. (1982). *Veterinary Record* **111**, 540 (Correspondence).
- Price, D.L. and Porter, K.R. (1972). The response of ventral horn neurons to axonal transection. *Journal of Cell Biology* **53**, 24-37.

- Rambourg, A., Clermont, Y. and Beaudet, A. (1983). Ultrastructural features of six types of neurons in rat dorsal root ganglia. *Journal of Neurocytology* **12**, 47-66.
- Reichmann, W.J. (1961). Use and abuse of statistics. Pelican Book A707. Penguin Books. Appendices 1 and 3.
- Robinson, J.M. (1985). Improved localisation and intracellular sites of phosphatases using cerium and cell permeabilisation. *Journal of Histochemistry and Cytochemistry* **33**, 749-754.
- Rochlitz, I. (1984). Feline dysautonomia (the Key-Gaskell or dilated pupil syndrome): a preliminary review. *Journal of Small Animal Practice* **25**, 587-598.
- Rochlitz, I. and Bennett, A.M. (1982). *Veterinary Record* **112**, 614. (Correspondence).
- Roth, J. and Berger, E.G. (1982). Immunocytochemical localisation of galactosyltransferase in HeLa cells : co-distribution with thiamine pyrophosphatase in trans-Golgi cisternae. *Journal of Cell Biology* **92**, 223-229.
- Rothman, J.E. (1981). The Golgi apparatus : two organelles in tandem. *Science* **213**, 1212-1218.
- Sabate, I.M., Stephenson, C., Bishop, A.E., Probert, L., Cole, G.A., Hodson, N.P., Edwards, G.B., Yeats, J., Bloom, S.R. and Polak, J.M. (1983). Pathological changes in the regulatory peptides of the gut in equine grass sickness. *Journal of Pathology* **139**, 484.

- Schwartz, J.H. (1985). Synthesis and distribution of neuronal protein. In Kandell, E.R. and Schwartz, J.H. (Eds.). Principles of Neural Science, 2nd Edition. Elsevier, New York.
- Shanthaveerappa, T.R. and Bourne, G.H. (1965). The thiamine pyrophosphate technique as an indicator of the morphology of the Golgi apparatus in the neurons. II. Studies on the cerebral cortex. *Cellule* 65, 201-209.
- Sharp, N.J.H., Nash, A.S. and Griffiths, I.R. (1984). Feline dysautonomia (the Key-Gaskell syndrome). A clinical and pathological study of 40 cases. *Journal of Small Animal Practice* 25, 599-615.
- Siesjo, B.K. (1978). Brain Energy Metabolism. John Wiley and Sons.
- Smuckler, E.A. and Clawson, G.A. (1985). Nuclear envelope structure and RNA maturation. UCLA Symposia on Molecular and Cellular Biology. New Series Vol.26. Alan R. Liss Inc. N.Y.
- Sommer, E.W., Kazimierczak, J. and Droz, B. (1985). Neuronal subpopulations in the dorsal root ganglion of the mouse as characterised by combination of ultrastructural and cytochemical features. *Brain Research* 346, 310-326.
- Sterman, A.B. (1982). Acrylamide induces early morphologic reorganisation of the neuronal cell body. *Neurology* 32, 1023-1026.

- Sterman, A.B. (1983). Altered sensory ganglia in acrylamide neuropathy. Quantitative evidence of neuronal reorganisation. *Journal of Neuropathology and Experimental Neurology* 42, 166-176.
- Stewart, W.J. (1977). A case of suspected acute grass sickness in a thoroughbred mare. *Australian Veterinary Journal* 53, 196.
- Syversen, T.L.M. (1977). Effects of methylmercury in in vivo protein synthesis in isolated cerebral and cerebellar neurons. *Neuropathology and Applied Neurobiology* 3, 225-236.
- Tartakoff, A.M. (1980). The Golgi complex : crossroads for vesicular traffic. *International Review of Experimental Pathology* 22, 227-251.
- Tartakoff, A.M. (1983). Perturbation of vesicular traffic with the carboxylic ionophore monensin. *Cell* 32, 1026-1028.
- Torrison, M.R. and da Silva, P.P. (1984). Compartmentalization of intracellular membrane glycoproteins is revealed by fracture-label. *Journal of Cell Biology* 98, 29-34.
- Torvik, A. (1976). Central chromatolysis and the axon reaction : a reappraisal. *Neuropathology and Applied Neurobiology* 2, 423-432.
- Torvik, A. and Skjorten, F. (1971). Electron microscopic observations on nerve cell regeneration and degeneration after axon lesions. I. Changes in the nerve cell cytoplasm. *Acta Neuropathologica (Berl.)* 17, 248-264.
- Vaillant, C. (1987). Regulatory Peptides. 6th Waltham Symposium. *Journal of Small Animal Practice* 28, 355-363.

- Vaillant, C. and Sharp, N.J.H. (1984). Abnormalities in the peptidergic enteric innervation in the Key-Gaskell syndrome. *Journal of Anatomy* **138**, 562.
- Veterinary Clinical Observation Unit (V.C.O.U.) Report (1970). Grass sickness survey in Scotland. *Veterinary Record* **86**. Members Information Supplement **35**, 55.
- Wiley, R.G., Donohue-Rolfe, A. and Keusch, G.T. (1985). Axonally transported *Shigella* cytotoxin is neuronotoxic. *Journal of Neuropathology and Experimental Neurology* **44**, 496-506.
- Wiley, R.G. and Stirpe, F. (1987). Neuronotoxicity of axonally transported toxic lectins, abrin, modeccin and volkensin in rat peripheral nervous system. *Neuropathology and Applied Neurobiology* **13**, 39-53.
- Wood, J.G., McLaughlin, B.J. and Barber, R.P. (1974). The visualisation of concanavalin A binding sites in Purkinje cell somata and dendrites of rat cerebellum. *Journal of Cell Biology* **63**, 541-559.
- Yamamoto, A., Masaki, R. and Tashiro, Y. (1985). Is cytochrome P-450 transported from the endoplasmic reticulum to the Golgi apparatus in rat hepatocytes. *Journal of Cell Biology* **101**, 1733-1740.
- Yoshino, Y., Mozai, T. and Nakao, K. (1966). Biochemical changes in the brain in rats poisoned with an alkylmercury compound, with special reference to the inhibition of protein synthesis in brain cortex slices. *Journal of Neurochemistry* **13**, 1223-1230.

Young, R.R., Asbury, A.K., Adams, R.D. and Corbett, J.L. (1975).

Pure pandysautonomia with recovery. Description and discussion of diagnostic criteria. *Brain* 98, 613.

Yusuf, H.K.M., Pohlentz, G., Schwarzmann, G. and Sandhoff, K.

(1983). Ganglioside biosynthesis in Golgi apparatus of rat liver. Stimulation by phosphatidylglycerol and inhibition by tunicamycin. *European Journal of Biochemistry* 134, 47-54.

